Organisation de Coopération et de Développement Economiques
Organisation for Economic Co-operation and Development

**15-May-2007**

_____

**English text only**

**NUCLEAR ENERGY AGENCY**
**COMMITTEE ON THE SAFETY OF NUCLEAR INSTALLATIONS**

**Best Practice Guidelines for the use of CFD in Nuclear Reactor Safety Applications**

**JT03227125**

**Document complet disponible sur OLIS dans son format d'origine**
**Complete document available on OLIS in its original format**

**ORGANISATION FOR ECONOMIC CO-OPERATION AND DEVELOPMENT**

The OECD is a unique forum where the governments of 30 democracies work together to address the economic, social and environmental challenges of globalisation. The OECD is also at the forefront of efforts to understand and to help governments respond to new developments and concerns, such as corporate governance, the information economy and the challenges of an ageing population. The Organisation provides a setting where governments can compare policy experiences, seek answers to common problems, identify good practice and work to co-ordinate domestic and international policies.

The OECD member countries are: Australia, Austria, Belgium, Canada, the Czech Republic, Denmark, Finland, France, Germany, Greece, Hungary, Iceland, Ireland, Italy, Japan, Korea, Luxembourg, Mexico, the Netherlands, New Zealand, Norway, Poland, Portugal, the Slovak Republic, Spain, Sweden, Switzerland, Turkey, the United Kingdom and the United States. The Commission of the European Communities takes part in the work of the OECD.

OECD Publishing disseminates widely the results of the Organisation's statistics gathering and research on economic, social and environmental issues, as well as the conventions, guidelines and standards agreed by its members.

\* \* \*

This work is published on the responsibility of the Secretary-General of the OECD. The opinions expressed and arguments employed herein do not necessarily reflect the official views of the Organisation or of the governments of its member countries.

NUCLEAR ENERGY AGENCY

The OECD Nuclear Energy Agency (NEA) was established on 1st February 1958 under the name of the OEEC European Nuclear Energy Agency. It received its present designation on 20th April 1972, when Japan became its first non-European full member. NEA membership today consists of 28 OECD member countries: Australia, Austria, Belgium, Canada, the Czech Republic, Denmark, Finland, France, Germany, Greece, Hungary, Iceland, Ireland, Italy, Japan, Luxembourg, Mexico, the Netherlands, Norway, Portugal, Republic of Korea, the Slovak Republic, Spain, Sweden, Switzerland, Turkey, the United Kingdom and the United States. The Commission of the European Communities also takes part in the work of the Agency.

The mission of the NEA is:

- to assist its member countries in maintaining and further developing, through international co-operation, the scientific, technological and legal bases required for a safe, environmentally friendly and economical use of nuclear energy for peaceful purposes, as well as

- to provide authoritative assessments and to forge common understandings on key issues, as input to government decisions on nuclear energy policy and to broader OECD policy analyses in areas such as energy and sustainable development.

Specific areas of competence of the NEA include safety and regulation of nuclear activities, radioactive waste management, radiological protection, nuclear science, economic and technical analyses of the nuclear fuel cycle, nuclear law and liability, and public information. The NEA Data Bank provides nuclear data and computer program services for participating countries.

In these and related tasks, the NEA works in close collaboration with the International Atomic Energy Agency in Vienna, with which it has a Co-operation Agreement, as well as with other international organisations in the nuclear field.

## COMMITTEE ON THE SAFETY OF NUCLEAR INSTALLATIONS

The NEA Committee on the Safety of Nuclear Installations (CSNI) is an international committee made up of senior scientists and engineers, with broad responsibilities for safety technology and research programmes, and representatives from regulatory authorities. It was set up in 1973 to develop and co-ordinate the activities of the NEA concerning the technical aspects of the design, construction and operation of nuclear installations insofar as they affect the safety of such installations.

The committee's purpose is to foster international co-operation in nuclear safety amongst the OECD member countries. The CSNI's main tasks are to exchange technical information and to promote collaboration between research, development, engineering and regulatory organisations; to review operating experience and the state of knowledge on selected topics of nuclear safety technology and safety assessment; to initiate and conduct programmes to overcome discrepancies, develop improvements and research consensus on technical issues; to promote the coordination of work that serve maintaining competence in the nuclear safety matters, including the establishment of joint undertakings.

The committee shall focus primarily on existing power reactors and other nuclear installations; it shall also consider the safety implications of scientific and technical developments of new reactor designs.

In implementing its programme, the CSNI establishes co-operative mechanisms with NEA's Committee on Nuclear Regulatory Activities (CNRA) responsible for the program of the Agency concerning the regulation, licensing and inspection of nuclear installations with regard to safety. It also co-operates with NEA's Committee on Radiation Protection and Public Health (CRPPH), NEA's Radioactive Waste Management Committee (RWMC) and NEA's Nuclear Science Committee (NSC) on matters of common interest.

# BEST PRACTICE GUIDELINES FOR
# THE USE OF CFD IN NUCLEAR REACTOR SAFETY APPLICATIONS

J. Mahaffy (PSU),

B. Chung (KAERI),

F. Dubois (IRSN),

F. Ducros (CEA),

E. Graffard (IRSN),

M. Heitsch (GRS),

M. Henriksson (Vattenfall),

E. Komen (NRG),

F. Moretti (U. of Pisa),

T. Morii (JNES),

P. Mühlbauer (NRI),

U. Rohde (FZR),

M. Scheuerer (GRS),

B. L. Smith (PSI),

C. Song (KAERI),

T. Watanabe (JAERI),

G. Zigh (USNRC)

# EXECUTIVE SUMMARY

## Background

In May 2002, an "Exploratory Meeting of Experts to Define an Action Plan on the Application of Computational Fluid Dynamics (CFD) Codes to Nuclear Reactor Safety Problems" was held at Aix-en-Provence, France. One of three recommended actions was the formation of this writing group to report on the need for guidelines for use of CFD in single phase Nuclear Reactor Safety (NRS) applications. CSNI approved this writing group at the end of 2002, and work began in March 2003. A final report was submitted to GAMA in September 2004, summarizing existing Best Practice Guidelines (BPG) for CFD, and recommending creation of a BPG document for Nuclear Reactor Safety (NRS) applications. This action was approved by GAMA and CSNI, resulting in the creation of this document.

## Objective of the Work

This document is intended to provide an internally complete set of guidelines for a range of single phase applications of CFD to NRS problems. However, it is not meant to be comprehensive. We recognize that for any specific application a higher level of specificity is possible on questions of nodalization, model selection, and validation. This document should provide direct guidance on the key considerations in known single phase applications, and general directions for resolving remaining details. It is our intent that this will serve as a template for further application specific (e.g. PTS, induced break) BPG documents that will provide much more detailed information and examples.

**Results and their Significance**

After review of other Best Practice Guidelines, and discussion with many CFD practitioners and developers, we have assembled guidance covering a fully verified and validated NRS analysis. The document begins with a summary of NRS related CFD analysis in countries represented by the authors, to give a feeling for the existing range of experience. Some key terminology in the field is defined in the field. These definitions are not meant simply for novices, but also provide experienced users with an understanding of how some terms (e.g. verification and validation) are used within this document.

Chapter 3 deals with definition of the problem and its solution approach. This includes isolation of the portion of the NRS problem most in need of CFD, and use of a classic thermalhydraulic (TH) safety code to provide boundary conditions for the CFD based upon less detailed simulation of the balance of plant. The chapter discusses the Phenomena Identification and Ranking Table (PIRT) process, which identifies phenomena critical to the problem, provides a basis for selection of an appropriate simulation tool, and establishes the foundation for the validation process needed for confidence in final results. The chapter also discusses theory and modelling needs associated with a number of special phenomena important to NRS but not commonly modelled in the CFD community.

CFD is not always the optimal approach to problem solution. In many cases the level of detail required for results can be obtained with thermalhydraulic systems codes of special purpose reactor component in much less time than required for a CFD analysis. Chapter 4 provides guidance in choosing between these options, and also discusses use of a transient calculation with tightly coupled CFD and TH codes.

Chapter 5 discusses selection of physical models available as user options. As is appropriate for single phase CFD, most of the emphasis is on selection of turbulence models. Recommendations are provided for high level selection between Reynolds Averaged Navier Stokes (RANS), Large Eddy Simulation (LES), and hybrid approaches such as Detached Eddy Simulation (DES). Specific turbulence models available with each of these approaches are also described. Recommendations are also provided for models associated with buoyancy, heat transfer, free surfaces, and fluid structure interactions.

Chapter 7 focuses on the numerical approximations available to solve the flow equations. Guidelines are provided for nodalization, and for choice of discrete approximations to the differential equations. Guidance is also given on convergence of iterative solutions, and numerical techniques for following free surfaces.

Results from any simulation must be properly justified. Chapter 7 discusses general assessment strategy. Chapter 8 covers approaches to limiting errors associated with discretization and numerical solution methods (verification). This step is a necessary precursor to quantifying errors associated with physical models (validation) as described in Chapter 9. All of these steps must, of course, be properly documented both for immediate review and archival purposes. Guidance on documentation is provided in Chapter 10.

Chapter 11 provides some examples of NRS applications. These are not intended as comprehensive illustrations of best practices, but illustrate some of these practices for very specific NRS applications. The first two examples are boron dilution and pressurized thermal shock. These scenarios have been analysed for many years by a number of organizations, and references to some of these other studies can be found in Chapter 1. The third example explores the use of Fluent for simulation of dry cask storage of spent fuel. This is example is highly suited to single phase CFD analysis.

**Conclusions and Recommendations**

The need for Best Practice Guidelines and their systematic use by analysts became very clear during the assembly of this report. With the exception of individuals working within the ECORA project, most CFD practitioners worked from personal experience, advice from co-workers, and at times code manuals. For those with experience in development and use of classic thermalhydraulic safety codes this should come as no surprise. Even if this document is not used on a regular basis for CFD projects, it should have significant value as a repository of expertise for training inexperienced CFD users.

As reflected in the content of this document, computer simulation is much more than generating input and observing results. In an NRS project producing trusted results, these activities do not even occupy the majority of the staff time expended. A project must begin with a clear written statement of the problem, including identification of the specific system and scenario to be analysed. This statement is then reviewed by a panel of experts in a PIRT process, to identify parameters of interest and to rank physical phenomena (and by inference regions of the system) that most strongly influence these parameters. This identification of important phenomena guides the analyst in selection of an appropriate CFD code and in selecting optional physical models within that code. With knowledge of the system and significant physical phenomena, the panel is also responsible for identification of existing information that can be used to validate models over the range of conditions in the specified scenario.

The panel's identification of significant physical phenomena, and associated validation is also an initial guide for spatial (and if appropriate temporal) discretization. If a specific validation problem has already been performed with the selected code, it should be reviewed for appropriate nodalization. If new validation calculations are required, a verification process is necessary to estimate errors associated with discretization before any comparison with data. This may result in an iterative adjustment of discretization until quantitative assurance is available that error associated with selection of the spatial mesh (and where appropriate time step) does not contaminate conclusions of the of the validation exercise.

If validation does not include simulations of the full system considered by the project, verification of the final discretization will also be needed before accepting results. Frequently, available time and computer resources restrict the rigor in estimation of discretization error. However, analysts must not use these restrictions as an excuse to abandon verification. Useful information can be obtained from comparison with results from a mesh that is coarser than the one used for final results, and verification tests with subsections of the mesh can also be productive.

This document suffers from two major shortcomings. The first is that we are producing a snapshot of guidelines at a relatively early phase in the use of CFD for nuclear reactor safety applications. As more general experience is gained, we expect that extensions and revisions will be desirable. The second is in the necessary decision to cover a wide range of CFD safety applications. As more experience is gained through OECD sponsored benchmarks and other activities, we recommend that this document be used as a template for application specific best practice guidelines. For example experience with ISP 47 could be used to generate detailed guidelines for modelling hydrogen mixing and combustion in a containment.

## ACKNOWLEDGMENTS

## TABLE OF CONTENTS

# 1   INTRODUCTION

## 1.1      Document Content

This document's primary purpose is to provide practical guidance for application of single phase Computational Fluid Dynamics (CFD) to the analysis of Nuclear Reactor Safety (NRS). We will consider use of CFD programs solving Reynolds Average Navier-Stokes (RANS) equations on both regular and unstructured meshes, as well as use of Large Eddy Simulation (LES), and Detached Eddy Simulation (DES). Very little will be said about Direct Numerical Simulation (DNS), as it is only practical for a very limited range of applications. We have attempted to cover the full range of issues associated with a high quality analysis. This begins with proper definition of the problem to be solved, permitting selection of an appropriate simulation tool. For the probable range of tools, we provide generic guidance on selection of physical models and on numerical issues including creation of an appropriate spatial grid. To complete the process of analysis, we also provide guidance for verification of the input model, validation of results, and documentation of the process.

Although our primary target audience could be considered to be less experienced CFD users, the document should be valuable to a wider audience. High quality CFD analysis is a complex process with many steps, and many opportunities to forget important details. More experienced CFD users should find value in the checklist of steps and considerations provided at the end of the document. Project managers should find the discussion useful in establishing level of effort for a new analysis. Regulators should find this to be a valuable source of questions to ask those using CFD to support licensing requests.

There are already a number of other useful documents providing guidelines for the use of CFD. The most notable in the area of reactor safety analysis was produced by the ECORA project [1]. The European Research Community On Flow, Turbulence And Combustion (ERCOFTAC) produced a more general set of guidelines for creation of CFD input models [2, 3]. Similar guidelines were produced specifically for marine applications by MARNET [4]. The AIAA has produced a short guidelines document on verification and validation [5]. More details on verification and validation can be found in a book by Patrick Roach [6], and publications by William Oberkampf and his colleagues at Sandia National Laboratories [7, 8].

This work was intended to be as internally complete as possible and specific guidance that might also be available in the above publications, is provided here in the context of NRS and our experience with CFD. However, "internally complete" does not imply that the document is exhaustive. For any specific application (e.g. mixing in a lower plenum) very detailed information can be gathered and recorded on spatial nodalization, code specific model selection, and experimental basis for validation. Our intent is that this document be updated as needed and followed by a series of best practice guideline reports for specific NRS applications.

## 1.2      Background of Document

In May 2002, an "Exploratory Meeting of Experts to Define an Action Plan on the Application of Computational Fluid Dynamics (CFD) Codes to Nuclear Reactor Safety Problems" was held at Aix-en-Provence, France. The outcome was a recommendation that three writing groups be created to provide recommendations on:

1. Guidelines for Use of CFD in Nuclear Reactor Safety Applications;

2. Assessment of CFD Codes for Nuclear Reactor Safety Problems;

3. Extension of CFD Codes to Two-Phase Flow Safety Problems.

The rationale behind this split of effort was that applications of single phase CFD were wide-spread in the Nuclear Reactor Safety (NRS) community and in need of systematic guidelines for use. A need was also identified for an organized and documented collection of appropriate assessment cases. Within the context of NRS two-phase CFD was considered to still be in its infancy, needing further thought on paths for development and appropriate assessment. The CSNI approved these writing groups at the end of 2002, and work began in March 2003.

The first group's final report was submitted to GAMA in September 2004, summarizing existing Best Practice Guidelines (BPG) for CFD, and recommending creation of a BPG document for Nuclear Reactor Safety (NRS) applications. This action was approved by GAMA and CSNI, resulting in the creation of this document.

**1.3     History of CFD use in Nuclear Reactor Safety Analysis**

Systems thermal-hydraulic codes have dominated flow modelling for NRS analysis. However, use of single-phase CFD still has a long history, beginning with special codes mainly developed at government laboratories, and expanding rapidly after widespread acceptance of commercial CFD codes. Research summaries are provided here for more than historical reasons. References provided in this section are also meant to summarize current worldwide use of CFD in NRS applications, and to give an idea of the existing pool of expertise in the area. However, understand that these summaries simply reflect the experience of authors of this report. We have not attempted to cover activities in all countries concerned with nuclear safety.

*1.3.1     Czech Republic*

The first consistent application of CFD-type computer codes in nuclear safety dates back to the 1970's, when there was bilateral cooperation between NRI Rez and FEI Obninsk (Russia) in the field of flow and heat transfer in LMFBR fuel assemblies. An extensive experimental programme of wind tunnel measurements of turbulent flow in enlarged models of fuel assemblies, and of temperature fields in a sodium rig with BN-type reactor fuel assemblies was supplemented by development of FEM-based computer codes [9-11]. Here, the main subject of research was the effect of displacements of fuel rods from their nominal positions on the temperature field.

In the 1990's, the German CFD code FLUTAN (developed in FZK on the basis of the US code COMMIX) was used to calculate development of a cold plume in the cold leg and reactor downcomer of the Czech Dukovany nuclear power plant with VVER-440/213 reactors. Altogether 50 seconds of transient started by HPIS were calculated and formation of the cold plume was studied. The result was presented at the NURETH-8 conference in Kyoto, 1998 [12]. Then, extensive application of the commercial CFD code FLUENT started, first within the International Standard Problem ISP-43 „Rapid Boron Dilution Transient Tests for Code Verification [13-15]. Within the EU project ECORA (5th Framework Programme) and SETH project, pre-test calculations of the test Nr. 17 on theSwiss PANDA facility were performed [16].

Within another EU project FLOMIX-R (5th Framework Programme), two tests focused on mixing of coolant in a VVER-1000 geometry (Gidropress stand) were calculated with FLUENT 6. Effects of modelling an elliptic perforated bottom and inclusion of wall-to-fluid heat transfer were tested along with different models of turbulence and numerical methods [17, 18]. Also within the FLOMIX-R project,

one test on a Vattenfall experimental facility (a steady state and one transient) and two tests on the FORTUM test facility (Loviisa VVER-440-type reactor) were also analysed with FLUENT 6 [18].

### 1.3.2    France

In France, single phase CFD calculations began to be used for NRS at the end of the late 80s for Fast Breeder Reactors (FBR, mainly by NOVATOME, CEA and EDF), about ten years later for PWRs by all the community (FRAMATOME, EDF, CEA and IRSN) and in the beginning of the 21th century for gas cooled reactors (GCRs) mainly by the CEA.

Some single phase CFD codes, mainly devoted to Nuclear applications, have been developed in France, among them : TRIO-U and CAST3M (CASTEM Fluid, TONUS) by the CEA, and ESTET and N3S by EDF.   Industrial codes such as CFX, Fluent and STAR CD are also used by the different organizations.

In terms of applications, up to now four safety analyses involving CFD comparison calculations have been carried out by IRSN and CEA, they are related to the following issues:

- Single phase Pressurised Thermal Shock : the comparison study was based on CFX and TRIO-U calculations to assess EDF/FANP STAR CD ones;

- Primary Flowrate (Hot Leg Heterogeneity): the comparison study was based on Banquise tests and used CFX [19] and TRIO-U calculation in order to assess EDF's demonstration based on STAR CD;

- Hydro-thermal-mechanical analysis of thermal fatigue in a mixing tee [20] : a comparison study involving CAST3M [20] and TRIO-U calculations was carried out, while EDF has used ESTET for the same application;

- Inherent boron dilution: the comparison study based on CFX and TRIO-U calculations of ROCOM, UPTF and Plant, has shown that the extrapolation of UPTF test results to a French PWR can't be done directly [22].

At the same time, many studies have been and are being performed by the French nuclear community; amongst these we can point out:

- For Water reactors at CEA and IRSN : TRIO-U studies of the mixing in the lower plenum in case of Steam Line Break [23, 24], CFX and TRIO-U studies of Induced Break in case of High Pressure Accident [25, 26],and TONUS and CFX studies of H2 risk in the containment with or without recombiners[27, 28];

- For GCR at CEA, GCR core blocking and other configurations with TRIO-U and CASTEM_Fluid [29].

Finally, we also note that multi-phase CFD applications are beginning to appear [30, 31, 32].

### 1.3.3    Germany

In Germany, the first nuclear reactor safety related applications of CFD codes were concerned with the simulation of natural convection in large tanks. Experimental and numerical investigations were performed at Forschungszentrum Rossendorf (FZR) in 1996 [33]. In 1998 Knebel et al. [34] provided and

overview of general features, characteristics and fields of CFD application in nuclear reactor safety, focusing on three examples. These are the calculation of the single-phase natural circulation of air flow in the primary system of a light water reactor for total LOCA conditions, the mixing of low-borated water with higher-borated water in the downcomer and the structures below the core of a light water reactor pressure vessel under forced and natural circulation conditions, and validation calculations for the two-fluid model in bubbly two-phase flow with closure relations for the interfacial forces and for a boiling model.

At the research centre in Karlsruhe, the CFD-code FLUTAN [35] was developed for the simulation of flows in the containment. A catalytic recombiner was modelled with the CFD-code CFX by Heitsch 1998 [36], in order to remove hydrogen and other burnable gases from the containment atmosphere of nuclear power plants during an accident. A comparison of different CFD codes for the calculation of Boron mixing transients was made during the OECD/NEA International Standard Problem ISP 43 [13].

In the first half of 2002, German nuclear research centres under the leadership of Gesellschaft für Anlagen- und Reaktorsicherheit (GRS) initiated a concerted action for the "Development and Application of CFD Software for Phenomena in the Primary System of Light Water Reactor". The goal of this CFD network is the development of a CFD software package for the efficient and accurate simulation of reactor safety relevant fluid flow and heat transfer processes (http://domino.grs.de./cfd/cfd.nsf). For this purpose 'Best Practice Guidelines (BPG)' have been developed and are continuously applied. They were developed in the framework of the European project ECORA aiming at the evaluation of CFD for reactor safety analysis [1, 37]. Detailed information and public reports are available at http://domino.grs.de/ecora/ecora.nsf.

A comprehensive experimental data base on turbulent mixing in PWRs was created within the European project FLOMIX-R [38]. Selected experiments from this data base were used for CFD code validation [39]. Reactor dynamics simulations on boron dilution transients were performed using realistic data on mixing [40].

In co-operation with ANSYS-CFX, the CFX MUSIG (**Mu**lti-**Si**ze **G**roups) model was extended to a multi-phase approach [44]. M bubble size groups for N disperse phases can be considered in this model providing a mechanistic approach for the dynamic modelling of two-phase flow regime transitions. Experimental investigations at the TOPFLOW test facility in FZ Rossendorf were focussed on bubbly flow in vertical tubes [45] and stratified flow in horizontal channels [41]. The models validation was performed against data provided by high resolution measurement techniques [46].

Joint projects between research centres, ANSYS CFX and industries (e.g. FANP, Vattenfall) are performed on CFD simulation of boiling in heated channels and transport of insulation material particles in the reactor sump during long-term emergency cooling [42, 43].

### 1.3.4 *Italy*

A group of researchers of the Department of Mechanics, Nuclear and Production Engineering (DIMNP) of the University of Pisa is involved in research activities related to the development, the application and the assessment of CFD codes in the field of nuclear reactor safety.

Experimental activities are also underway at the Scalbatraio Laboratory (which is part of the DIMNP) aimed at investigating some heat and mass transfer phenomena relevant for the nuclear reactor safety, and the experimental data are compared against results of CFD simulations. In particular, the EFFE facility is aimed at investigating the passive cooling of innovative reactor containments by falling water

film evaporation [47], while the CONAN facility is used for studying condensation in the presence of non condensable gases [48, 49, 50].

In the frame of the International Standard Problem No. 47, computational studies of the TOSQAN benchmark have been performed [51]. Moreover, the DIMNP researchers have been involved in the application of the French Trio_U code to coolant mixing problems (i.e. ROCOM and UPTF facilities) in the frame of cooperation agreements with the Commissariat à l'Energie Atomique of Grenoble.

Some other CFD-related activities carried out at the DIMNP deal with natural convection and natural circulation stability [52, 53, 54], and to the analysis of hydrogen recombiners [55].

### 1.3.5 Japan

Japan also has a long history using laboratory developed CFD codes, and recent active use of commercial tools. JNC (Japan Nuclear Cycle Development Institute) started (late in 1980) to develop a thermal-hydraulic system code for fluid flow simulation in LMFBR (Liquid Metal Fast Breeder Reactor) plant and CFD codes to solve nuclear reactor safety problems peculiar to LMFBR. The SSC code solves the overall behaviour of LMFBR plant thermal-hydraulics by using a network of one-dimensional objects that simulate pipes, pumps, core, intermediate heat exchanger, SG, etc. Using these calculated results as the boundary conditions, the 3D behaviour of sodium flow in the upper plenum and core are solved by CFD codes such as the AQUA code, the ASFRE(single phase) and the SABENA(two phase) codes [56]. Recently, JNC has been coupling a CFD code with a subchannel code to simulate the thermal-hydraulic behaviour of the core in more detail. As for the problems peculiar to LMFBR, JNC has developed the CFD codes to solve high-cycle fatigue induced by temperature fluctuations observed in thermal striping [57], sodium fire in a room with a sodium leak, sodium and water chemical reaction induced by steam generator tube rupture [58], and distorted distribution of sodium flow in a deformed sub assembly.

A rupture of secondary piping occurred at the Mihama Power Station on August 9, 2004. The Japan Nuclear Energy Safety Organization (JNES) and the Japan Atomic Energy Research Institute (JAERI) calculated the 3-D turbulent flow in the secondary cooling system in order to predict the distribution of the thinning mass of the pipe wall due to erosion/corrosion caused by turbulence downstream of an orifice.

One of the most innovative design improvements of the advanced PWR that is under licensing process in Japan is the neutron reflector replacing the conventional baffle-former structure. JNES has developed the u-FLOW/INS code to evaluate coolability of the neutron reflector heated by γ- rays, and has validated the code using data from a one fifth scale of hydraulic flow test [59].

Other recent CFD analyses in Japan include:

- JNES has also studied a behaviour of hydrogen mixing and combustion in a containment by using the DEFINE code [60];

- The boiling two-phase flow in the secondary side of the steam generator has been simulated by the Institute of Nuclear Safety Systems [61];

- The two-fluid model of the PHOENICS code was used to analyze the experiment conducted by Nuclear Power Engineering Corporation, and the effects of the interfacial friction and the heat transfer rate were studied. Studies of in-vessel and ex-vessel flow phenomena for the gas-cooled reactor are currently in progress at JAERI;

- Steady and transient analyses are performed using the STAR-CD code, and the calculated results are compared with the experimental results obtained by the high temperature test reactor in JAERI;

- Single and two-phase thermal stratification phenomena in cold legs are also being studied using the FLUENT code in JAERI.

### 1.3.6    Korea

Most of the CFD analyses for the nuclear reactor systems in Korea can be categorized into two groups: One is related to the system design analysis works and/or the safety analysis for developing new reactors such as APR1400, SMART, KALIMER and NHDD projects; the other is associated with the safety analysis of the operating reactors such as the OPR1000 and CANDU-6.  CFD has been applied to analysis of detailed thermal-hydraulic phenomena in the complex geometries of nuclear reactors under mostly single phase flow conditions and in some cases under two-phase flow conditions

Fluid and thermal mixing in the PWR reactor systems of OPR1000 and APR1400 are usually done using CFD codes by mainly focusing on the following technical concerns:

Impact of complicated three-dimensional flow structures inside a reactor vessel on problems such as boron dilution [62, 63];

- ECC bypass phenomena and jet (steam or water) impingement behaviour expected to occur in a reactor vessel downcomer with the DVI type of safety injection [64, 65, 66];

- Thermal stratification in a horizontal piping with blockages [67];

- Thermal mixing of condensing steam in a large subcooled water pool (IRWST) [68];

- Flow behaviour affecting the wall thinning of the piping due to a Flow Accelerated Corrosion (FAC) at the pressure boundary of nuclear reactor systems

- Subcooled boiling phenomena [69];

- Severe accident–related issues such as the thermal loads on the reactor vessel due to a core melt and hydrogen behaviour in a containment [70].

Fluid and thermal mixing in a CANDU reactor system is also being analyzed, but mainly from the view of a fuel channel analysis by focusing on the thermal stratification, moderator behaviour and fuel channel integrity during a LOCA, with heat transfer and chemical reaction in mind. [71, 72]  Most of these research projects are using commercial CFD codes such as CFX, Fluent and STAR-CD, but in some cases in-house codes have been applied.

CFD codes are also widely used for analyzing basic thermal-hydraulic phenomena, especially for poorly understood phenomena before experiments are performed to support new reactor development.

The Nuclear Hydrogen Development and Demonstration (NHDD) project for developing a VHTR in Korea has adopted CFD for preliminarily analyses of single phase flow behaviour in the reactor system during steady-state operation or postulated transient conditions. [73, 74] The sodium cooled reactor development project (KALIMER) as well as the integral reactor development and demonstration project (SMART-P) also use commercial or in-house CFD codes for detailed analysis of multi-dimensional flow

phenomena in complicated flow geometries (e.g., multi-dimensional ECC water flow behaviour in a downcomer annulus) and to compare the analysis results with other design analysis tools or experimental data. [75, 76]

It is expected that the use of CFD codes for a nuclear reactor analysis will be expanded to obtain the more realistic analysis information, particularly for confirmation and/or reduction of plant safety margins.

### 1.3.7    *The Netherlands*

In the Netherlands, CFD started to be used for NRS analyses in the mid 90s. These NRS analyses were concerned with the transport of hydrogen, or helium as a substitute for hydrogen, and the transport and condensation of steam in model containments. The application of CFD to containment flows has remained important until today. Containment analyses using CFD have been performed for:

- the PHEBUS test facility within the PHEBUS project, and PHEBEN-2 5th framework EU project;

- the PANDA test facility within the TEMPEST 5th framework EU project

- the TOSQAN, MISTRA, and THAI  test facilities within the International Standard Problem 47 (ISP-47);

In order to perform these containment analyses, models to describe physical phenomena such as condensation and evaporation on walls and in the bulk flow have been implemented in commercial CFD codes such as CFX-4, CFX-5, FLUENT-6, and STAR-CD using user coding. Hydrogen deflagration studies using CFD have been performed for the FLAME test facility

The application of CFD to single-phase primary system flows started in 2000, and has remained important. The following types of single-phase primary system flow analyses have been performed:

- single-phase Pressurized Thermal Shock (PTS) analyses of the UPTF facility, representing a full scale mock-up of the primary system of a four-loop PWR, within the ECORA 5th framework EU project;

- singe-phase PTS analyses of the 1:5 linear scale ROCOM facility, representing a four-loop KONVOI type reactor, within the FLOMIX-R  5th framework EU projects

- Boron Dilution Transients (BDT) within the FLOMIX-R 5th framework EU;

- high cycle thermal loading in the T-junction of CEA FATHERINO-2 test facility, using Large Eddy Simulation.

The above selected examples refer to R&D NRS applications where the developed CFD models have been validated using experimental data from test facilities. The ultimate goal is to apply the validated CFD modelling to full scale industrial applications. Examples of such industrial NRS applications are:

- hydrogen and steam distribution analyses for selected LOCA scenario's in the Borssele nuclear power plant;

- analyses of potential hydrogen deflagrations in the Borssele nuclear power plant;

- BDT analyses for the Borssele nuclear power plant;

- analyses for the modification and optimisation of the cooling of the reactor pool of the HFR research reactor.

In 2000, CFD began to be used for NRS analyses for the following Heavy Liquid Metal (HLM) flow applications:

- the MYRRHA ADS system (free surface analyses for the HLM target, analyses for the lower plenum of the MYRRHA pool);

- the target of the European Spallation Source (ESS) (flow distributions, stability, and asymmetry, and the effect of the heat removal capability, and the transport of micro bubbles)

- validation of CFD methods for application to HLM within the ASCHLIM 4th framework EU project

In the late 90s, CFD started to be used for Innovative / GEN IV concepts:

- decay heat removal analyses, fast depressurization analyses, and activated dust transport analyses for High Temperature Reactor (HTR) concepts;

- heat transfer under supercritical water conditions for the High Performance Light Water Reactor (HPLWR) concept / Supercritical Water.

A few selected recent publications illustrating the application of CFD in the Netherlands are listed in references [77] through [82]

### 1.3.8    Sweden

The first Swedish attempts to use CFD for safety analysis and development of nuclear reactor systems dates back to the 1980's, which is about a decade later than the first use for other areas (e.g. circulation of lakes and reservoirs). In 1988-1989 the code PHOENICS started to be used more regularly both by the utility Vattenfall and the vendor Asea-Atom. For instance natural convection outside the moderator tank was studied for the inherent safe reactor concept PIUS [83]. Modelling of the flow in the region above the steam separators and the dryers in a BWR was used for analysis and prediction of steam quality after the steam dryers, ref. [84].  The 3D flow pattern and heat transfer in U-bend steam generators was also investigated, ref. [85].  The model gave unexpectedly good agreement (within 2 percent) between calculated and transmitted heat.

Other early uses of CFD were for prediction of flow pattern and mixing in the downcomer of a BWR [86], flow in the annulus to the steam outlets [87], and flow and heat transfer of condensers [88]. More recent CFD applications relate to:

- Boron dilution transients, first for the Vattenfall scale 1:5 model [89], and laters for the International Standard Problem No. 43 (Model at University of Maryland) [90];

- Thermal mixing in a T-junction comparing DES and RANS calculations to model tests [91];

- Fluid Structure Interactions (FSI) comparing results from the HDR experiments in Germany to numerical simulations with RELAP 5 [92] and ADINA [93] (performed both with and

without FSI effects caused by the flexible core barrel) and giving quite good ADINA for the first 100 ms of the transient, when only single phase fluid existed in the vessel;

- CFD simulations of flow in the LWR tube bundles and vertical channels [94 through 99]; and

- Large scale investigations of gas mixing and stratification in the PANDA experiments [100] , performed in the EU project ECORA.

### *1.3.9    Switzerland*

First CFD activities within Switzerland date from 1982, when analyses of Hypothetical Core Disruptive Accidents (HCDAs) in Fast Breeder Reactors (FBRs) were carried out. This work was coordinated with the UKAEA and EURATOM, and contracts were signed between partners to jointly develop the fluid/structure code SEURBNUK-EURDYN [101], and validate the code against test data from the COVA [102] series of small-scale tests. In a separate agreement with the CEA, data from the MARA tests performed at the Cadarache site were also used for validation purposes. Further work involved a linked 2-D fluid/structure (SEURBNUK) and 3-D structure dynamics (ADINA) study on whether the roof cover of the Super-Phoenix FBR could withstand the impact caused by a fast rising sodium surface, driven by an HCDA [103].

Switzerland entered the commercial CFD area by licensing the 3-D CFD code ASTEC [104] from AEA Technology, and using it to examine decay-heat removal by natural circulation in FBR cores in the context of the SONACO experiments being carried out at PSI. The code was also used to perform preliminary studies of an early design of a spallation source target, in support of an initiative to build a molten lead-bismuth target for the SINQ facility at PSI.

The association with AEA Technology was strengthened by licensing their 3-D CFD code FLOW3D , which later became known as CFX-4 [105]. The code was required in support of the ALPHA project [106], directed towards analysis of passive decay-heat removal for the Generation III Simplified Boiling Water Reactor (SBWR) concept of GE. The work focussed on two aspects of passive containment cooling: the growth and break-up of large bubbles formed by discharge of steam/nitrogen mixtures through vent lines into the suppression pool, and mixing of the pool by the subsequent bubble plume. Both activities entailed using CFX-4 in two-phase mode, the former involving installation of the Level Set interface-tracking algorithm into CFX-4 [107], and the latter the development of two-phase RANS and LES turbulence models [108].

Further work involved extension of the design and safety studies of spallation source targets, which ultimately are of interest in the Accelerator Driven System (ADS) concept [109, 110], in which neutrons from the source are used to support a continuing reaction in an otherwise sub-critical core.

Other single-phase CFD applications relate to:

- Boron Dilution [111], using both CFX-4 and CFX-5;

- Mixing in PWR downcomers, as part of the EU 5th FWP FLOMIX-R [112] using CFX-4 and CFX-5;

- Participation in International Standard Problem ISP-47 [], performing analysis with CFX-4 of the CEA experiments and TOSQAN and MISTRA, related to wall condensation in containments; and

- Severe accident studies involving aerosol deposition [114], initially using CFX-4, but more recently using FLUENT.

### *1.3.10    United States.*

The earliest known use of CFD for NRS in the United States was associated with the COMMIX code [116] developed by Bill Sha and his colleagues at Argonne National Laboratory.   COMMIX started as a single phase 3-D porous media code to improve modelling of reactor vessel flow, employing the novel porous media formulation (NPMF) [117] to provide a wide range of modelling capabilities.   In 1979 with assistance from Brian Launder, a modified k-ε two-equation turbulence model (with addition of buoyancy terms) was incorporated into the code.

Two other laboratory code series developed CFD capabilities slightly later than COMMIX. KFIX [120] was one result of a long history of flow simulation codes developed by the Fluid Dynamics Group (T-3) of the Theoretical Division at the Los Alamos National Laboratory (LANL). Although normally used for 3-D two-phase flow analysis without turbulence modelling, later versions contained a Prandtl mixing length model for single-phase turbulence.   The COBRA-TF [121] series developed at Pacific Northwest National Laboratory (PNL) followed a similar pattern, adding a mixing length turbulence model to the basic two-phase 3-D flow capabilities around 1982.   Westinghouse's containment code GOTHIC [122] evolved from COBRA-TF, becoming a totally different program over the years, and adding a k-ε two-equation turbulence model in 1995.   Currently GOTHIC also provides options for k-ε models with 2nd and 3rd order Reynolds stress approximations and a k-ε model based on Renormalized Group (RNG) theory.   It is Westinghouse's workhorse for containment safety analysis including hydrogen mixing and dispersal and deposition of radionuclides.

The earliest safety issues addressed by CFD in the U.S. were associated with Large Break Loss of Coolant Accidents (LBLOCA).   In the late 1970's the U.S. Nuclear Regulatory Commission (NRC) became concerned about the integrity of core barrels during the rapid depressurization associated with a LBLOCA.   T-3 at LANL created an appropriate dynamic structural analysis tool [123] tightly linked to KFIX.   Analysis with these coupled programs provided the first accurate comparisons with German experimental data [124].

Pressurized thermal shock first became an issue in the U.S. in the early 1980's.   This also is a coupled CFD and structural analysis problem, but transient linkage does not need to be as tight as with core barrel deflections.   COMMIX was chosen by EPRI to help resolve the issue [125].   At the same time the NRC did an extensive series of analyses using KFIX.   The issue did not re-emerge for over a decade.

In the early 1990's COMMIX was successfully used to analyse the severe accident scenario now known as an induced break [126].   A related Westinghouse experiment showed:

1.  thermally stratified counter-current flow in the hot leg;

2.  recirculation in the core, upper plenum and SG inlet lower plenum, and

3.  the establishment of stable circulating flow through SG.

COMMIX modelled all reactor components in the experiment and showed good agreement with the data.

In the mid-1990's a fundamental shift occurred at the NRC in application of CFD to NRS problems.   Experienced CFD practitioners were recruited to the NRC staff, and a licence purchased for

Fluent (1997). A great deal of work was done without publication, including calculations to clarify issues related to PTS, the AP1000 upper head, and boron dilution. To improve fundamental understanding, NRC has done calculations exploring stratification in tanks (including AP600 CMT), mixed convection on a flat plate, and turbulence in pipe flow and jets. They also have worked on SETH-PANDA separate effects containment tests (gas jets, stratification, and mixing). NRC staff have published reports on boron dilution [127], spent fuel heatup [128], and steam generator inlet plenum mixing during a severe accident [129] (induced break).

# 2.  TERMINOLOGY

Discussion of terminology has to begin with "Computational Fluid Dynamics".  At its most general level any computer based simulation of fluid flow falls in this domain.  However, specialists in the field tend to apply two levels of restrictions to use of the phrase.  In normal usage CFD now implies solution of Navier-Stokes (as opposed to Euler) equations with some special provision for modelling turbulence.  With improvements in hardware and software technology, description of a simulation as CFD has also come to normally imply the presence of some fairly sophisticated means of dealing with the problem geometry, usually involving a complex and flexible process for spatial discretization.

## 2.1      Spatial Mesh

Until recently CFD tools have tended to work on a regular, logically rectangular mesh.  Logically rectangular simply means that you can apply some transformation to the mesh and get a picture that looks like a orderly lattice of rectangular boxes.  This mesh class comes in two flavours: orthogonal where all grid lines meet at right angles; and non-orthogonal where no restriction is placed on angles between mesh lines.  Now many CFD tools have the capability to work with an unstructured mesh.  Common elements here are triangles in 2-D and tetrahedrons in 3-D, although mixtures with other geometric cell forms are possible and at times desirable.  The primary advantages of an unstructured mesh are the ability to nodalize very complex geometries and better load balancing in parallel calculations.  The primary disadvantages of unstructured codes are complexity of software implementations and higher level of errors associated with spatial discretization.

A third option exists for discretization of space, overset-grid (or Chimera) methods [130].  This technology was largely developed in the U.S. by NASA and the DoD, for analysis of flow past very complex systems, such as the space shuttle.  The underlying idea is to break a complex geometry into a collection of much simpler regions.   Each region can be resolved with a relatively simple structured mesh, and all meshes have a zone of overlap with their neighbours.  One major advantage of the method is the ability to model motion such as rotating turbine blades, changes in position of control surfaces, or manoeuvring of a full body.  This capability has also been applied to resolution of vortices shed at trailing edges.  The primary disadvantage occurs during development of the portion of the software associated with interpolation of results in the overlap zones between the overset grids.

## 2.2      Turbulence

An early decision in modelling any turbulent flow is the high level approach to turbulence modelling.  Details of this selection are provided in Section 5, but brief definitions of four approaches are provided here as part of basic CFD terminology.  Distinctions between the approaches are based on the standard view of turbulence as a superposition of eddies with a continuous distribution of sizes.  Selection of modelling approach is a question of how much of this eddy spectrum is resolved in the direct solution of the Navier-Stokes equations and how much is relegated to special auxiliary models.

### 2.2.1    Reynolds Average Navier Stokes (RANS)

RANS is most clearly defined in simulations of "steady" flow.  The time independent mean flow field is obtained from Navier-Stokes equations, and mean effects of all turbulence are captured in a

separate model. In transient simulations, the time averaging imposed on the Navier-Stokes equations is on a large enough scale that everything recognized as turbulence is filtered, and must be modelled separately.

### 2.2.2 Direct Numerical Simulation (DNS)

DNS takes advantage of the fact that turbulence is part of any detailed solution of the Navier-Stokes equation. In this approach a fine enough computational mesh is introduced to resolve all significant scales of turbulence and no special turbulence models are needed. Unfortunately, turbulence theory tells us that the smallest persistent eddy diameter is roughly proportional to the Reynolds number to the minus three-quarters power ($1/Re^{3/4}$). This means that the number of mesh points in 3-D DNS scales like $Re^{9/4}$, and only a very limited range of problems can be solved with DNS on current computers.

### 2.2.3 Large Eddy Simulation (LES)

LES is a family of methods that compromise between RANS and DNS. Large-scale eddies are resolved in the flow equation solution, and effects of small-scale eddies are obtained from a special model. This implies a cutoff size in the LES model separating the two scales. This cutoff is small enough that turbulence models for smaller scales can be significantly simpler than those required for good results with RANS.

### 2.2.4 Detached Eddy Simulation (DES)

DES is a further compromise between RANS and LES, to capture key physical phenomena in the lowest possible amount of computer time. A decision is made on spatial regions that are adequately modelled by RANS and those requiring LES. An example is simulation of vortex shedding from the trailing edge of some solid structure, perhaps as part of an acoustic or fatigue analysis. Boundary layers and more far-field flows can be simulated well with RANS. However, a region downstream of the structure would require a finer mesh, and a flag activating LES.

## 2.3 Verification and Validation

When discussing verification and validation (V&V) for a simulation, it's useful to precisely define a few terms. Although there is some variance in definitions within the V&V community, these are generally small. We have adopted definitions provided by the AIAA [5]. First a very specific distinction is drawn between error and uncertainty.

Error -   A recognizable deficiency in any phase or activity of modelling and simulation that is not due to lack of knowledge.

Uncertainty -   A potential deficiency in any phase or activity of the modelling process that is due to lack of knowledge.

It is also important to distinguish between two types of uncertainty. Aleatory (or stochastic) uncertainty results from a physical process that is fundamentally random. Processes in this class may be totally characterized by known probability density functions, and the only unknown is the particular state of the random process at any instant. The second class of uncertainty is Epistemic and reflects a broader lack of knowledge. One common example is a parameter in a model which is a contant (not stochastic), but for which the value is not precisely known. It is also possible to have unknown information in the specification of a stochastic process (unknown distribution function, unknown mean, unknown varience). In this case the uncertainty is both aleatory and epistemic.

The processes of verification and validation are separated as follows:

Verification - The process of determining that a model implementation accurately represents the developer's conceptual description of the model and the solution to the model;

Validation - The process of determining the degree to which a model is an accurate representation of the real world from the perspective of the intended uses of the model.

For the user of a CFD code verification primarily covers quantification of error associated with the selection of mesh, time step, and iteration convergence criteria, and with specification of initial and boundary conditions in an input model. Details of the V&V process are covered.

# 3. PROBLEM DEFINITION

In this section we discuss two important steps in problem definition. The first is clean isolation of the problem to be analysed and the second is the PIRT process. PIRT was originally defined in the context of classic thermal-hydraulic safety analysis, but the procedures are not specific to that arena, and it is gaining acceptance in the wider CFD community. We close the section with discussion of considerations of special phenomena necessary during the process of problem definition.

## 3.1    Isolation of the Problem

Hitherto, reactor systems and containments have generally been modelled as networks of 0-D and 1-D elements. Primary systems have been represented by a series of control volumes, connected by flow junctions; the primary system codes RELAP5, TRACE, CATHARE and ATHLET, for example, are all constructed in this way. The flow conservation equations are applied to the volumes and junctions, and heat transfer and appropriate flow resistance correlations are imposed, depending on the flow regime. It is evident, however, that in some components the flow is far from being 1-D: for example, in the upper and lower plenums and downcomer of the Reactor Pressure Vessel (RPV), and to some extent the core region, particularly if driven by non-symmetric loop operation. Natural circulation and mixing in containment volumes are also 3-D phenomena, and a number of "CFD-type" codes have been specially developed to deal with such flows: for example GOTHIC, TONUS and GASFLOW. However, the meshes employed are very coarse by CFD standards, and rely on correlations rather than resolving boundary layers and underlying physics. Here, we conveniently delegate the coarse-mesh, system/containment part of the simulation as the *macro-scale* calculation, and the fine-mesh, CFD part as the *meso-scale* calculation.

A recent example of meso-scale calculation can be found in [132]. Comparative simulations of hydrogen mixing including mitigation in a full containment of type VVER 440/213 for a small break severe accident scenario were carried out with CFX, FLUENT and GASFLOW. The meshes employed by FLUENT and CFX were about one order of magnitude bigger than that of GASFLOW.

It is inconceivable that CFD approaches will be able in the near future to completely replace the now well-established system/containment code approach to reactor transients. The number of meshes which would need to be employed would be well beyond the capabilities of present computers, and reliable closure relations for 3-D multi-phase situations are still a long way from maturity. Additionally, no readily available CFD code has a neutronics modelling capability.

A more efficient option would be to perform local CFD computations only where and when a fine-mesh resolution is required. The problem with this is that most of the macro-scale phenomena relating to safety are transient, and the local meso-scale situation may be strongly influenced by the macro-scale parameters. This means directly interfacing a CFD module to an existing system/containment code in order to perform a localized 3-D computation within the framework of an overall macro-scale description. This arrangement is attractive, since it retains the accumulated experience and reliability of the traditional system/containment code approach, but extends their capabilities in modelling meso-scale phenomena. However, the issue of isolating the CFD problem arises.

Unless there is full coupling between the macro- and meso-scale parts of the simulation, meaning that the CFD computation is carried out throughout the entire system transient, it has to be decided whether the coupling between the scales is one-way or two way.

In the case of one-way coupling (no feed-back of the CFD calculation on the macro-scale behaviour), the two calculations can be run independently, with the CFD part of the calculation run in a post-processing mode, with time-dependent boundary conditions supplied by the system/containment calculation. Calculations with a system code usually start from a steady state. When the CFD simulation also starts from the same steady state, the initial conditions for the CFD would be determined from a steady state CFD simulation based upon this initial macro-scale steady state (that is, a steady state is calculated with the CFD code using boundary conditions supplied by steady state calculation with the system code). Very frequently, however, the CFD simulation starts during the transient, so that this approach cannot be used. Then, a quasi-steady situation should be selected as the initial state for the CFD simulation and this quasi-steady state is again calculated by the CFD code using corresponding boundary conditions based on the calculation of the system code. Simulations of Pressurized Thermal Shock are the typical examples. They usually start at the time when the Emergency Core Cooling System (ECCS) starts to deliver cold water into the primary circuit. At this time, the situation in that part of the primary circuit selected as computational domain for the CFD simulation need not be steady and some conservative assumptions must be adopted (e.g., flow stagnation). Another option would be to start the CFD calculation at an earlier time in the Pressurized Thermal Shock (PTS) transient when some "plateau" in thermal-hydraulic parameters within the selected computational domain is detected in the system calculation. From the point of view of Best Practice Guidelines (BPGs), sensitivity to initial conditions needs to be carried out, the time-step for the CFD simulation should be set in accordance with the time variation in the boundary conditions, and an assessment should be made of the validity of assumed top-hat profiles at the inlets and outlets (using sensitivity studies, if necessary). Two-way coupling is more difficult, but some cases could be handled by iteration between the macro-scale and meso-scale computations.

The isolation problem is bypassed if there is full, two-way coupling between the code systems. The disadvantage then is that the meso-scale calculations would have to be performed throughout the transient, even if the 3-D aspects at this scale are not always important, and this brings with it a large CPU overhead and/or restrictions on the number of meshes that could be employed. However, there would be no logistics problem associated with specifying initial conditions: for example, the transient may start from a steady-state flow situation, already established, and known cell-wise, in the 3-D component. As before, the validity of the 1-D approximations to the velocity and temperature profiles at the inlets and outlets would need to be examined.

## 3.2    PIRT

The process of constructing a Phenomena Identification and Ranking Table (PIRT) originated as part of the U.S. NRC's Code Scaling, Applicability, and Uncertainty (CSAU) evaluation methodology [131]. CSAU was a demonstration methodology for use of best estimate simulation codes in licensing of nuclear power plants under rules approved by the U.S. NRC in September 1988. The PIRT process was created as a systematic and documented means of completing a CSAU exercise with a limited amount of resources. Phenomena and processes are ranked in the PIRT based on there influence on primary safety criteria, and efforts focused on the most important of these. This process has proven valuable in other contexts and its specifications have been broadened over the years (see Ref. 133). In recent years the value of the PIRT process has been recognized outside the nuclear safety community as an important component of any validation process [8].

The PIRT process begins with some crucial steps performed by the organization needing the PIRT. First, objectives of the exercise must be clearly documented. One key conclusion of Wilson and

Boyack [133] is that the value of the final PIRT is directly proportional to the degree of detail in the initial specification of a transient scenario and system in which the scenario occurs. An organization will obtain more efficiency from a series of specific PIRT exercises (e.g. Direct Vessel Injection (DVI) line break in AP600 reactor design) rather than trying to cover a range of analyses with a very general PIRT exercise (e.g. small break loss of coolant accident in a pressurized water reactor).

With well defined objectives, scenario and system in hand, the next step is selection of the panel of experts. This should begin with the selection of a panel coordinator. In addition to relevant technical expertise, this individual needs to be experienced in the PIRT process and to have strong interpersonal skills, including the ability to gracefully sort relevant from irrelevant team member contributions. The coordinator should have direct access to management members who have requested the PIRT, access to staff outside the panel who can perform studies needed to clarify the importance of any given phenomena, and sufficient wisdom to use these resources effectively.

The panel should have the necessary breadth and depth to handle the problem as defined. Depth is achieved by carefully selecting high quality experts. Breadth is obtained by attention to each individual's fields of expertise. At least one member should have a primary focus in each of the following areas, relevant to the scenario and system under study:

- Experimental programs and facilities;

- Simulation code development (numerical implementation of physical models);

- Application of relevant simulation codes to this and similar scenarios;

- Configuration and operation of the system under study.

The panel of experts begins by reviewing objectives, system, and scenario, and then defining parameters of interest. For a Large Break Loss of Coolant Accident (LBLOCA) in a given PWR, the critical parameter is peak clad temperature. In other cases the list of parameters of interest could be much longer, and might be modified as phenomena and processes are identified and ranked.

With this initial groundwork in place, the next phase is identification of relevant existing information, primarily experimental data and results of related analysis. This relies heavily on the knowledge and experience of panel members, but can also be scheduled to permit research by available staff.

The central work follows with identification of phenomena and processes associated with the system under the specified scenario. Wilson and Boyack recommend starting with identification of high level system processes (e.g. depressurization, debris transport). Next some structure is supplied by dividing the scenario into time phases in which dominant processes do not change significantly, and splitting the system into components or subsystems, which can be expected to spatially isolate some key phenomena. This provides a matrix of zones in time and space for which all plausible phenomena and processes can be identified. Some or all of the steps to this point could be handled without assembling the panel in one location. However, a face to face brainstorming session is needed at this point to assemble the initial list and move on to ranking of importance.

The ranking process is iterative both within the initial panel session and on a longer time scale as more information becomes available from experiments and analysis. A good starting point is to rank phenomena and processes as having low, medium, or high significance. When more resolution is required, panels have split each of these categories into three subdivisions giving a nine level scale, or simply split

the high and low categories into two subdivisions, giving a five level scale. It is common after the discussion associated with the first round of ranking to realize that phenomena considered early in the process were under or over-emphasized. This results in further discussion and shuffling before the first draft of the PIRT is produced. Discussions may also expose a clear lack of available knowledge, and result in requests for specific sensitivity calculations before release of a final PIRT.

Interpretation of the PIRT depends on details of the objectives. If the PIRT is used to aid design of an experiment, rankings are with respect to need for accurate measurements and need for care in scaling to properly capture its effect in a full-scale system. If the PIRT is to be used to improve modelling in a simulation code, ranking addresses the level of detail required in special models programmed for the phenomenon or process. If the PIRT is directed towards a simple sensitivity study the ranking can be used to limit the number of input parameters studied. Phenomena with low importance may be dropped from the sensitivity analysis, or their impact estimated with bounding calculations. If the class of uncertainty analysis described in Section 9.3.2 is used, then this ranking should not be used to restrict the number of parameters subject to random perturbations. However, more care should be taken in generating probability density functions for parameters associated with highly ranked coefficients.

The ranking table is only a useful overview of the process, and the primary value rests in the full documentation produced by the panel of experts. Sections of the document provide:

- A detailed description of the system, scenario, and objectives;

- Discussion of the parameters of interest and range of their values that meet the objectives;

- A clear definition of the phenomenon and processes considered by the panel;

- State of the existing knowledge base that could impact final results, including adequacy of the

- Experimental data base,

- Simulation code's physical models, and

- Code verification and validation;

- Discussion of the ranking scale used and formal methodology selected for assigning ranks;

- Technical justification for each rank assigned in the table.

As already indicated, creation of a PIRT is an iterative process. After it is first applied results of requested experiments, sensitivity studies, or other results from simulations may require revisions to the original PIRT and associated documentation. However, the value of the PIRT process lies not in absolute accuracy at a point in time, but in its rational guidance in allocation of limited resources to a complex research process.

## 3.3    Special Phenomena

### 3.3.1    *Containment Wall Condensation*

It is now recognized that traditional approaches to containment modelling using lumped-parameter models need to be supplemented by 3-D models, and purpose-built "CFD-like" containment

codes such as GOTHIC [134], using very coarse meshes (by CFD standards), but with industrial-standard turbulence models. Discrepancies still remain in validation of these 3-D containment codes, however, and their source cannot always be identified because of lack of detailed information in integral tests. When sufficient computer resources are available, CFD codes, with much finer meshes, have the potential to improve simulation accuracy, but need extended modelling capabilities. In particular, a CFD code used for containment simulations must have some provision for condensation of steam on walls or condensers.

Steam condensation in the presence of high non-condensable mass fractions at low gas mass fluxes (i.e. below 2 kg/m$^2$s)is encountered in the context of passive containment cooling for advanced light water reactors incorporating building condensers. Typical condenser operating conditions are saturated steam/air mixtures at 110$^o$C with 1 kg/m$^3$ air partial density on the primary side and boiling water at 100$^o$C on the secondary side.

It is possible to directly calculate the condensation process from first principles or to introduce empirical models for heat and mass transfer. Both models are based on the assumption that, in the presence of a non-condensable gas, the thermal inertia of the condensate layer is negligible and can be ignored. This means that a two-component, single-phase simulation can be carried out, with the mass transfer of the steam handled by adjusting its species concentration appropriately.

For the direct modelling approach, the computational mesh next to the condensing surface is chosen fine enough for the steam concentration gradient to be resolved in the laminar sub-layer, where turbulent mass transfer can be neglected [136]. (This means that the model has to be used in combination with a low Reynolds number turbulence model.) The condensation mass flux to the wall $q_m''$ is then evaluated from the gradient of the steam mass fraction $Y$ according to Fick's law:

$$q_m'' = -\frac{\rho D}{(1 - Y_w)}\frac{\partial Y}{\partial n}$$

in which $\rho$ is the mixture density, $D$ the binary diffusion coefficient, and $n$ is the normal distance from the wall. Saturation conditions are assumed at the wall itself, so that from the local wall surface temperature $T_w$ the partial pressure of steam $P_{st}$ can be found from tables. Since the total pressure is known as one of the local state variables, and stored by the code, the partial pressure of the non-condensables can be derived, and from this the mass fraction of steam at the wall $Y_w$; the mass fraction gradient is assumed linear near the wall, and may be determined from differences in local values. The latent heat is extracted from the fluid cell and placed in the wall material (for a conjugate heat transfer problem) to be conducted away internally, while sensible heat transfer to the wall is handled by the code in the normal way.

For the non-local model, fine-mesh resolution near the condensing wall is not required, and a suitable mass/heat transfer correlation is used to represent condensation for the mesh cell next to the wall. In principle, any standard heat transfer correlation can be used (e.g. Gido-Koestel [137]), and the mass transfer calculated by dividing by the latent heat at the steam partial pressure. As before, the condensate film is ignored in this treatment. An alternative treatment which employs the turbulent mass transfer coefficient based on the wall function concept rather than a heat transfer correlation is applied in reference [138]. It must be remembered, however, that if a correlation is used, it corresponds to the total heat transfer, including the sensible heat, so this must not be added again by the code.

Currently, no definite guidelines exist for choosing between use of a correlation or a wall function approach when using a non-local model. The wall function approach has the advantage of being

consistent with the rest of the near wall modelling in the simulation, and is simpler to implement. However, a correlation may be more exact in special cases like rough walls  or finned tubes, which are not resolved in the mesh. A difficulty with correlations is that they were not derived for local values but for a global or averaged estimation over a total wall and not a tiny piece of it. Therefore uncertainties arise in calculating required averaged parameters like bulk temperature or height of condensate film along a wall. Care is needed when applying heat transfer correlations in order to provide a mesh independent calculation and to stay within the limits under which the correlation was derived.

Thus, from the standpoint of Best Practice Guidelines, it is necessary to ensure the following.

- The fluid mesh cell next to the condensing surface is appropriate to the condensing model chosen. Fick's law model must be applied within the laminar sub-layer (for concentration), and the correlation model outside the turbulent boundary layer. The concentration gradients tend to be sharper than those for heat and momentum transfer, and consistency checks need to be made that the fluid mesh is appropriate for all transport quantities.

- The turbulence model must be consistent the mass/energy transfer model adopted.

### 3.3.2    Pipe Wall Erosion

The secondary circuit of a PWR is usually made of carbon steel. Pipe wall erosion (known as flow accelerated corrosion) can bring about wall thinning of secondary piping to an extent that the pipe wall thickness reaches the minimum thickness required by the design criterion.  This phenomenon has resulted in severe piping ruptures at the Surry nuclear plant in 1989 and the Mihama plant in 2004. Flow accelerated corrosion (FAC) is a form of localized attack that occurs in areas where the turbulence intensity at the metal surface is high enough to cause disruption of the normally protective oxide surface film.

Programs for inspecting pipe wall thinning exist at all plants. Inspection locations are generally established in accordance with the inspection program guidelines of each country. The inspection frequency for pipe wall thickness measurements is based on a combination of predicted and measured erosion/corrosion rates. Kastner's correlation [139] has been most used as the prediction formula of the thinning behaviour of carbon steel piping by erosion/corrosion. It should, however, be noticed that this formula only estimates the maximum amount of thinning and gives no information on its distribution.

Detailed ultra-sonic wave measurements of the distribution of pipe wall thinning were performed after the Mihama accident to find the causes of the pipe rupture in one of the steam generator secondary flow circuits and to elucidate the phenomenon. The 3-D turbulent flow in the secondary cooling system of the Mihama Plant has been analyzed by the modern CFD codes (FLUENT, Star-CD and PLAHSY [140]) in order to simulate the measured distribution of thinning [141].

An investigation of the relation between the calculated values of turbulence intensity and the thinning obtained by the Kastner's correlation revealed that the calculated kinetic energy of turbulence near the pipe wall surface would have good correlation with the wall thinning.

The measured thinning distribution on the pipe wall downstream of the orifice agreed well with the calculated distribution of turbulent kinetic energy near the wall surface by the CFD codes. This 3D-CFD calculation was extended to the full secondary piping system to study the reasons for the enhancement in the wall thinning in one plant secondary loop (A-loop) relative to that in another loop (B-loop) and found the following differences of flow pattern in A and B piping:

- Strong counter-clockwise rotating flow was generated in the first elbow of A-loop piping, and;

- Weak clockwise rotating flow was generated in the first elbow of B-loop piping.

These differences caused the different circumferential distribution of calculated turbulence energy near the wall surface behind the orifices of the A and B loops. The distribution of calculated turbulence energy was found to have some similarities to the measured wall thinning distribution. Both showed uneven distribution in the A loop, and uniform distribution in the B loop.

Experience analyzing the Mihama accident has produced a number of specific guidelines for application of CFD to this class of problem.  The coolant in the secondary piping system at normal operation is considered to flow in a steady turbulent condition. The standard k-ε turbulent model can provide satisfactory results for calculating this flow. However, the scaled test performed after the Mihama accident revealed oscillating and twisting flow in the A-loop.  This required transient analysis using LES to model the turbulent flow.

A standard wall function is applicable to the steady turbulent flow of normal operation. However, for the observed oscillatory flows a non-slip boundary condition with very fine mesh near the wall using the low Reynolds number type k-ε model or the LES model may be better than the wall function. This provides high accuracy evaluation of turbulent kinetic energy near the pipe needed for evaluation of wall thinning by FAC.

Special consideration must also be given to spatial nodalization.  The shape of roundness of the corner in a junction in the pipes should be exactly reflected in the calculation grid, because details of the junction shape have a strong effect on the flow.

### 3.3.3    Thermal Cycling

Thermal striping (presence of high-frequency thermal fluctuation on the inner surface of a component) can be the cause of the propagation of deep cracks, present in the component wall. Failures of parts of structures of NPPs caused by thermal fatigue include Genkai Unit 1 (Japan), Tihange Unit 1 (Belgium), Farley Unit 2 (USA), PFR (UK), Tsuruga Unit 2 (Japan), and Loviisa (Finland). Thermal striping is a very complex phenomenon involving several fields of science: thermal-hydraulics (which can produce the thermal fluctuations), stress analysis (which can transform the thermal loads into mechanical stresses), and science of materials (which can describe the effects of mechanical stresses on behaviour of cracks). Therefore, some kind of multi-physics coupling of codes is required.

In thermalhydraulic analysis of thermal fatigue it is necessary to know how different frequencies and amplitudes of time-dependent mechanical stress affect crack propagation in order to evaluate suitability of a selected computational model to analyse the problem of thermal fatigue. Based on experience described in Chapuliot et al. [142], the frequency range from 0.1 Hz to 10 Hz should be studied. The upper bound of frequencies (10 Hz) is also found in ref.[144]. Higher frequencies are not so dangerous from the point of view of crack propagation.

Thermal fluctuations of various frequencies and amplitudes can be caused by turbulence, or by large-scale instabilities like pulses, pump fluctuations, gravity waves, etc. Some low-frequency fluctuations depend on geometry even of the plant itself which causes problems with selection of the computational domain and formulation of boundary conditions. Critical geometries are represented mainly by T-junctions, valves, and parallel jets (e.g., in upper plenums). Simulation approaches can be based on RANS or U-RANS with superimposed thermal fluctuations of selected frequency and amplitude, or on

LES/VLES/DES models. The sinusoidal form of temperature fluctuations used in the RANS approach does not properly represent random nature of the real fluctuations. There are simulations using a "pseudo-DNS calculation", that is, using the assumption of unsteady laminar flow with fine grid and small time steps (but not so fine grids and so small time steps to simulate all needed space and time scales as in the true DNS). Such an approach is possible with all commercial CFD software supposing that enough computer memory and time are available.

Validation of computer codes for simulation of thermal stripping is limited by the fact that suitable experimental data is very scarce. On real plants, temperatures (or deformations) of the solid walls are measured predominantly at the outer surfaces of conduits. Temperature fluctuations are damped by wall conduction as demonstrated analytically by Kashahara [143], so the measured amplitudes are small.

Ref. 144 makes the following recommendations based on solution of a benchmark problem (T-junction of a Liquid Metal Fast Breeder Reactor (LMFBR) secondary circuit):

- The range of the damaging frequencies from the wall thickness should be determined first (frequencies lower than this band do not produce sufficient $\Delta T$ across the wall, and frequencies higher than this band cannot penetrate the wall);

- The duration of the transient simulation should be deduced from the lower bound of the range, considering that the transient duration should cover at least 10 periods of this low frequency;

- The time step of the computation must be small enough to resolve oscillations at the higher bound of damaging frequencies;

- Since realistic boundary conditions should be used and there are some limitations as to the size of computational domain, the boundary conditions should include possible secondary flows (e.g. swirl flow) and low-frequency variations of temperature and/or velocity (boundary condition sensitivity analyses are a good practice);

- Transient simulation using a Large Eddy Simulation model is recommended, requiring that discretization schemes must be at least of order 2 in space and in time;

- Care must be given to the transient behaviour of the computational mesh adjacent to the wall in association with a transient heat transfer coefficient with induced filtering of high frequencies.

### 3.3.4    *Hydrogen Explosion*

The hydrogen-air reaction has the potential to threaten containment integrity or any other equipment in a Nuclear Power Plant (NPP). Hydrogen becomes an issue during severe accidents with considerable gas releases mainly by oxidation of fuel cladding. Under design basis accident conditions releases of hydrogen are considerably lower. During normal operation radiolysis of water produces some hydrogen as a stoichiometric mixture with oxygen. In order to preserve containment integrity under all conditions or to avoid hydrogen combustion at all, several mitigation strategies were developed. These include inertisation (BWR), dilution, installation of catalytic recombiners or the use of igniters. Underlying physical and chemical processes of hydrogen combustion including modelling approaches are rather complex and are dealt with in detail in reference [145].

*Hydrogen combustion*

The nature of hydrogen production and release determines the possible forms of hydrogen combustion. Hydrogen mostly appears in lean (under-stoichiometric) mixtures together with air and steam and may accumulate non-uniformly in clouds (premixed combustion) in the containment. The dimensions of a containment are too big and too complicated to investigate hydrogen combustion experimentally in full scale. All known experimental facilities have either much smaller dimensions or they address only selected aspects of hydrogen combustion. In the nuclear context any modelling approach has to pay special attention to scaling aspects from experiments in reduced geometry, to full size, and to given geometric complexity.

Hydrogen combustion can occur as deflagration or detonation including a transitional process called DDT (deflagration to detonation transition). Deflagrations are the most common combustion mode and may range from slow deflagrations (flame speeds below 100 m/s) to fully accelerated turbulent combustion with flame speeds up to 1000 m/s. The release of hydrogen may be continuous with occasional combustion events. In this case a standing flame close to the gas release source can also develop.

For assessment of containment integrity, temperature and pressure loads including pressure differences between compartments are of primary interest. Most models concentrate therefore on these parameters. This requires the correct prediction of flame propagation mechanisms (branching) and flame speeds. For deflagrations it can be shown that reaction kinetics is much faster than the mixing processes bringing reaction partners together. The most common CFD modelling approach addresses simply the mixing process and assumes infinitely fast chemical kinetics. This concept is called the Eddy Break-up model and was introduced by Magnussen and Hjertager [146]. The reaction rate is defined by:

$$R = -\rho * \frac{\varepsilon}{k} * C * M_{\lim} \quad (1)$$

with:

$\rho$ - density

$k, \varepsilon$ - turbulent energy and dissipation

$C$ - numerical constant

$$M_{\lim} = \min\left( m_F, \frac{m_O}{i}, B\frac{m_P}{1+i} \right) (2)$$

$M_{\lim}$ describes the presence of fuel, oxidizer and products respectively, weighted by the stoichiometric relations within the reaction. The influence of products (water vapour) can be switched on or off by the factor B in eq. (2). The constant C has to be fitted to experiments. There is a direct proportionality of the reaction rate to the inverse turbulent time scale defined by $k/\varepsilon$. This creates a mesh dependency of the reaction rate and calls for careful validation of the model. For the factor C a number of modifications and extensions have been proposed. These are focused on local extinction of the reaction if turbulence becomes locally too high or on a reduction of the dependency on spatial resolution by introducing the laminar burning velocity [147]. Scaling of the Eddy Break-up model from experimental level to full scale containment application has to be made with great care. If possible the mesh resolution relative to existing length scales should be preserved between experiment and application.

Each recent commercial CFD code also offers other modelling options for simulating premixed hydrogen deflagrations. Among these are flame front or pdf (probability density function) models. A promising approach is the combination of a flamelet pdf model with a turbulent burning speed closure. The numerical effort is however strongly increased compared with the Eddy Break-up or Eddy Dissipation formulation, which often prohibits their application to containment scale. A comparative application of several combustion models in a large simplified EPR containment can be found in [148] and in [149]

A general weakness of existing models is the completeness of combustion. Models consume all hydrogen but this is in contradiction to experimental findings, which have always detected a low percentage of remaining unreacted hydrogen (about 0.5 to 0.8 % by volume).

The transition from deflagration to detonation (DDT) cannot be predicted to date. But assuming a stable detonation is much easier to calculate and shows comparable loads. In the case of a detonation it is not necessary to care about turbulence levels because the reaction is determined by the chemical reaction kinetics. Detonation algorithms are much simpler than for deflagration and computing times are rather short (about one order of magnitude shorter than for deflagrations).

For some applications it is enough to calculate AICC (adiabatic isochoric complete combustion) pressures, the potential of a mixture to create an accelerated deflagration (expansion ratio or sigma criterion) or the principal possibility of a detonation (7-lambda criterion). All these parameters are conservative and do not need much computational effort.

*Mitigation strategies*

There exist several options to reduce or avoid the potential consequences of hydrogen combustion. Inertisation of possible release areas by either nitrogen or $CO_2$ makes any combustion impossible. Dilution is designed to avoid the transition to detonation. It needs less additional mass to be injected into the containment and produces hence less extra pressure built-up. Both options can be simulated by basic features of recent CFD codes. The choice of the turbulence model will be important. In view of the large geometric dimensions and long simulation times only two equation models appear currently feasible. BPG for turbulence should be followed as much as possible in order to obtain predictable simulations.

Another option is the implementation of catalytic recombiners in the containment or in parts of the primary circuit to recombine hydrogen back to water in a smooth way. These have been installed or are planned for most PWR containments. These recombiner systems can be designed to cover hydrogen releases for design basis accidents or to reduce remaining loads in a severe accident.

A model of the processes ongoing in a catalytic recombiner needs to include the catalytic surface reactions (Arrhenius formulation), diffusion and convection of species, heat conduction in solids and thermal radiation. An example of a CFD model can be found in [150]. If only the impact of recombiners in terms of hydrogen management in a containment has to be estimated then a much more simplified model can be used which can easily implemented in any CFD code.

### 3.3.5 *Fire Analysis*

A variety of fire modelling tools employing different features are currently available. The most appropriate model for a specific application often depends on the objective for modelling and fire scenario conditions. Fire models have been applied in nuclear power plants in the past to predict environmental conditions inside a compartment room of interest. The models typically try to estimate parameters such as temperature, hot smoke gas layer height, mass flow rate, toxic species concentration, heat flux to a target, and the potential for fire propagation in the pre-flashover stage compartment fire.

Fire models are generally limited by their intrinsic algorithms and by other factors impacting the range of applicability of a given model feature. These features are inherent in the model's development and should be taken into consideration in order to produce reliable results that will be useful in decision-making.

The engineer must bear in mind that most fire models were developed for general application and not specifically for the conditions and scenarios presented in nuclear power plants. A fire model's features and ability to address these conditions should be considered when selecting an appropriate fire model. These considerations affect the accuracy or appropriateness of the fire dynamics algorithms used for a unique analysis of a given space. The conditions can include but are not limited to the following:

- The types of combustibles and heat release rates;

- Types and location of ignition sources;

- The quantity of cables in cable trays and other in-situ fire loads in compartments;

- Location of fire sources with respect to targets in the compartments;

- High-energy electrical equipment;

- Ventilation methods;

- Concrete building construction, large metal equipment, and cable trays that will influence the amount of heat lost to the surroundings during fire;

- Compartments that vary in size but typically have a large volume with high ceilings;

- Transient combustibles associated with normal maintenance and operations activities.

Techniques used to model the transfer of energy, mass, and momentum associated with fires in buildings fall into three major categories.

- Single equations: used to predict specific parameters of interest in nuclear power plant applications such as adiabatic flame temperature, heat of combustion of fuel mixtures, flame height, mass loss rate, and so forth. These equations can be steady state or time dependent. The results of the single equation can be used either directly or as input data to more sophisticated fire modelling techniques.

- Zone models: assume a limited number of zones, typically two or three zones, in an enclosure. Each zone is assumed to have uniform properties such as temperature, gas concentration, and so forth. Zone models solve conservations equations for mass, momentum, energy, and in some examples, species. However, zone models usually adopt simplifying assumptions to the basic conservation equations to reduce the computational demand for solving these equations.

- Field models: field or Computational fluid dynamics (CFD) models divide an enclosure into large number of cells and solve the Navier-Stokes equations in three dimensions of the flow field. CFD models also require the incorporation of sub-models for a wide variety of physical phenomena, including convection, conduction, turbulence, radiation, and combustion. The resulting flows or exchange of mass, energy, and momentum between

computational cells are determined so that the three quantities are conserved. Accordingly, CFD models need intensive computational power, but these models can be run on high-end PC computers. The CFD models can provide detailed information on the fluid dynamics of an enclosure fire in terms of three-dimension field, pressure, temperature, enthalpy, radiation, and kinetic energy of turbulence. These models have been used to model a variety of complex physical phenomena such as the impact of a suppression system (e.g., a sprinkler system or water mist system) on a specific type of fire, or smoke movement in a large compartment with complex details such that detection can be optimized. CFD models can provide a fundamental understanding of the flow field models for known compartment geometry, along with the physical phenomena that interact with the flow field.

Fire differs significantly in its behaviour from other fluids and gases due to its complex chemical, thermal and turbulent behaviour and interaction. Because of this complexity, any simulation tool must be capable of handling the chemical reactions; the turbulent flows and radiative and convective heat transfer within the analysis. Fire suppression using mist-spray is an additional factor to take into account when choosing a CFD tool to analyze fire.

Fluent, STAR-CD and CFX are among the commercially available software that include modelling capabilities to deal with the complex nature of fire physics. Fire Dynamic Simulator (FDS), developed, maintained and freely distributed by the National Institute of Standards and Technology (NIST), is also capable of modelling fire growth and suppression. The drawback with FDS is its limited choice in the type of configuration it can deal with. FDS solves the conservation equation in rectilinear coordinates only, and is not designed to handle geometries with curves. Additionally, FDS is not capable of solving a conduction equation through thick walls. Also, the only available models to treat turbulence is LES with a Smagorinsky model and DNS. LES requires very fine mesh with y+ of order of unity, while DNS is even more restrictive and requires even finer mesh resolution than LES. For chemical reactions FDS uses a mixture fraction combustion model. The model assumes that combustion is mixing-controlled, and that the reaction of fuel and oxygen is infinitely fast, regardless of the temperature. If the fire in under-ventilated, fuel and oxygen may mix but may not burn. Also, the user has to provide the products of the reaction that are difficult to estimate. For most cases, the user assumes complete combustion and relies on yield ratios for smoke and other constituents which are usually unavailable especially if you are dealing with incomplete reaction which is the case in most fire simulations. In the calculation of surface heat flux combined with LES, FDS uses ad-hoc correlations of both natural and forced convection. This approximation will have a major effect on the prediction of heat flux to the walls and targets which are important parameters to the fire analysis. For more information on this model, visit www.nist.gov.

In order to evaluate the capabilities of fire models for nuclear power plants applications, an International Collaborative Fire Model Project (ICFMP) was organized. The objective of the project is to share the knowledge and resources of various organizations to evaluate and improve the state of the art of fire models for use in nuclear power plant fire safety and fire hazards analysis. The project is divided into two phases. The objective of the first phase is to evaluate the capabilities of current fire models for fire safety in nuclear power plants. The second phase will implement beneficial improvements to current fire models that are identified in the first phase, and extend the validation database of those models. Currently, twenty-two organizations from six countries are represented in the collaborative project.

So far, this organization has formulated five benchmark exercises. These were intended to simulate a basic scenario defined in sufficient detail to allow evaluation of the physics modelled in the fire computer codes. An assessment of appropriate input parameters and assumptions, interpretation of results, and determination of the adequacy of the physical sub-models in the codes for specific scenarios will establish useful technical information regarding the capabilities and limitations of the fire computer code.

Uncertainties in the predictions based on validations of each code will provide a basis for the confidence on the set of results developed in the exercise.

As with any flow simulation, guidelines have to be followed to choose the grid to correspond to the appropriate chosen turbulence model. Additionally, the grid has to satisfy grid independent solution to obtain the correct heat flux and temperature to the targets.

The right reaction model has to be chosen to correctly simulate the oxidation kinetics of the fuel and the inclusion of the effect of turbulence. A lower oxygen limit (LOL) is used in many of the models to simulate the under-ventilation and extinction of the fire. The specification of LOL has a large effect on the prediction of the extinction and could be a large source of user effects.

Ventilation systems should be modelled correctly, as the flow pattern from mechanical ventilation systems will affect the temperature in local areas, and will be a source of uncertainty.

A correct and robust radiation model is required to assess heat flux to the walls and targets from fire.

### 3.3.6    Water Hammer

There is a long history of water hammer analysis, beginning with simple back-of-the-envelop calculations, which do a reasonable job estimating peak pressures. One-dimensional analysis generally provides quite good simulation of the initial pressure wave propagation, and usually works well for checking equipment against peak loads. Classic thermalhydraulic safety codes have been successfully used for such analysis. However, one-dimensional analysis tends to under-predict decay of the peak pressure over relatively long transients (very long piping runs and/or multiple wave reflections). One major reason is the development of asymmetric flow instabilities [151, 152], that must be captured with multidimensional (CFD) flow simulations. A recent summary of water hammer analysis and experiments has been provided by Ghidaoul et al [153].

Unfortunately, because of the practical success of 1-D analysis, and the expense of full CFD calculations, there is insufficient CFD experience to provide specific user guidelines for those wishing to perform detailed water hammer simulations. The best general advice is to start with a good nodalization for 3-D flow in a pipe, and to use the data provided by Brunone et al [151] for initial validation.

### 3.3.7    Liquid Metal Systems

The application of established CFD codes to liquid metal flows, such as sodium in breeder coolants or lead/lead-bismuth in spallation targets, is of limited value and requires special care. As long as only an isothermal single-phase flow is considered, which is fully characterized by just a Reynolds number, the usual CFD codes are fully applicable. However, the situation changes if additional phenomena such as

- free surface flows,

- gas bubble two-phase flows, or

- temperature gradients and related buoyancy flows

are of any relevance. Due to the much higher surface tension and the drastically lower Prandtl number of liquid metals compared to water, the CFD modeling of liquid metal flows cannot rely on turbulence models developed and tested for water flows. For instance, the ratio between the boundary layer

thickness for momentum and temperature is opposite for liquid metals and water, which results in a very different thermalhydraulic behaviour. Thus, for physical reasons, a separate benchmarking of the CFD modelling of liquid metal flows is inevitable. In general, this is less developed. This situation, in turn, heavily relates to the missing measuring techniques allowing resolution of such flow fields with a precision which is needed for code validation. The recent developments of ultrasonic velocity measurements, local electric potential probes and magnetic flow tomography [154, 155] changed this situation qualitatively.

Initial benchmarking activities for liquid metal turbulence models were done in the European community with the recently finished ASCHLIM project (Assessment of Computational Fluid Dynamics Codes for Heavy Liquid Metals). In particular, analyses of the TEFLU sodium jet experiments [156] have provided useful insights into appropriate turbulence models. A number of tests were run with the FLUTRAN code in which use of Reynolds analogy was replaced by more detailed models of the turbulent energy flux term. In particular the Turbulent Model for Buoyant Flows (TMBF) was found to work quite well for these experiments with significantly less expense than a full Reynolds stress model.

One clear conclusion from this experience is that users attempting simulation of liquid metal flows with commercial CFD codes should select a turbulence model with separate modelling of the turbulent energy transport, and validate the results very carefully.

### 3.3.8    Natural Convection

Natural convection is caused by density differences in a fluid or by mixing of fluids of different density. The density differences can be caused by heating from internal or external sources. Natural convection can be used as a passive mechanism of heat removal. Buoyancy driven flow can also occur in the case of mixing of fluids of different densities, (e.g. steam and nitrogen, liquid regions with different solute concentrations). This case is relevant for boron dilution scenarios in PWRs.

Comparisons to experiments have shown that classical turbulence models applied in a Reynolds Averaged Navier Stokes (RANS) solver can be applied to flow situations having Rayleigh Numbers up to about $10^5..10^6$. The CFD modelling of temperature stratification for higher Rayleigh Numbers of the system shows deficiencies. Classical turbulence models assume the isotropic approach of the Reynolds stresses and the Boussinesq approximation for the dependency of the density on the temperature. Possible solutions with increasing computational effort are directed to:

- consideration of additional sources in the turbulence equations;

- application of a Reynolds Stress turbulence model, which consider the anisotropy of the Reynolds stresses; and

- using a Large Eddy Approach, which solves for the large-scale fluctuating flows and uses sub-grid scale turbulence models for the small-scale motion.

*Consideration of additional sources in the turbulence equations*

If we take in consideration turbulence models, which are based on the modelling principle of turbulent kinetic energy (two-equation family turbulent models like k-epsilon and its modifications, SST Shear Stress Transport), the transport equation for turbulent kinetic energy has the form:

$$\frac{\partial k}{\partial t} + \overline{u_i}\frac{\partial k}{\partial x_i} = \frac{\partial}{\partial x_i}\left(\nu + \frac{\nu_t}{\sigma_k}\right)\frac{\partial k}{\partial x_i} + \underbrace{\nu_t\left(\frac{\partial \overline{u_i}}{\partial x_j} + \frac{\partial \overline{u_j}}{\partial x_j}\right)\frac{\partial \overline{u_i}}{\partial x_j}}_{P_k} \quad \underbrace{-g_i\overline{u_i'\rho'}}_{G_k} - \epsilon - 2\nu\left(\frac{\partial k^{\frac{1}{2}}}{\partial x_i}\right)^2$$

where $k = \frac{1}{2}\sum_{i=1}^{3} u_i u_i$ is turbulent kinetic energy, $u_i$ is mean velocity in the $i$ direction, $\nu$ is the fluid kinematic viscosity, $\nu_t$- is the turbulent viscosity, $G_k = -\sum_{i=1}^{3} g_i\overline{u_i'\rho'}$ is a source term due to turbulent mass fluxes, $g_i$ is the component of gravity vector in $i$ direction, and $\varepsilon$ is the dissipation rate of turbulent kinetic energy. In two-equation turbulent models a separate transport equation is solved for the dissipation rate of turbulent energy.

The local approximation for the buoyancy driven source term of turbulent kinetic energy, which is often used in CFD codes (CFX, Fluent), is based on principle that we prescribe :

$$G_{\rho_i}^{th} = \frac{-\mu_t}{\rho \, Pr_t} g \varDelta\rho$$

where $\rho$ is the mean density, $\mu_t$ is the turbulent dynamic viscosity, $Pr_t$ is the turbulent Prandtl number, $g$ is the acceleration due to gravity and $\varDelta\rho$ is the density difference.

If we define the source term in the form $G_{\rho_i}^{th} = -\sum_{i=1}^{3} g_i\overline{u_i'\rho'}$ with anisotropic contributions from the components of the turbulent mass fluxes, then we must model transport equations for the individual components of the turbulent mass fluxes:

$$\frac{\partial \overline{u_i'\rho'}}{\partial t} + \overline{u_j'}\frac{\partial \overline{u_i'\rho'}}{\partial x_j} = \underbrace{\frac{\partial}{\partial x_j}\left(\underbrace{\alpha\frac{\overline{\partial \rho}}{\partial x_k}u_i + \nu\overline{\rho\frac{\partial u_i}{\partial u_k}} - \overline{\rho u_i u_k}}_{D_{\rho i}^t}\right)}_{D_{\rho i}} \underbrace{-\frac{\overline{\rho}}{\rho}\frac{\partial p}{\partial x_i}}_{\Pi_{\rho i}} - \underbrace{(\alpha+\nu)\overline{\frac{\partial \rho}{\partial x_k}\frac{\partial u_i}{\partial x_k}}}_{\epsilon_{\rho i}}$$

$$\underbrace{-\overline{u_i u_k}\frac{\partial \rho}{\partial x_k}}_{P_{\rho i}^\rho} \underbrace{-\overline{\rho u_k}\frac{\partial U_i}{\partial x_k}}_{P_{\rho i}^U} \underbrace{-g_i\beta\overline{\rho^2}}_{G_{\rho i}^{th}} + \underbrace{g_i\beta_c\overline{\theta_c}}_{G_{\rho i}^c} + \underbrace{\overline{f_i^L\theta}}_{G_{\rho i}^L} + \underbrace{\overline{f_i^r\theta}}_{G_{\rho i}^\Omega}$$
$$\underbrace{\phantom{-\overline{u_i u_k}\frac{\partial \rho}{\partial x_k} -\overline{\rho u_k}\frac{\partial U_i}{\partial x_k}}}_{Production}$$

where $D_{\rho i}^v$ is the molecular diffusion of density flux, $D_{\rho i}^t$ the turbulent diffusion of density flux, $\Pi_{\rho i}$ the pressure scrambling effect, $\varepsilon_{\rho i}$ the molecular destruction term, $P_{\rho i}^\rho$ the production term due to mean density gradient, $P_{\rho i}^U$ the production term due to mean velocity gradient , $G_{\rho i}^{th}$ the production term due to density buoyancy, $G_{\rho i}^c$ the production term due concentration buoyancy, $G_{\rho i}^L$ magnetic field effect, Lorentz force, and $G_{\rho i}^\Omega$ system rotation effect.

$$\frac{\partial \overline{\rho'^2}}{\partial t} + \overline{u_i}\frac{\partial \overline{\rho'^2}}{\partial x_i} = \frac{\partial}{\partial x_k}\left(\underbrace{\alpha\frac{\partial \rho^2}{\partial x_k}}_{D^v_{\rho^2}} \underbrace{-\overline{\rho^2 u_k}}_{D^t_{\rho^2}}\right) \underbrace{-2\overline{\rho u_k}\frac{\partial \rho}{\partial x_k}}_{P_{\rho^2}} \underbrace{-2\alpha\overline{\frac{\partial \rho}{\partial x_k}\frac{\partial \rho}{\partial x_k}}}_{\epsilon_{\rho^2}}$$

$$\underbrace{\qquad\qquad\qquad\qquad}_{D_{\rho^2}}$$

The turbulent mass flux equations must be supplemented by a transport equation for turbulent density variance

where $D_{\rho^2}$ is the total diffusion of density variance, $D^v_{\rho^2}$ the molecular diffusion of density variance, $D^t_{\rho^2}$ the turbulent diffusion of density variance, $P_{\rho^2}$ production term due to mean density gradient, and $\varepsilon_{\rho^2}$ the molecular destruction term.

In the case of the fully differential model, we have to solve four additional balance equations together with the two equations for $K$ and $\varepsilon$. This increases the computational efforts significantly.

Instead of differential balance equations we can also assume a set of algebraic equations for the turbulent mass fluxes and turbulent density variance as a simplification. An algebraic model is less expensive with respect to computation time, but still reflects the physical phenomena, which are produced by the buoyancy effect. The algebraic model was derived by neglecting the transport effects,

$$\overline{\rho u_i} = -C^\rho\frac{k}{\epsilon}\left(\overline{u_i u_j}\frac{\partial \rho}{\partial x_j} + \xi\overline{\rho u_j}\frac{\partial U_i}{\partial x_j} + \eta\beta g_i\overline{\rho^2} + \epsilon_{\rho i}\right)$$

If we further neglect the molecular dissipation rate and for the transport equation we also neglect the transport effects of density variance we obtain a fully algebraic model:

$$\overline{\rho u_i} = -C^\rho\frac{k}{\epsilon}\left(\overline{u_i u_j}\frac{\partial \rho}{\partial x_j} + \xi\overline{\rho u_j}\frac{\partial U_i}{\partial x_j} - 2\overline{\rho u_k}\frac{\partial \rho}{\partial x_k}C\frac{k}{\epsilon}\right)$$

$$\overline{\rho u_i} + C^\rho\frac{k}{\epsilon}\xi\overline{\rho u_j}\frac{\partial U_i}{\partial x_j} - C^\rho\frac{k}{\epsilon}2\overline{\rho u_k}\frac{\partial \rho}{\partial x_k}C\frac{k}{\epsilon} = -C^\rho\frac{k}{\epsilon}\overline{u_i u_j}\frac{\partial \rho}{\partial x_j}$$

$$A\overline{\rho u} = b \Rightarrow \overline{\rho u} = A^{-1}b$$

wh

ere the matrix A has the form:

$$
\mathbf{A} = \begin{bmatrix} 1 + \tau \left( \xi \frac{\partial U_1}{\partial x_1} - C' \frac{k}{\epsilon} 2 \frac{\partial \rho}{\partial x_1} \right) & \tau \left( \xi \frac{\partial U_1}{\partial x_1} - C' \frac{k}{\epsilon} 2 \frac{\partial \rho}{\partial x_2} \right) & \tau \left( \xi \frac{\partial U_1}{\partial x_1} - C' \frac{k}{\epsilon} 2 \frac{\partial \rho}{\partial x_3} \right) \\ \tau \left( \xi \frac{\partial U_2}{\partial x_1} - C' \frac{k}{\epsilon} 2 \frac{\partial \rho}{\partial x_1} \right) & 1 + \tau \left( \xi \frac{\partial U_2}{\partial x_1} - C' \frac{k}{\epsilon} 2 \frac{\partial \rho}{\partial x_2} \right) & \tau \left( \xi \frac{\partial U_2}{\partial x_1} - C' \frac{k}{\epsilon} 2 \frac{\partial \rho}{\partial x_3} \right) \\ \tau \left( \xi \frac{\partial U_3}{\partial x_1} - C' \frac{k}{\epsilon} 2 \frac{\partial \rho}{\partial x_1} \right) & \tau \left( \xi \frac{\partial U_3}{\partial x_1} - C' \frac{k}{\epsilon} 2 \frac{\partial \rho}{\partial x_2} \right) & 1 + \tau \left( \xi \frac{\partial U_3}{\partial x_1} - C' \frac{k}{\epsilon} 2 \frac{\partial \rho}{\partial x_3} \right) \end{bmatrix}
$$

The vector of unknown turbulent mass fluxes is

$$
\overline{\rho \mathbf{u}} = \begin{bmatrix} \overline{\rho u_1} \\ \overline{\rho u_2} \\ \overline{\rho u_3} \end{bmatrix}
$$

$$
\mathbf{b} = \begin{bmatrix} -\tau \left( \overline{u_1 u_1} \frac{\partial \rho}{\partial x_1} + \overline{u_1 u_2} \frac{\partial \rho}{\partial x_2} + \overline{u_1 u_3} \frac{\partial \rho}{\partial x_3} \right) \\ -\tau \left( \overline{u_2 u_1} \frac{\partial \rho}{\partial x_1} + \overline{u_2 u_2} \frac{\partial \rho}{\partial x_2} + \overline{u_2 u_3} \frac{\partial \rho}{\partial x_3} \right) \\ -\tau \left( \overline{u_3 u_1} \frac{\partial \rho}{\partial x_1} + \overline{u_3 u_2} \frac{\partial \rho}{\partial x_2} + \overline{u_3 u_3} \frac{\partial \rho}{\partial x_3} \right) \end{bmatrix}
$$

and the vector of right side

Mixed approaches are also possible, where e.g. the differential balance equation for the turbulent density variance is solved together with a set of algebraic equations for the turbulent mass fluxes.

*Application of a Reynolds Stress turbulence model, which considers the anisotropy of the Reynolds stresses*

The concept of turbulent mass fluxes presented above can also be used in turbulence models based on the principle of modelling each component of the Reynolds stress (Reynolds stress model RSM). For each component of the turbulent Reynolds stress with equal indexes $\overline{u_i u_i}$, $i = 1, 2, 3$ a source term directly equivalent to the turbulent mass flux in the proper direction is used in the transport equation: $G^{th}_{\rho_i} = - g_i \overline{u'_i \rho'}$ This new source term of density fluxes then includes anisotropy from the Reynolds stress components.

An analogous approach as described above can be applied for the turbulence modelling in the case of temperature induced density differences [157]. Instead of the turbulent mass fluxes, turbulent heat fluxes are balanced in this case. Density differences in this case are replaced by temperature differences, multiplied by the thermal expansion coefficient of the fluid, turbulent temperature variance is considered instead of turbulent density variance.

# 4.   SELECTION OF APPROPRIATE SIMULATION TOOL

The aim of this section is to provide guidance for the appropriate selection of a simulation tool from the common known approaches extending from "classical thermohydraulic system code" to "component code" up to "CFD code". Considering that the recommendation will be based both on the underlying theoretical hypotheses that have led to the corresponding models and on the supposed validation state of each tool, this selection approach may be valid for both single and two phase applications.

Beyond the standard use of each code within its usual application field, we will also explore the possible complementary use of the different tools to deal with a given issue; either independently or in a more integrated way that will lead to coupled approaches. The underlying framework is a multi scale description of the reactor coolant circuit, each of the following approaches clearly referring to an appropriate "scale description".

## 4.1    Classic Thermal-Hydraulic System Code

Thermalhydraulic (TH) system codes have evolved over many decades to provide simulation of the response of full nuclear power plants to a wide range of accident scenarios. Each has been designed to perform simulations of a wide range of reactor plant designs and a full range of relevant experimental facilities. They must be able to model 1-D two-phase flow through any configuration of piping, and normally have provisions for some classes of 3-D regions.

Typically over half of the source code in a systems code is devoted to managing this flexibility. Of this most is associated with input processing required to define the system configuration and set initial and boundary conditions. Other significant functions associated with general flow topology are initialization and management of flexible data structures, full system restart dumps, and output of graphical.

The input processing capabilities built into current system codes are combinations of ASCII and binary restart information. Although powerful modelling capabilities are provided via this route, development of an ASCII input model for a reactor transient can require months of even a very experienced analysts time. As a result the classic TH systems codes are now operating as computational engines within a broader suite of software tools, which provide a graphical user interface (GUI) for model construction, execution of the simulation, and display of results. In the U.S. the Symbolic Nuclear Analysis Program (SNAP) provides the interfaces to TRACE or RELAP5 (along with other packages for analysis of the containment and neutron kinetics). In France CATHARE is supported by a similar interface. These GUIs are designed for intuitive assembly of complex systems, and radically reduce time for model creation and analysis of results. They also significantly reduce the opportunities for user errors in the creation of the initial model.

### 4.1.1    Underlying hypotheses and main outcomes

The hypotheses that lead to the equations solved in system codes allow the complete description of the whole primary circuit through a blending of one dimensional approach for the tubes; a zero

dimensional approach for some technological objects (lower and upper plenum; water box, pump, …), and coarse 3D description within homogenized approaches for some other parts (the core; the vessel). The fluid equations are solved in conjunction with wall conduction equations (including radiation effects), a transient simulation of the plant control system, and at times with a solution of the neutron kinetics equations.

A key hypothesis in these codes is that turbulent diffusion terms are not important as direct contributions to the flow equations. Euler rather than Navier-Stokes equations are used. Within the standard range of mesh sizes employed with TH system codes, numerical diffusion is substantially larger than actual turbulent diffusion, so this assumption is justified. Turbulence is taken into account in correlations for heat transfer and friction (wall and interfacial) coefficients.

Physical models associated with two-phase flow and heat transfer are limited by various assumptions. Quantities used for interfacial terms such as flow regimes, bubble diameter, or droplet diameter are normally based on local conditions and not on the flow history. Heat transfer coefficients are based on data for fully developed flow and normally do not account for entrance effects. One exception is the occasional inclusion of grid spacer effects in rod bundle heat transfer correlations.

The main outcomes are fluid and solid state variables representing averages over substantial volumes. This is especially true of 0-D models, but it is also important to remember that 1-D volumes no matter how short frequently represent an average over a wide cross-sectional flow area, and that even 3-D volumes are huge compared to those used in a CFD analysis (see Section 4.2). These codes do a credible job predicting quantities with relatively slow spatial variation, but should not be expected to capture local phenomena with safety consequences such as hot spots on a fuel rod.

### 4.1.2    Classical validation process

The physical modelling of two phase flow relies on numerous closure laws that have been tuned to obey known correlations or for complex situations to follow experimental results obtained from some "as close as possible to real world" experiments. The resulting simulation tool can therefore be considered as a spatial-temporal interpolator between these results, with the capability to be used for new reactor concepts. Flow maps and transition between different flow patterns are a key issue of the validation.

The validation process has always followed a standard tiered approach. To the extent possible individual physical models (e.g. film boiling heat transfer coefficient) are evaluated through comparison against Separate Effects Test (SET) data. The next level of complexity consists of component tests (e.g. reactor core, upper plenum). Finally the full system capabilities of the code are evaluated against integral systems tests, which may be scaled facilities such as ROSA [158], or full nuclear plants such as Ringhals. Typically, analyses of separate effects and integral systems dominate the validation process.

As with all other general purpose simulation codes, validation must be tied to specific applications. Limited resources generally require careful focus of the validation process, which can be provided by the PIRT process (see Section 3.2).

### 4.1.3    Circumstances of standard use (recommended use)

The use of a TH system code is recommended for two main safety issues:

- To provide the main information relative to some Nuclear Reactor Safety (NRS) related events that involve a system effect (in the sense that they result from an equilibrium that develops over the whole circuit or at least over circuit parts that can not be investigated with other approaches);

- To provide proper boundary conditions (inlet and outlet condition) to other approaches.

These codes are appropriate for a full range of two-phase flow regimes. They are limited in the range of geometries that can be well modelled by the lack of turbulent diffusion terms. They are not suitable for large open regions of a system containing circulating flows (e.g. containment), as the circulation patterns will be controlled by numerical rather than turbulent diffusion.

In addition to safety analysis, the relatively fast run times for most TH system codes, make them good candidates for use in real time training simulators. This speed compared to standard CFD codes is simply a result of the smaller number of finite volumes in spatial discretizations. Were the number of elements in a CFD spatial mesh are counted in the millions, the number of volumes in a real-time TH systems simulation are counted in the hundreds. The most complex TH systems simulations tend to still be on the order of ten thousand volumes. This advantage is only slightly offset by the fact that TH codes typically compute and store somewhat over an order of magnitude more state variables.

Over the 30 year course of evolution for most TH codes, the primary source of run time improvement has been the radical increase in compute CPU speed. As in any field of computer based simulation, problems that we would not have considered for real time simulation a few years ago are now feasible in that context. In the most recent years some of these codes have also taken advantage of parallel processing to improve wall clock execution times. A secondary source of speed improvement has been a steady improvement in robustness as various adverse peculiarities of numerical solutions have been fixed.

The best example of real time TH simulation is the SCAR project in France. This tool is a version of CATHARE adapted for coarse grain parallelism (typically eight processors). In the U.S. TRACE was designed to support distributed parallel calculations, and is currently used by Knolls Atomic Power Laboratory for real time simulation of Naval nuclear power plants.

### 4.1.4 *Main scales involved*

Scales vary with location in the system and transient being modelled. However, the typical size of mesh is on the order of a meter. In a core volume heights are seldom less than a third of a meter. In some sections of piping volume lengths may be many meters.

## 4.2 Component Code (Porous CFD)

Although 3-D modelling within system codes such as TRACE and CATHARE can be regarded as porous media models, in this section we discuss more special purpose codes utilizing a porous media approach such as COBRA-TF [121].

### 4.2.1 *Underlying hypotheses and main outcomes*

The equations are derived after averaging the solid and the fluid, i.e. resulting in a homogeneous or porous media. The solids are not simulated, but modelled through the closure laws such as wall friction coefficient. The heat conduction is solved in fuel elements in order to provide the heat flux to the fluid (source term in energy balance equation). The closure laws are devoted to rod bundles geometry, typical of LWR reactor cores or Steam Generators. The validation covers steady-state and transient conditions that are used for design, optimization and safety analysis. The boundary conditions are provided by the system scale (off- or on-line coupling). For core applications, coupling with neutronics is also necessary in order to provide an accurate power distribution.

### 4.2.2 *Classical validation process*

The validation process is based on experimental data obtained in rod bundles mock-up for a specific range of application (geometry, pressure, mass flow…). These data are used either to derive specific closure laws (e.g. Critical Heat Flux) or to optimize/tune existing models from the literature

### 4.2.3 *Circumstances of standard use (recommended use)*

The use of component code is recommended to provide a multi-dimensional response within the component, i.e., reactor core, steam generator or heat exchanger, both for steady-state and transient conditions

### 4.2.4 *Main scales involved*

For reactor cores, there are classically two levels of application: the so-called "sub-channel" level and the fuel assembly level. The sub-channel level is mostly used to assess the Critical Heat Flux (CHF) margin, using local parameters such as mass flow and quality. A one-way coupling (zoom) between fuel assembly level and sub-channel level is necessary to provide the boundary conditions.

## 4.3 CFD Code

Computational Fluid Dynamics (CFD) has developed over the last 25 years into a reliable tool for analyzing complex flow situations, and has become an invaluable aid to design practice in, for example, the automotive, aerospace and turbo-machinery industries. However, CFD is not as mature a technology as seen in commercial codes available for thermal and stress analysis in solid structures. The main difficulty is that industrial-type CFD is highly non-linear, and resolution of flow structures spanning a wide range of scales (e.g. boundary and free-shear layers, vertical structures, zones of recirculation, etc.) is required.

Though universities and government laboratories may continue to pursue in-house CFD development, this activity is strictly limited to departmental specialities, and the major steps forward in CFD technology from an industrial standpoint are now being undertaken by commercial vendors of CFD software. The major players in this league are CFX, FLUENT (both now owned by ANSYS) and STAR-CD. Worldwide, current estimates of regular users of commercial CFD codes is 25,000 to 30,000, and the number has been growing steadily by 15% to 20% annually for some years. This growth has enabled the major CFD vendors to sponsor, and more generally to become actively involved in, the development of innovative numerical modelling techniques, which they hope will convert into profit-based growth in the future. Examples are direct funding of master and doctoral programmes at universities and direct participation in EU-funded framework programmes.

The general picture emerging is that CFD is rapidly expanding, with a very large database of proven capability. The driving force for program development is generally not the nuclear community, as it was for the classical thermal-hydraulic system codes (see Section 4.1). Nonetheless, many of the application areas overlap those associated with NRS: flows in complex geometries, mixing in stratified fluids, flow separation and re-attachment, turbulence, multi-phase phenomena, chemical species interaction and combustion. Consequently, practitioners in NRS-related areas can indirectly benefit from the advancements in the technology taking place elsewhere. However, because of the complexity of modern commercial CFD packages, great care is needed in input preparation and equation solving to avoid errors. Some of these points are expanded in this document.

### 4.3.1    *Underlying hypotheses and main outcomes*

CFD is now a well established science, and is generally accepted as describing the broad topic encompassing the numerical solution, by computational methods, of the governing equations which describe fluid flow: i.e. the set of the Navier-Stokes equations, mass continuity, and additional conservation equations, such as for heat and species concentration. This is done on scales down to those of the largest turbulence eddies and boundary layer widths, in marked contrast to those of the system codes described above.

It is an intrinsic assumption in CFD that the details of the geometry are important to the flow, and must be represented accurately. Most CFD codes therefore employ body-fitted meshes, in which the faces of the mesh cells coincide with the physical boundaries of the problem (walls, inlets, outlets). For complex geometric situations, this means that very careful and time-consuming mesh generation, with mesh refinement in regions of strong gradients, is an important precursor to any complex CFD simulation. The application of CFD to complex flow problems requires considerable experience, and critical interpretation of the results must be undertaken from a position of fundamental knowledge of fluid dynamics and heat transfer.

Nonetheless, the codes are only as good as the physical models programmed into them: in particular, for single-phase applications, the turbulence model must be scrutinized carefully to determine whether it is appropriate to the situation being modelled. In addition, because of the complexity of modern commercial CFD packages, great care is needed in input preparation and equation solving to avoid errors.

A typical Reynolds number encountered in NRS applications will be of the order $10^5$ to $10^6$. Consequently, turbulent flow conditions are to be expected. Industrial CFD simulations generally incorporate Reynolds-Averaged Navier Stokes or RANS turbulence models (usually the High Reynolds Number k-ε model), which return only mean values for the velocities and temperatures. However, turbulence is not only a small-scale phenomenon. For the Reynolds number quoted above, the ratio of the largest to smallest turbulent eddies is $10^7$ to $10^8$. The RANS models average over all of these length scales to produce their estimates of the mean quantities. Most of the information relating to the scale of variation (turbulent flows are highly irregular and unsteady) is lost in this process, though the mean turbulent kinetic energy, $k$, does provide a measure of the average size of the velocity fluctuations. In addition, it has been recognized that some NRS applications (e.g. flow in Tee-junctions) require the use of more sophisticated turbulence modelling approaches, such as Large Eddy Simulation (LES), in which the largest of the turbulence scales are computed explicitly, while smaller scales are modelled, or even Direct Numerical Simulation or DNS, in which all turbulence scales, down to Kolmogorov scales are computed, with no modelling assumptions. Such calculations are, of necessity, three-dimensional and time-dependent. Hence they are very computationally expensive.

The k-ε model, though now over 30 years old, is still regarded as the industrial standard turbulence model, simply because it is robust and cheap. This is not to say that industry is satisfied with the results given by the model, only that huge amounts of extra effort are required to moderately improve predictions, and therefore in the industrial context are not justified. Basically, the model is one of momentum transfer (except for a few special flow types, such as impinging jet heat transfer), and extra problems with transfer are not due to basic deficiencies in the model, but result from treating turbulent heat transfer in accordance with the Reynolds analogy, which relates the turbulent heat flux to the mean temperature gradient via a turbulent Prandtl number. The choice to use Reynolds analogy is a balance between accuracy and the need for computational speed.  At some point in the future computer speeds and storage will be high enough that more detailed treatment of turbulent heat transfer will be more prevalent. Nonetheless, the model also has rather well-known deficiencies regarding certain flow types (swirling flows, spreading of jets). This means that, for most CFD applications to NRS, there is a definite need to

benchmark the various simulations being undertaken, and validate the code predictions against experimental data, where available.

CFD is not a quick-and-easy science, and should not be employed in NRS problems unless the precision of the data to be extracted justifies the computational effort needed to obtain it. Don't use a pair of scissors to cut the grass on a football field. On the other hand, don't cut your hair with a lawn mower. Take the instrument most appropriate to the job at hand that can deliver the level of accuracy required at the minimum effort. The principal outcome from a CFD calculation is meso-scale fluid dynamic and heat transfer data.

### 4.3.2    *Classical validation process*

Today, CFD is a very exact technology. However, like any precision instrument, a state-of-the-art, general-purpose, commercial CFD package is a very complex entity, and demands respect in its application. The widespread use of such codes in industry, and the increasing reliance which is now placed on the predictions from the codes, has prompted several recent initiatives to produce a documented 'Code of Conduct' or 'Best Practice Guidelines'. The objective of the present document is to provide such guidelines for application to NRS. Nonetheless, quality assurance in regard to CFD is best achieved by means of benchmarking and validation.

Validation examines whether the physical models used in computer simulations agree with real world observations. It is a process that addresses the question 'Have we solved the right equations?'. Validation is one of the two fundamental tiers upon which the credibility of numerical simulations is built: the other is verification. The basic validation strategy is to identify and quantify both error and uncertainty through comparison of simulation results with experimental data.  See Chapter 9 for a more detailed discussion of validation.

Validation bases for CFD (many of them with on-line access) exist for a variety of specialist application areas. The document produced by the OECD/NEA Writing Group on the "Assessment of CFD Codes for Nuclear Reactor Safety Problems", NEA/SEN/SIN/AMA (2005) 3, lists the existing databases, and makes proposals for extending the concept to NRS issues.

The remarkable growth in the power of high performance computing from PC cluster systems to massively parallel supercomputers has had a dramatic impact on engineering research by enabling large-scale simulations of previously intractable phenomena. In particular, the growth of PC clusters has been mirrored by the global number of emerging companies investing in hardware, software, support and training. As a result, numerous companies are now turning towards clusters to expand their computational resources.

### 4.3.3    *Circumstances of standard use (recommended use)*

The use of CFD codes is recommended if there are important 3-D aspects of the system's thermalhydraulics that need to be resolved at smaller scales than can be handled by standard system and containment codes. Typical instances in NRS problems include: flow-induced vibration of structures; erosion of surfaces; boron dilution; mixing and stratification; heterogeneous flow situations; pressurized thermal shock; hydrogen distribution, chemical reactions and detonation in containments; and many other situations.

The choice of code is often made on the basis of familiarity, convenience, tradition or cost, or a combination. At least for the large commercial codes, it is only seldom that the final choice is influenced by code capabilities, since all contain similar models. Exceptions may be if a fluid/structure interaction problems needs to be solved and the CFD vendor has an agreement) and more important a user-friendly

interface) with one of the important stress-analysis programs, or that the situation demands the use of an advanced turbulence modelling capability, such as LES. Most commercial CFD codes these days have interfaces to standard mesh-generation and post-processing software. However, the most critical consideration is correct use of the selected CFD code, and the present document aims to provide information on how to do this.

### 4.3.4   *Main scales involved*

In principle, CFD can be used to obtain fluid-dynamic and thermal data at all meso-scales. Thus, the flow around individual fuel rod spacer grids can be computed as can the main flows in the hot and cold legs, the downcomer and upper and lower plenums of a PWR. In practice, such an undertaking would be grossly over-ambitious, for the foreseeable future. Even with geometry data supplied by a CAD/CAM/CAE package, mesh generation, utilizing unstructured grids and automatic mesh generation options, would be a major undertaking. The number of meshes needed would be staggering, and CPU times for running transient safety cases unattainable.

Thus, from a purely practical viewpoint, the CFD problem has to be isolated (see the discussion in Section 3.1). For the example given here, the gross flow and heat distribution phenomena in the RPV and attached piping could be handled, but the core and perhaps the core-support structure would need to be modelled using a porous-medium approach in order to obtain a tractable CFD problem. Likewise, a detailed description of the flow in a small number of sub-channels could be attempted, with appropriate inlet and outlet boundary conditions supplied by external means.

In summary, the main scales for NRS simulations using CFD codes could be from millimetres to centimetres, and perhaps tens of centimetres, depending on the specific application. In many circumstances, a combination of each of these scales is included in different places in the fluid domain.

### 4.4   **Potential Complementary Approaches**

Reactor safety analysis is normally carried out using one-dimensional, area-averaged two-phase flow equations.   Three-dimensional analysis has been available in some safety codes such as CATHARE[159]; TRAC[160], FLICA [161]  for many years.  However, these 3-D tools have had a number of restrictions related to nodalization, field equations (usually Euler), and other aspects of physical modeling. The existing safety codes generally give good estimates of the system performance for a wide class of flow conditions.  However, in some situations a detailed understanding of the flow may be required in a limited region of the system.  In this case a 3-D Reynolds Averaged Navier-Stokes (RANS) code may be applied for the detailed analysis and the safety code used to provide boundary conditions reflecting feedback from the balance of the system. This addresses basically three description scales: (i) the system scale; (ii) the macro scale corresponding to the description of the core in terms of an "equivalent porous medium", and (iii) to the CFD scale. This basically addresses three possible and interesting coupling strategies: System/CFD; System/macro scale and macro scale/CFD.

### 44.1   *State of the art of some CFD-1D coupling*

Some basic coupling issues have already been addressed through the linkage of 1-D and 3-D flow solutions in some TH systems codes.  However, many new questions must be addressed and old ones revisited when linkage is to the more complex mesh geometry associated with CFD. Some of them are given below.

- What should be the temporal nature of the coupling (implicit or explicit) ?

- What should be the spatial nature of the coupling: system code and CFD domains should be separated (interfacial coupling) or partially or totally overlapping?

- What should be the features for interpolation of variables (if required), with a system code being based on staggered grid whereas CFD codes may be based on finite element or co-located finite volume grid?

- What are the quantities that should be conserved at the discrete levels when coming from one code to the another?

- How to treat the restriction (in the 3D =>1D sense) and the prolongation, reconstruction (in the 1D =>3D) of the variables profiles?

- How to treat coupling of codes using different variables and different numbers of field equations?

- What are the consequences of possible occurrence of inconsistency in the equations of state and other closure models?

Many other problems will certainly appear and will be treated in the near future. A state of the art can be found out looking at some of the related studies and papers: see ref [162], [163], [164], [165], and [166]. Explicit coupling has been tried and seems to be sufficient at least for simple cases (see ref [165] and [166]); explicit and semi-implicit coupling have been tried for more complex and applied ones (see [164]). Up to now single phase cases have been reported.

### 4.4.2    *Recommendations for NRS :*

At this state very few guidelines can be provided for such coupling. The main recommendations that may be given come from "common sense":

- Try to perform the coupling in region where the physics is simple; try to change the space location of the coupling to investigate its effects;

- Follow the respective guidelines coming along with both the system and CFD codes;

- First of all, try simple test cases such as the ones proposed in previous references to be sure that the coupling is validated or at least mastered;

- Participate in the R&D in this area.

# 5. USER SELECTION OF PHYSICAL MODELS

Nuclear reactor applications generally involve very complex and full-scale geometries. CFD simulations are often a compromise between the execution times, and solution fidelity obtained from optimal physical models and adequate discretization of the spatial domain. In striking a balance it is also important to follow verification procedures outlined in Chapter 8, to insure that the influence of models described in this chapter is not degraded by discretization errors.

After identifying whether or not a problem is phenomenological scale independent, (i.e., do Reynolds or Grashoff numbers appear as key parameters?) the user should follow the provided methodology in order to select the most appropriate turbulence modelling and wall associated functions.

Most of reactor thermal-hydraulic phenomena include local effects and global effects such as thermal stratification (buoyancy effects), impinging jets, level swelling, counter-current flows, thermal conductivity, etc., which are taken into account by user selection of models for such things as the Boussinesq approximation, heat transfer, free surfaces, and fluid structure interaction.

## 5.1 Guidelines for turbulence modelling in NRS applications

This section begins with a summary of its goals and limitations, briefly surveys related documents, and provides an overview of the current modelling approaches (e.g. RANS, LES, DES).

### 5.1.1 Limitations and aims of the present section

Most NRS flows are time turbulent (at least unsteady and/or transitional); which means that their main features are fluctuating in time and that their main effects and "properties" are far from the laminar steady case. This has crucial influence on at least three particular items (i) the flow topology (ii) the momentum and heat exchange capabilities between the flow and the surroundings and (iii) the ability of scientific community to model these flows (i.e. to derive reliable ways to quantitatively predict their effects in any situations). This has been the starting point for many attempts to provide theoretical, mathematical and practical modelling of turbulence phenomena. However, due to the long history and continuing efforts to propose such models, the collection of available models is very large and producing complete and exhaustive guidelines for all of them is far beyond the scope of this section.

This section provides a brief classification of turbulence models and survey of their limitations. However, the focus is on providing a non-expert reader with a methodology for selecting the most appropriate turbulence model for an application. In consequence, this section is organized as follows. First a brief bibliography of existing related documents is provided. Next some insights are provided into turbulence modelling and some modelling procedures, to help the user understand the modelling frameworks and therefore the information they need to provide. The following section deals with turbulence model classification and limitations associated with each class. Attention is then paid to the difficult question of the wall treatment before we provide an attempt of a methodology to select the best available model. We close the discussion of each type of turbulence model with specific recommendations related to its use.

### 5.1.2    *Related existing documents*

Related existing documents may be divided into two types:

1.    Documents that follow the same objective as the present section, to provide "guidelines" for use of turbulence models in numerical simulation. The main interesting document is the "best practice guidelines" of the Special Interest Group on "Quality and Trust in Industrial CFD" produced by Ercoftac [2]. Additional similar documents have been provided by the ECORA project [1] and MARNET-CFD [4].

2.    Documents that may provide direct validation of a given modelling (or most of the time of a family of models) against a specific configuration and/or topic. These documents should be considered at least two levels.

- Documents that deal with the validation of a model against a specific flow configuration that may be understood as an isolated effect (separate effects tests). Typical documents are the Ercoftac data base [167], and specific tests of modelling such as found in references [168], [169].

- Documents that deal with a complete realisation that validate a modelling against combined effects and for which the validation goes beyond the simple model validation (integral effects tests). The best methodology in this case may be to look for a relevant experiment and to identify the modelling that has led to success. See the CSNI writing group report on assessment of CFD codes [19] for a review of existing data and pay a particular attention to the papers related to specific nuclear applications [170].

### 5.1.3    *Some insights into the turbulence phenomena, some modelling procedures*

One basic definition of the phenomena is [186] that turbulence may occur as soon as a region of the flow is dominated by inertia (i.e. as soon as the Reynolds number is high enough), which is nearly always the case in the flow related to NRS issues (see Section 11.3 for a notable exception). From a phenomenological point of view, turbulence is felt through the temporal and spatial unsteadiness of the flow features (velocity, thermodynamic state variables), leading to increased flow mixing. These features are general ones and weakly depend on the driving force: imposed flow rate; gravity; pressure drops; flow separations… Even if it is rather difficult, a distinction should be made (at least for a modelling purpose) between "unsteady" and "fully turbulent" flows. The latter concerns the flows for which development has been "sufficient" so that turbulence can be considered as mature. The difference may appear as a "philosophical consideration" but bear in mind that a model validated for a given flow configuration in a given state (consider a canonical attached turbulent boundary layer) will generally encounter real difficulties predicting the way the flow has reached this state (i.e. the transition steps). Additional features to consider for turbulent flow are that:

- A description of the very large extent of spatial and temporal scales[1] involved in turbulence is the well-known Kolmogorov cascade (see [186]);

- The mean flow inhomogeneities do have an effect on these scales.

---

[1] The large scales size "L" (the integral scale as far as the turbulence spectrum is concerned) is most of the time directly given by some specific size of the considered physical domain (a fraction of the pipe diameter for a pipe flow; of the diameter injector in case of injection…) whereas the size of the smallest scales ("$\eta$" for the Kolmogorov scales) are related to the flow Reynolds number : the higher the Reynolds number; the larger the range of scales, the ratio of large to small scales being $L / \eta = O(Re^{3/4})$, see [184] for additional information)

*Mathematical modelling*

From a mathematical point of view turbulence results from the nonlinearity of the Navier-Stokes (NS) equations, whose expressions are known but cannot lead to a Direct Numerical Resolution in all configurations (in terms of numerical equation integration) for CPU cost reasons. The numerical resolution thus leads to a modelling process for which key issues are:

1. to choose a modelling context from deterministic (DNS), statistical (RANS), or hybridisation between both (LES, DES);

2. to derive an adapted model (through theoretical and/or empirical considerations); and

3. to test it in dedicated situations.

*Turbulent flow classifications*

There are many ways to classify turbulent flows for turbulence modelling validation issues. One choice may be to consider the issue both for single and global effects. Indeed, the rather complex configurations arising in industrial situations [2] have led people to consider "canonical" situations that may be identified in industrial flows.

1. The first level of complexity consists of flows dominated by a single and identified phenomenon and a single and identified regime for a given identified geometry. Usual isolated effects lead to consideration of: simple shear flows (attached shear flows (boundary layer, wall jet); free shear flows (mixing layers; wake; plume, plane or round jets); impinging flows. The related regimes may be stably (unstably) stratified flows, flows dominated by buoyancy leading to mixed or natural convection, or forced convection. Geometries are rather simple ones and may refer to "canonical configurations" including plane wall; round tube; plane or round jets; the related flows are driven by a nearly two dimensional strain.

2. The second level of complexity includes configurations with secondary flows, and configurations with a strong coupling between turbulence and another key physical phenomenon such as rotation or chemical processes (e.g. combustion). This also includes flows with strong turbulence state variation (transition between laminar and turbulence state or occurrence of unsteadiness that cannot be considered as fully developed turbulence).

3. The two previous items mainly refer to steady flows. More complex flows involve strongly unsteady flows for which the time scale of variations is of the order of turbulence time. Unsteadiness may originate from unsteady boundary conditions; from flow separations, from coupling between turbulence and other phenomenon (e.g. acoustics or material vibrations). These circumstances are seldom compatible with the hypotheses of turbulence modelling and the predictive capacity of this latter will be very difficult to access.

The mathematical tools applied to the derivation of practical models has led to two different approaches: Deterministic and Statistical modelling. The first corresponds to motion equation integration, eventually including closure equations that model turbulence effects in a deterministic way.

The most deterministic model is Direct Numerical Simulation (DNS). This achieves the direct resolution of all temporal and spatial scales of a flow through the detailed solution of the Navier-Stokes equations. This has been performed for many simple low Reynolds flows (single or two phase, sometimes reactive flows) leading to the knowledge that the complete unsteady Navier-Stokes equations are able to describe all the turbulence phenomena. Unfortunately, turbulence theory tells us that the smallest persistent

eddy diameter is roughly proportional to the Reynolds number to the minus three-quarters power ($1/Re^{3/4}$). This means that the number of mesh points in 3-D DNS scales like $Re^{9/4}$, and only a very limited range of problems can be solved with DNS on current computers. The range of problems amenable to this approach will expand gradually with the increase in computer speeds and memory. However, within foreseeable future application of DNS to NRS will be restricted to improving understanding of local phenomena.

Large Eddy Simulation (LES) also involves deterministic modelling. The LES framework refers to the numerical resolution of the space and time low pass filtered Navier-Stokes equations, leading the resultant turbulent motion to be composed of scales extending from the largest down to the ones of the filter size. The description of the motion on the resolved spectral band (containing the most energetic scales) is as with DNS a direct result of the solution of the Navier-Stokes equations. The effects of the filtered scales on the resolved ones are modelled through different procedures (phenomenological; formal, structural, statistical, etc.). Two main motivations governing this type of modelling are worth mentioning: (i) the effects that have to be modelled take place at very small scales and exhibit a rather universal behaviour and (ii) the explicit description of the most energetic scales is sufficient to capture the main features of the flow. The resulting modelling is therefore potentially very powerful provided that the filter (which size is generally linked to the mesh size) can take place at sufficiently small scales. Unfortunately for very high Reynolds flows the mesh associated with a physically reasonable filter can have far too many cells to be computationally feasible. This limitation can be mitigated by selective use of LES within hybrid methods, as discussed later in this chapter.

Statistical modelling corresponds to the use of the famous Reynolds Averaged Navier-Stokes (RANS) equations, resulting from the application of a statistical filter to the Navier-Stokes equations. All turbulence effects are then modelled in a statistical way, leading to consideration of the filtered solution as a statistical result. This derivation concerns both the steady (RANS) and unsteady (U-RANS or T-RANS) modelling. The corresponding modelling has historically been the first developed because of limits on computer resources. Special models must be provided (e.g. k-ε, k-ω) to describe the effects of turbulence over all the physical scales. This approach permits a larger minimum mesh size than required for DNS or LES, and explains the lower simulation costs. Unfortunately this modelling approach has suffered from recurrent difficulties as physicists have tried to discover models covering a large range of applications.

Fig. 5.1 illustrates the underlying modelling framework as far as the turbulence spectrum is concerned. It shows turbulence frequencies resolved by the solution of the Navier-Stokes equations on the left, and those covered by special models on the right.

A

E(k)

k

E(k)                        B

k

E(k)

k

E(k)

k

E(k)

C

k

E(k)

k

E(k)                        D

k

E(k)

k

kC

kc
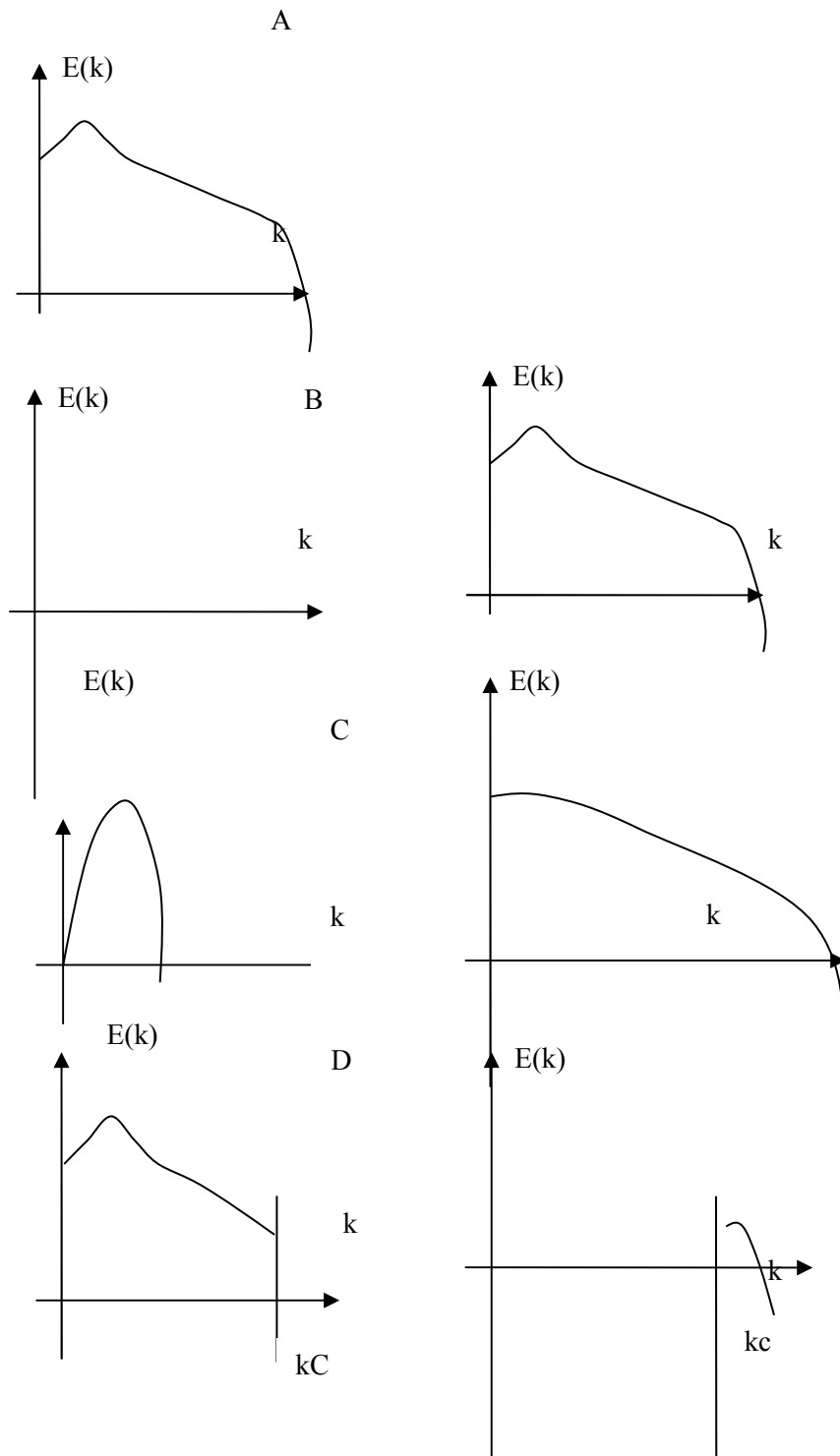
Fig. 5.1 Part of the turbulent spectrum that is explicitly simulated (Left) and modelled (Right) for DNS (A); steady RANS (B); U-RANS (C) and LES (D); from [172].

### *5.1.4 Turbulence model classification and known limitations*

Turbulence models are classified first by whether they are purely statistical over the full range of turbulence scales (e.g. RANS), or use the Navier-Stokes equations to deterministically model turbulence over at least a portion of the eddy spectrum (e.g. LES)

*RANS and U- or (T-) RANS) turbulence models*

RANS methods are the most widely used approach for CFD simulations of industrial flows and as such have received the most modelling support from vendors of commercial CFD codes.

The simplest modelling is linear, expressing a direct proportionality between the unknown Reynolds stress tensors (e.g. $\overline{u'\varphi'}$ with $\varphi$ standing for $u, T, Y_k$) and the resolved shear $\nabla\overline{\varphi}$. Additional models must be provided for the associated eddy coefficients $\alpha_t$ (turbulent viscosity for momentum and diffusivity for temperature and species). This is the Boussinesq hypothesis that is connected with the Eddy Viscosity Models (EVM). The eddy viscosity hypothesis assumes that the Reynolds stresses can be related to the mean velocity gradients in a manner analogous to the relationship between the stress and strain tensors in laminar Newtonian flow. The eddy coefficient is proportional to the product $uL$ of a turbulent length $L$ and a turbulent velocity $u$, or to the product $kT$ of a turbulent energy $k$ and a turbulent time scale $T$.

Early methods made use of algebraic formulations (also called zero-equation model see [172] and [173] ). These models were all directly designed for a given type of flow. Most of them are based on the description of a canonical configuration such as boundary layer, mixing layer, etc., and are therefore not suited to a large range of applications. According to our classification, the range of application is limited to a few cases of flow of first level complexity. The use of algebraic models is not recommended for general flow simulations, due to their limitations in generality and their geometric restrictions.

Algebraic models have been largely replaced by more general transport equation models for both implementation and accuracy considerations. These transport models are the lowest level of turbulence models, which offer sufficient generality and flexibility for general use. The simplest of them rely on a one equation turbulence model, transporting turbulent kinetic energy (k). Although the range of flows that can be treated is wider than that for algebraic models, it is not considered sufficient for general purpose application. The Spalart-Almaras model [174] is one of the most famous of these models.

The most popular modelling approach now uses two transport equations to model the behaviour of turbulence. They are based on the description of the dominant length and time scale by two independent variables. The most famous model of this family is the k-ε model. Here in addition to an equation transporting the turbulence kinetic energy (k), a second equation transports the rate at which turbulence kinetic energy is dissipated (ε). The second most common two equation model is k-ω, where ω is a specific dissipation rate of turbulence kinetic energy, obtained from solution of the second transport equation. In both cases results of the transport equations are used in a simple algebraic expression to obtain a turbulent viscosity, and often Reynolds analogy is then applied to obtain thermal diffusivities. A hybrid of these approaches has been developed by Menter [176] that takes advantage of the superior k-ω performance near walls, and transitions to a k-ε model away from walls.

When using RANS or its transient implementations it is important to understand limitations of the available turbulence models. Because there are so many variations on the two equation approach (k-l, k-ε, k-ω, SST, k-ε-V2, non linear k-ε, …), the user should read and understand the documentation of these

models provided for the specific code being used. When questions arise on optimal choice for a given flow configuration, validation tests should be run and compared for several candidate models.

Since k-ε is a common first choice, it is useful to list some of its short-comings and behaviour relative to other turbulence models. First, this model and its close relatives can not be expected to perform well in cases where there are strong anisotropies in the turbulence. Reynolds stress models or an LES (or hybrid RANS/LES) approach should be explored in this situation. Look for degraded results from k-ε within:

- impinging jets;

- reattachment regions;

- flow separation in a strong adverse pressure gradient;

- regions with strongly swirling flows or other sources of high curvature in the streamlines;

- buoyancy driven flows such as a thermal plume;

- secondary flows;

- laminar or transitional flows;

- round jets.

The k-ε model behaves well for most configurations at the first level of complexity. In addition the family of the first order turbulence closure involving transport equations is very wide and real improvements have been achieved beyond standard k-ε models such as k-ε-v2 or SST, in particular for some cases of separation and buoyancy dominated flows. These advanced models behave well for most configurations at the first level of complexity and for some at the second level complexity.

Models that are more complex have been developed and offer more general platforms for the inclusion of physical effects. They are based on transport equations for the unknowns. The most complex RANS model used in industrial CFD applications are Second Moment Closure (SMC) models. Instead of two equations for the two main turbulent scales, this approach requires the solution of seven transport equations for the independent Reynolds stresses and one length (or related) scale. These models are based on transport equations for all components of the Reynolds stress tensor and the dissipation rate. These models do not use the eddy viscosity hypothesis, but solve an equation for the transport of Reynolds stresses in the fluid. The Reynolds stress model transport equations are solved for the individual stress components. Algebraic Reynolds stress models solve algebraic equations for the Reynolds stresses, whereas differential Reynolds stress models solve differential transport equations individually for each Reynolds stress component. The exact production term and the inherent modelling of stress anisotropies theoretically make Reynolds Stress models more suited to complex flows, including non-equilibrium flows. The range of application of these models covers the first, second and some configurations of third level complexity. However with this modelling power comes a real difficulty of use, including the boundary condition requirements and possible less robust numerical features when turning from EVM to SMC.

RANS and U-RANS respond reasonably well to the mesh convergence studies described in Section 8.5 as part of verification activities necessary before attempting to validate an application. This is particularly true for representation of large scale flow features.

Recommendations for RANS and U-RANS

So-called buoyancy driven boron dilution transients (BDT) and pressurized thermal shock (PTS) scenarios have been analysed using transient statistical modelling (U-RANS or T-RANS) in the ECORA and FLOMIX-R projects. As a result of numerical simulations of turbulent mixing inside pressurized water reactors (PWRs) it was found, that two-equation turbulence models like k-ε or SST were suitable for momentum-driven mixing. Reynolds stress models provided better results for buoyancy driven mixing. The ECORA and FLOMIX-R projects have demonstrated that T-RANS CFD modelling has indeed some shortcomings in situations when the time scale of the main flow is of the same order of magnitude as the time scale of the large turbulent eddies in the downcomer of the RPV [16] and [18]. Obviously, more advanced scale-resolving CFD methods based on LES, DES, or SAS are required for such cases.

*Large Eddy Simulation (LES)*

This modelling approach is usually based on a Boussinesq hypothesis ( the subgrid tensor $\langle u'\varphi'\rangle - \langle u'\rangle\langle \varphi'\rangle$ is considered as proportional to the resolved gradient $\nabla\langle \varphi\rangle$ , $\langle \varphi\rangle$ standing for the low pass filtered part of the whole field $\varphi$ ). The previous limitations arising from this statement in the context of RANS are restricted to the unresolved small scales for LES, which have led people to consider this approach as very promising. The first historical model was proposed by Smagorinsky for meteorological purposes (see [175]). The last thirteen years have led to a very large collection of new models that can be classified into several families (see [177] and [178] for a complete review).

- Algebraic models providing an eddy diffusivity based on a given operator coming along with a fixed constant (Smagorinsky model [175] or the Structure Function model family [186], WALE [179] ) or with a constant evaluated through a local evolution of the flow state (Dynamic modelling [180]). These models are globally dissipative.

- Models based on formal analytical evaluation of the subgrid scale tensor from the resolved scales: this includes the scale similarity model from Bardina (see [182181]) and all the modelling based on deconvolution procedures (see the ADM method [181]).

- Models based on the subgrid scale energy transport equation. Also mainly diffusive, these models may be attractive because they allow the introduction of more physics and are easy to introduce in codes already having RANS models.

- Models based on the numerical dissipation inherent in the discrete approximations of differential operators. These approaches are referred to as Monotonic Integrated for LES (MILES) and are very tempting when an appropriate dissipative numerical scheme is available in a solver ( see [178] and [197]).  In effect a numerical viscosity (or diffusion coefficient) replaces the use a specific subgrid model at filtered length scales.

Combinations of previous modelling

Recent modelling and, in particular, dynamics modelling have been shown to behave well over a very large range of canonical configurations listed above as troublesome for RANS, including rotation, curvature, separation, and transitional flows. Due to its formulation; LES is the only model able simulate high frequency events or events where the time scale of the main flow is of the same order of magnitude as the time scale of the large turbulent structures.

Recent LES developments have started to extend the application domain of LES to real gas and reacting flows (see [183] and [185] for a review), to fluid/particles flows [184] for example) and to two

phase flows. These models potentially cover all the flow configuration complexity levels previously defined. However, these successes are moderated by the fact that they have usually required rather fine meshes and are very expensive simulations when compared to their U-RANS counterparts.

One common problem observed with LES is lack of intrinsic convergence in mesh refinement studies (also true for DES). This can be caused by intrinsic inconsistencies between turbulence resolved by the detailed Navier-Stokes solution, and small scale turbulence covered by a subgrid model. When solutions on successive meshes are viewed too closely, the lack of convergence can also be associated with the fundamentally chaotic Navier-Stokes solution. Studying convergence of instantaneous values for local state variables will normally not be profitable in these situations. The key to convergence studies for LES (and DNS) is selection of target variables that represent averaged flow behaviour important to the goals of the analysis (e.g. mean flow velocities, turbulence spectrum).

When performing convergence studies with LES it is also important not to put too much weight on experience from such studies using RANS or U-RANS. The mesh structure required for a given level of discretization error will be different, and the degradation of results as mesh is coarsened can be more pronounced with LES.

Recommendations for LES

LES is currently available in some commercial solvers as well as in many special codes developed at universities and government laboratories. It should be used in conjunction with non-diffusive high order schemes (centred or stabilized centred schemes) for space discretization of convection and with high order time integration methods. This recommendation does not hold in case of the MILES approach but this latter type of modelling has to be considered with care because numerical diffusion can vary significantly more from the physical diffusion terms than is reasonable.

For most applications the space filter applied in generating the LES equations is directly connected with the local mesh size and is clearly a key-point of the modelling procedure. As a general rule of thumb either the code logic or the user should ensure that 4 to 5 mesh cells are available to span (in each direction) the smallest eddy resolved by the Navier-Stokes solution. In addition the mesh should be able to describe not only the main flow gradient as for a RANS simulation but also the turbulent mechanisms, including low and high speed streaks in case of wall resolved turbulent flows (y+=1), and the main modes of instability in case of mixing layer or jet. As a consequence the mesh has to be 3D in all situations.

Because LES is based on the explicit description of the main energy containing scales, numerical solution of transient behaviour also needs caution. The time filter introduced by the selection of time step size should not mask the space filter for turbulence modelling. An eddy moving more than one mesh cell in one time step will not be adequately resolved. Protection from this problem is guaranteed for solutions using explicit time integration, were the restriction of CFL number less than one based on local velocities is tighter than a restriction on eddy motion based on mean flow velocity. If an implicit method is employed in the transient solution, the user needs to be certain that maximum time steps continue to resolve eddy motion (see [205]). The time step size also needs to be substantially less than the smallest eddy decay time, but this is normally less restrictive than a CFL test.

When large CPU resources are available LES can be used with success for moderate Reynolds numbers flows (such as the ones involving natural convection) in very complex geometries (see for example [189], [190]) and for rather high Reynolds number flows for simulation of for local effects. High Reynolds number flow within a complex and large geometry requires an unaffordable CPU effort today. LES is the only practical tool available for situations where high unsteadiness is to be described. In research from the THERFAT FP5 EU project, it was concluded that LES is required instead of T-RANS for the prediction of the high cycle thermal loading in T-junctions [192]. Despite the previous references;

there is relatively little experience within the nuclear community and other related industries in the application of these relatively new and more detailed scale-resolving CFD methods for NRS applications.

*Wall resolved or wall approximated turbulence modelling*

The near wall region is usually governed by the velocity shear and heat transfer, and is very important for most NRS applications. This region is very complex regarding the physics of turbulence because it contains the main turbulence production and dissipation areas. This modifies the turbulence structure beyond the assumptions of standard turbulence models. Describing carefully what happens in this region is theoretically possible for all the previously described turbulence models, but it requires their extension and, for numerical simulation, this usually requires a very fine mesh near the wall, which is not always possible. This difficulty is treated through the use of wall functions avoiding the expense of the wall resolution. RANS models were first developed with approximate wall boundary conditions. This has opened a large area of additional models for the law of the walls. The spirit of this modelling was to replace the complex flow simulation near the wall by empirical closure laws. These are generally based on the assumption that the flow in this region is close to an incompressible, turbulent, attached, and fully developed boundary layer at zero pressure gradient, which can be basically considered as an extension of the RANS concept. One looks for an algebraic relation between parietal transfer of momentum $\tau_w$ or energy $\phi_w$ and the resolved unknowns where they are available "far" from the wall $U, T(y_{1stpo\,int}, \upsilon_{1stpo\,int,})$, leading to the well known "log law". Many models have been used in practice (logarithmic laws, Werner and Wengle modelling; Schuman laws…), having more or less the same physical bases. Additional closures concern the turbulence modelling itself. An overview of wall laws guidelines for RANS is provided in ref [2]). The range of validity of this modelling depends on the behaviour of the flow within the boundary layer. Strong compressible flows, or flows strongly heated may be not accurately described. Impinging and separating regions are also poorly described through these wall functions. The validation of LES use with standard wall functions is less complete than for the RANS counterparts: some drawbacks have been identified concerning very High Reynolds number flows (see [195]). This also leads to constraints in the meshing itself. For RANS, U-RANS and LES, the limitations of standard wall functions have led to consideration fully wall resolved solutions. This has been possible for RANS, but currently requires too much computer time and memory for LES simulations of high Reynolds flows. Wall functions are therefore the only way to consider practical LES applications for industrial use now.

See Section 6.2 for a discussion of nodalization requirements when wall functions are in use.

*General information on hybrid methods*

LES modelling has been used with wall laws coming from the RANS modelling but adapted in an unsteady way [194]. This can be considered as the first RANS/LES coupling method and has opened the field of hybrid modelling (between statistical and deterministic approaches). Unsteady flows requiring a time evolving solution in situations where standard U-RANS solution fails have therefore been treated in many ways following more or less the same spirit. The main underlying ideas in the hybrid approaches being :

- to promote the use of an attached U-RANS solution in the near wall region;

- to switch from this U-RANS framework in the near wall region towards a LES concept in the core of the flow.

The expected gain of this methodology is the gain in capability of describing all the unsteadiness in the core of the flow without paying for a complete LES resolution in the near wall region; which is too expensive.

As said, previous LES with standard wall functions can be considered as the first realisation of this family of models. More recent works have proposed two different natural trends:

- To start with low Reynolds U-RANS models and to derive a more or less natural way to make the model close to an LES formulation in the core of the flow (the DES framework [196]); and

- To consider an extension of standard LES plus wall function methods, for example by switching from standard wall laws to U-RANS modelling in the near wall regions (see [173]).

Detached Eddy Simulations (DES) have recently been applied to the flow and thermal mixing in a T-junction [198], based on an experimental investigation [199]. The DES-calculations were compared with results from time-dependent RANS calculations using the RNG k-ε model, and both simulation techniques were used on two different grids. The RANS turbulence models showed discrepancies as compared to experiments, and the disparities could not be reduced by grid refinement or by using unsteady inlet boundary conditions.

The DES-results showed more realistic fluctuations with strong temperature and velocity gradients, caused by vortex shedding behind the incoming branch flow and the instabilities due to the separation zone. The predicted mixing was clearly influenced by the secondary flows caused by upstream bends in the piping system. Although there were quantitative differences between experiments and DES-computations, the results clearly showed the importance of using a scale-resolving simulation technique such as DES or LES for this type of flow situation.

One particular hybrid implementation is Scale-Adaptive Simulation (SAS), a recently developed methodology, which allows an improved prediction of unsteady flows [200, 201, 202]. It involves the introduction of the von Karman similarity length scale, LvK, into the turbulence model. LvK allows the model to adjust to resolved scales in a simulation. Essentially, SAS is an improved U-RANS approach, which avoids the occurrence of unphysical single-mode unsteady flow features, as observed in classical U-RANS methods. As a result, unsteady regions display a breakdown of the large turbulent structures to smaller and smaller scales as typical for turbulent flows. The method by itself distinguishes between stable and unstable regions of the flow. In stable regions, the model operates in classical RANS mode, whereas in unstable regions, the model displays a LES-like behaviour. As the SAS model formulation dos not involve the grid spacing, it avoids the undefined model regimes of DES. In case of overly coarse grids or too large time steps, the model reverts back to the underlying RANS formulation.

The SAS model is based on a re-evaluation of the k-L model proposed by Rotta [203]. It was shown that some of the arguments used in the derivation of that model have been overly restrictive. As a result, The Rotta model features a length scale based on the third velocity derivative, which is not attractive in CFD simulations. The re-formulation of the model results if the use of the second derivative – leading to the von Karman length scale as the natural length scale.

The SAS term has also been transformed into the SST turbulence model [204]. It gives an additional term in the ω-equation, which can be implemented with relative ease. Figure 5.2 shows the behavior of the standard SST and the SST-SAS model for the flow around a cylinder.
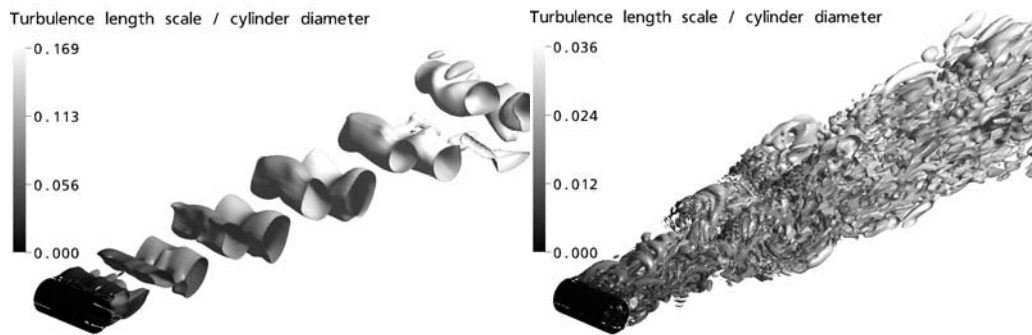
Figure 5.2 Comparison of standard SST model and SST-SAS model for flow around cylinder.

The problem of standard U-RANS models is clearly visible, producing only single mode solutions. The SST-SAS model can represent the true nature of the flow, by allowing a break-down of the turbulent structures into a spectrum (down to the grid limit).
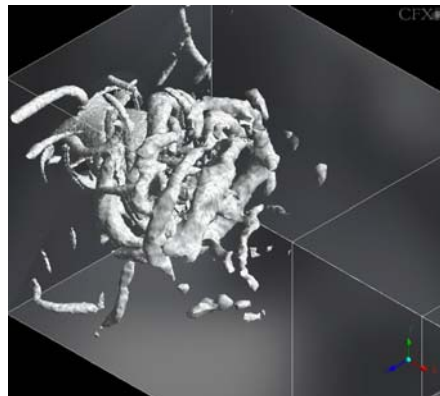


Figure 5.3 Iso-surfaces of $S^2$-$\Omega^2$ for ITS combustion chamber computed with SST-SAS model

Figure 5.3 shows the flow from a combustion chamber simulation using the SST-SAS model. Again, turbulent structures develop and represent the flow instability observed also in the experiments (not shown).

Recommendations for Hybrid methods

The validity range of such modelling and their sequels is not very well established and it is clearly misleading to consider that hybridizing two models naturally leads to each keeping their own good qualities and to remove their drawbacks. The use of such modelling is now to be considered with care even if there are very promising. However, a distinction has to be made between the use of LES plus wall functions, which is already an "old" technique and really new hybrid techniques that most of the time have been developed for extra-NRS area motivations.

The basic recommendation for LES plus wall function is to combine the previous recommendations for LES (concerning both time and spatial schemes, the time stepping and boundary conditions) and the recommendations for the mesh size constraints.

There are no precise recommendations yet for other hybrid methods but one can imagine that the previous recommendations are valid.

*Inlet boundary conditions*

The turbulent state of the incoming flow has an influence on the downstream flow development. The implication on the turbulence modelling is twofold:

- Some models directly require the knowledge of the incoming turbulence state (k and ε profiles for the k-ε model should be prescribed for example). There is no directly available data to universality prescribe such quantities. The code thus generally contains specific internal treatment allowing a synthetic state of the turbulence at the inlet, which relies on hypotheses that are not always valid. As one form of remediation, the user may need to consider extension of the computational domain in the upstream direction far enough to capture all significant influences on the flow behaviour in the region of interest (for example if the investigation concerns a region downstream of an elbow; the elbow has to be considered).

- For LES, specific treatments in the upstream direction have been derived but require further development (see [206], [207], and [208].

### 5.1.5    *A methodology to select an appropriate turbulence model?*

NRS applications usually encompass a large collection of the complexities described in Section 5.1.3. Three key steps in assembling the best set of CFD modelling options are:

1. to analyse the flow regimes to identify the main features (complexity) of the flow to be reproduced to assess a "correct" flow representation and those that can be omitted with acceptable physical realism and preserved predictive capabilities;.

2. to select the most appropriate framework of modelling that is pertinent for the flow and reasonable as far as the CPU cost/precision of the whole simulation is concerned. DNS being on the research side; the choice may be done between LES; hybrid methods, RANS/LES coupling,  U_RANS or RANS modelling;

3. to select a model within a given context, that is compatible with the chosen framework and for which there is a validation assessing its capability to take into account the required flow features. This step addresses the choice of wall resolved or wall modelled strategy.

To end this section we note that the choice of a turbulence model is a matter of compromise between the accuracy of the global model and its costs and feasibility.  For NRS applications, one may prefer a given solution falling within accepted uncertainties than the use of the "best" model for a given situation. In that respect it should be noted that current uncertainty methodologies will probably require a prohibitive amount of computing resources to estimate error bounds associated with a turbulence model for full 3D unsteady situations.  When uncertainty analysis is not feasible, a CFD user should at least:

- Use "new" or "marginally known model" with care

- Compare the results coming from different modelling to access the sensitivity of the results to a given model and reconsider the first choice in case of inconsistencies

## 5.2    Buoyancy Model

The physical problem of buoyancy dominated flows is the additional generation of turbulence based on buoyancy effects. The fluids of different densities can be modelled rather with the Multicomponent Model or alternatively with the Boussinesq approximation. The Boussinesq approximation can be used to account for buoyancy forces until density differs by about 10 % between the fluids. The Multicomponent Model (mass fractions with different densities, viscosities etc.) contains components of a fluid which are mixed at the molecular level. The two or more components and its properties are calculated from those of the constituent components. The components can exist in variable mass fractions. A single velocity field is calculated for each multicomponent fluid. Individual components move at the velocity of the fluid of which they are part, with a drift velocity superimposed, arising from diffusion. The properties of multicomponent fluids are calculated on the assumption that the constituent components form an Ideal Mixture. Concerning the turbulence modelling for buoyancy dominated flows, the standard k-ε turbulence model has limitations (see Section 5.1.4). One possible solution can be the introduction of gravity terms into two-equation models or the use of higher order Reynolds-Stress models. The exact production term and the inherent modelling of stress anisotropies theoretically make Reynolds Stress models more suited to buoyant flows. Taking into consideration that buoyancy effects take place at rather large scales, LES is by its own framework a solution to ensure an explicit and complete description of all the buoyant events and their effects, provided the use of LES is recommended for the considered flow (see Section5.1.4).

## 5.3    Heat Transfer

Heat transfer is one of the key phenomena for reactor thermalhydraulics. The evaluation of heat transfer in reactor cores is of particular importance for the design of economical and safe reactors. Characteristics of heat and fluid flows should be correctly predicted under operational and accidental conditions in order to maintain the coolability and the structural integrity of the core. Single-phase heat transfer is important in fast reactors and gas reactors, while two-phase heat transfer dominates accident analysis in water reactors.  Given the single-phase flow focus of this document, we will not discuss two-phase heat transfer.

In sodium-cooled fast reactors the temperature difference between the core inlet and exit is more than 100 K in normal operation. Several heat transfer phenomena need to be taken into account in thermalhydraulic analyses of the reactor vessel, including thermal stratification, non-uniform flow, stagnation, and thermal striping. Thermal stratification is seen in reactor transients such as shutdown. In this case, core exit temperatures and flow rates decrease rapidly, and the mixing with high-temperature coolant is reduced in the upper plenum. The temperature difference can exceed 100 K in the vertical direction, and the effects on circumferential structures are large. Non-uniform flows are caused by complex structural shapes and their locations. Thermal striping refers to temperature fluctuations in the mixing process of hot coolant from the fuel bundle and cold coolant from the control rod bundle. The temperature difference around the upper structures can also exceed 100 K.

Non-uniform flows and insufficient mixing are also important in high temperature plenums in gas reactors. Thermal stratification is significant in water reactors during ECCS water injection. For instance, in case of an accident with ECCS actuation cold water is injected into cold legs. The temperature difference between primary coolant and ECCS water can be more than 200 K, and the effects on piping would be significant when the flow rate of primary coolant is small ( see Section 11.2).

These examples of heat transfer phenomena are all in three dimensions and closely related to single-phase turbulent flows. Precise predictions of these phenomena are difficult when using conventional reactor safety analysis codes based on one-dimensional modelling. CFD codes with turbulence models and grid flexibility are often used to simulate these phenomena. Heat transfer models for CFD are reviewed subsequently, together with representative turbulence models.

Heat transfer in fluids is governed by conservation equations for mass, momentum and energy. For turbulent flows, which are widely seen in nuclear applications, the dependent variables in the conservation equations are usually divided into average and fluctuating parts, and Reynolds or ensemble averaging is used to obtain equations for the mean flow variables. The mass and momentum equations are solved for the averaged velocity and pressure fields. The Reynolds stresses, $\overline{\rho u_i u_j}$, appear as additional unknowns in the momentum equations. The turbulent heat fluxes, which are made up of velocity and temperature fluctuations, $\overline{\rho u_i t}$, are included in the averaged energy conservation equation. The turbulent heat fluxes and thus the temperature field are substantially affected by the flow field, and heat transfer models are strongly related to turbulent flow models..

The Reynolds stresses and the turbulent heat fluxes can be modelled using gradients of mean velocity and temperature, respectively. These models are called eddy viscosity or eddy diffusivity models. The eddy viscosity for momentum and the eddy thermal diffusivity for energy can be calculated in several ways, as outlined in Section 5.1.4.

The purpose of the models described in Section 5.1.4 is to obtain the eddy viscosity, which in turn is needed to calculate the Reynolds stresses, The eddy thermal diffusivity can be obtained by dividing the eddy viscosity by a turbulent Prandtl number (Reynolds analogy). The turbulent Prandtl number is a constant in most cases, but it is possible to assume a spatial distribution. This model for turbulent heat flux is widely used in combination with the two-equation models. Turbulent thermal intensity, which is defined as the variance of the temperature fluctuation, and its dissipation could also be calculated using two additional transport equations in the two-equation model for the turbulent heat flux. This model is used when the similarity between the velocity field and the temperature field is not good (e.g. Section 3.3.7).

When using transport equations to calculate the eddy viscosity and the eddy thermal diffusivity for buoyant flows, some modifications are necessary. The transport equations for the turbulent kinetic energy and its dissipation rate, contain production terms due to buoyancy. The transport equations for the Reynolds stresses and the turbulent heat fluxes in second-moment closure models are analogously modified. Although the Boussinesq approximation can be applied to flow fields with buoyancy effects, the density variation in the fluid should be small (or a linear function of temperature). An equation of state is taken into account if the density difference becomes significant. Equivalent models based on the equation of state are available and can be used for such cases.

In some instances the simpler models just described are inadequate for capturing heat transfer, and the Reynolds Stress models described in Sections 3.3.8 and 5.1.4 must be applied.

Turbulent heat transfer models taking temperature fluctuations into account are not used generally in reactor analyses. In sodium-cooled fast reactors, the molecular Prandtl number is very small, and the velocity and temperature boundary layer thickness can therefore differ significantly. For such cases, the use of at least a separate two-equation model for the temperature fluctuations is recommended to obtain the turbulent heat flux near structures. The heat conductivity of sodium is, however, very large, and the effect of viscous diffusion on heat transfer is not significant up to large Reynolds numbers. Although the turbulence effect is relatively large for the flow field compared with the temperature field, the turbulent heat flux should be evaluated for precise predictions of heat transfer phenomena in complicated geometries

such as the reactor core and heat exchangers. Computer and simulation technologies are developing day by day, and the detailed heat transfer analyses will be popular even in nuclear application fields in the future.

In commercial CFD codes like ANSYS CFX, STAR-CD, and FLUENT, the one- and two-equation models, the second-moment closure model, and large eddy simulation models are provided for turbulent flow analyses with default constant values. However turbulent heat flux models are not available in all codes. The energy equation is instead closed using the Reynolds analogy.

## 5.4    Free Surface Modelling

The discussion here will be restricted to incompressible, single-phase aspects of free-surface modelling in which there is no phase change, but the physical properties (density, viscosity, thermal capacity and thermal conductivity) of the single fluid change discontinuously across the interface. Even with this restriction, there remain several interesting application areas in NRS, including level swelling in BWR suppression pools, estimates of the free-surface levels in accumulator tanks in PWRs, level-tracking in condenser units, and generally free-surface behaviour under seismic loads.

An interface between a gas and liquid is often referred to as a free surface. The reason for the "free" designation arises from the fact that the location is not known a priori, but forms part of the solution procedure. Large differences in the densities of the gas and liquid can occur: for example the ratio for water and air is about 1000. A low gas density means that its inertia can generally be ignored compared to that of the liquid. In this sense, the liquid is the driving force for the interface motion, the only influence of the gas being the pressure it exerts on the liquid surface.

The presence of a free or moving boundary introduces serious complications for any type of analysis. Free surfaces require the introduction of special models to define their location, their movement and their influence on the flow. Generally speaking, there are two free surface modelling methods. Conceptually, the simplest means of defining and tracking a free surface is to construct a Lagrangian grid that is imbedded in, and moves with, the fluid. This model is ideal for continuous free surfaces for which a very accurate interface prediction is required. Other free-surface tracking methods use a fixed, Eulerian grid as the basis for computations, so that more complicated surface motions may be treated. This is well-suited for large deformation problems, such as filling, sloshing, droplet break-up and other discrete processes.

For the Lagrangian grid methods (examples are front-tracking [209] and boundary-integral [210] methods), the principal limitation is that they cannot track surfaces that break apart or intersect. Even large amplitude surface motions can be difficult to track without introducing regridding techniques such as for the Arbitrary-Lagrangian-Eulerian (ALE) method [211]. On the other hand, since the proper boundary condition can be applied at the surface, the most precise evolution of the shape and location of a surface with time can be obtained. Recently, numerical methods without grids have been developed in order to avoid the regridding methods necessary for ALE. For example, the MPS scheme represents a fluid by a large number of calculation points (particles) moving with flow [212]. In this method, the partial differential operators appearing in the Navier-Stokes equations are replaced by the appropriate interaction modelling between particles.

Modern examples of Eulerian approaches are the Volume of Fluid (VOF) method, Level Sets [213, 214], and Phase Field Methods [214]. Historically, the earliest numerical method devised for time-dependent, free-surface, flow problems was the Marker-and-Cell (MAC) method [216]. This scheme is based on a fixed, Eulerian grid of control volumes. The location of fluid within the grid is determined by a set of marker particles that move with the fluid, but otherwise have no volume, mass or other properties. A free surface is defined to exist in any grid cell that contains the markers and that also has at least one

neighbouring grid cell that is void. The MAC method succeeded in solving a wide range of complicated free-surface flow problems. One reason for this success is that the markers do not track surfaces directly, but instead track fluid volumes. Surfaces are simply the boundaries of the volumes, and in this sense surfaces may appear, merge or disappear as volumes break apart or coalesce. The principal limitation of marker particles is that they don't do a very good job of following flow processes in regions involving converging/diverging flows. When fluid elements get pulled into long, convoluted strands, the markers may no longer be good indicators of the fluid configuration.

The Volume-of-Fluid (VOF) Method [217], which is the method that has been used most frequently and widely so far, is based on the concept of a fluid volume fraction. If we know the fraction of fluid in each cell (control volume) it is possible to locate surfaces, as well as determine surface slopes and surface curvatures. Surfaces are easy to locate because they lie in cells partially filled with fluid or between cells full of fluid and cells that have no fluid. Slopes and curvatures are computed by using the fluid volume fractions in neighbouring cells. The essential element in this process is to remember that the volume fraction should be a step function, i.e. having a value of either one or zero. The application of free-surface boundary conditions consists of assigning the proper gas pressure (plus equivalent surface tension force) as well as determining what velocity components outside the surface should be used to satisfy a zero shear-stress condition at the surface. In practice, it is sometimes simpler to assign velocity gradients instead of velocity components at surfaces. Finally, to compute the time evolution of surfaces, a technique is needed to move volume fractions through a grid in such a way that the step-function nature of the fluid volume fractions is retained. A straightforward numerical approximation cannot be used because numerical diffusion and dispersion errors destroy the sharp, step-function, nature of the distribution of the fluid volume fractions. The principal limitation of the method is that an exact determination of the shape and location of the surface cannot be made in two or three dimensions. For accurately tracking sharp liquid-gas interfaces, it is necessary to actually treat the interface as a discontinuity. This means it is necessary to have a technique to define an interface discontinuity, as well as a way to impose the proper boundary conditions at that interface. It is also necessary to use a special numerical method to track interface motions though a grid without destroying its character as a discontinuity.

The Level Set (LS) technique [214] is also Eulerian in nature, and similar to VOF in principle, except that a continuous function is used to delineate the phase boundary. The Level Set Function $\Phi$ is defined as the signed minimum distance to the interface, positive on one side and negative on the other. Thus, the sign of the function at any point defines in which phase the point lies, and its magnitude defines its distance from the interface. The interface itself is the surface $\Phi=0$. Clearly, $\Phi$ is continuous across the interface, and its normal gradient is unity at the interface. With $\Phi$ known throughout the flow field, the normal gradient and curvature of the interface can be determined in the same way as with VOF, using values in neighbouring cells. Again, as with VOF, the Level Set Function $\Phi$ is advected with the flow field. The basic overhead of the method computationally is that it is necessary to re-initialize $\Phi$ after each advection step to ensure that the isosurfaces of $\Phi$ remain locally parallel to the interface. This is necessary because of the "blending" procedures that need to be introduced for the discontinuous changes in the physical properties.

In summary, probably the most popular and successful method for free surface modelling is the VOF technique, mainly because of its simplicity and robustness. It is implemented, for example, in the commercial CFD code FLUENT [218]. Research to improve the VOF method is still underway, and is focused on deriving better, more accurate, ways to move fluid fractions through the grid [219, 220]. Likewise, Level Sets have been introduced into Beta-versions of FIDAP [221] and CFX-4 [222], and a hybrid formulation in which LS is combined with a marker approach is also being pursued [223]

## 5.5 Fluid-Structure Interaction

As with any project, analysis of fluid-structure interaction begins with selection of the right team of analysts. Individuals who are highly experienced with CFD are normally not well trained in the analysis of structural vibrations. One member of the project team should have a high level of training in the area of structural vibrations, and in the use of associated computer software.

The next consideration is the type of coupling needed between the CFD and structural mechanics programs. Frequently the question to be answered by such analysis is whether or not the flow drives a resonant frequency in the structure. For a rough answer to that question, run the CFD alone, and then supply the surface pressure results as boundary conditions to the calculation of structural dynamics. In this instance the CFD side should normally be a transient LES or DES calculation, to best capture the pressure oscillations. However, special purpose post-processing models exist that generate appropriate pressure oscillations from the results of steady RANS calculations. Separate calculations are also appropriate when the goal of analysis is to check for mechanical failure under extreme conditions such as LBLOCA. In this situation RANS analysis is usually adequate.

Tightly coupled flow and structural calculations are needed if detailed knowledge is needed of structural vibrations. Paterson et al [224] have shown that feedback of structure motion into the fluid calculation can result in a significant broadening of the resonance peak, and modification to flow patterns. Their work adapted in-house CFD and structural codes to permit, feedback every time step, including a moving fluid mesh at the structure boundary. The paper provides useful guidance to anyone adapting local codes to this class of calculation.

## 6. USER CONTROL OF THE NUMERICAL MODEL

User control of numerical models comes primarily through selection of discretization in space and time, and through care in selection of convergence criteria for any iterative solution procedures. These issues are addressed both here through guidance on initial choice, and in Section 8 where guidance is provided for checking of errors associated with these choices. Available options are discussed for numerical approximations to differential operators, as are other options such as surface tracking that can improve modelling fidelity.

### 6.1    Transient or Steady Model

The choice between transient and steady state is only an issue with RANS based simulations. More detailed simulations based on LES, DES, and DNS are fundamentally transients. Most selections are based on common sense, and the only serious problems in making the choice arise in configurations that appear steady based upon imposed boundary conditions, but may be shedding vortices (e.g. from a trailing edge) or contain fundamentally unstable macroscopic flow patterns.

The best option for questionable flows is to run a transient and inspect the flow patterns. If the user wishes to start the analysis running a CFD code in steady state mode, it is important to understand the code's algorithm for obtaining steady state. If the specific CFD code achieves steady state solutions through some pseudo-transient iteration procedure, it will generally not converge if the flow is fundamentally transient. However, if it's algorithm is a direct solution of flow equations with no time derivative terms, it may provide an smooth answer that masks actual transient behaviour.

In the event that vortex shedding is detected a more important question is level of detail required in simulating a flow. RANS does not do a particularly good job of resolving these vortices, and consideration should be given to use of a code with LES or DES options (see Section 5.1.4).

### 6.2    Grid Requirements

The computational grid is a discretized representation of the geometry of interest. It should provide an adequate resolution of the geometry and the expected flow features. The grid's cells should be arranged in a way to minimize discretization errors. Specific recommendations here follow closely those provided by ECORA and ECOFTAC [1, 2].

### 6.2.1    *Geometry Generation*

Before the grid generation can start, the geometry has to be created or imported from CAD data or other geometry representations. Attention should be given to:

- Use of correct coordinate systems;

- Use of correct units;

- Completeness of the geometry: If local geometrical features with dimensions below the local mesh size are not included in the geometrical model, for instance fuel element assemblies, they should be incorporated via a suitable empirical model.

- Oversimplification due to physical assumptions: Problems can for instance arise when the geometry is over-simplified, or when symmetry conditions are used which are not appropriate for the physical situation.

- Location of boundary conditions: The extent of the computational domain has to capture relevant flow and geometrical features. A major problem can be the positioning of boundary conditions in regions of large gradients or geometry changes. If in doubt, the sensitivity of the calculation to the choice of computational domain should be checked.

When the geometry is imported from CAD data, these data should be checked thoroughly. Frequently, CAD data have to be adapted (cleaned) before they can be used for mesh generation. For instance, some mesh generators require closed three-dimensional volumes (solids) for mesh generation, and these are not always directly obtained from CAD data. As a consequence, the CAD data have to be modified. However, care must be taken to ensure that these changes to the geometry do not influence the computed flow.

### 6.2.2 Grid Design

In a CFD analysis, the flow domain is subdivided into a large number of elements or control volumes. In each computational cell, the model equations are solved, yielding discrete distributions of mass, momentum and energy. The number of cells in the mesh should be sufficiently large to obtain an adequate resolution of the flow geometry and the flow phenomena in the domain. As the number of elements is proportional to storage requirements and computing time, many three-dimensional problems require a compromise between the desired accuracy of the numerical result and the number of cells. The available cells need to be distributed in a manner that minimizes discretization errors. This leads to the use of non-uniform grids, hybrid grids consisting of different element types, overset grids, and local grid refinement.

Modern CFD methods use body-fitted grids where the cell surfaces follow the curved solution domain. Different mesh topologies can be used for this purpose as follows:

- Structured grids consist of hexahedral elements. Cell edges form continuous mesh lines which start and end on opposite block faces. The control volumes are addressed by a triple of indices ($i,j,k$). The connectivity to adjacent cells is identified by these indices. Hexahedral elements are theoretically the most efficient elements, and are very well suited for the resolution of shear layers. The disadvantage of structured grids is that they do not adapt well to complex geometries, although this problem can be eliminated through the use of an overset grid.

- Unstructured grids can be generated automatically by assembling cell by cell without considering continuity of mesh lines. Hence, the connectivity information for each cell face has to be stored in a table. This results in an increase of storage requirements and calculation time. Often, tetrahedrons are used as mesh elements. Special types of unstructured grids are:

- Hybrid grids which combine different element types, i.e. tetrahedral, hexahedra, prisms and pyramids.

- Block-structured grids which are assembled in an unstructured manner from a number of structured mesh blocks.

### 6.2.3 *Grid Quality*

A good mesh quality is essential for performing a good CFD analysis. Therefore, assessment of the mesh quality before performing large and complex CFD analyses is very important. Most of the mesh generators and CFD solvers offer the possibility to check the mesh parameters, such as grid angles, aspect ratios, face warpage, right-handedness, negative volumes, etc. The CFD user should check the guide of the applied mesh generators and CFD solver for specific requirements. General recommendations for generating high quality grids are:

- Avoid grid angles below 20° and above 160°

- Avoid jumps in grid density: Growth factors between adjacent volumes should be smaller than 2

- Avoid non-scalable grid topologies: Non-scalable topologies can occur in block-structured grids and are characterised by a deterioration of grid quality under grid refinement.

- Avoid grid lines which are not aligned with the flow direction (e.g. tetrahedral meshes, in thin wall boundary layers). Computational cells which are not aligned with the flow direction can lead to significantly larger discretization errors.

- Avoid high grid aspect ratios: This criterion depends on the flow solver. For standard iterative solvers, aspect ratios should not be larger than 10 to 50 to obtain convergent solutions. Solvers with multi-grid acceleration can absorb higher aspect ratios.

- Use a finer and more regular grid in critical regions, e.g. regions with high gradients or large changes such as free surfaces.

- Avoid the presence of non-matching grid interfaces in critical regions. An arbitrary grid interface occurs when there is no one-to-one correspondence between the cell faces on both sides of a common geometry face

- In areas where local details are needed, the local grid refinement can be used to capture fine geometrical details. If grid refinement is used, the additional grid points should lie on the original boundary geometry, and not simply be a linear interpolation of more grid points on the original coarse grid.

If the target variables of a turbulent flow simulation include wall values, like wall heat fluxes or wall temperatures, the choice of the wall model and the corresponding grid resolution can have a large effect on the results. Typical 'wall functions' are:

- Calculation of the wall shear stresses and wall heat fluxes based on logarithmic velocity and temperature profiles

- Calculation of the wall shear stresses and wall heat fluxes based on linear velocity and temperature profiles

- Calculation of the wall shear stresses and wall heat fluxes based on linear/logarithmic velocity and temperature profiles

Wall functions of this kind are used for all RANS turbulence models, and also for LES and DES simulations. The choice of the wall model has a direct influence on the mesh design. The following values are recommended for the distance of the first grid point away from the wall:

- Logarithmic wall functions: $30 < y^+ < 500$. The upper limit is Reynolds number-dependent. The limit decreases for decreasing Reynolds numbers. A logarithmic near-wall region does not exist for very small Reynolds numbers.

- Linear wall functions: $y^+ < 5$. Linear wall functions can only be used in combination with special low-Re versions of the k-ε turbulence model. k-ω-type models usually do not need special modifications.

- Linear/logarithmic wall functions: $y^+ < 500$. Linear/logarithmic wall functions can only be used in combination with special low-Re versions of the k-ε turbulence model. k-ω-type models usually do not need special modifications.

*Here $y^+$* is the non-dimensional wall distance:

$$y^+ = \frac{\rho u_\tau y}{\mu} = \frac{\sqrt{\rho \tau_w}\, y}{\mu}$$

The recommendations above are strictly only valid for two-dimensional attached flows. The logarithmic law is not valid for separated flows. Close to separation, the wall shear stress $\tau_w$ goes to zero, and with it the non-dimensional wall distance $y^+$, irrespective of the physical wall distance, $y$. In contrast, the linear near-wall law remains valid, but requires finer resolution. The combination of logarithmic and linear wall functions yields the best generality and robustness against small variations of the near-wall grid distance.

For two-dimensional flows, the following equation is valid:

$$u_\tau = U_e \sqrt{\frac{c_f}{2}}$$

$U_e$ is the velocity at the boundary layer edge or a characteristic reference velocity. The skin friction coefficient $c_f$ for turbulent flows is typically in the interval from 0.003 … 0.005. With these two values, the friction velocity $u_\tau$ and the distance of the first grid point away from the wall can be a priori estimated as:

$$y = \frac{y^+ \mu}{\rho u_\tau}$$

Finally, some recommendations regarding the choice of element types are made:

- Hex elements are the most efficient elements from a numerical point of view. They require the least memory and computing time per elements. They can be well adapted to shear layers

(long and thin), for instance in the vicinity of walls. However, generation of hex meshes in complex geometries often requires a large manual and cognitive effort.

- If this effort seems too high, use of tetrahedral meshes is a viable alternative. Tetrahedral elements require roughly fifty percent more memory and computing time per element than hex elements. They are not very efficient for the resolution of shear layers: Either a large number of tetrahedral elements must be used, or the grid angles become very small. If wall values are the target values of a calculation, pure tetrahedral meshes should either be avoided or used with great care.

- The combination of tetrahedral elements in the flow domain and prism elements close to walls is a *reasonable* alternative to the use of pure tetrahedral grids. The combination of tetrahedral elements in the flow domain, and hex elements close to walls (with pyramids as transition elements) is a *good* alternative to pure tetrahedral grids.

- Non-matching grid interfaces, which combine different grid types and/or mesh densities, should be avoided, if possible. They can have a negative impact on accuracy, robustness (convergence) and parallel scalability (depending on the numerical algorithm and the application).

Based on these observations, the following rules and priorities can be formulated to obtain the best accuracy and efficiency:

1, Use of pure hex element grids, if the grid generation effort is manageable

2. Use of hybrid grids with hex elements close to walls, and tetrahedral elements in the core of the domain

3. Use of hybrid grids with prism elements close to walls, and tetrahedral elements in the core of the domain

4. Use of pure tetrahedral element grids

The order becomes reversed if the manual grid generation effort is the sorting parameter. The final decision and compromise which grid to use is up to the user. However, the reasoning which has led to the use of a particular grid and topology should be part of the final documentation of the analysis.

A grid dependence and sensitivity study should always be performed to analyse the suitability of the mesh and to provide an estimate of the numerical error of the results. At least two (better: three) grids with significantly different mesh sizes should be employed. If this is not feasible, results obtained with different discretization schemes in time and space can be compared on the same mesh (see Section 8.5).

## 6.3    Discretization Schemes

Ideally, selection of discretization schemes should be automated within the CFD code and not a user option.  Unfortunately the current state of CFD presents the user with a list of potential discretization schemes with some general advice on situations in which each is appropriate.  Selection of temporal and spatial discretization is a balancing act between too much numerical diffusion for low order schemes, and spatial wiggles (unphysical non-monotonic behaviour) in key state variables with higher order schemes.

The concept of numerical diffusion was quantified for first order numerical schemes by Tony Hirt in 1967 [225].  Consider a simple 1-D advection equation, approximated with backward Euler time

(fully implicit) and first order upwind spatial discretization. Applying Hirt's analysis, the numerical solution can be shown to closely approximate the analytic solution of an advection-diffusion equation

$$\frac{\partial \rho}{\partial t} + \frac{\partial}{\partial x}(\rho V) = D \frac{\partial^2 \rho}{\partial x^2} \ ,$$

where the numerical diffusion coefficient D is

$$D = \frac{V}{2}(V\Delta t + \Delta x).$$

Anyone contemplating use of numerical methods that are first order accurate in time or space, should obtain typical values for turbulent diffusion coefficients (or molecular diffusion coefficients if the flow is laminar), and use the previous formula to estimate the time step and/or mesh size needed to make the numerical diffusion substantially less than the physical diffusion. In the case that physical diffusion is unimportant to a problem, numerical diffusion should at least be limited to the point that it doesn't significantly distort the results of advection terms.

In general use of first order discretization should be avoided. The one significant exception comes in steady flow solutions. In some cases a CFD code will be unable to converge its steady state iteration when using an appropriate higher order spatial discretization. In this situation an initial steady solution can usually be obtained with a first order spatial method, then this used as a starting point for iteration to steady state with the higher order method. However, even this approach does not always work, and the CFD code may be trying to tell you that vortex shedding is significant, and no steady solution exists.

Higher order methods remove second derivative terms from Taylor truncation error analysis that give rise to obvious numerical diffusion. However, they do not completely suppress numerical diffusion. A recent study Vyskocil [226] is one of many examples of the numerical diffusion that can be introduced by higher order methods, particularly in problems involving continuity or shock waves. He was able to demonstrate degradation of results for several spatial discretizations, propagating a thermal wave in a flow field. The problem for the analyst is in quantifying the magnitude of numerical diffusion relative to turbulent diffusion in a given simulation.

The Richardson based error analysis described in Section 8.5 is a way to determine that errors introduced by numerical diffusion are bounded. However, Richardson analysis tends to break down in continuity or shock waves (particularly near the inflection point), and even when working well doesn't allow direct comparison of numerical and physical diffusion. Another approach is to perform numerical experiments with simple continuity waves as in Vyskocil's work and analyse the results with the "C-Curve" method originally developed to extract diffusion coefficients from experiments (see Levenspiel [227]). Application of this technique to a simple numerical problem was described by Macian and Mahaffy [228] as part of a study on limiting numerical diffusion in boron dilution problems. The method is basically 1-D, so is most useful for examining the behaviour of portions of a mesh after the nature of the flow field has been established. Boundary conditions must be used carefully to isolate the chosen section of the mesh and to drive a continuity wave along the direction of flow observed in the full calculation.

Higher order upwind methods are typically selected for use in RANS calculations. However, LES, DES, and DNS calculations need the lower numerical diffusion associated with central difference methods (typically 4th order or higher). For methods operating on a logically rectangular mesh, performance is optimal when flow is aligned with a mesh direction. Results should be studied with

particular care when flow is diagonal to the mesh lines. All higher order methods have the potential for cell to cell spatial oscillations in key state variables, and results, particularly near continuity or shock waves, should be watched carefully for this behaviour. When these oscillations are severe, they can be controlled by a flux correction method (available in any serious CFD code). Such techniques are automatically applied to limited areas, and reduce the spatial accuracy to first order in these regions.

Local application of flux correction prevents the type of numerical diffusion associated with global use of a first order upwind method. However, a user needs to be cautious of two potential side effects. Many flux correction algorithms can take a wave with a very gradual rise on the leading edge, and artificially sharpen it to something with a very steep leading edge. If propagation of sound or continuity waves is an important phenomenon in a given simulation (.e.g. boron dilution), some simple numerical studies should be run to understand the impact of selected numerical methods on wave shape, and a decision made on the physical significance of any distortions. The second side effect of flux correction is propagation of the local reduction of accuracy to the global solution. This is particularly a concern if internal code criteria for engaging flux correction are too loose, and can be checked using Richardson analysis on simplified test problems (see Section 8.5).

When evaluating tests of discretization schemes, it is important to keep a proper prospective. Understand that the results of a Richardson error analysis will probably indicate lower effective order of accuracy than advertised for the selected discretization scheme. The important goals are to demonstrate convergence of the solution as the mesh or time step is refined (see Section 6.4.1) and to achieve acceptably low numerical distortion of important physical phenomena at the discretization used in the final analysis.

## 6.4    Convergence Control

There are two meanings of *convergence* in common use in CFD. Both forms of convergence must be checked to understand the accuracy of a calculation.

### 6.4.1    *Differential versus Discretized Equations*

The first convergence refers to the formal process which brings the exact solution of the discretized equation set ever closer to the exact solution of the underlying partial differential equations, as each of the discretization sizes for independent variables approaches zero. That is:

$$T_j^n \rightarrow \overline{T}\left(x_j, t_n\right) \text{ as } \Delta x_j, \Delta t \rightarrow 0 .$$

In practice, the definition is not very useful, since exact solutions of algebraic equations (with no round-off errors, for example) are generally difficult to obtain, and exact solutions of the partial differential equations even more so, except for a few over-simplified demonstration cases. However, in the case of linear equations, it is possible to link the concept of convergence with *consistency* and *stability*, which are easier to demonstrate.

A system of algebraic equations generated by a space and time discretization process is said to be *consistent* with the partial differential equation if, in the limit of the grid spacing and the time step tending to zero, the algebraic equation is identical with the partial differential equation at each grid point, at all times. Consistency may be demonstrated by expressing the differences appearing in the discretized equations in terms of Taylor expansions in space and time, and then collecting terms. For consistency, the resulting expression will be identical with the underlying partial differential equation, apart from a set of remainder terms, which should all tend to zero as $\Delta x_j$, $\Delta t \rightarrow 0$. In CFD, almost universally, the numerical

schemes for solving the fluid flow and energy equations are consistent, due simply to the methodology employed in their development.

Numerical stability, however, is far more difficult to prove, and most of the formal procedures are limited to linear equations. In a strict sense, stability only applies to marching problems (i.e. to the solution of hyperbolic or parabolic equations) and will be defined here accordingly. A numerical scheme is considered to be *stable* if errors arising from any source (e.g. round-off or truncation) do not grow from one time step to the next. The most common example of instability arises from the use of explicit time-differencing for convective problems in which the time step exceeds the Courant-Friedrich-Levy (CFL) criterion [229]. Physically, this corresponds to information being numerically transported within a time step faster than the physical communication process, either by sonic or fluid velocities. In practical terms, small disturbances grow until the solution is destroyed. There are classical methods available for determining the stability of numerical schemes, but most of the work refers to linear systems.

The Lax Equivalence Theorem states that, given a well-posed, linear, initial-value problem (well-posed means that the solution develops in a continuous manner from the initial conditions), and a finite difference approximation to it that satisfies the consistency condition, stability is a necessary and sufficient condition for convergence of the numerical result to the analytic solution as discretization is refined. The theorem is very powerful since, as we have noted, it is much easier to demonstrate consistency and stability than convergence directly, though convergence is the most useful property in the sense of quality and trust in the solution. Though the theorem is stated in terms of finite differences, it applies too to other discretization schemes, such as finite volume and finite element. The theorem can only be rigorously applied to linear, initial-value problems, whereas with CFD the governing equations are non-linear, and of the boundary- or mixed initial/boundary-value type. In these circumstances, the Lax Equivalence Theorem should be regarded as a necessary, but not sufficient, condition, and used heuristically to provide a pragmatic solution strategy; i.e. one that is consistent and stable.

Although user's have no iron-clad guarantee of convergence to the solution of the Navier-Stokes differential equations, they should use common sense to look for obvious signs of trouble. Frequently analysts assume that step to step oscillations associated with bounded numerical instabilities are oscillating about the correct mean solution to the problem. This may not be the case and isolated time step sensitivity studies should be performed on any such case to determine shift in mean behaviour with time step size. Error studies discussed in Sections 8.5 and 8.6 are also important in this respect. Although convergence of results as time step or mesh size are reduced towards zero is not a guarantee that the numerical solution is converging to the solution of the set of PDE's, it is a good indicator. If no convergence can be seen in these sensitivity analyses, there is no hope of converging to the PDE solution.

### 6.4.2    *Termination of Iterative Solvers*

The second meaning of convergence refers to the criterion adopted to terminate an iterative process. Such processes nearly always arise in CFD simulations, because of (1) implicit or semi-implicit time differencing, and (2) the non-linear nature of the governing equations.

For a fully coupled solver, all the governing equations are considered part of a single system, and are solved together. This means that all variables are updated simultaneously, and there is just one overall iteration loop. For highly non-linear equations in three dimensions, as occur in industrial CFD applications, this entails a large memory overhead, and until recently such approaches were considered impractical. However, with the advent of large-memory machines and fast CPUs, the approach has become tractable, and today many modern commercial CFD software is built around the concept of fully-coupled solvers.

An alternative is to treat each of the governing equations in isolation, assuming all other variables are fixed, and invert the sub-system matrix on this basis. This procedure is often called the *inner iteration*. The other equations are then all solved in turn, repeating the cycle, or *outer iteration,* until all the equations are satisfied simultaneously.

The solution of the fully coupled system of equations, and the inner loop of the non-coupled system, requires the solution of a set of linear, simultaneous equations; in other words, the inversion of a matrix. Except for small problems, for which inversion by Gaussian elimination can be attempted, the solution algorithm is usually iterative. In fact, the success of finite-volume discretization schemes in CFD is largely due to the fact that the algorithms produce diagonally-dominant system matrices. Such matrices can be readily inverted using iterative methods.

A multitude of such methods have been derived, ranging from the classical Jacobi, Gauss-Seidel, Successive-over-Relaxation (SOR) and Alternative Direction Implicit (ADI) algorithms, through the more modern Krylov family of algorithms (e.g. Conjugate-Gradient, GMRES) up to the more up-to-date Multigrid and Algebraic Multigrid methods. All such methods involve pivoting on the diagonal entry for each row of the matrix, and the success and speed of convergence of the iteration process is essentially governed by how much this term dominates over the sum total of the others in the row (supported by under-relaxation if necessary) and the accuracy of the initial guess.

When using iterative solvers, it is important to know when to stop and examine the solution (steady-state problems), or move on to the next time step (transient solutions). The difference between two successive iterates, measured by an appropriate norm, being less than a pre-selected value is not sufficient evidence for solution convergence, but the information may be used to provide a proper estimate of the convergence error as follows. The largest eigenvalue (or spectral radius), $\lambda_m$, of the iteration matrix, may be estimated from the (*rms* or $L_2$) norms at successive iteration steps according to:

$$\lambda_m \approx \left\| r^n \right\| / \left\| r^{n-1} \right\| \text{ where } r^n = \Phi^{n+1} - \Phi^n ; \ \Phi \text{ is a dependent variable, and } n \text{ the iteration number.}$$

A good estimate of the convergence error $\varepsilon^n$ is then

$$\varepsilon_m \approx \left\| r^n \right\| / (\lambda_m - 1)$$

Though the analysis is based on linear systems, all systems are essentially linear near convergence, and, since this is the occasion when error estimates are needed, the method can be applied to non-linear systems as well. Further details are given in [230].

It should be emphasized that with commercial CFD software incorporating sequential (i.e. partially coupled) solvers, it may not be possible to have sufficient user access to control the convergence error in the way described above. For example, many solvers based on pressure-velocity coupling algorithms rely on minimizing the mass residual in the continuity equation. It is recommended that the residuals for each of the momentum equations, as well as for the energy equation for problems involving heat transfer, be controlled as well, just as they would be for fully coupled solvers. There is another issue as well: some "juggling" between the convergence criteria for the inner and outer iterations may be necessary to avoid wasting machine time. Obviously, it is not worth insisting on high accuracy for the inner iteration, when the outer iteration is still far from convergence. The reader is referred to the code documentation on how best to optimize tolerances for maximum CPU efficiency. However, as the solution approaches convergence in the outer iteration, minimization of all the residuals should be enforced.

Regardless of the underlying iteration scheme, CFD users should perform some simple numerical studies to understand the effect of convergence criteria on solution accuracy. After a base run, a second run should be performed with all iterative convergence criteria halved. After plotting results for key variables, the user can make a practical decision on significance of the discrepancies. To make a conservative judgement of impact, all differences in results should be doubled.

## 6.5      Free Surface Consideration

As discussed in Section 5.4, the presence of free surfaces introduces particular difficulties in the CFD analysis, whichever tracking algorithm is used. This is essentially due to the fact that the location and movement of the free surface has to be computed simultaneously with the flow field.

The simplest is not to explicitly track the interface at all. This can be accomplished within a two-phase two-fluid code by using the void fraction (gas volume fraction) variable to describe where each phase is located. This approach is only acceptable if the free surface location is only required approximately, since volume fraction information is only known cell-wise, and will become diffuse as a result of the numerical diffusion associated with the solution scheme. Though "surface-sharpening" algorithms may be introduced to offset the interface diffusion, these tend to be ad hoc schemes, and do not guarantee mass and momentum conservation. From the standpoint of BPGs:

- It will not be possible to obtain completely grid-independent results, but repeat runs with different meshes should be performed to give an indication of the degree of precision of the results.

- Numerical diffusion should be minimized by employing high-order space and time differencing algorithms.

- Mass conservation must be checked if surface-sharpening algorithms are employed.

The most popular surface tracking methods are the front-capturing, Eulerian Volume of Fluid (VOF), and Level Sets (LS). In principle, for incompressible fluids, the VOF methods preserve mass exactly, since the volume fraction $F$ is a conservation property. In practice, however, a surface reconstruction algorithm has to be employed to define the actual interface location from the volume fraction information in each cell and their neighbours. In the most popular of these algorithms (PLIC-VOF) the interface is piecewise linear, with discontinuities at mesh boundaries. This can sometimes lead to small, isolated parcels of one fluid becoming trapped in the other fluid domain. Cleaning up can lead to mass-loss errors.

In the LS method, the Level Set Function $\Phi$ is not a conservation quantity, and is often challenged on the issue of poor mass conservation. However, some successes have been reported, so that from a BPGs viewpoint we can nominate this property as one of the target variables.

Thus for both VOF and LS approaches:

- Mass conservation check is the ultimate test of a good solution.

- The solution of the advection equation for $F$ or $\Phi$ should be at least the same order as for the rest of the flow solution, otherwise it is impossible to judge the overall accuracy of the solution. Schemes should be at least $2^{nd}$ order to limit numerical diffusion.

- Grid independence checks should be made, as usual. The exercise has somewhat more importance in free-surface flows because of the "numerical blending width" – usually a few mesh cells – over which the discontinuous change in physical variables across the interface is handled.

- The advection of the interface is often explicit: that is, the position of the interface is treated as "frozen" over the time step, even if the basic flow solver is implicit. This means that there will be a CFL time-step limitation controlled by the interface motion through the mesh.

- The surface tension force is usually incorporated as a body force spread over a number of meshes in a band adjacent to the interface [231]. Sensitivity of results to the width of the band should be investigated.

# 7. ASSESSMENT STRATEGY

Here, assessment is understood as the expression of belief (based on validation calculations) that a given computer code is able (when properly used) to simulate with acceptable fidelity a given set of situations (at least parts of a nuclear reactor transient). Assessment therefore requires validations of a verified computer code on suitable experiments.

The overall situation is schematically shown in Fig. 7.1. The complete process can be separated into the following eight activities, see Oberkampf [8]:

1. Identification and specification of the intended application;

2. Planning of verification and validation activities, especially use of the PIRT (see Section 3.2);

3. Development, implementation, and documentation of verification activities;

4. Design and execution of validation experiments based upon the PIRT results;

5. Development and definition of useful metrics;

6. Assessing the results of the validation metrics;

7. Assessment of the predictive accuracy of the code;

Accurate and complete documentation of the validation planning, results and consequences, concluding with a clear statement on predictive confidence for the intended application of the code.

Verification as used here is in fact an experiment-independent activity since in a strict sense of this term only analytical solutions (including Manufactured Solutions, see Roache [6]) are used in verifying that the numerical properties of a given computer code correspond to those stated in the code documentation ("solving the equations right"). Nevertheless, results of calculations performed by means of a high-precision code (e.g., DNS) or selected separate-effect and well-designed experiments in simple geometries can contribute to the verification process. A poor match of calculation to a separate-effect experiment originally used to formulate a particular model indicates the potential for a coding error. A good match is an indication of correct coding. The strength of these indications depends on how strongly the experiment isolates the effects of the model in question.

Validation ("solving the right equations") should be based on well-designed separate-effects or integral experiments with instrumentation enabling elimination of user effects (e.g., mistakes in modelling of initial and boundary conditions) and determination of sources of possible differences of experimental and analytical results. In any case it must be proved that all suitable tools of the code have been utilised and user errors have been eliminated. It is a good practice to plan the validation experiments as needed during the validation process rather than just once before all needs are understood. After validation computations are finished and the results evaluated, it is possible to review the existing validations and to

produce a new, updated statement on the state of assessment of the code for given range of problems. Therefore, assessment should be understood as an ongoing, iterative process.

The assessment process is not cheap and easy, especially experiments and validation calculations when done at the highest level of precision and complexity. On the other hand, safety of nuclear power plants belongs to a class of problems, where the ability to do full scale testing is very limited, in some cases even impossible, so that computational simulations are the only possible tool. Erroneous results of computational analyses could therefore have dangerous consequences. It is very desirable to improve our confidence and understanding in these simulations.

```
┌─────────────────────────────────────────┐
│ Intended application, planning, PIRT     │
└─────────────────────────────────────────┘

  ┌──────────────┐      ┌──────────────┐
  │ Experiments  │      │ Verifications│
  └──────────────┘      └──────────────┘

       ┌──────────────┐   ┌──────────────┐
       │ Validations  │   │Demonstrations│
       └──────────────┘   └──────────────┘

            ┌──────────────┐
            │  Assessment  │
            └──────────────┘
```
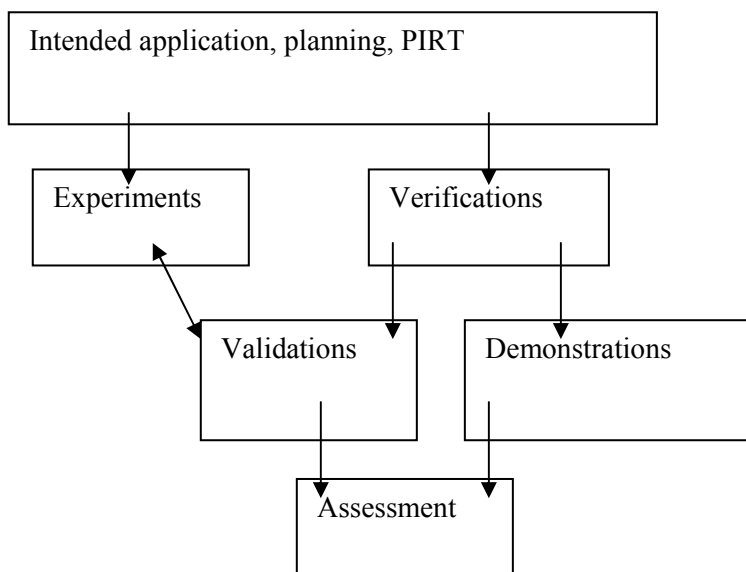
Fig. 7.1: Basic components of an assessment process.

## 7.1    Task 7.1 Demonstration of Capabilities

Within safety analyses of nuclear power plants, there are situations when no validation calculations of the situation with the given computer code have been done so far, and even experimental data are sparse or non-existent. Under these conditions, computational simulations can be termed "demonstration calculations". These demonstration calculations, where no or very limited and almost non-conclusive comparisons with experiments have been done are very frequently found in the literature. They demonstrate certain capability of a code to perform such calculations and illustrate the required computational time and memory. These parameters could add some ground on decisions as regards to assessment of the code, but in no case can replace verification and validation. A specific group of such "demonstration" calculations consists of simulations of experiments on mock-ups of parts of NPP's. These test facilities are in some cases quite large so that only very coarse computational grids are possible given the capacity of present (or available) computers. The assessment matrix should contain such experiments and simulations, but validation calculations aimed at individual physical phenomena involved in the experiment should also be made based on more detailed experiments on simpler models.

## 7.2 Interpretation of Results

In analyses of computational results, several levels of comparisons can be observed (see Oberkampf et al [8]). At the lowest level, statements can be issued whether important physical phenomena observed in real world are seen in the analysed computation. This is a purely qualitative evaluation of results ("viewgraph norms" in the cited reference), most frequently represented by comparison of colour pictures of measured or observed situation with computed physical quantity at selected locations. Existence of maxima and minima of important state variables and their locations, existence of regions with recirculation flows or other distinguished flow regions found in real world should be the first criteria for success or failure of this qualitative analysis.

The next level of analysis of results is quantitative comparison of target variables (see Section 9.2). These variables strongly depend on the intended application of the code and could therefore range from integral quantities like averaged values of velocity or temperature at selected planes or volumes to local quantities. Here, selection of suitable metrics is important, but simple graphical comparison of measured and computed values is the most frequent case. It is very important that both experimental uncertainty and numerical error are estimated and shown.

The highest level of comparison of results requires ensembles of experiments and computations to be performed so that experimental uncertainty and simulation results- are represented as estimated probability distributions. Then, a graph showing differences of the mean, or expected values of computational and experimental distributions with contours of one and two standard deviations can be produced.

# 8.    VERIFICATION OF THE CALCULATION AND NUMERICAL MODEL

## 8.1    Introduction

In Section 2.3 'verification' is defined as the process of determining that the implementation of a physical model or numerical method accurately represents the developer's conceptual description of the model and the solution to the model. However, this definition partially hides a distinction that must be made between code and solution verification.  The developer in question may be the developer of the computer code or the developer of the input model that specifies the details of a particular problem solution (code user).  A code user clearly has responsibility for verification that quantifies and limits discretization error and for verification of the initial conditions, boundary conditions and other special options provided in the input model.  However, a code user must also confirm that the code has been adequately verified by obtaining and reviewing verification documentation from the developers.  If such documentation is unavailable or inadequate, then appropriate caveats must be provided in documentation of results and/or the user needs to perform what code verification is possible.

To the extent possible, code verification examines implementation of the full mathematical model through comparison to exact analytical results, manufactured solutions [232], or previously verified higher accuracy simulations.  Of these options the method of manufactured solutions is the most powerful, but requires that the user be able to provide source terms as a function of spatial location and time for every partial differential equation active in the problem solution.

Unfortunately, analytical results and manufactured solutions are only useful for verification of the portions of a code responsible for approximating partial derivatives and solving the system of  PDEs associated with the flow problem.  They do not help verify coding of complex algebraic expressions used for contributions such as turbulent diffusion coefficients, wall heat transfer functions, reaction rates and the equation of state.  Rigorous verification in these cases is often only possible for code developers.  For them the first step is a good quality assurance (QA) procedure (see Section 8.7).  Another good practice for developers is to independently code the algebraic expressions implementing physical models and carefully compare results from the two independent model implementations.  At a less rigorous level, developers should also drive implementations of physical models in a separate program and compare directly against the data from which the original algebraic model was obtained.  Discrepancies strongly suggest, but do not prove an error in the model implementation.

If the code developers' verification is inadequate, the code user needs to either independently verify the software, or understand that the validation process (Chapter 9) may be effectively checking an undocumented model (published form plus implementation bug).  In this case extra caution is necessary to validate the model against the full operating space of the system and scenario being simulated.  Scaling behaviour seen in the documented model is not completely assured in the implemented model.

Comparison to data can also contribute to verification, if there is sufficient knowledge about the expected performance of the numerical method or the physical model for a given test case. Usually this information comes from publications or other external sources. Use to support code verification does not rely on good agreement with the data, but rather that the differences between a simulation and corresponding data are as expected from independent comparisons to results from verified codes using the

same numerical method and/or relevant physical model. This activity provides necessary, but not sufficient information for comprehensive verification of a code.

Error evaluation for the solution of a particular simulation involves sub-tasks:

- Quality Assurance of the system input model;

- Examination of iterative convergence;

- Basic consistency checks, for instance checks on global mass, momentum and energy conservation;

- Examination of spatial grid convergence;

- Examination of temporal convergence

Inconsistencies in any of these checks will quickly point to implementation problems in the input model (or on occasion the software). Once the verification checks have been passed, the validation task can start.

The following sections describe some of the techniques to perform the verification tasks listed above.

## 8.2 Error Hierarchy

The range of errors possible in a simulation should be addressed in a logical, hierarchical sequence to obtain efficient error quantification. In the case of CFD software, this sequence starts at round-off errors and then proceeds to iteration errors, discretization errors and, finally, model errors. The term 'error hierarchy' also implies that numerical errors can be strictly separated from model errors.

Round-off errors are caused by insufficient machine accuracy; they can be understood through some relatively simple studies. One quick way to check the impact of round-off errors is to run a relevant simulation with programs compiled with and without optimization engaged. Other variations on this approach are to run the same problem on codes generated by different compilers. These techniques do have the disadvantage of being susceptible to undiscovered (but very infrequent) compiler errors. Another approach is to execute the simulation with the program adapted for higher precision data and arithmetic than normally used. Most NRS simulations are done with 64 bit representation (double precision) of floating point numbers. If the problem (or relevant portion) can be rerun with a 128 bit representation (quad precision), useful information will be also be available on impact of round-off errors.

Most CFD codes use iterative schemes for matrix solution, and for dealing with the coupling and non-linearities of the underlying equation system. In both cases, insufficient convergence can cause unacceptable errors in final results. Only once these iteration errors have become sufficiently small, should discretization errors be investigated.

Discretization errors are the difference between the solution of the discrete approximation to the PDEs in the mathematical model and the actual PDE solution. In order to obtain mathematically sound solution error estimates, systematic grid width and time step reduction is necessary. Once the asymptotic range of the convergence properties of the numerical method is reached, the difference between solutions on successively refined grids can be used as an error estimator (see Roache [0]).

An alternative method to grid or time step refinement, is the calculation of the same problem with different discretization schemes, followed by a comparison of target variables. The rationale behind this method is that all consistent discretization schemes should converge to the same solution as the grid is refined towards zero mesh length. Differences in solutions which are obtained with different discretization schemes on the same grid, point to regions where the grid is still too coarse.

Comparison of solutions on the same grid but with different discretization schemes is for many three-dimensional problems more practical than the grid refinement technique discussed above, because it does not have the excessive disk space and calculation time requirements (for instance halving the grid distance in three directions leads to an increase in grid points by a factor of 8, and an increase of calculation times by factors larger than 8). A disadvantage of comparing solutions on the same grid but with different discretization schemes is the lack of a mathematical theory for error quantification as with Richardson extrapolation, see Roache [6]. Therefore, this method yields only heuristic criteria and 'indicators'. However it is a fairly economic technique because the cost for going from a first-order scheme to a second-order scheme (or from a flux-blending to a second-order scheme is often fairly small. The same arguments apply in an analogous fashion to temporal discretization schemes, if 'grid width' is replaced by 'time-step'.

### 8.2.1    *Target Variables*

Numerical errors should be monitored for a limited number of representative target variables defined during the PIRT process as being representative of the goals of the simulation.  It is usually inefficient to evaluate and check all values of all variables. These target variables can for instance be maximum or minimum dependent variable values or integral quantities like efficiencies, and heat transfer coefficients. Under optimal conditions these variables are computed during run-time and for steady state solutions displayed as part of the convergence history. They should be readily available to existing post-processing tools.

### 8.3    **Round-Off Errors**

Round-off errors can be significant for high-Reynolds number flows where the boundary layer resolution can lead to very small cells near the wall. The number of digits of a single precision simulation can be insufficient for such cases. The only way to avoid round-off errors with a given CFD code is the use of a double precision version. In case of an erratic behaviour of the CFD method, the use of a double precision version is recommended.

### 8.4    **Iteration Errors**

A first indication of the convergence to the solution is the reduction of the residuals (or residual norms) of the difference equations. However, different types of flows require different levels of residual reduction. For example, swirling flows can often exhibit significant solution changes, even when the equation residuals have been reduced by more than 5 - 6 orders of magnitude. Other flows can be well converged with a reduction of only 3 - 4 orders of magnitude.  As a result, it is also necessary to monitor the solution during convergence and to plot the pre-defined target quantities of the simulation as a function of the residuals. A visual observation of the solution fields at different levels of convergence is recommended. We also recommend monitoring the global balances of conserved variables, like mass, momentum and energy during the iterative process.

In summary, iterative convergence can be ensured by the following steps:

- Plot evolution of residual norms as a function of iteration number;

- Report global mass balance as a function of iteration number;

- Plot target variables as function of iteration number;

- Report target variables as a function of residual norms.

These steps are generally easy to follow for a steady state calculation. For a transient requiring iterative equation solution at each time step, detailed review of convergence histories for all time steps can be too labour intensive. Review should be restricted to a limited number of specific time steps, including those with unusually large iteration counts. If these convergence studies are not possible due to unavailable data, at least two runs should be made with significantly different convergence criteria, and results compared.

## 8.5    Spatial Discretisation Errors

Spatial discretization errors result from the use of finite-width grids and from the approximation of the differential terms in the model equations by difference operators. Experience shows that only space discretization methods with second and higher order truncation error are able to produce high-quality solutions on practical grids. It is worth noting that for some grids only first order methods will produce converged steady state solutions. However, in such cases solutions need to be regarded with caution. The convergence is a result of a numerical viscosity larger than the actual turbulent viscosity. In some instances the first order solution can be successfully used as an initial guess at the steady state for a higher order analysis. In others the numerical viscosity is simply masking fundamentally transient behaviour in the flow (see Section 6.1).

As the truncation error order of a given discretization scheme usually can not be changed by an end user, spatial discretization errors can only be influenced by the provision of optimal grids. It is important for the quality of a solution, that the grid points are concentrated in regions of large truncation errors, which are often the regions of large solution variation. It is also important for the reduction of spatial discretization errors, to provide high-quality numerical grids. Guidelines for grid generation are given in Section 6.2.

For mathematically sound grid convergence tests, simulations should be carried out on at least three successively refined grids, and the target quantities should be given as a function of the grid width. Using Richardson extrapolation [233] an estimate can be made of error in the target variable due to discretization in space as follows:

$$\varepsilon_1 = \frac{\Theta_1 - \Theta_2}{r^p - 1} \qquad (8.1)$$

In this equation, $\Theta$ is the target variable (lift, drag, heat transfer coefficient, maximum temperature, mass flow rate, etc), $r$ is the grid refinement ratio (always greater than 1), and $p$ is the truncation error order of the discretization scheme. A subscript of one indicates results from the finest grid.

An independent estimate of the order of accuracy for the discrete approximation can be obtained from results on three successive grids.

$$p = \frac{\ln\left(\dfrac{\Theta_3 - \Theta_2}{\Theta_2 - \Theta_1}\right)}{\ln(r)} \qquad\qquad (8.2)$$

This value of p can only be expected to approach the theoretical accuracy of the numerical method when mesh size is small enough to be in the asymptotic region. In this region only the lowest order contribution to truncation error is significant, and the following indicator should be nearly constant:

$$E_h = \frac{\varepsilon}{h^p}. \qquad\qquad (8.3)$$

For practical three-dimensional simulations, limited computational resources often make it extremely difficult to obtain all three mesh solutions in the asymptotic region. In this situation useful information on mesh errors can still be obtained by driving sub-regions of the mesh with appropriate boundary conditions. A code user should also realize that practical implementations of numerical methods (particularly when flux limiters or highly distorted grids are involved) do not always perform at their advertised order of accuracy even in the asymptotic region.

It must be emphasised that this error estimation procedure does not impose an upper limit on the real error, but is an approximation for the evaluation of the quality of the numerical results. The best results are obtained for error estimates when:

- Order of accuracy used in Eqn. 8.1 is obtained from Eqn. 8.2

- All three meshes are in the asymptotic region;

- The solution at the estimation point is continuous with continuous derivatives;

- Points sampled for error analysis are not too close to inflection points in a plot of the target variable vs. the discretized dimension; and

- Any iteration employed in the solution is adequately converged.

Even if it is not possible to obtain results for three meshes within the asymptotic range, there is still hope for useful results from a Richardson analysis. Remember that the asymptotic range comes from consideration of terms in a classic Taylor series based truncation error analysis of the discrete approximations to the PDEs. Richardson analysis is simply an extrapolation using a curve fit to results from a sequence of mesh refinements in the form:

$$\Theta(h) = \Theta_{exact} + a\,h^p. \qquad\qquad (8.4)$$

where h is the relevant mesh (or time step) size. If results for a target variable at the same spatial location for three grids ($\Theta_1$, $\Theta_2$, and $\Theta_3$) lie on a smooth, monotonic curve, then use of Eqn (8.1) with Eqn (8.2) can be expected to give a sensible estimate of the error associated with the finest grid. Although the rigour of the results in the asymptotic range is missing, results in this case can still have value in determining regions where a mesh is inadequate.

Patrick Roache [6] deals with quality of error estimates through the use of a Grid Convergence Index (GCI) to measure error, and a factor of safety ($F_s$) to cover degradation of the error estimate due to results from a grid outside the asymptotic range.

$$GCI = F_s \left| \frac{\Theta_1 - \Theta_2}{\Theta_1} \right| \frac{1}{r^p - 1} . \qquad (8.5)$$

When the three grids used to calculate p are known to be in the asymptotic region, Roache recommends a value of 1.25 for the factor of safety, otherwise he recommends a value of 3.0.

For unstructured meshes, the above considerations are only valid in case of a global refinement of the mesh. Otherwise, the solution error will not be reduced continuously across the domain. For unstructured grid refinement the refinement ratio, $r$, can be defined as follows:

$$r_{effectve} = \left( \frac{N_1}{N_2} \right)^{1/D} \qquad (8.6)$$

where $N_i$ is the number of grid points and $D$ is the dimension of the problem.

We also recommend a visual check on convergence through graphical comparison of selected variables obtained on three grids. The following steps should be followed:

- Define target variable as described in Section 8.2;

- Provide three (or more) grids using the same topology (or for unstructured meshes a uniform refinement over all cells);

- Compute solution on these grids, and ensure convergence of the target variables ;

- Cross-plot selected variables for the different grids;

- Check if the solution is in the asymptotic range.

Plotting experimental data with the results for the two finest grids can give a quick feel for when it is time to go looking for other sources of error in the simulation results.

## 8.6 Time Discretization Errors

To reduce time integration errors for unsteady-state simulations, we recommend use of at least a second order accurate time discretization scheme (see discussion in Section 6.3). For oscillating flows the relevant frequencies usually can be estimated beforehand and the time step can be adjusted to provide at least 10 - 20 steps for each period of the highest relevant frequency. In case of unsteadiness due to a moving front, the time step should be chosen as a fraction of:

$$\Delta t \approx \frac{\Delta x}{U}$$

In this equation, $\Delta x$ is the grid spacing and $U$ the front speed.

Sometimes, under strong grid and time step refinement, flow features can be resolved which are not relevant for the simulation. An example is the (undesirable) resolution of the unsteady-state vortex shedding at the trailing edge of an airfoil or a turbine blade in a simulation with very fine grids and time steps. Another example is the gradual transition of a free surface flow simulation with a statistical Volume-

of-Fluid method to a Direct Numerical (Multi-Phase Flow) Simulation (DNS), with droplet formation, and wave excitation. This is a difficult situation, as it usually means that no grid and time step-converged solution exists above the DNS range, which can usually not be achieved.

In principle, the time dependency of the solution can be treated as another dimension of the solution error estimation. However, a four-dimensional grid study would be very demanding. It is therefore more practical to carry out the error estimation in the time domain separately from the space discretization. Starting with a sufficiently fine space discretization, the error estimation in the time domain can be performed as a one-dimensional study.

Studies should be carried out with at least two and if possible three different time steps for one given spatial resolution. The error estimators given in Section 8.5 can be used, if the spatial grid width is replaced by the time step. The following information should be provided:

- Unsteady-state target variables as function of time step (graphical representation);

- Error estimate based on (time-averaged) target variables;

- Comparison with experimental data for different time step values.

## 8.7    Software and User Errors

Software errors are defined as an inconsistency in the software package. This includes the code, its documentation and the technical service support. Software errors occur when the information provided to the user on the model equations is different from the actual equations solved by the code. This difference can be a result of: coding errors (bugs), deficiencies in the numerical algorithms, errors in the graphical user interface, documentation errors, and incorrect support information.

Many software errors can be detected by the verification tests described above. However, it is the task of software vendors to ensure the functionality of the software through a systematic program of quality control, including extensive testing.   If more than one software package meets a user's modelling needs, it is worth reviewing the quality control procedures for each candidate before making a final selection.

User errors result from the inadequate use of the resources available for a CFD simulation. The resources are for instance the problem description, computing power, CFD software, physical models in the software, and the project time frame. User errors can be caused by: lack of experience, lack of attention to detail, and simple mistakes. Typical user errors are oversimplification of a given problem (geometry, equation system, etc.), poor geometry and grid generation, use of incorrect boundary conditions, selection of non-optimal physical models, incorrect or inadequate solver parameters (time step, etc.), acceptance of non-converged solutions, and post-processing errors.

### 8.7.1    Quality Assurance

The most important step in error control is to understand that errors will occur regardless of the method used to generate source code or input models.  Procedures must be in place to eliminate (or at least minimize) programming or user input errors.  Quality Assurance (QA) procedures are a proven way to control the introduction of bugs and formalize test procedures.  These procedures work well for both code development and application input model development. However, it is important to realize that rigorous adherence to international standards for a QA program carries a fairly heavy price in two respects. Inclusion of formal QA adds at least 30% to the cost of a project.  In addition the system can become rigid

enough that the best CFD practitioners will leave to find a better work environment. However, even if a formal QA program is not in place, it is important to understand and apply the underlying principles.

In addition to discussion of QA principles directly applicable the creation and maintenance of code input models, this section contains a significant amount of information on software QA. This has been provided to aid in judging the adequacy of software verification documentation obtained from code developers.

Four key components of QA are documentation, development procedures, testing, and review. Written standards for these components should be established at the beginning of a project and accepted by all involved. Documentation of a new code or new simulation usually begins with a simple statement of requirements for what must be modelled, what approximations are and are not acceptable, and the form of implementation. A complete written description of the underlying mathematical model provides a basis for verification activities. A clear description should be provided of relevant experiments for use in validation activities. Any uncertainties in the input model and in code models should also be described for later studies of sensitivity of results to model uncertainties. A test plan describes calculations based on the validation experiments, and any necessary verification tests including discretization error studies described in previous sections.

Documentation should be generated in two drafts. The first precedes the creation of software or an input model. When used for a specific system simulation this initial QA document builds on documentation from the PIRT process ( see Section 3.2). The second draft is issued as a final report including the final form implemented and results of all proposed tests. Both drafts should be accompanied by two phases of independent review, the first focusing on the viability of the proposed approach, and the second focusing on the completeness of testing. Combined review of the documentation and actual software or CFD input model is a powerful technique for catching and correcting errors. Even before independent review, the act of describing implementation with words, forces a careful reconsideration of the software or input model. In the case of software QA, this pair of documents should be generated for every significant new capability added to the code.

Code developers should also have a reference QA document providing procedures for code or input model creation that reduce chances for initial introduction of errors, without significant reduction in developers' effectiveness. Software should be easy to read, easy to maintain, and easy to extend. A similar statement can be made for code input, but meeting these objectives is dependent on the choice of CFD code. Relatively simple guidelines can have a major impact on the ability of new software to meet these objectives. Standards should be set for indentation, naming of variables and program units (functions, subroutines, …), capitalization, modularity, data storage and flow, data typing, use of pointers, and internal documentation (comments). Software development should begin by understanding all steps in the problem solution and documenting the storage needed for input, output, and temporary storage. Based on this understanding, appropriate data structures are designed and implemented first, to provide a framework for implementation of the solution algorithm. It is also a good idea to evolve new software from existing code that does all or part of a specific task. This procedure simplifies verification by permitting direct comparison of results from two procedures that should give either the same results or differences that can easily be quantified with side calculations.

Code users also need clear guidelines for documentation of input models, and where appropriate style and order of creation of the input model. However, the first significant step in controlling user errors is to include the quality of the user interface(s) as a strong component in the selection criteria for a CFD software package. Look for capabilities that minimize opportunity for simple typographic errors and provide clear easily accessible guidance in option selection. Important features to consider include:

- the ability to define geometry directly from CAD files:

- automated aids to mesh generation;

- menu driven interface for option selection and specification of initial conditions;

- direct links to useful documentation describing each menu and menu item;

- error checking on inconsistent input and values that are out of range.

For QA of both software and code input consideration should be given to a more automated form of source file documentation via a configuration management procedure. This starts with a systematic record of all changes, dates of change and individuals responsible for the changes. When under software control this level of code management lets you remove old changes to a code or input model if they are found to be inappropriate, and facilitates specialized versions of an application input model for uncertainty or design optimization studies. Automated configuration control has been used for a long time on large software projects, and is being extended to code input files. Two currently popular configuration control tools are CVS and the more recent Subversion, which are both GNU open source software, and free

There are more test options available for software verification than for verification of an input model. These were outlined in the introduction to this chapter, and one (Method of Manufactured Solutions) is described in more detail in the next section. A code verification test suite is built up as verification tests are created for each code option, physical model or field equation added to the code. The problems are designed in conjunction with design of the coding for each new capability, and exercise every aspect of the code update including additions and modifications to all input and output and individual terms in any field equations added to the code. The test set also contains tests important interactions between new and existing code options, A thorough developer will use code coverage software to automatically check all lines of code tested by the verification set. New verification test problems are also used to populate a regression test suite. Here the goal is not to verify a new code feature, but to detect any changes in the operation of that feature as other updates are made to the code. This can usually be accomplished with a subset of the verification test set, and often with simplified versions of individual test problems. The accumulated regression test suite should be run by the code's custodian with each new version to demonstrate that the latest code modifications have not disabled any existing capabilities.

### 8.7.2     *The Method of Manufactured Solutions*

## 9.  VALIDATION OF RESULTS

Once the verification process has limited discretization and iteration convergence errors to acceptable levels, validation of physical models can proceed. This chapter discusses basic considerations for validation, as well as the associated uncertainty analysis needed to build final validation metrics, and to confirm completeness of the validation.

## 9.1    Validation Methodology

In the field of CFD, the real world is modelled first by a Conceptual Model (governing equations), and then by a Computational Model (computer code). Application of the computer code or, more specifically, of one concrete computational path to a scientific or industrial problem leads to a Computational Solution. The Computational Solution should be validated.

As defined in Section 2.3 of this document, **validation** is a process of determining the degree to which a model is an accurate representation of the real world from the perspective of the intended uses of the model (AIAA Guide [5]). Here, real world is a system (engineering hardware), for which a reliable engineering simulation tool is needed.  Such a system is typically very complex with many coupled physical phenomena, taking place in complicated geometry. Therefore, a **tiered approach** is recommended for validation of models of such systems. In Oberkampf and Trucano [7] and Oberkampf et al. [8], the following four progressively simpler tiers are defined:

- Complete System;

- Subsystem Cases;

- Benchmark Cases;

- Unit Problems.

Careful attention to the tiered approach minimizes one of the most insidious problems in code validation, cancellation of errors.  Confidence is built in relevant models contributing to the CFD simulation by first testing isolated physical processes and simple geometries, and then moving up through testing with higher levels of complexity in process interaction.

Validation of a CFD code should then start from the unit problems, where only one element of complex physics is allowed to occur in each problem, so that elements of complex physics are isolated as tractable items. Unit problems are characterized by very simple geometries, very often two-dimensional, or three-dimensional with important geometric symmetry features. Experiments should be on highly instrumented test facilities producing highly accurate data supported by extensive uncertainty analysis of the data for validation calculations at this level. If possible, repeated runs should be performed, even at separate facilities, to aid identification of random and systematic (bias) errors in the experimental data. All the important code input data, initial conditions, and boundary conditions should be accurately measured and documented. If some significant parameters that are needed for the CFD simulation were not measured, reasonable or plausible values for the missing data should be assumed. In this case, an estimation of possible effect of missing information on computed results should be performed. A rigorous (and seldom feasible in the CFD field) approach in this case requires multiple computations and a statistical uncertainty analysis to estimate sensitivity of target variables to the possible range of unknown (or uncertain) system parameters..

Benchmark cases typically involve only two or three types of coupled flow physics in more complex geometry than in the unit problems, retaining the features, critical to these types of physics. Most of the required modelling data, initial conditions, and boundary conditions are measured, but some of the less important experimental data are not measured in some cases. As in the case of unit problems, whenever missing input data are replaced by assumed values, uncertainty analysis should be performed.

For subsystems and complete systems, it is difficult, and sometimes impossible to quantify most of the test conditions required for thorough validation of the computational model. Three or more types of

physics are coupled (some coupling reduction is typical for subsystem cases). Some of the necessary or the most important modelling data, initial conditions, and boundary conditions are measured. There is typically less experimental data and less measurement precision provided at this level than in the case of unit problems and benchmark cases. Taken as stand-alone validation, these factors reduce reliability of detailed conclusions on suitability of the computational model to the intended application. However, taken in conjunction with unit and benchmark tests, subsystem and complete system tests provide necessary validation of interactions between individual process models.

Traditional experiments are intended to improve understanding of the physical world and have been classified by Oberkampf, Trucano [7] as:

- „physical-discovery experiments", which are conducted primarily for the purpose of improving the fundamental understanding of some physical process;

- experiments, conducted primarily for construction or improving mathematical models of fairly well-understood flows;

- Experiments, that determine or improve the reliability, performance or safety of components, subsystems, or complete systems.

Validation experiments have the primary goal of quantifying differences between a portion of the physical world and the equivalent portion of a virtual world. As a result, design of a validation experiment requires both skilled experimentalists, and individuals with detailed knowledge of the contents and behaviour of the simulation tool (both developers and code users). The experiment should be designed to answer questions about a specific application, and the design should be guided by the PIRT process (see Section 3.2) to capture the essential physics of interest, and to measure state variables most sensitive to the relevant model implementations in the code. Special care should be taken with the experiment to obtain initial and boundary conditions for use in the simulation. This includes precision measurements of hardware geometry and instrument location rather than use of dimensions from design drawings. This data as well as data from instrumentation during the experiment should be accompanied by reliable estimates of random (precision) and bias (systematic) errors. In the case of initial and boundary conditions, these errors form the basis of uncertainty analysis for key computed results. For physical state data these errors should be included in consideration of validation metrics.

Scoping studies with the simulation code may provide guidance to the design process. However, the communication of results between experimentalists and analysts should end when it is time to actually perform the experiment, and simulation of the experiment. Results from the two groups should be obtained independently and only compared after each activity is complete. It is common to perform a second post-test round of simulation, but care should be taken that changes to the input model only reflect differences in initial and boundary conditions between design and actual execution of the experiment.

The last step in the validation process is formulation of conclusions. Validation cannot be understood as a binary ("yes" or "no") problem. From an engineering viewpoint, validation is an estimation problem: What is the measure of agreement between the computational result and the experimental result, and how much is the measure affected by numerical error in the computational solution and by the experimental uncertainty? The answers are clearly application dependent and also user dependent. Acceptance criterion is in most cases determined very vaguely, and there is also a risk of faulty conclusions. There is a "model builder's risk", that is risk of rejection of a model when the model is actually valid, based on errors on both computational side and the experimental side, and there is also a "model user's risk" in accepting the validity of a model when the model is actually invalid and the original favourable agreement has compensating, or cancelling errors in the comparisons. Oberkampf and Trucano

believe that compensating error in complex simulations is a common phenomenon. It is also well known, that model user's risk is potentially the more disastrous since it produces a false sense of security. It is also more likely to occur in practice, since there is a tendency to find agreement of results and not to spend more time and resources pursuing possible problems in either the computations or the experiments.

**9.2      Target Variables and Metrics**

Target variables for validation should be selected during the PIRT process (Section 3.2) by the panel of experts. Because PIRT is recognized to be an iterative process, it should be realized that the list of target variables may change as experience is gained with the experiment or with computational scoping studies. Note that target variables may be fundamental quantities such as velocity, temperature, and pressure, or derived quantities such flow rates, heat transfer coefficients or a maximum, minimum, or average over more fundamental data.

Selection of suitable validation metrics is a very important part of the validation process. Oberkampf and Barone [234] provide a detailed discussion of considerations for selection of metrics. Two key considerations are that the metric include a comparison to a reliable measure of experimental uncertainty, and that presentation of metric values not include qualitative judgements such as "very good agreement". It is not the analyst's job to make such judgements. To obtain reliable values for experimental uncertainty, results should be available from redundant validation experiments. With the data from multiple runs of the same experiment, a basic metric would be the difference between a computed value and the mean of the experimental values at the same location, presented with a confidence interval for true experimental data. In this case the metric involves statement of three numbers: the estimated error between results of the simulation and the true experimental value, an estimated range within which the true value of this error lies, and the confidence level that the error lies within the quoted range (usually chosen as 90% or 95% for the statistical analysis). Useful global metrics can be constructed by integrating the local error estimates or corresponding fractional errors over time or space as appropriate. However, the corresponding integration of confidence intervals (or intervals ratioed to the mean experimental value) simply become confidence indicators, due to loss of rigor in the interpretation of the resulting interval. Care must also be taken in using such global metrics because regions with relatively large error may be masked by the averaging process.

To place the metric in the proper perspective, information on experimental error should also be provided, that to the extent possible clearly distinguishes between truly random error, and systematic (bias) error. Consider the hypothetical comparison in Figure 9.1 of calculated and measured mass flow rate at a specific location. The error bars could be the result of phenomena that vary randomly with time during any run of the experiment. Another possibility is that they reflect calibration error resulting in a fixed offset (bias) of data in any given experiment. This offset might vary randomly from experiment to experiment as a result of the calibration process. In later evaluation of validation metrics, the nature of the experimental error in Figure 9.1 can make a significant difference in conclusions about the quality of one or more models used in the numerical simulation. If the error is truly random within each experiment, one might conclude that the simulation adequately captures the physical phenomena. However, if the error is a bias, the simulation misses a key trend in the data, and depending on needs for the final application, one or more relevant models could be judged to be inadequate.
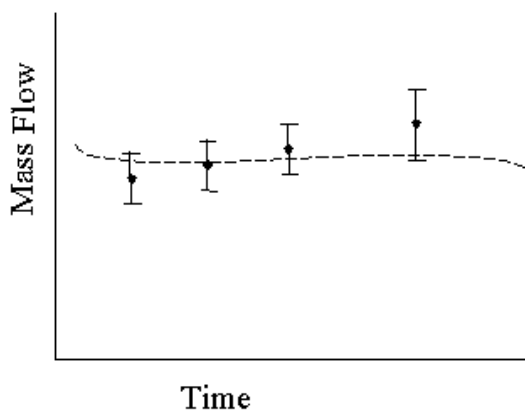
**Figure 9.1  Comparison a calculation to data**

## 9.3      Treatment of Uncertainties

A complete validation process should incorporate knowledge of uncertainty associated both with an experiment and with the associated simulation.   Analysis of experimental uncertainties is well established and described in Section 9.3.1.   Analysis of uncertainty associated with the simulation of an experiment, is more complicated, and a current statistical approach is described in Section 9.3.2.  Although Oberkampf and Truncano [7] present a metric incorporating experimental uncertainty, use of both classes of uncertainty in a quantitative validation metric is still a matter of research.

### *9.3.1      Experimental Uncertainties*

*Overview*

The field of experimental uncertainty analysis has a very long history, although the history of use within nuclear reactor safety is not nearly as long as it should be.  The material in this section is based on relatively recent attempts to standardize the process in the ISO, "***Guide to the Expression of Uncertainty in Measurement"*** (hereafter referred to as the ISO Guide) [235], the AIAA Standard S-071-1995 "***Assessment of Wind Tunnel Data Uncertainty"*** (hereafter referred to as the AIAA Standard) [236], and the ASME PTC 19.1-1998 "***Test Uncertainty"*** (hereafter referred to as the ASME PTC) [237].   Two key terms defined in this discussion are "accuracy (of measurement)" and "error (of measurement)", respectively defined as "the closeness of agreement between a measured value and a true value of the measurand" and "the true, unknown difference between the measured value and the true value".

The ISO Guide defines the term "uncertainty (of measurement)" as a "parameter, associated with the result of a measurement that characterizes the dispersion of the values that could reasonably be attributed to the measurand". The AIAA Standard and the ASME PTC define the term "uncertainty (of measurement)" as "an estimate of measurement error" and "an interval about the measurement or result that contains the true value for a given confidence level", respectively.

The ISO Guide classifies uncertainties into two groups according to the way in which their numerical value is estimated. Those which are evaluated by statistical methods are *category-A*, and those which are evaluated by other means are *category-B*. The AIAA Standard and the ASME PTC recommend

the classification system for uncertainties by their effect. That is, if an uncertainty source causes scatter in test results, it is a random uncertainty and has been caused by *random errors*. If not, it is a systematic uncertainty and has been caused by *systematic errors*. However, the estimation procedures for the *category-A* and *-B* uncertainties are almost identical to those for the random and systematic uncertainties, respectively.

If the nature of an elemental error is fixed over the duration of the defined measurement process, then a 95% confidence estimate of the error is classified as a systematic uncertainty. If the error source tends to cause scatter in repeated observation of the defined measurement process, then the error source contributes to the random uncertainty.

In nearly all experiments, the measured values of different variables are combined using a data reduction equation to form some desired result. A general representation of a data reduction equation may be

$$R = f(\overline{X}_1, \overline{X}_2, \ldots, \overline{X}_J) \qquad (9.4.1)$$

where $R$ is the experimental result determined from $J$ measured variables $X_i$. Each of the measured variables contains systematic errors and random errors. These errors in the measured values then propagate through the data reduction equation, thereby generating the systematic and random errors in the experimental results $R$. Figure 9.2 illustrates the propagation of errors into an experimental result.
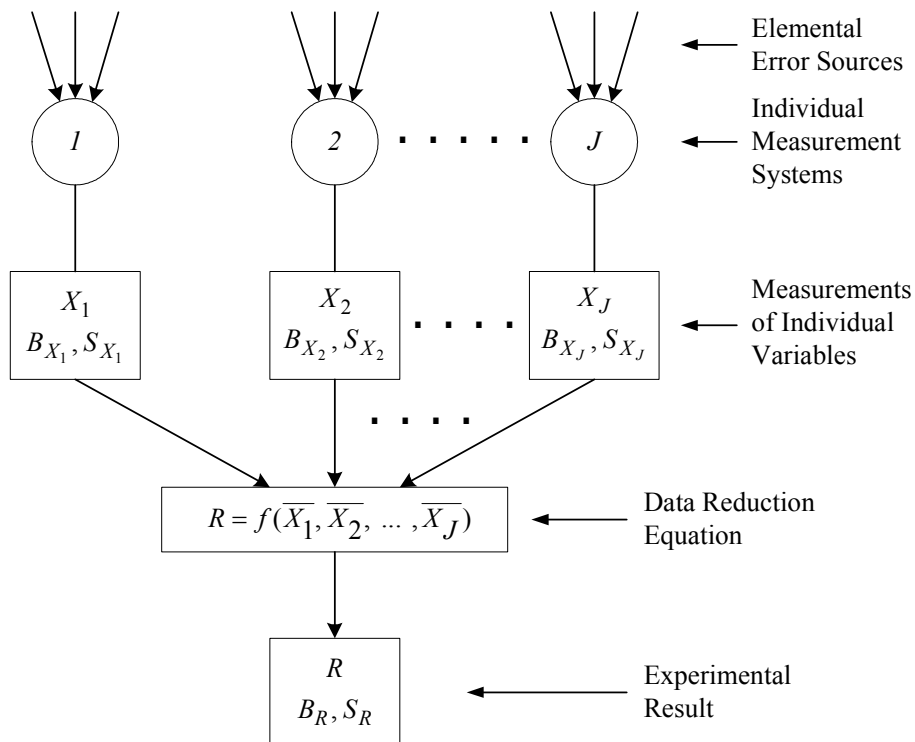


**Fig. 9.2  Propagation of errors into an experimental result**

The ISO Guide, the AIAA Standard, and the ASME PTC recommend a simplified $U_{RSS}$ uncertainty estimation model for the vast majority of engineering experiments. With this model, several simplifying assumptions have been made, namely:

(a) All random uncertainty sources are estimated as $2S_{\overline{X}}$, which is a 95% confidence estimate of the effect on the average of a particular random uncertainty source.

(b) These uncertainty estimates are grouped as systematic or random and root-sum-squared to obtain the systematic (B) and random (P) uncertainties of a measurement for large samples.

(c) These are then root-sum-squared to obtain a 95% confidence uncertainty as follows:

$$U_{95} = \left[B^2 + P^2\right]^{1/2} = \left[B^2 + \left(t_{95}S_{\overline{X}}\right)^2\right] = 2\left[(B/2)^2 + \left(S_{\overline{X}}\right)^2\right]^{1/2} \qquad (9.4.2)$$

Here the multiplier 2 is really Student's $t_{95}$ (the coverage factor for 95% confidence level) which is taken as 2 for more than 30 degrees of freedom. The AIAA Standard suggests that the coverage factor for 95% confidence level be taken as 2 if the number of samples is larger than 10, i.e. the degree of freedom is higher than 9.

Frequently in this analysis all systematic uncertainty sources are assumed normally distributed and are estimated as $2\sigma$ for 95% coverage. However, justification for this is weak. See the discussion in Section 9.3.2 and the references provided in that section for more rigorous approaches to this aspect of the problem.

*Uncertainty of Measurements of Individual Variables*

The total uncertainty in a measurement is the combination of uncertainties due to both systematic error and random error. The ASME PTC divides uncertainty sources introduced in a measurement process into following categories:

(1) Calibration uncertainty

(2) Data acquisition uncertainty

The ASME PTC and the AIAA Standard recommend performance of an overall system calibration or an end-to-end calibration under operating conditions to minimize the systematic uncertainty that can arise from errors in the transducers or sensors, the signal conditioning devices, the recording devices, etc.

(3) Data reduction uncertainty

The typical uncertainty source in this category stems from curve fits.

(4) Uncertainty due to methods

The ASME PTC defines these uncertainties as additional uncertainty sources that originate from the test techniques or methods inherent in the measurement process. The ASME PTC provides some common examples as follows:

- uncertainty in the assumptions or constants contained in the calculation routines;

- uncertainty due to intrusive disturbance effects caused by installed instrumentation;

- spatial or profile uncertainty in the conversion from discrete point measurements to station averages;

- environmental effects on probes such as conduction, convection, and radiation;

- uncertainty due to instability, non-repeatability, and hysteresis of the test process

Some of these uncertainties are more difficult to estimate than the uncertainties in other categories, and might not be considered appropriately in uncertainty estimation.

(5) Uncertainty due to the physics of the process under investigation

A typical example of this uncertainty source would be variation in measurements due to the presence of turbulence in a flow experiment, especially in a turbulent mixing experiment. Even with no uncertainty associated with instrumentation or boundary conditions, turbulence will produce uncertainty in final measured values for many state variables.

(6) Others

Estimation of Random Uncertainty

Since random error introduces variation or scatter in repeated measurements (or readings) of a parameter, the uncertainty due to random error may be estimated by inspection of the measurement scatter. An estimate of the population standard deviation is the standard deviation of the data sample, determined by:

$$S_X = \sqrt{\sum_{k=1}^{N} \frac{\left(X_k - \overline{X}\right)^2}{N-1}} \qquad (9.4.3)$$

where $N$ is the number of measurements made and $\overline{X}$ is the mean of the individual measurements $X_k$ given by

$$\overline{X} = \frac{1}{N} \sum_{k=1}^{N} X_k \qquad (9.4.4)$$

When a mean value of $X_i$ is used to determine the experimental result ($R$), as shown in Eq. (9.4.1) and Fig. 9.2, the appropriate estimate of the population standard deviation is the standard deviation of the sample mean which is given by

$$S_{\overline{X}} = \frac{S_X}{\sqrt{N_m}} \qquad (9.4.5)$$

The random uncertainty of the mean of the measurement of the individual variable is given by

$$P_{\overline{X}} = t_{95} S_{\overline{X}} = 2 S_{\overline{X}} = 2 \frac{S_X}{\sqrt{N_m}} \qquad (9.4.6)$$

when the degree of freedom is sufficiently large so that $t_{95} = 2$ can be used for the multiplier (large sample assumption). The ISO Guide, the AIAA Standard, the ASME PTC, and other literatures

[238, 239] provide the detailed method to calculate the degree of freedom and the coverage factor of the student $t$-distribution for small sample case.

The AIAA Standard suggests that a consideration of the appropriate time interval for collection of $N$ readings (or measurements) be critical if the appropriate estimate of the population standard deviation is to be estimated. Consider, for example, a steady experiment in which some of the test variables have a time variation shown typically in Fig. 9.3. If the time interval for collecting $N$ readings is much shorter than the interval for variation of some of the variables, a value of $X_i$ determined over such a relatively short time interval $\Delta t_1$ should be considered as a single reading whether the value of $X_i$ is the average of 10, $10^3$, or $10^6$ readings taken during $\Delta t_1$. Therefore, the population standard deviation should be estimated by the standard deviation of a data sample given by Eq. (9.4.3). On the other hand, if the collection of $N$ readings is taken during the time interval $\Delta t_2$ which is much longer than the time interval of the variation of $X_i$, then the appropriate estimate of the population standard deviation is the standard deviation of the sample mean given by Eq. (9.4.5).



*Time, t*
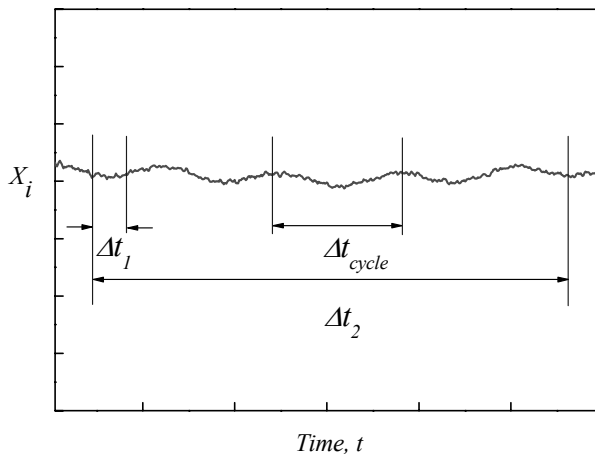
**Fig. 9.3 Variation of a variable X$_i$ with time for a steady experimental condition**

Another important consideration is how to define the number $N_m$ in Eq. (9.4.5) when the collection of readings is made during the time interval $\Delta t_2$. There are some candidates for the number $N_m$ such as the total number of readings, $N$ in Eq. (9.4.3), the number of cycles of the variation of the variable $X_i$ during the time interval $\Delta t_2$, etc.

With regard to the total number of readings, the larger number of readings during the same time interval gives more accurate statistical estimation of the population when the data reading rate is comparable to the major change rate of the variable $X_i$. In this case, the number $N_m$ can be defined as the total number of readings ($N$) taken during the time interval $\Delta t_2$. However, beyond a certain data reading rate that is sufficiently high enough to reflect all the subtle changes of the variable $X_i$, the higher data reading rate does not actually give an improved statistical estimation of the population because it is the case that we have multiple replicated identical elements in a sample space. Therefore, the random uncertainty of a measurement will be underestimated if the number $N_m$ is defined as the total number of readings ($N$) taken with the sufficiently high data reading rate during the time interval $\Delta t_2$. On the other hand, the upper bounds estimate of the random uncertainty of a measurement will be given if the number $N_m$ is defined as the number of cycles of the variation of the variable $X_i$ during the time interval $\Delta t_2$, i.e.,

$N_m = \dfrac{\Delta t_2}{\Delta t_{cycle}}$ . Unfortunately, the existing literature does not provide detailed guidance about the choice of

*sampling rate*. Therefore, it is wholly dependent on an uncertainty analyst how to define the number *N*, and the analyst should report the detailed information about the number *N*.

Estimation of Systematic Uncertainty

The estimate of systematic uncertainty is based on engineering judgment and analysis of elemental systematic errors. The ASME PTC provides the following examples for the basis of the estimation:

- comparison of standards with instruments used in the actual test environment;

- documents from instrument manufacturers and other references;

- inter-laboratory or inter-facility tests;

- comparison of independent measurements that depend on different principles or that have been made by independently calibrated instruments;

- special calibrations which perturb a known cause of systematic error through its complete range to determine the range of systematic uncertainty;

- model of the process which is known to generate the error;

- engineering judgment or experience.

The systematic uncertainty of the measurements of the individual variables is the root-sum-square of the elemental systematic uncertainties ($b_i$) for all elemental error sources in Fig. 9.2

$$B = \left[ \sum_{i=1}^{K} b_i^2 \right]^{1/2} \qquad (9.4.7)$$

where *K* is the total number of systematic error sources. For each error source in the measurement, the elemental systematic uncertainty must be estimated from the best available information.

*Uncertainty of an Experimental Result*

Uncertainties in measurements of individual variables are propagated to the result through the data reduction equation of Eq. (9.4.1). The effect of the propagation can be approximated by the Taylor series method.

When a set of individual variables ($\overline{X}_i$) is measured in and experiment and a single result (*R*) is calculated, this case is called a single test result. If multiple test results can be run at the same condition and each parameter is measured during each test, then these multiple sets of data can be used to determine multiple results. The reported result will usually be the mean of the results ($\overline{R}$). This is called a multiple test result.

In the calculating error associated with a result R, the sensitivities of R to the individual variables ($\overline{X}_i$) are needed.  . The sensitivity coefficient of each variable is defined as:

$$\theta_i = \frac{\partial R}{\partial \overline{X}_i} \qquad (9.4.8)$$

Random Uncertainty of a Result

Single Test

When a test result is given by Eq. (9.4.1), the ASME PTC suggests that the standard deviation of a single test result may be determined from the propagation equation as

$$S_R = \left[ \sum_{i=1}^{J} \left( \theta_i \cdot S_{\overline{X}_i} \right)^2 \right]^{1/2} \qquad (9.4.9)$$

where $S_{\overline{X}_i}$ is the standard deviation of the mean of each individual variable obtained from Eq. (9.4.5).

The random uncertainty of a single test result for the large sample condition is given by

$$P_R = t_{95} S_R = 2 S_R \qquad (9.4.10)$$

On the other hand, the AIAA Standard gives the following suggestion for a single test with averaged readings. If an experiment is run such that all of the $X_i$ could be determined as averages over appropriate time intervals, then multiple individual test results can be determined, and the standard deviation of an experimental result should be determined from the method for the multiple tests, not from the above propagation equation.

This suggestion can be interpreted as follows: Each experimental result ($R_k$) is not determined from the measured means of individual variables ($\overline{X}_i$) but determined from single measurements of individual variables ($X_{i,k}$), thus N experimental results are evaluated and finally the experimental result ($R$) is obtained from the arithmetic mean of $N$ experimental results ($R_k$). In this case, the standard deviation of the mean of experimental results is expressed by

$$S_R = \frac{1}{\sqrt{N_m}} \left[ \sum_{k=1}^{N} \frac{\left( S_k - \overline{S} \right)^2}{N-1} \right]^{1/2} = \frac{1}{\sqrt{N_m}} \left[ \sum_{k=1}^{N} \frac{\left( S_k - \overline{S} \right)^2}{N-1} \right]^{1/2} \qquad (9.4.11)$$

where $N_m$ holds the same meaning with $N_m$ in Eq. (9.4.5).

When the degree of freedom is sufficiently large, the random uncertainty of the mean of experimental results is also given by Eq. (9.4.10).

Multiple Tests

When more than one test is conducted with the same instrument package and under the same test conditions, the average result is given by

$$\overline{R} = \frac{1}{M} \sum_{i=1}^{M} R_i \qquad (9.4.12)$$

where $M$ signifies the number of tests available.

The estimate of the standard deviation of the distribution of the results is

$$S_R = \left[ \sum_{i=1}^{M} \frac{\left(R_i - \overline{R}\right)^2}{M-1} \right]^{1/2} \qquad (9.4.13)$$

where $S_R$ includes random errors within tests and variation between tests.

The sample standard deviation and the random uncertainty of the mean result from multiple tests are respectively given by

$$S_{\overline{R}} = \frac{S_R}{\sqrt{M}} \qquad (9.4.14)$$

$$P_{\overline{R}} = \frac{t_{95} S_R}{\sqrt{M}} = \frac{2 S_R}{\sqrt{M}} \qquad (9.4.15)$$

when the large sample assumption is adequate.

The random uncertainty of the multiple tests includes the variation among the results due to the imperfect reproduction of test conditions and/or test procedure, which is not contained in the random uncertainty of the single test. Therefore, the random uncertainty of the multiple tests does not always give lower value than that of the single test, especially when the test result is very sensitive to the change of some individual variables and the reproducibility of these variables is not satisfactory.

The variation of the test results due to the imperfect reproduction of test conditions and/or test procedures may be handled by normalizing the test results, as proposed in the example of the ASME PTC.

Systematic Uncertainty of a Result

When the results are given by Eq. (9.4.1), the systematic uncertainty of a result is expressed by the systematic uncertainties ($B_{\overline{X}_i}$) of the measurements of the individual variables ($X_i$) by

$$B_R = \left[ \sum_{i=1}^{J} \left( \theta_i \cdot B_{\overline{X}_i} \right)^2 \right]^{1/2} \qquad (9.4.16)$$

The special cases of correlated systematic uncertainties and asymmetric systematic uncertainties are dealt in detail in Ref. [240] and [241], respectively.

Total Uncertainty of a Result

The 95% confidence total uncertainty of a result is determined by the root-sum-square of the systematic and random uncertainties. When the degree of freedom is sufficiently large, the total uncertainty is given by

$$U_{R_{95}} = \left[ B_R^2 + P_R^2 \right]^{1/2} = \left[ B_R^2 + \left( t_{95} S_R \right)^2 \right] = 2 \left[ \left( B_R / 2 \right)^2 + \left( S_R \right)^2 \right]^{1/2} \quad (9.4.17)$$

where $B_R$ is obtained from Eq. (9.4.16) and $S_R$ is obtained from either Eq. (9.4.9) and (9.4.11) for single test result or from Eq. (9.4.14) for multiple tests result.

### 9.3.2    *Uncertainty in the Simulation Results*

Generally uncertainty analysis for CFD calculations is done at a very simple level in which response to variation of individual parameters is observed.  This is a simple sensitivity analysis, normally restricted to location and perhaps magnitude of boundary conditions (see the following two subsections. This limited approach is primarily driven by research deadlines and limits on computer resources. However, the more rigorous uncertainty analysis now associated with use of best estimate calculations in formal reactor licensing is applicable to CFD calculations.  The primary guideline for anyone wishing to attempt this level of uncertainty analysis for CFD is to purchase large parallel computer clusters.  This uncertainty analysis works exceptionally well at a facility with a large number of processors to run all of the necessary variations on the base simulation. More discussion of statistical uncertainty analysis is provided in Section 9.3.2.3.

*Inlet boundary position and inlet boundary condition*

It is well known that the choice of inlet boundary position and inlet boundary conditions (turbulence level, variation in inlet velocity field in space and time) can have a significant influence on the flow pattern far downstream from the inlet. Sensitivity tests should be applied as part of the quality assurance for the simulation project.

Experience concerning the impact of boundary conditions has been gained within projects such as the EU Project FLOMIX-R [18, 242].  This project was aimed at describing the mixing phenomena relevant for both safety analysis (particularly in steam line break [242] and boron dilution scenarios), and mixing phenomena of interest for economical operation and the structural integrity. Measurement data from a set of mixing experiments, gained by using advanced measurement techniques with enhanced resolution in time and space were used to improve the basic understanding of turbulent mixing and to provide data for CFD code validation.  Turbulent mixing in one-phase flow was investigated in the complex geometry of a reactor pressure vessel (RPV) with structures representative of  lower plenum internals and the core support plate. Target variables were the distribution of a tracer solution concentration at the core inlet. For code validation purposes, tracer concentration and velocity distributions in the downcomer were measured and compared with CFD results.

Sensitivity tests on inlet boundary position and inlet boundary condition have been performed for this special application. It was concluded, that the inlet boundary conditions are of minor importance, if the inlet boundary position was put far upstream from the RPV inlet nozzle (inlet boundary position A in Fig. 9.4). This is of special importance in the case of low flow rates and the occurrence of density differences, when stratification occurs in the cold leg pipe.

In cases with high flow rates (high momentum injection), results were not sensitive to inlet boundary conditions like inlet value of turbulent energy or radial distribution of velocity and turbulent energy over the inlet pipe cross section even at an inlet positioned close to the downcomer (inlet boundary

position B in Fig. 9.4). The major influence on the flow field in the downcomer is the impinging jet from the loop onto the inner downcomer wall, and perhaps the downcomer cross section extension below the inlet nozzles. As a result, the assumed turbulence values at the inlet nozzles do not play an important role for the flow field and mixing in the downcomer. Slightly different results were achieved if the concentration profile was changed at the same inlet position. For the momentum driven mixing cases, modelling of the four cold legs, bends, gave only slightly different results compared to having an inlet close to the downcomer.

*Outlet boundary position and outlet boundary condition*

The influence of the outlet boundary position on the flow field and mixing in the flow domain is normally small if the position is far away from the area of interest. However, backflow from the outlet into the flow domain could influence the results and should be avoided if possible. The use of a pressure controlled outlet boundary condition should be used instead of a mass flow outlet condition. For the fluid mixing simulations in the downcomer and lower plenum of the reactor pressure vessel, it was sufficient to put the outlet boundary position above the core inlet plane.
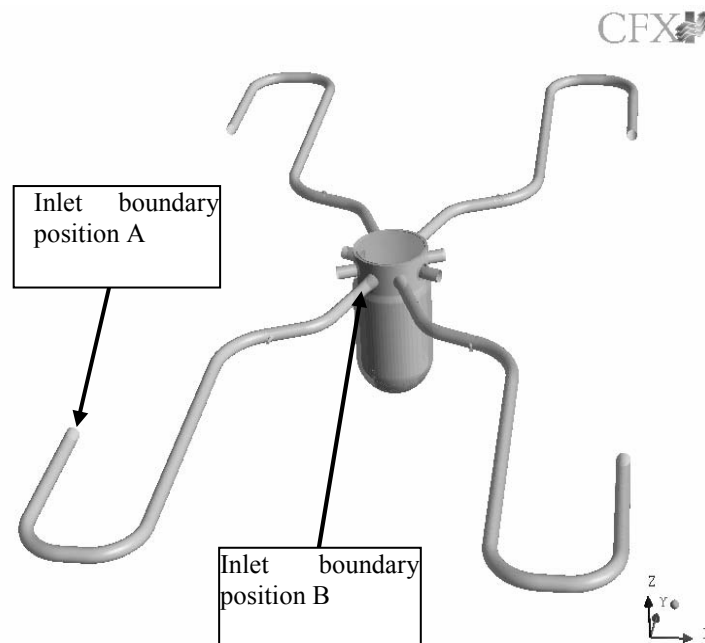


Fig. 9.4 Sketch of the ROCOM mixing test facility with indication of inlet boundary positions

*Statistical Uncertainty Analysis*

Anyone applying CFD to NRS problems should start by understanding the uncertainty methodologies accepted by their regulatory authorities. Most such methodologies are currently based on application of order statistics and Wilkes formula [243, 244]. This class of analysis begins with the specification of probability density distributions for uncertain input or other parameters associated with the

simulation. Next a set of simulations are run using a Monte Carlo approach with these distributions for random selection of the parameters in each run. Results for a specific target variable (say peak clad temperature) are collected from the set of runs and ordered by their magnitude. A desired confidence level $\beta$ (often 95%) is set for the proposition that the highest obtained value of the result lies at or above a value $\gamma$ of its cumulative probability distribution (also usually 95%). When values of $\beta$ and $\gamma$ are selected for a single output, Wilkes formula provides a way to obtain the necessary number simulations ($\beta=1-\gamma^N$). Generalizations of Wilkes formula are also available when a level of confidence is needed for more than one output from a given set of runs.

Descriptions and examples of this approach can be found in papers by Glaeser [245] and Guba et al [246]. An interesting discussion on alternate approaches and interpretations can be found in a string of papers in the journal "Reliability Engineering and System Safety" [247, 248, 249].

Application of a statistical methodology lends credibility to bounds placed on results from simulation. However, the analyst should always remember that the results are only as good as the input. In this case the results depend heavily on selection of an appropriate list of uncertain parameters, and selection of appropriate probability density functions for these parameters. This information should flow from the PIRT process.

Selection of probability density function begins by considering whether each parameter exhibits aleatory or epistemic uncertainty (see Section 2.3). For aleatory uncertainty a probability density function can be obtained from theory and/or experiment. Often experimental results are used to provide a mean and standard deviation for a normal distribution. In a common instance of epistemic uncertainty insufficient information exists to precisely assign the value of a model parameter. Treatment of this uncertainty begins with an attempt to establish credible bounds on the parameter's value.. Most statistical uncertainty analyses model the lack of knowledge about this parameter by a uniform density function between these bounds. However, current research in this area indicates that there are more defensible approaches to providing epistemic parameters to a statistical uncertainty study. Some of this research has been summarized in a special edition of Reliability Engineering and System Safety (Vol. 85), edited and introduced by Helton and Oberkampf [250]. Evidence theory is a promising approach to dealing with this form of uncertainty. Helton et. al. [251] describe the application of evidence theory to sensitivity analysis. Oberkampf and Helton [252] provide a good summary of evidence theory in this context.

In some instances what appears on first sight to be an aleatory parameter, may need to be treated as a combination of aleatory and epistemic parameters. A quantity that is fundamentally stochastic may have been characterized by an experiment with insufficient data. A probability density function can be specified, but the mean value and/or standard deviation may be sufficiently uncertain that they must be represented by epistemic parameters.

With the procedure programmed to randomly set uncertain parameters of the simulation, make at least one check of the uncertainty analysis on a validation test problem. If the uncertainties calculated for key outputs do not bound the data, choices of uncertain input parameters and their probability density functions should be reviewed. This review can be aided by performing a global sensitivity analysis of outputs to the input parameters. This type of sensitivity study also serves as a check of phenomena ranking in the original PIRT process, and either reinforces confidence in the validation set, or suggest a need for additional validation. This sensitivity study should be performed even if the uncertainty study associated with a validation test properly bounds the data.

# 10.    DOCUMENTATION

It is necessary to document the content and results of any thermal-hydraulic computation, especially of verification or validation of a code/computation. Relevant information must be recorded, archived, and disseminated. The documentation must be complete, consistent and readable.

In any organization doing thermal-hydraulic computational analyses, a record management system must be established and documented. This represents a long-term activity. A good record of the simulation should be kept with clear documentation of assumptions, approximation, simplifications, geometry, and data sources. The documentation of the calculations should be organized so that another CFD expert can follow what has been done. The level of documentation required can depend strongly on the customer requirements as specified in the problem definition.

The ECORA project Best Practice Guidelines [1] contain proposals for the structure of three types of documents (Test Case Selection Report, Existing CFD Results Evaluation Report, and Validation Report) to be used within the project. General guidance on the content and form of appropriate documentation based on a long-term experience can be found in Trucano et al. [249]. According to this source, the following information should be included in any report on a thermal-hydraulic analysis (abridged):

1.  Information about the code application, the origin of this application, the particular modelling requirements that this application creates, and characterization of uncertainties that are associated with the application.

2.  Detailed discussion of the physical phenomena in the PIRT that are being validated by the computation.

3.  A comprehensive discussion of verification activities, both of the code and calculation, centered on the intended application.

4.  Documentation of how the code was used in the definition, design, and analysis of each validation experiment. Enough information should be included to allow repetition of the described calculations by others. Such information includes mesh construction information, calculation geometry, computational initial and boundary conditions, computational model inputs such as material-model input specifications, and selection of computational algorithm parameters such as iterative tolerances and numerical smoothing parameters.

5.  A complete description of each experiment, sufficient to allow experimental replication in the future.

6.  A description of the analysis of experimental data. It is important to document information about the uncertainty in the acquired experimental data, including estimation of both random and bias errors with information on the methods of these estimations.

7. The methods and results of the validation metrics (a synonym for "measure") applied in the validation experiment activity including definition of success and failure criteria for these metrics.

8. A characterization of the credibility of the code for the specified application, based on the results from the application of the defined validation metrics and the assessment.

9. Information about the contribution of the validation activity to the BE+U ("best-estimate+uncertainty") paradigm for predictive code application. A discussion should be given for the sources of uncertainty that were considered, as well as those sources that were neglected. Assumptions should be discussed concerning any probabilistic analyses.

Given the scope of this information, it should be evident that one or more documents will sometimes be required to archive all of the proposed content. Especially in the case of code validation, detailed description of experiment(s) is needed including evaluation of measurement uncertainties. When a demonstration simulation of a real industrial problem is attempted, preparation of a PIRT before the start of simulation is essential together with corresponding scaling considerations.

## 11.     SPECIAL CONSIDERATION OF SPECIFIC NRS CASES

### 11.1     Boron Dilution

#### 11.1.1     Key phenomena

During so-called boron dilution transients at pressurized water reactors, slugs of weakly borated water might be formed in one of the primary system loops due to different external or internal mechanisms (failure of the water make-up system, steam generator tube break, reflux-condenser mode during small break LOCA). By starting the coolant circulation in the corresponding loop (inadvertent pump start-up, re-start of natural circulation) the under-borated slug might enter the reactor core. This results in the insertion of positive reactivity and possibly leads to a power excursion. In this case the amount of reactivity insertion depends on spreading of the cold leg flow at the core barrel and subsequent turbulent mixing in the downcomer and lower plenum of the reactor pressure vessel (RPV).  In the case of start-up of the main coolant pump, the mixing is momentum controlled. In the case of low flow rates and higher density differences between the slug and the ambient water, the mixing forced by buoyancy forces. The specific case of slug mixing during pump start-up will be described below. Key phenomena include: the transition from resting fluid via laminar flow to turbulent flow; the jet impingement at the core barrel; the splitting of the flow into two main jets to the left and to the right of the core barrel; secondary flows in various parts of the downcomer; and a re-circulation area below the injection nozzle.

#### 11.1.2     Solution strategy

The solution strategy is based on the validation of the CFD models against experiments at test facilities before simulating the real plant transients. An experimental data base on turbulent mixing has been created within  the EC research project FLOMIX-R [255]. The objective of the project was to obtain complementary and confirmatory data on slug mixing using improved measurement techniques with enhanced resolution in space and time.  Results have contributed to the validation of CFD codes for the analysis of turbulent mixing problems.  A few benchmark problems based on selected experiments have been used to study the effect of different turbulent mixing models under various flow conditions, to investigate the influence of the geometry, the boundary conditions, the grid and the time step in the CFD analyses according to the ECORA Best Practice Guidelines [1].

The CFD analysis described here is for a slug mixing test performed at Rossendorf's ROCOM mixing test facility.  This is a 1:5 scaled model of a German Konvoi type reactor, including four loops with fully controllable main coolant pumps. The RPV model is manufactured from transparent acryl.  Mixing is determined from electrical conductivity measurements of the distribution of a salt tracer solution [254]. Higher measured salinity corresponds to higher boron dilution, or lower boron concentration.

#### 11.1.3     Geometry, grid, numerical schemes and model features

The geometric details of the vessel internals have a strong influence on the flow field and hence on the mixing. Therefore, an exact representation of the inlet region, extension of the downcomer below the inlet region and the obstruction of the flow by the outlet nozzles cut through the downcomer is necessary.

In the CAD-File all geometrical details are modelled accurately, such as: inlet nozzles including the diffuser; orifices of the outlet nozzles; the downcomer extension; the lower plenum; the core support plate; the perforated drum; the core simulator; the upper plenum; and the outlet nozzles. No additional physical models (Porous media, Body Forces) are necessary. The following internals were modelled in detail:

- The core plate contains 193 orifices with a diameter of d=20 mm each.

- The core contains 193 fuel element dummies. The fluid flows through the hydraulic core simulator inside the tubes. Although it was found in [242], that the influence of the core structure on the flow and mixing pattern at the core inlet is rather small, this region was also modelled in detail.

- The perforated drum contains 410 orifices of 15 mm diameter. The advantage of modelling the drum with the original geometry is a detailed study of the flow phenomena in the lower plenum, the disadvantage is the high numerical effort. Sensitivity tests on the influence of different ways of modelling the perforated drum (e.g. porous media, resistant coefficients, reduced number of holes) are presented in [242].

*Grid features*

RPV                                              Horizontal cut: Inlet nozzle plane (Hexa),
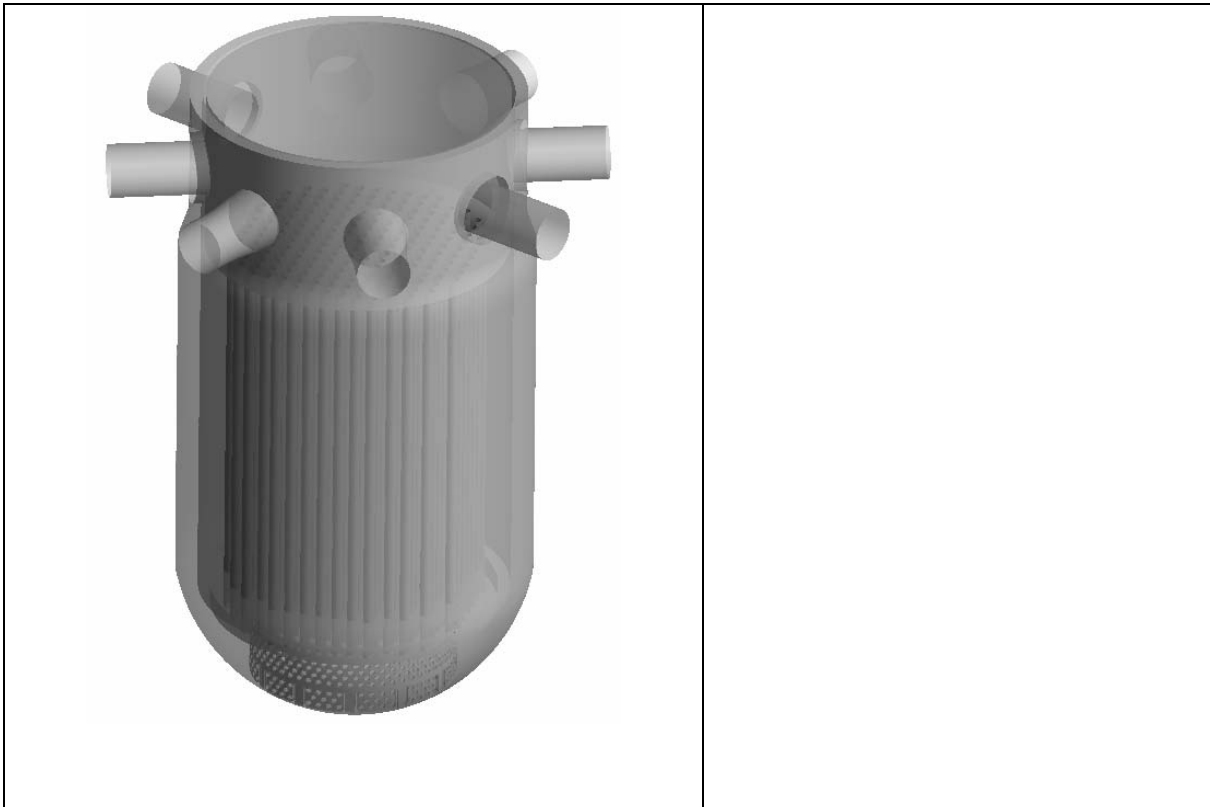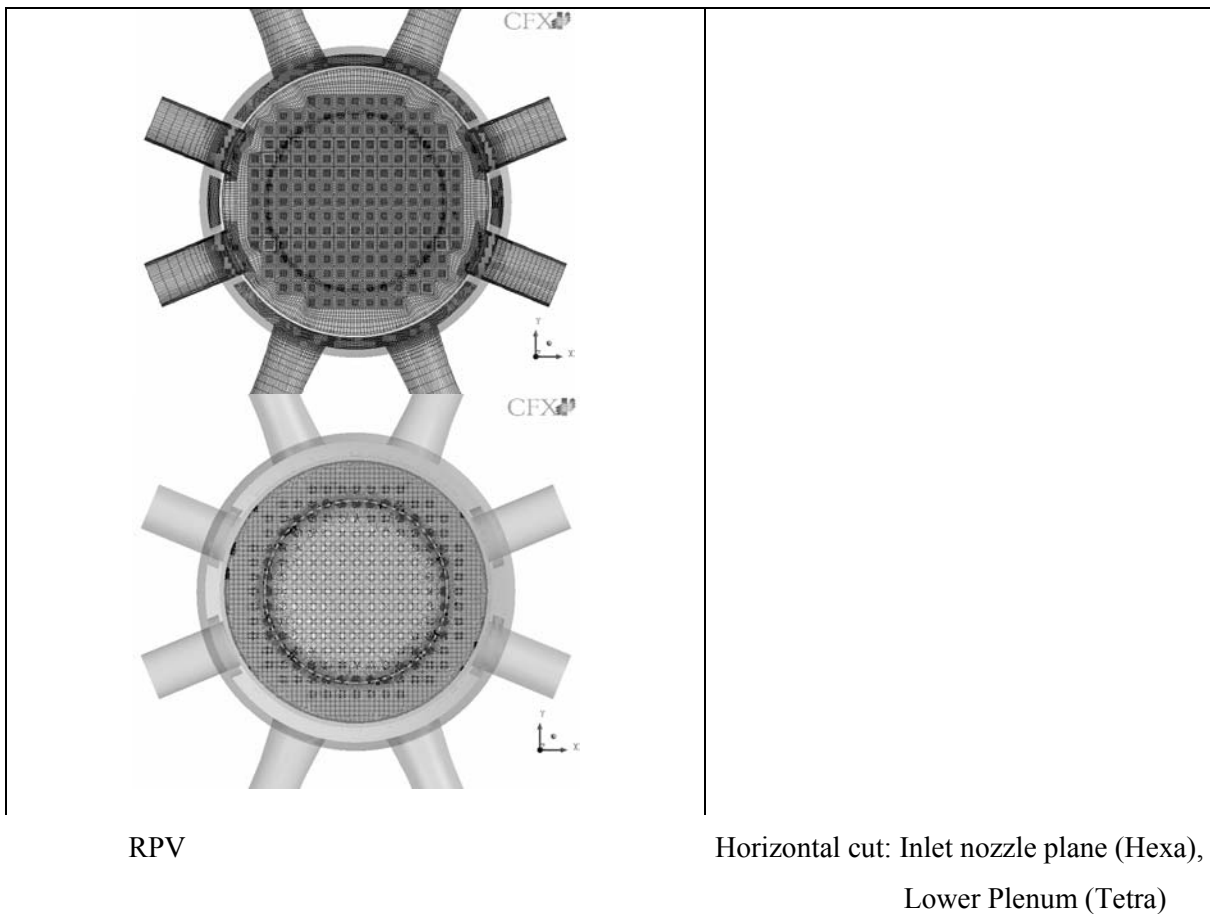
Lower Plenum (Tetra)

**Figure 11.1. Hybrid mesh based on tetrahedral and hexahedral elements**

The CFD code used for this analysis was ANSYS CFX-10. A hybrid mesh was used to model the RPV. The upper part was modelled with 1.2 million hexahedral cells, and the lower plenum including the perforated drum with 2.3 million tetrahedral elements. In addition 470000 wedges and 26000 pyramids were needed to optimize the grid (Figure 11.1). Mesh refinement was used in the area of the perforated drum and in the lower core support plate, and the Laplace grid-smoothing algorithm has been utilized.

*Discretization schemes*

The calculations were done with the CFX "High Resolution" option for spatial discretization, which adjusts local discretization to provide something close to second order spatial accuracy. The CFX "Fully implicit 2$^{nd}$ order backward Euler" option was chosen for integration in time. For both discretization schemes the target variable does not change significantly for iteration convergence criteria below 10$^{-4}$. The round-off error was studied by comparing the results obtained with single and double precision. No difference was observed.

*Time step*

Calculations have been performed with 3 different time steps: 0.05 s; 0.1 s and 0.5 s. An optimum with respect to computation time and convergence of the solution was achieved for a time step size of 0.1 s. The differences in the solutions between 0.05 s and 0.1 s time step sizes were small.

*Boundary conditions and model selection*

The inlet boundary conditions (velocity, mixing scalar etc.) were set at the inlet nozzles. No specific velocity profile is given. As an initial guess the CFX defaults for the turbulent kinetic energy and the dissipation rate were used. The outlet boundary conditions were pressure controlled and set at the outlet nozzles. Passive scalar fields were used to simulate transport of water salinity, used in the experiment to re describe the boron dilution processes. In loop 1 the pump starts linearly from 0 to 185 m³/h in 14 s, after 14 s the mass flow rate is constant at 185 m³/h, counter flows are developing at the other 3 loops. The initial space averaged value of the mixing scalar at the inlet nozzle of Loop 1 was used as the inlet boundary condition.

Calculations have been performed with the following turbulence models and wall boundary conditions:

| Turbulence model | Wall treatment |
|---|---|
| k-ε-Standard Turbulence Model | adiabatic with scalable logarithmic wall functions |
| Shear Stress Transport Turbulence Model | adiabatic with automatic Menter modified wall functions |
| Reynolds Stress Turbulence Model | adiabatic with scalable logarithmic wall functions |

In the case of a highly turbulent flow these three selections for turbulence modelling gave almost the same results for the velocity and mixing scalar profile in the downcomer. However, the SST model was preferred as it is more accurate than the k-ε model near the wall.

### 11.1.4 Results of the boron dilution transient

Due to a strong impulse driven flow at the inlet nozzle the horizontal part of the flow dominates in the downcomer (Figure 11.2). The injection is distributed into two main jets by impact on the core barrel, the so-called butterfly distribution. In addition several secondary flows are seen in various parts of the downcomer. Especially strong vortices occur in the areas below the non-operating loop nozzles and also below the injection loop. Here a recirculation area develops, which controls the size of other small swirls. The maximum value of the passive scalar field at the core inlet (representing the minimum boron concentration) is an indicator for possible reactivity insertion during a transient (Figure 11.3a). In the experiment as well as in the calculation the maximum value at the core inlet is determined at each time step over all fuel element positions, therefore the position can vary. The calculated maximum mixing scalar at the core inlet is very close to the experimental value. The local time dependent mixing scalar at the fuel element position in the center of the core inlet is shown in Figure 11.3b.

| 9 s after start-up | 10 s after start-up |
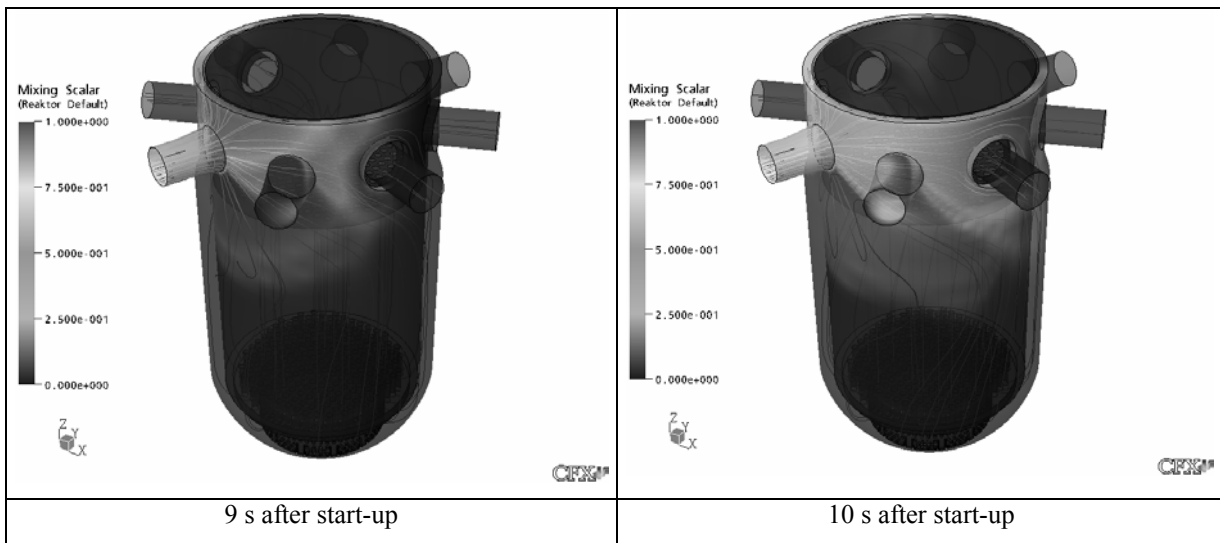
**Figure 11.2. Time dependent mixing scalar distribution in the downcomer, CFX-5**



| a)  Time dependent global maximum of the mixing scalar at the lower downcomer | b)  Time dependent local mixing scalar at the core inlet, center position |
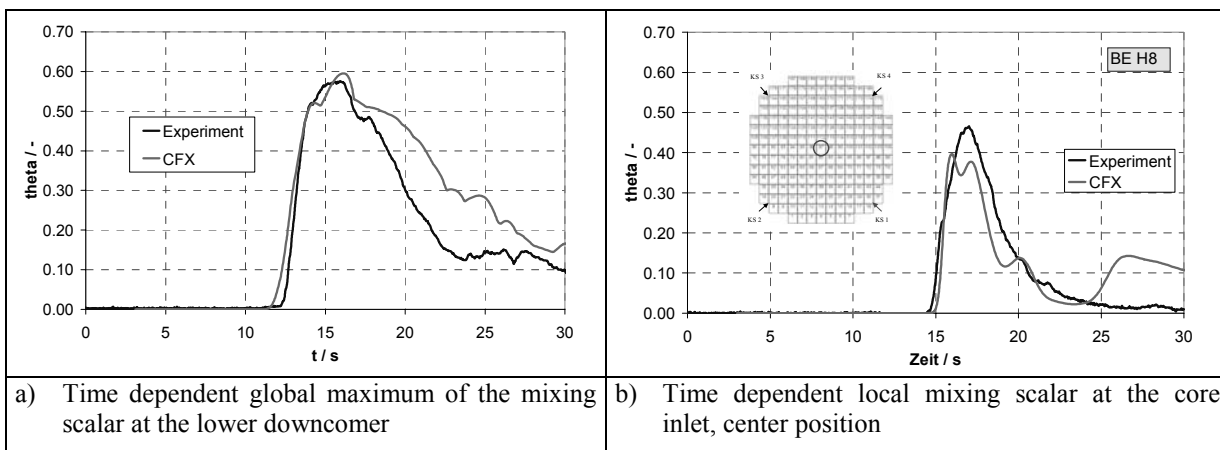
**Figure 11.3. Comparison of the time dependent mixing scalar at the core inlet sensor position (experiment, CFX-5 calculation)**

### *11.1.5    Conclusions*

The CFD calculations were carried out with ANSYS CFX-10. All internals of the RPV of ROCOM were modelled in detail.  A production mesh with 7 Million elements was generated. Detailed and extensive grid studies were made. It was shown, that a detailed model of the perforated drum gives the best agreement with the experiments.  However, no full grid independence of the CFD solutions was achieved.

Sensitivity studies have shown that the SST turbulence model and the automatic wall functions together with higher order discretization schemes should be used.

## 11.2    Pressurized Thermal Shock: UPTF Test 1

The Upper Plenum Test Facility (UPTF) was a full-scale representation of the primary system of the four loop 1300 MWe Siemens/KWU Pressurized Water Reactor (PWR) at Grafenrheinfeld in Germany. The test vessel upper plenum internals, the downcomer, and the primary coolant piping were

replicas of the reference plant. However, other important components of the PWR such as the core, the coolant pumps, the steam generator, and the containment were replaced by simulators which simulated the thermal-hydraulic behaviour in these components during end-of-blow down, refill, and reflood phases of a large break Loss-Of-Coolant Accident (LOCA). Both hot leg and cold leg breaks of various sizes have been simulated in the UPTF. The Emergency Core Cooling (ECC) injection systems of the UPTF were designed to simulate the various ECC systems of PWRs in Germany, Japan, and the US.

Temperature measurements have been performed at various locations in the UPTF geometry. The results of CFD simulations have been compared at those positions most relevant for Pressurized Thermal Shock (PTS). The temperature measurements in the intact cold leg, where the ECC injections occur, and the measurements in the downcomer directly under this cold leg were selected.   These measurement positions are indicated in Figure 11.4.
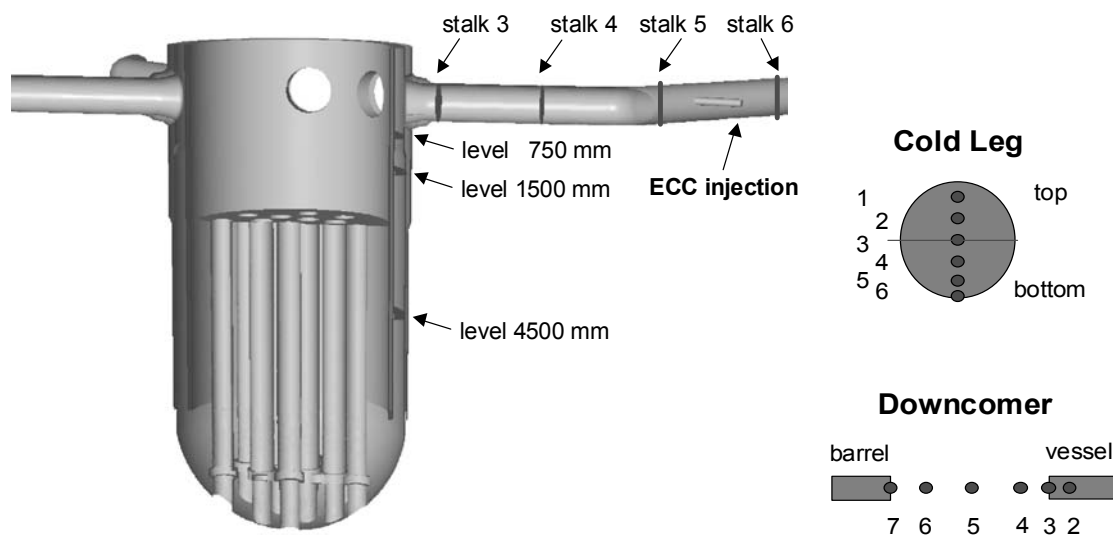


**Figure 11.4. Location of the key temperature measurement positions, and probe numbering**

### 11.2.1    UPTF Test 1 Conditions

UPTF Test 1 was performed to investigate fluid-fluid mixing in the cold leg and downcomer during a small break LOCA. This fluid-fluid mixing results from the high pressure injection of the cold ECC water into the cold leg at a time when the reactor coolant system is at an elevated temperature. The level of mixing controls the fluid temperatures in contact with pipe and vessel walls and hence the potential for a PTS safety issue.  In general, if the mixing is good, a slow cool down occurs which provides sufficient time to prevent the development of significant temperature gradients in the wall of the Reactor Pressure Vessel (RPV). Good mixing takes place when there is flow in the loops, even when the flow only results from natural circulation. However, in certain SBLOCA scenarios, it is possible that stagnant flow conditions occur in one or more loops. For this situation, the flow in the cold leg is thermally stratified. Namely, the ECC injection results in a cold stream, which flows along the bottom of the cold leg from the injection nozzle to the downcomer, whereas a hot stream flows along the top of the cold leg counter current to the cold stream. This situation was investigated in UPTF Test 1.

For UPTF Test 1, the primary system was initially filled with stagnant hot water at 463 K (190°C). The cold ECC water was injected into a single cold leg. The ECC water injection mass flow rate was equal to 40 kg/s and the temperature of this ECC water was 300 K (27°C).

*11.2.2    Summary of Results Calculated Using CFX-5*

Calculations summarized here were performed by the Nuclear Research and consultancy Group (NRG). The different turbulence models and meshes used in these computations are summarised in Table 11.1. Cases A and B have been executed in order to determine whether detailed modelling of the UPTF internals is required. Simulations showed spurious circumferential flow oscillations in the downcomer for an empty lower plenum in combination with the commonly applied porous medium approach for representation of the UPTF core. Furthermore, it has been shown that the pump volume has to be taken into account, since a large amount of the ECC water flows towards the pump and accumulates there. In a real accident scenario, it is therefore important to correctly predict the amount of ECC water flowing towards the pump, since this water will never reach the core.

**Table 11.1: Overview of the performed CFX-5 computations for UPTF Test 1.**

| Case | Turbulence model | Turbulence modification | Core model | Pump volume | Time step | Discretisation space , time | Mesh size |
|------|------------------|-------------------------|-----------|-------------|-----------|----------------------------|-----------|
| A | SST-k-$\omega$ | none | porous | no | 0.5 s | $1^{st}$, $1^{st}$ | 1.155.153 |
| B | SST-k-$\omega$ | buoyancy | internals | yes | 0.5 s | $1^{st}$, $1^{st}$ | 2.052.315 |
| C | k-$\varepsilon$ | buoyancy | internals | yes | 0.5 s | $1^{st}$, $1^{st}$ | 2.052.315 |
| D | SST-k-$\omega$ | buoyancy | internals | yes | 0.5 s | $2^{nd}$, $1^{st}$ | 2.052.315 |
| E | SST-k-$\omega$ | buoyancy | internals | yes | 0.05 s | $2^{nd}$,$2^{nd}$ | 2.052.315 |
| F | SST-k-$\omega$ | buoyancy | internals | yes | 0.05 s | $2^{nd}$,$2^{nd}$ | 2.871.450 |
| G | RSM | buoyancy | internals | yes | 0.05 s | $2^{nd}$,$2^{nd}$ | 2.871.450 |

Turbulence modelling has been investigated by comparing results of a simulation using the SST-k-$\omega$ turbulence model without (case A) and with (case B) inclusion of the turbulence production/destruction term due to buoyancy. From a comparison of these two cases, it has been concluded that this modification to the standard turbulence model is required in order to achieve a good representation of the stratification occurring in the cold leg. Once this term is included, the results of the SST-k-$\omega$ (case B) and standard k-$\varepsilon$ turbulence model (case C) are practically identical. Finally, an $\omega$-based Reynolds stress turbulence model has been used (case G). The results from this calculation show a better agreement with experimental observations for the amplitude of the oscillations in the downcomer. These oscillations are over predicted by the two-equation turbulence model (case F). It is important to notice that correct prediction of these oscillations is required in order to analyse phenomena like PTS and thermal fatigue. Since these oscillations have a significant effect on the wall temperature, and thus on the correct prediction of the severity of the PTS. An attempt was made to quantify the oscillations in the experiments. However, the Fast Fourier Transformation of the experimentally observed oscillations did not show any dominant frequencies present in the signals. Besides determining the effect of the geometrical assumptions and turbulence modelling, as described before, the other calculations in Table 11.1 are related to the ECORA Best Practice Guidelines. Since modelling the UPTF geometry is computationally very demanding, it is impossible to strictly follow the BPG, which, e.g., state that a 2×2×2 refinement should be performed. Instead, a 1st order solution (case B) has been compared with a 2nd order solution (case D). This comparison demonstrated that it is plausible to assume that the mesh in the cold leg is sufficiently fine; but that the results in the downcomer are still mesh dependent. Therefore, a mesh which is locally refined in the downcomer was generated. In this new mesh, care was taken to ensure correct y+ values (case F). The temporal discretization has been checked by performing a simulation with a reduced time step size and 2nd order temporal discretization (case E). This reduced time step size is needed in order to reliably capture the oscillations in the downcomer which determine the vessel wall temperature.

Case F in Table 11.1 is the reference case, since here the best mesh and time step size was used. In Figure 11.5 the temperature distribution on the vessel cold leg walls can be seen. Strong mixing of the cold ECC water with the hot liquid, initially present in the system, is observed in the region of the upward directed ECC injection tube. Further downstream, strong stratification is observed in the cold leg. The cold water flows towards the reactor vessel and in the direction of the pump simulator, where the cold water accumulates until it has reached the level of the top of the cold leg (after about 160 s). The stratification in the part of the cold leg leading to the reactor vessel remains at a constant level throughout the transient. The cold water plume flows downwards past the vessel wall. Some slow oscillations can be observed in the circumferential direction. In the same figure, a detailed view of the flow in the downcomer is presented. At the connection of the reactor vessel with the cold leg, the flow remains attached to the vessel wall, but starts to detach and re-attach at a lower level in the downcomer. These oscillations, which are much faster than the circumferential oscillations, cause hot and cold regions to emerge. In the bottom of the reactor vessel the hot and cold regions are fully mixed by the turbulent flow between the lower plenum internals.
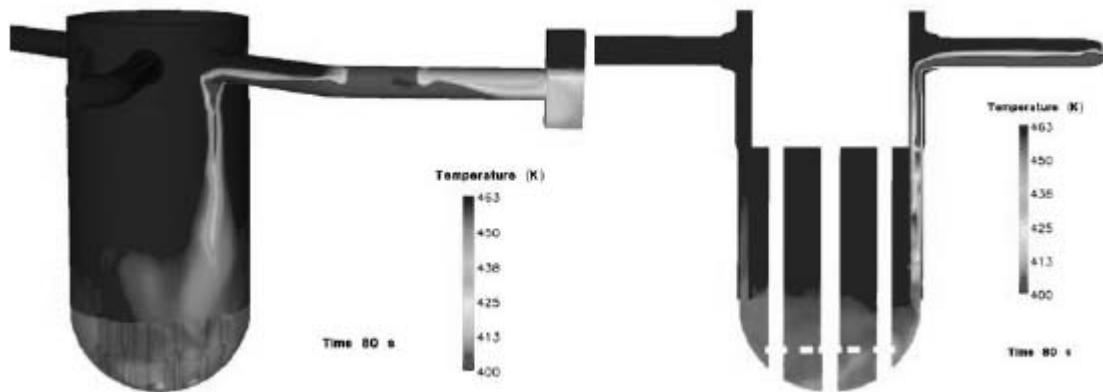


**Figure 11.5. Vessel and fluid temperatures on the vessel and cold leg walls (left) and a cross-section through the middle of the cold leg with ECC injection (right)**

The computed temperature profiles in the cold leg are compared with the experimental results from the UPTF Test 1 in Figure 11.6. From this comparison, we conclude that the stratification in the cold leg is accurately predicted by the CFD code. The calculated lowest temperature in the cold leg, which is the most important factor for determining the severity of the thermal shock, is within 3 % of the experimental value. A second comparison is made for the results in the downcomer in Figure 11.7 and Figure 11.8. In the experimental results in the downcomer large oscillations are observed at every height. In the CFD results, these oscillations are not found at the highest measurement positions. This is caused by the previously mentioned attachment of the cold plume to the vessel wall, which results in an overestimation of the cooling of the vessel wall. The predicted temperature drop $\Delta T = T - T_{initial}$ is typically overestimated by 50 to 100 %. At the lower level (see Figure 11.8) oscillations are observed, but the temperature drop still remains overestimated by 60 to 90 %.
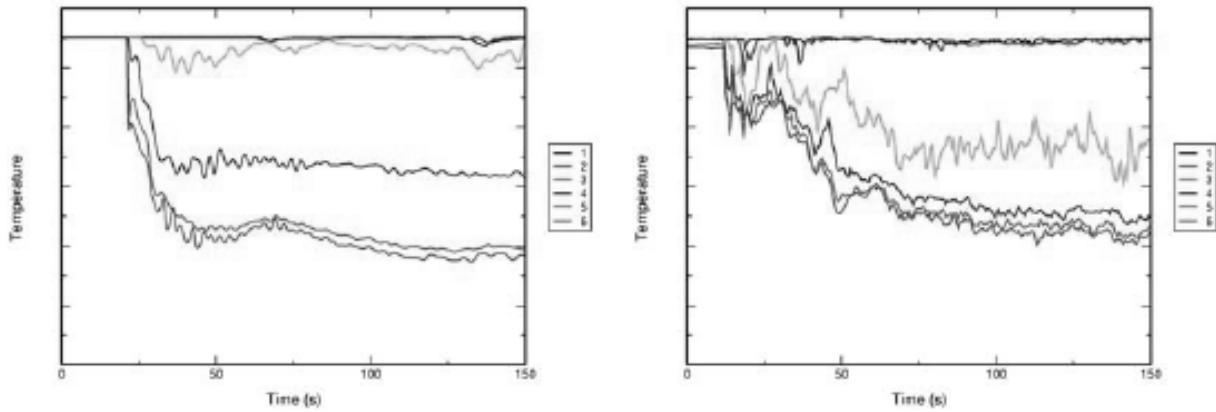
**Figure 11.6. Stalk 3 results of the CFX-5 reference calculation (left) and UPTF experiment (right). For location see Figure 11.4**
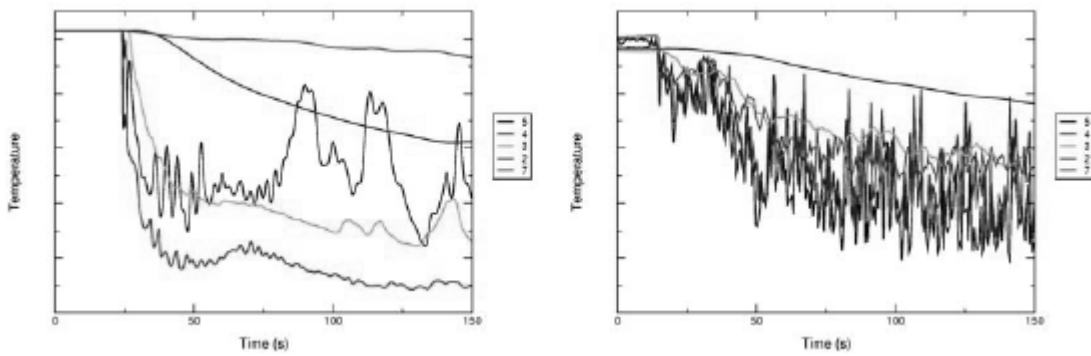


**Figure 11.7. : Level 750 mm results of the CFX-5 reference calculation (left) and UPTF experiment (right). For legend see Figure 11.4**
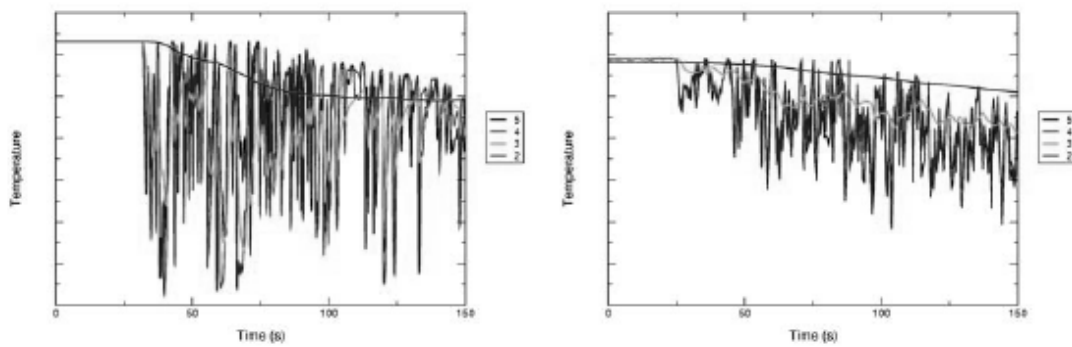


**Figure 11.8. Level 4500 mm results of the CFX-5 reference calculation (left) and UPTF experiment (right). For legend see Figure 11.4**

### 11.2.3    Conclusions

This study clearly indicated a need for buoyancy modifications to turbulence source/sink terms. Further work is needed in nodalization and model studies to resolve serious discrepancies in results within the downcomer.

### 11.3 Spent Fuel Dry Storage Cask

The objective of this task was to validate a general purpose Computational Fluid Dynamics (CFD) method to perform thermal evaluations of a Ventilated Concrete Storage Cask VSC 17 system. In addition, the effectiveness and validity of an effective thermal conductivity model $k_{eff}$ was quantified and validated. The ($k_{eff}$) model is used to represent the combination of radiation and conduction heat transfer by an equivalent thermal conductivity in the region that houses the spent fuel. The ($k_{eff}$) method has long history of use with Finite Element Analysis (FEA) codes and has been proven to favourably predict a dry cask's thermal response. In the presented analysis, Fluent [259], a commercially available CFD software package, was used. Fluent is finite control volume based, more suited than FEA codes like ANSYS to model convection in open flow regions of the storage system. As such, there is a need to investigate the applicability of a $k_{eff}$ model in the context of Fluent.

Two types of flows exist in spent fuel dry storage casks such as the VSC-17. Inside the sealed canister, compressed helium flows through the fuel rod assemblies due to buoyancy forces, while air flows outside the canister in an open system manner also as a result of buoyancy (density difference). The standard k-ε model with standard wall function is often used to bridge the viscous layer near the wall to the fully turbulent core region in the middle of the channel. As such, the second objective of this validation is to compare the performance of different turbulence models as well as the laminar flow option.

Run #1 among the runs shown in Table 11.3 of the VSC-17 experiments performed in 1990 at Idaho National Laboratory [256] was selected for detailed modelling with the Fluent code. The VSC-17 is a multi-assembly storage cask comprised of a ventilated concrete storage module. Detailed temperature data was taken during testing and is available for multiple locations and axial levels throughout this cask.

### 11.3.1 Description of the VSC-17 Spent Fuel Storage Cask Experiments:

The VSC-17 spent fuel storage system is a passive heat dissipation system for storing 17 assemblies/canisters of consolidated spent nuclear fuel. The VSC-17 system consists of a ventilated concrete cask (VCC) enclosing a multi-assembly sealed basket (MSB) containing spent nuclear fuel as shown in Figure 11.9 and Figure 11.10. Decay heat generated by the spent fuel is transmitted through the containment wall of the MSB to a cooling air flow. Natural circulation drives the cooling air flow through an annular path between the MSB wall and the VCC liner wall and carries the heat to the environment without undue heating of the concrete cask. The annular air flow cools the outside of the MSB and the inside of the VCC.

The cask weighs approximately 80 tons empty and 110 tons loaded with 17 canisters of consolidated fuel. The VCC has a reinforced concrete body with an inner steel liner and a weather cover (lid). The MSB contains a guide sleeve assembly for fuel support and a composite shield lid that seals the stored fuel inside the MSB. The cavity atmosphere is helium at slightly sub-atmospheric pressure. The helium atmosphere inside the MSB enhances the overall heat transfer capability and prevents oxidation of the fuel and corrosion of the basket components.

The performance testing consisted of loading the MSB with 17 fuel cans containing consolidated Pressurized Water Reactor (PWR) spent fuel from Virginia Power's Surry reactors and Florida Power & Light's Turkey Point reactors. At the time of the cask tests, this fuel was generating about 14.9 kW of total decay heat. Temperatures of the cask surface, concrete, air channel surfaces, and the fuel compartments (containing the fuel cans) were measured, as were cask surface gamma and neutron dose rates. Testing was performed with vacuum, nitrogen, and helium backfill environments in a vertical cask orientation, with air circulation vents open, partially blocked, and completely blocked. Of these tests, Run #1 is the nominal case (no blocked vents) with helium gas in the MSB.

Detailed descriptions of the VSC-17 experiments, including system geometry, instrumentation locations, specifics of fuel loading, and estimates of the heat generation rates in the spent fuel assemblies are included in the original documentation of the testing [256]. The availability of as-built information and an extensive amount of data make this an excellent choice for evaluation of the accuracy and completeness of computer models for spent fuel storage systems.



**Figure 11.9 Photo of the concrete shell and sealed canister**
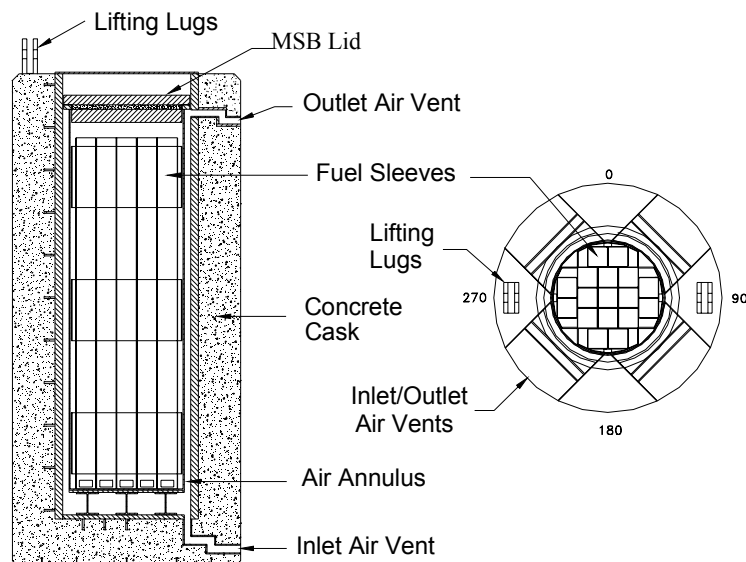


**Figure 11.10 Schematic of the ventilated concrete cask system.**

### 11.3.2 *Effective Thermal Conductivity Model for Consolidated Fuel Canister:*

The tightly packed fuel rods within the stainless steel fuel canisters are modelled as a homogeneous solid material region with a specified uniform heat generation rate and an effective thermal conductivity. The option in Fluent for anisotropic thermal conductivity was used to represent the different effective conductivities of the fuel region in the axial and radial directions. For axial heat transfer, the conductivity of the fuel ($UO_2$) material and the fill gas was ignored, and it was assumed that significant axial conduction occurs only in the zircaloy cladding of the fuel rods. The effective conductivity in the axial direction was represented as an area-weighted fraction of the conductivity of zircaloy-4, using an area-weighted ratio of the cladding to the total cross-section of the homogeneous region. This relationship was implemented in Fluent based on the temperature-dependent thermal conductivity of Zircaloy 4.

For heat transfer in the radial direction through the fuel region, the Fluent model makes use of the effective thermal conductivity values for consolidated 17x17 fuel. The k-effective values for the consolidated fuel cans in the VSC-17 are based on a calculational 'database' generated by a separate 2D Fluent analysis for consolidated WE 17x17 fuel using a detailed two dimensional model of a single fuel can. Calculations were performed with Fluent for a single consolidated fuel can of WE17x17 fuel rods for fuel can wall temperatures ranging from 93°C to 400°C. A 'database' was created for fuel can total decay heat rates of 0.5 kW, 0.75 kW, 1.0 kW and 1.2 kW, somewhat exceeding the range of decay heat values of the fuel cans loaded into the VSC-17 cask. However, there were only very small differences in the effective thermal conductivity values as a function of wall temperature obtained with the standard methodology for the full range of heat rates evaluated. Therefore, the effective thermal conductivity obtained for a heat load of 1.0 kW was used for all fuel cans in the CFD calculations, regardless of actual fuel can heat load, which varied from about 0.744 kW to 1.048 kW in the quadrant represented in the Fluent model.

The effective thermal conductivity values in the radial direction of the fuel region were obtained as a function of temperature using the standard k-effective methodology [257]. This is the approach generally employed in vendor's Safety Analysis Report (SAR) analyses to determine peak fuel temperatures in spent fuel casks when the fuel assemblies are modelled as a homogeneous material. Following the documented form of the basic k-effective model, this approach yielded an effective thermal conductivity for the homogeneous fuel 'block' as a function of local computational cell temperature. The model is implemented in Fluent as temperature-dependent k-effective values.

### 11.3.3 *Decay Heat Generation (Thermal Source Term) for Consolidated Fuel Cans*

Individual consolidated fuel cans in the VSC-17 had heat generation rates ranging from 0.707 kW to 1.05 kW. The fuel cans were loaded in the basket to give as close to a symmetrical heat load as possible, with fuel cans near 1.0 kW in the central 3x3 grid, and fuel cans with heat loads near 0.7 kW on the periphery of the basket (refer to Figure 3.13 of McKinnon [256]). Most of the temperature measurements obtained within the fuel cans and the basket are from thermocouples located in one quadrant of the basket. In this quadrant, the peripheral fuel cans all have decay heat values of approximately 0.744 kW, and the inner fuel cans have decay heat values ranging from 0.962 kW to 1.048 kW. The specific heat generation rates for these fuel cans were applied to the homogeneous regions modelling the corresponding fuel cans in the 1/4 section of symmetry representation of the MSB in the Fluent model.

The decay heat for a given fuel can was applied as a uniform volumetric heat generation rate throughout the homogeneous region, modified only to include an axial power profile based on the measured axial power distribution in the fuel cans (refer to Figure 3.14 of McKinnon [256]). The heat generation is applied over 388 cm (153 inches). The actual heated length for this fuel is estimated at 145.5 inches (i.e., an original length of 144 inches, plus 1.5 inches of growth due to burn-up.) This

approximation will result in slightly lower peak fuel temperature predictions than would be obtained if the shorter (actual) heated length were to be used.

### 11.3.4    Mesh Considerations and Turbulence Modeling in the Air Annulus Region

The mesh spacing between the VCC liner and MSB outer shell wall is an important consideration in selecting turbulence model for airflow through this annular gap.  The near wall modelling significantly impacts the fidelity of numerical solutions, inasmuch as walls are the main source of mean vorticity and turbulence.  After all, it is in the near-wall region that the solution variables have large gradients, and the momentum and other scalar transports occur most vigorously.  Therefore accurate representation of the flow in the near-wall region determines successful predictions of wall-bounded turbulent flows.  In this study, two types of mesh distribution were used in the annular region.  The first mesh was chosen to use semi-empirical formulas called "standard wall functions" to bridge the viscosity-affected region between the walls and the fully-turbulent core region.  The use of wall functions obviates the need to modify the turbulence models to account for the presence of the wall.  This type of modelling is usually used for high Reynolds number flows.  In the second mesh, the viscosity-affected region is resolved with a mesh all the way to the wall, including the viscous sublayer.  This type of approach is referred to by "near wall modelling" approach.   The dimensionless distance between the wall and the cell centre near the wall (y+) for the second mesh is around 1, while the first mesh used y+ of around 20.

Reynolds number estimates were made using velocities from initial runs for the cooling air in the annulus and helium fill inside the MSB.  Cooling air in the annulus between the MSB and VCC had an average velocity of 1 m/s, corresponding to a Reynolds number above 3000 based on the channel hydraulic diameter.  This is clearly above the critical Reynolds number of 2300 for internal flows, putting the flow in the transitional range between the laminar and turbulent zone.  As we are dealing with buoyancy driven flows, both the Rayleigh (Ra) number based on the hydraulic diameter of the channel and the modified Rayleigh number defined as ($Ra_{modified} = Ra* W/H$) where W and H are the width and height of the air channel) were also calculated.  Based on both, Rayleigh and the modified Rayleigh number, laminar flow was obtained.  On the other hand, buoyancy driven Helium flow cooling the inside of the canister was calculated as laminar based on both the Rayleigh and the Reynolds numbers due to the higher kinematic viscosity, and the low achieved velocities of the helium gas within the MSB resulting in a Reynolds number of around 200.  This is clearly in the laminar flow regime.

These preliminary calculations showed that a turbulence model was not needed for the buoyancy-driven recirculation of the helium gas within the basket, and laminar flow conditions were assumed in this region of the model.  The airflow in the inlet and outlet vents and annular gap between the MSB and the concrete outer shell, however, is expected to be in the transitional regime. It was therefore necessary to specify an appropriate turbulence model for the airflow in order to obtain accurate predictions of local velocities and temperatures in the air stream, and local wall temperatures on the surfaces of the annulus and inlet/outlet vent structures.

As noted above, two types of meshes were used in the air annular region and in the inlet/outlet regions to define conditions that would be more consistent with both types of turbulence modelling.  Additionally, as the calculated Reynolds number was close to the critical Reynolds number of 2300, a laminar model with finer mesh was also tested.

### 11.3.5    Thermal Radiation Modeling within the VSC-17 System

There are quite a few radiation models that are implemented in Fluent.  Each model has its advantages and limitations.  On previous applications, both, the Discrete Transfer Radiation (DTRM) and Discrete Ordinate (DO) models were used and gave comparable results.  As a result, the DO model was

chosen. In this approach the radiative transfer equation (RTE) for an absorbing, emitting and scattering medium is solved for a finite number of discrete solid angles. The fineness of the angular discretization is controlled by the user. Unlike the DTRM, the DO model does not perform ray tracing. Instead, the DO model transforms the RTE equation into a transport equation for the radiation intensity in the spatial coordinates (x, y, z). The DO model solves for as many transport equations as there are directions defined by the angular discretization. The solution method is identical to that used for the fluid flow and energy conservation equations. In the solution of the VSC-17 problem, four angular discretizations were used in each direction of the spherical coordinates system (theta (θ) and phi (φ)).

### 11.3.6   *Boundary Conditions*

The external boundary conditions on the VSC-17 consisted of free convection to ambient air on the top and side surfaces, radiation to the ambient, and conduction through the base to a concrete pad and its underlying soil. Since the experiment was conducted inside a building, solar insolation was not taken into account. These boundary conditions were represented in the Fluent model of the VSC-17 by specifying appropriate convective heat transfer coefficients on the cells representing the outer surface at the top and sides of the VCC, and an appropriate thermal resistance on the cells representing the base of the system. Thermal radiation properties and resolution control for the view factor calculations were set via internal boundary conditions on solid cells adjacent to fluid (gas) cells. The specified values for these boundary conditions are summarized below.

- Ambient temperature of 21°C (based on test report)

- Solar heat loading not accounted for

- Ambient pressure boundaries at the inlet and outlet vents

- Heat transfer coefficient of 5 W/m$^2$-K on the top and sides of the VCC

- Heat transfer coefficient of 10 W/m$^2$-K on the top of the VCC weather cover

- Conduction resistance 5.87 m$^2$-K/W on the base of the VCC, to a 15°C fixed soil temperature (equivalent to conduction through 3 m of soil)

- Surface emissivities set to

  – 0.4 for fuel cans,

  – 0.6 for basket, supports and MSB body, and

  – 0.7 for A36 steel used for VCC annulus and inlet/outlet liners.

The values of heat transfer coefficients were determined using standard correlations for convective heat transfer and were adapted to include additional losses through thermal radiation determined via simple hand calculations. The heat transfer coefficient on the weather cover is higher than that of the surrounding concrete to account for its higher temperature and consequently higher heat transfer rate due to thermal radiation.

The values of surface emissivities were selected based on 'typical' values for the corresponding materials, since measured values for the particular components of the VSC-17 were not obtained in the testing. The most complete set of data is Hottel's measured values as listed in McAdams [258]. Most other

text books reference this data. For the 304 stainless steel used in the consolidated fuel can walls, McAdams lists an emissivity range of 0.44-0.36 for temperatures ranging from 420 to 914°F for a sample described as "light silvery, rough, brown, after heating". Since the measured temperatures for the VSC-17 fall in the middle of this range, a value of 0.4 is selected as the baseline. Values for non-stainless steels span a large range. McAdams [258] shows emissivity for mild steel with a very thin oxide layer can range from 0.1 to 0.3, whereas oxidized steel surfaces are shown as 0.66 for rolled sheet, 0.79 for steel oxidized at 1100°F, and 0.8 for sheet steel with a strong, rough oxide layer. A value of 0.7 for the A-36 steel of VCC liner was assumed. A-516 pressure vessel steel is the primary material for the MSB. The internal components will operate at elevated temperatures but will not see an oxidizing environment. The outside shell of the MSB is subject to rust and oxidation, however it would be expected to be less likely to oxidize than the A-36 steel used in the liner and MSB lid. The assumed emissivity for all of the A-516 components is 0.6.

### 11.3.7    Material Properties

Thermal properties for the solid materials in the VSC-17 were obtained from the test documentation (specifically, McKinnon's Table 5.2 [256]. Gas properties for air and helium were determined using the functions provided in the Fluent material set. Temperature dependent thermo-physical properties were used for cooling air and helium.

| Material | Thermal Conductivity W/m-°C (Btu/ft-hr-°F) |
|---|---|
| Concrete | 1.47 (.85) |
| Steel liner (A36) | 41.5 (24) |
| Steel basket assembly (A512) | 41.5 (24) |
| Steel fuel cans (SS304) | 16.3 (9.4) |
| RX-277 (radiation shield in lid) | 0.52 (0.3) |

**Table 11.2  Solid material thermal conductivities (from McKinnon, 1992)**

### 11.3.8    Spatial Differencing and Solution Method

The steady-state solution for the VSC-17 model in Fluent was performed with the SIMPLE algorithm using a conjugate gradient solver. Second order Upwind spatial differencing was used for all variables except the pressure equation (continuity equation), where a body force weighting method was used.

These simulations were run from a zero-flow initial condition using a pressure boundary at the airflow inlet. The criterion for solution convergence is typically when the total heat flux is within 20W, corresponding to an energy error of approximately 0.5%.

### 11.3.9    Simulation Results

The VSC-17 tests provided a large amount of thermocouple data of recorded temperatures inside the fuel cans, within the basket structure, and on the inner and outer surfaces of the VCC structure. The measured data and the locations of the instrumentation are given in the background references for the experiment (specifically, in Table C.1 of McKinnon 1992). From this information it is noted that the peak measured temperature was consistently recorded at thermocouple location L6-3. This thermocouple location was at the 3050 mm elevation of the thermocouple lance in the central fuel can. Therefore location L6-3 was used as the Peak Clad Temperature (PCT) for evaluating the Fluent model results, although additional comparisons were also made with temperatures measured in the basket, on the MSB shell surfaces, and on various surfaces of the VCC.

### 11.3.10   Thermal Performance Data

A total of 98 thermocouples (TCs) were used to measure the thermal performance of the cask. The inside of the MSB was instrumented through the use of seven TC lances, as shown in Figure 11.11. Each TC lance contained six calibrated Type J (Iron-Constantan) insulated junction TCs, which provided a total of 42 internal lance TCs.  A total of 53 Type J TCs were used to determine the temperature of the MSB, cask lid, and concrete.  Ten TCs were attached to the outer surface of the cask; five were attached to the MSB lid; two were attached to the weather cover; ten were imbedded in the concrete; nine were attached to the outside barrel of the MSB; nine were attached to the inner liner of the VCC; and one TC was installed in the center of each air inlet and outlet vent.  An additional three TCs were used to monitor the ambient temperature in the Hot Shop. The location of the TC lances and the elevations of the TCs are shown in Figure 11.12.  Each TC lance had six TCs installed in an 8-mm-diameter (0.315-inch) tube as shown in Figure 11.11. Lances were inserted through instrumentation penetrations in the test lid and into selected guide tubes placed in six fuel canisters and into one simulated guide tube attached to the basket. The selected axial and cross-sectional locations of the TC lance thermocouples made it possible to evaluate temperature symmetry and to determine axial and radial temperature profiles for the cask.
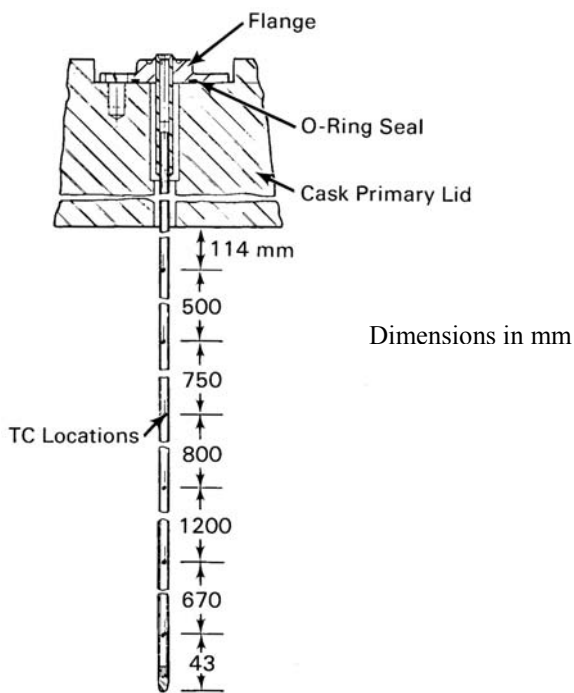


**Figure 11.11, Thermocouple Lance**

Dimensions in mm
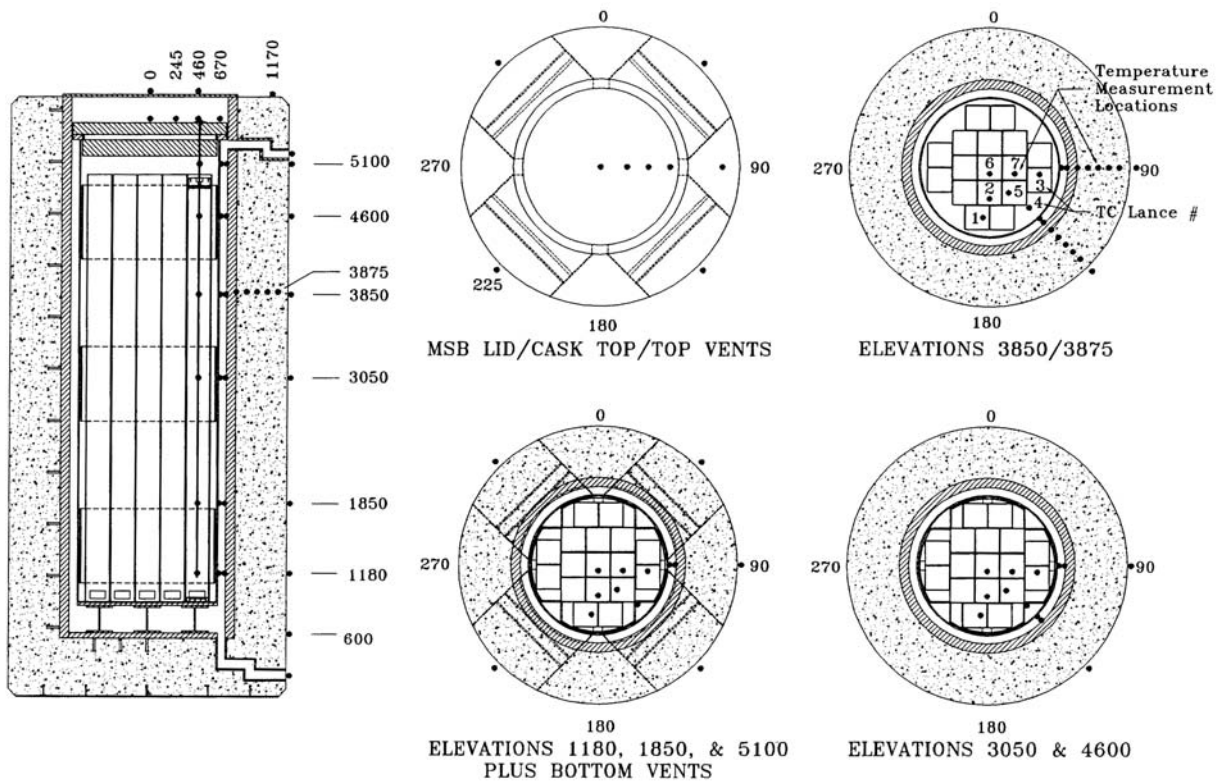
**Figure 11.12 Temperature Measurement Locations Used During the VSC-17 Performance Test**

| Test # | 1 | 2 | 3 | 4 | 5 | 6 |
|---|---|---|---|---|---|---|
| Backfill gas | Helium | Helium | Helium | Helium | Nitrogen | Nitrogen/vacuum |
| Pressure, mbar absolute | 817.5 | 1074.1 | 935.3 | 975.2 | 843.6 | 8.6 |

**Table 11.3  Performance Test Run Designation**

### 11.3.11   Summary of Results

Three turbulence models as well as a laminar regime were used to model the air flow passage between the MPC and the concrete liner.  The first two models among the three chosen turbulence models were the transitional SST k-ω model, and the low-Reynolds k-ε model.  Both of these models use damping functions that take into account the effect of the cell Reynolds number on the calculation of the time and length scale of turbulence.  Both of these models are used with the fine grid near the wall (y+ ~1) to enable integration through the viscosity-affected near wall region.  The third chosen turbulence model was the standard k-ε in conjunction with standard wall function to bridge the fully turbulent core region to the viscosity-dominated region near the wall.  This model does not use finer mesh near the wall.  In the present application a y+ close to 20 was used.

Temperature profiles from the four CFD approaches described above are compared to the experimental data and shown in Figure 11.13 through Figure 11.24.  The axial temperature profile experimental data for Lances 3, 5, 6 and 7 inside the fuel region, liner wall and MPC wall were chosen to compare to calculated CFD results.  Additionally, radial profiles from the centre of the fuel region to the periphery of the overpack concrete shield at elevation of 3.0 m and 3.85 m were used to compare the experimental data to the CFD results.

As a first observation, all the four options used to model the turbulence in the air cooling channel were successful in predicting the location of the peak cladding temperature. The peak cladding temperature value is of great importance in dry cask applications. For long term normal storage conditions, dry cask peak cladding temperature is limited to 400 C to avoid spent fuel rod failure due to thermal loads. CFD results obtained for the laminar option are shown in Figure 11.22 through Figure 11.24. Modelling air flow using the laminar option over-predicted the peak cladding temperature as well the axial temperature distribution in the entire fuel region as shown in Figure 11.22. Additionally the liner wall axial temperature distribution as well as the MPC wall axial temperature distribution was over-predicted using the laminar regime option to model the air cooling channel. The over-prediction of the temperature distribution inside the cask and the air channel led to the over-prediction of the radial temperature profile in the overpack region. The standard k-ε model was a better choice than the laminar option, but due to the lack of grids near the MPC wall and the liner wall, this model was unable to capture the exact temperature distribution at the liner wall. This model over-predicted the heat exchange between the two walls. Usually, a standard k-ε model combined with standard wall function is used when high Reynolds number flow exists. In case of transitional Reynolds numbers, as in this example, some type of damping function to enable computation across the laminar viscous sub-layer is required in conjunction with fine mesh near the wall, as was done with the first two turbulence models chosen in this analysis. The standard k-ε predicted the peak cladding temperature as shown in Figure 11.19, but under-predicted the liner wall axial temperature distribution as shown in Figure 11.21, for the reasons enumerated above. In the review and confirmation of CFD calculations of other dry cask designs, the standard k-ε model, proved to be non-conservative and under-predicts the peak cladding temperature when compared to transitional k-ω turbulence and low Reynolds k-ε model.

Both, the transitional SST k-ω and the low Reynolds k-ε turbulence models predicted the temperature distribution fairly well in the fuel region inside the canister as well as the passage of cooling air. Both, Figure 11.13 and Figure 11.16 show that these two models predicted the location and the value of the peak cladding temperature. Additionally the axial temperature profile of the liner wall and MPC wall were fairly well predicted given the complex nature of this buoyancy driven flow as shown in Figure 11.15 and Figure 11.18. The improvement in the prediction of the liner wall distribution was the result of the fine mesh used near the walls and the capability of these two models to handle low Reynolds turbulent flow. Additionally, the radial temperature distribution at 3.05 m and 3.85 m compares favourably using these two models as shown in Figure 11.14 and Figure 11.17.
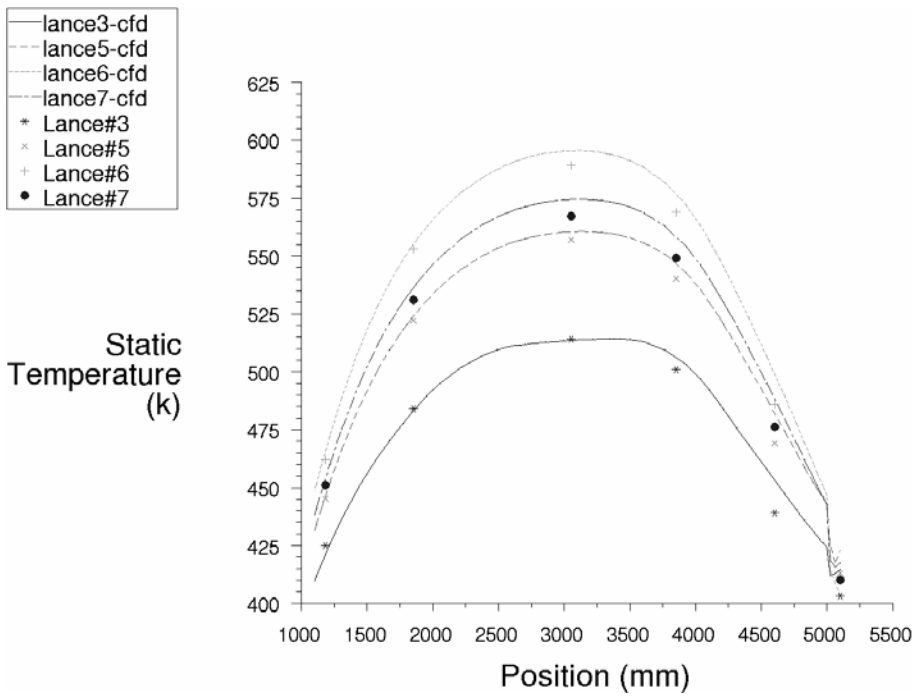
**Figure 11.13 Fuel region axial temperature, using SST k-ω turbulence model**
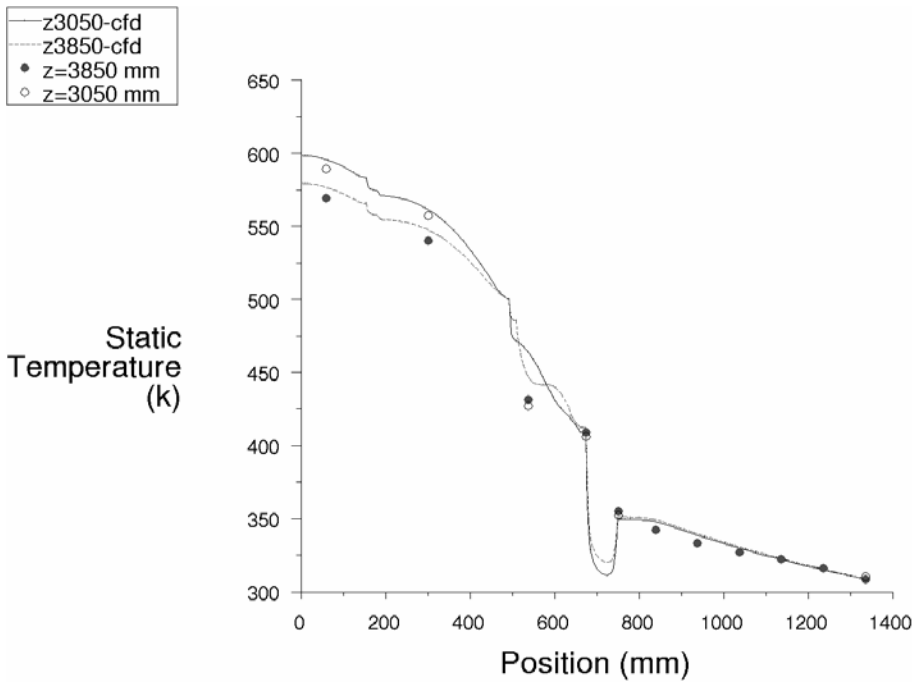


**Figure 11.14 Radial temperature plot at 3.05 and 3.85 m elevation using SST k-ω turbulence model**
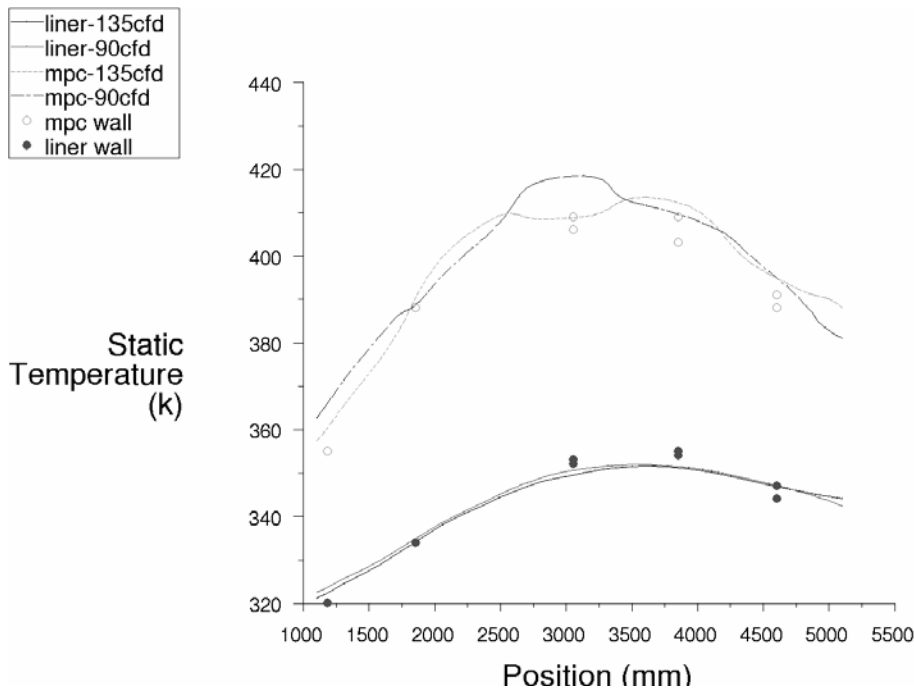
**Figure 11.15 MPC and liner walls axial temperature, using SST k-ω turbulence model**
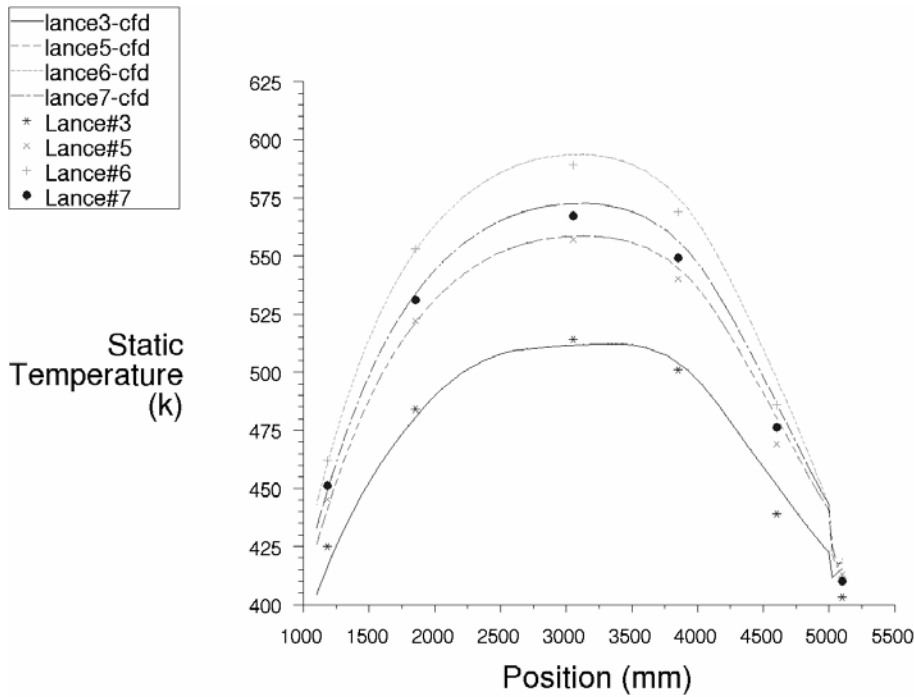


**Figure 11.16  Fuel region axial temperature, using low Reynolds k-ε turbulence model.**
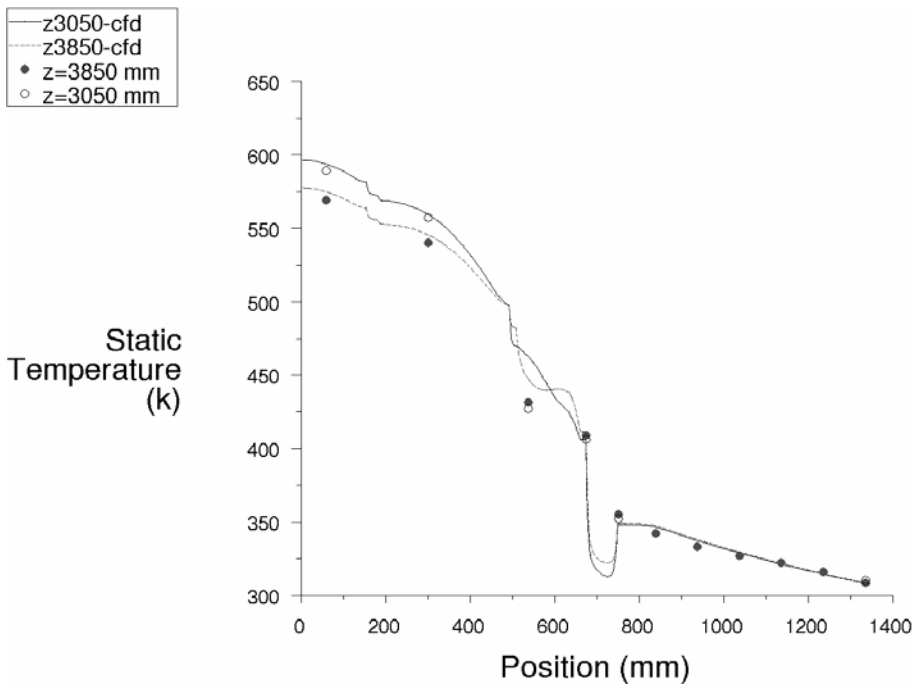
**Figure 11.17 Radial Temperature at 3.05 and 3.85 m elevation, using low Reynolds k-ε turbulence**
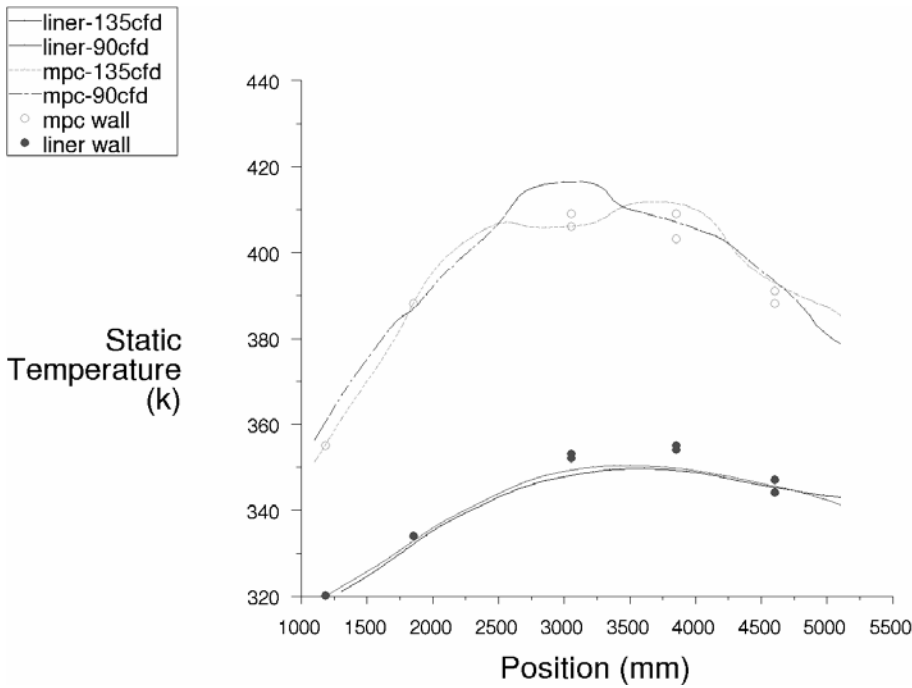


**Figure 11.18 MPC and liner walls axial temperature, using low Reynolds k-ε  turbulence model**
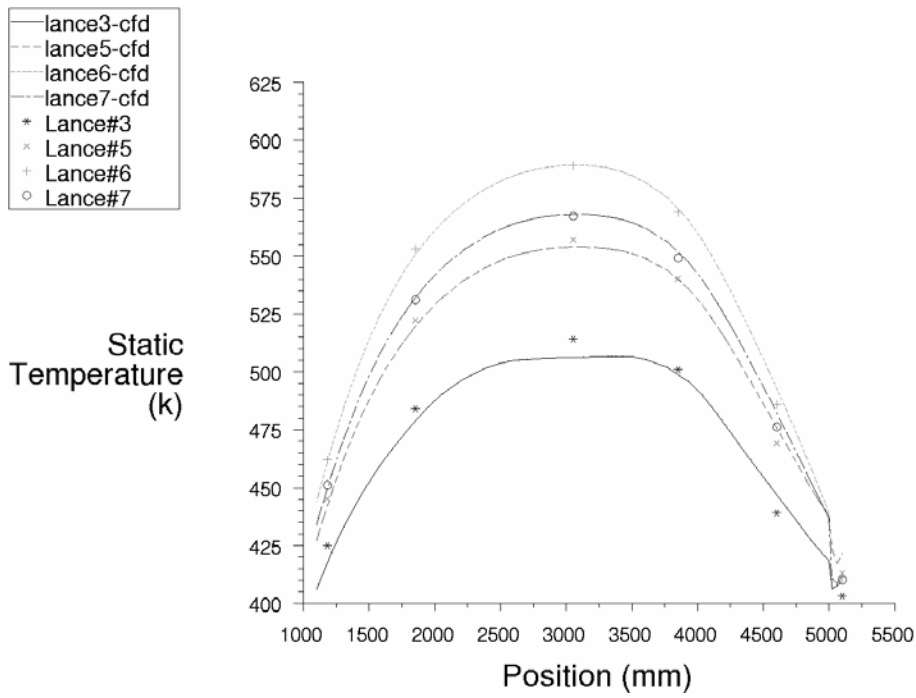
**Figure 11.19 Fuel region axial temperature, using standard k-ε turbulence model**
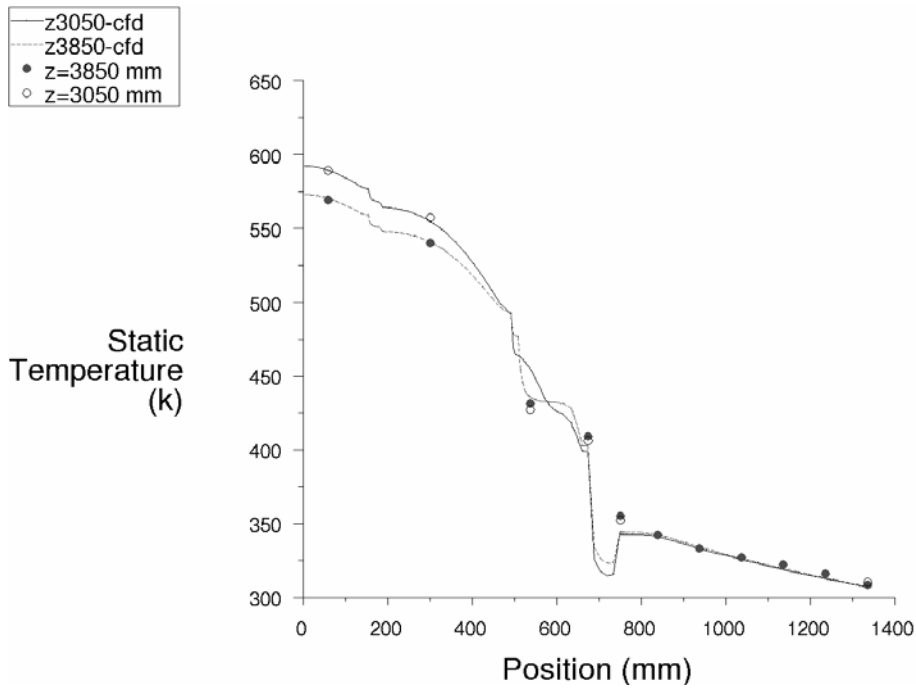


**Figure 11.20 Radial temperature at 3.05 and 3.85 m, using standard k-ε turbulence model**
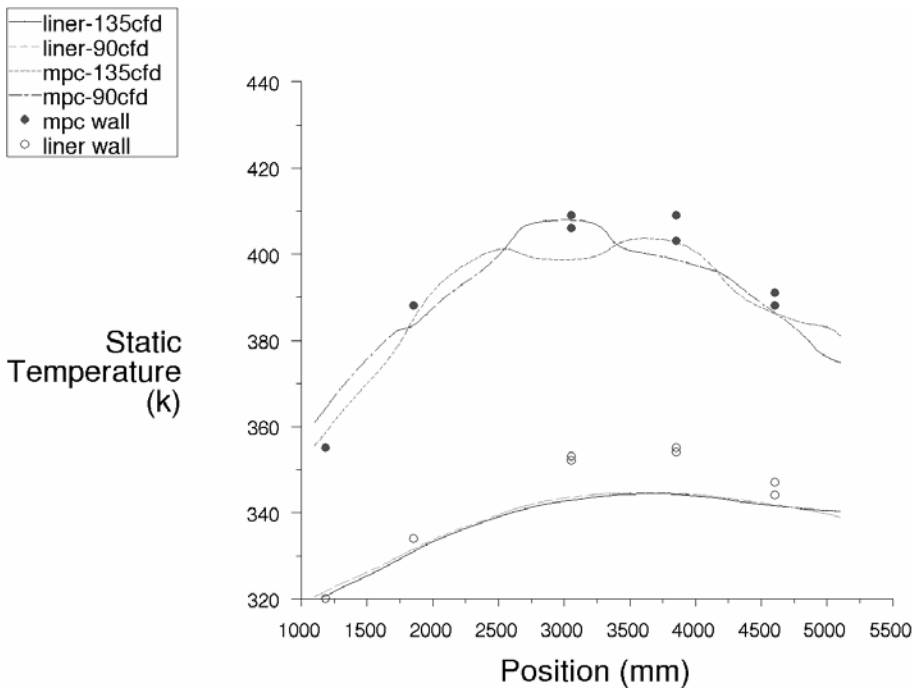
**Figure 11.21 MPC and liner walls axial temperature, using standard k-ε turbulence model**
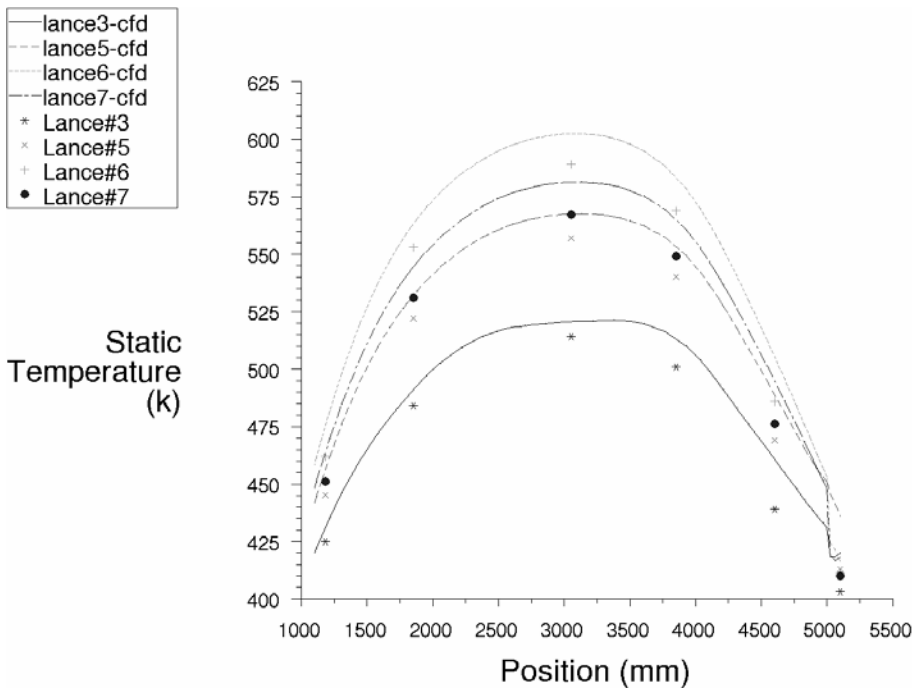


**Figure 11.22  Fuel region axial temperature, using laminar option**
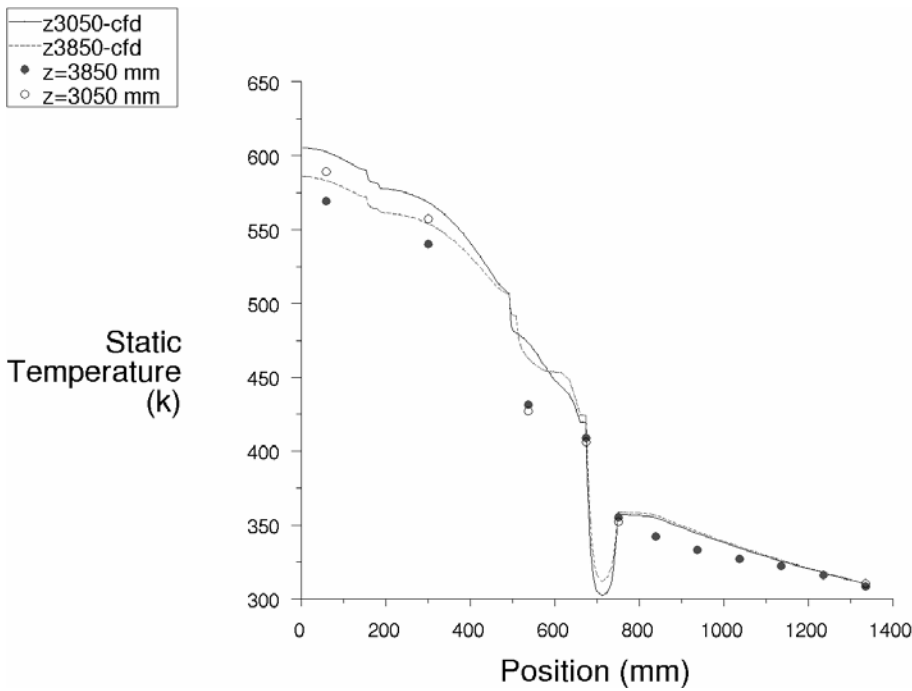
**Figure 11.23 Radial temperature at 3.05 and 3.85 m, using laminar option**
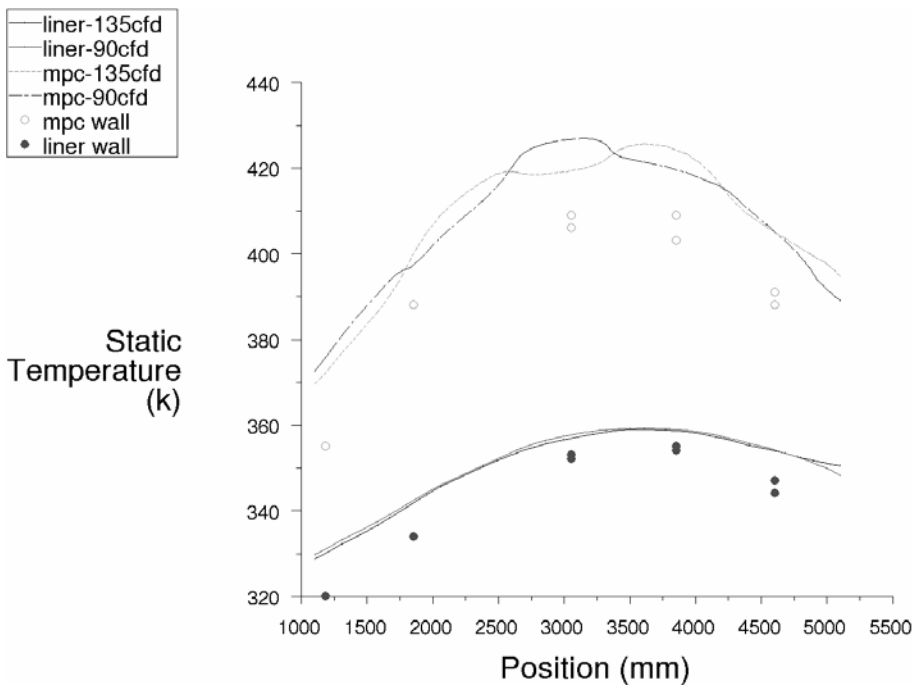


**Figure 11.24 MPC and liner walls axial temperature using laminar option**

## 11.4    Hydrogen Mitigation in the Containment of the PAKS NPP

Within the PHARE project "Hydrogen management for the VVER-440/213 containment" [132] of the EC, the project partners were requested to provide simulations for the hydrogen behaviour in the containment during a severe accident, The problem was selected from existing Probabilistic Safety Assessments (PSA), and flow boundary conditions for steam and hydrogen into the containment were

provided by a MAAP calculation [260] of the reactor system response to the severe accident. Comparison was made of the consequences for two variations on the accident scenario. The first case had no counter-measures against hydrogen accumulation and the second case included catalytic recombiners to remove as much hydrogen as possible from the containment atmosphere. Ignition of the atmospheric gas mixtures was not considered, but could be included as an extension of the project scope. The main result of the project was information on the effectiveness of different arrangements of catalytic recombiners in removal of atmospheric hydrogen and therefore reduction of the risk of damage by ignition.

The problem was very complex in geometry (full containment with numerous internals and additional engineered systems) and spanned a long time (25000 s of transient). Additionally, none of the available commercial CFD codes were equipped with all the models needed. Special models had to be implemented before running the simulations:

- Bulk condensation of steam,

- Wall condensation of steam as a single phase implementation,

The following engineered systems were modelled:

- Condensation of water vapour in pressure suppression pools of the bubble condenser system (found in VVER-440 containments),

- Catalytic recombiners for hydrogen removal.

For the given type of problem CFD codes were selected for application because hydrogen mixing is a typical 3-D problem which requires a high spatial resolution of the given geometry to detect potential agglomeration of hydrogen. The use of full Navier-Stokes solvers was necessary in order to capture the momentum of the flow from the reactor pipe break as well as through various flow paths within the containment.

Experimental data for validation of CFD codes are not available for the interplay between all phenomena expected in the containment. However, combined-effect tests addressing mixing like the HYJET [261] experiments at Battelle Model-Containment and SETH tests at the PANDA facility [262] were used before this project started to validate CFX and FLUENT and to improve skills of the analysts. Recombiners in a multi-room arrangement (Battelle Model-Containment) were investigated in the HYMI [263] project of the EC and analysed with CFX. ISP 47 [113] simulations were used to extract information about the validity of the condensation models in CFX.

Best Practice Guidelines were applied in that sense that the experience collected from previous validation steps was applied. For example the numerical investigation of jets through openings (important for flame acceleration) led to a minimum resolution of 3x3 to 5x5 cells. Another aspect is to enable the possibility of counter-current flows through openings, which also require at least 3 or 4 or more cells over the height of the opening [262].

Computational times were very high, requiring about 50 days for one of the two cases on six to eight processors in a PC-cluster. This prevented the direct investigation of mesh influence and turbulence models on the results. Instead, in order to ensure a higher reliability of results the project partners used different meshes and different codes for the same problem. For all user-models implemented in the codes prior to the containment simulations special verification tests were carried out and differences carefully analysed.

### 11.4.1 Calculations performed

The codes involved in the simulations were FLUENT (VTT Finland), CFX (SERCO UK, GRS Germany) and GASFLOW (VEIKI Hungary). GASFLOW as a nuclear in-house code uses a completely different approach for mesh generation than CFX and FLUENT. VTT and GRS created two independent meshes of the PAKS containment. SERCO used the VTT grid in CFX. VTT implemented all necessary user-models in FLUENT, while SERCO and GRS shared the same modelling work for CFX.

The following table gives some details of the simulations performed.

| | FLUENT (VTT) | CFX (SERCO) | GASFLOW (VEIKI) | CFX (GRS) |
|---|---|---|---|---|
| Grid | Hexahedral (body-fitted) | Hexahedral (body-fitted) | Rectangular | Hybrid (Hexas, Tetras, Pyramids) (body-fitted) |
| Number of Cells | 167170 | 167170 | 23030 | 237400 |
| Wall Condensation Model | User Model | User Model | Built-in | User Model |
| Bulk Condensation | User Model | User Model | Built-in | User Model |
| Recombiner Model | User Model | User Model | Built-in | User Model |
| Bubble Condenser System | User Model | User Model | User Model | User Model |
| Mitigation Option (# of Recombiners) | 30 | 20 | 30 | 20 |

Results reported from the calculations include pressures and temperatures as well as distributions of hydrogen, steam and oxygen within all compartments of the containment. Additionally, some time dependent quantities useful for describing the ignition potential of the actual gas mixture in the containment were calculated. These are the lower and upper ignition limits (lower: >4 % hydrogen, >5 % oxygen and <55 % steam; upper: >8 % hydrogen, >5 % oxygen and <55 % steam), the size of ignitable clouds and the AICC (adiabatic isochoric complete combustion) pressure for selected regions in the containment. This pressure is easily calculated and can serve as an upper limit for most combustion situations if these really would occur.

### 11.4.2 GRS Simulations

Results from GRS for the two scenarios with and without hydrogen mitigation are summarized in this section. More details of these calculations can be obtained from references [264] and [265].

The final grid for the simulation without recombiners is shown in Figure 11.25. In this picture the main equipment of the primary circuit can be seen. In the upper part of the picture two channels establish the connection to the pressure suppression system of this reactor system. This pressure suppression system (bubble condenser) consists of a tower to guide the hydrogen-steam-air mixture to twelve large water pools, where the steam condenses. The non-condensable gas components leave the water pools and flow to four large air spaces (air traps), from which they cannot return to the reactor system.

The mesh in the bubble condenser (only the lower section is visible in Figure 11.25) is considerably coarser than in the main part of the containment. In the bubble condenser detailed flow fields are not of interest; only gas composition and pressure need to be known to establish the link to the main part of the containment.

The SST (Shear Stress Transport) turbulence model available in CFX (version 5.7.1) was chosen for this work in conjunction with a combined linear and logarithmic wall function. This selection was made based on comparisons between simulations of several SETH tests [262] using SST and k-ε turbulence model options.
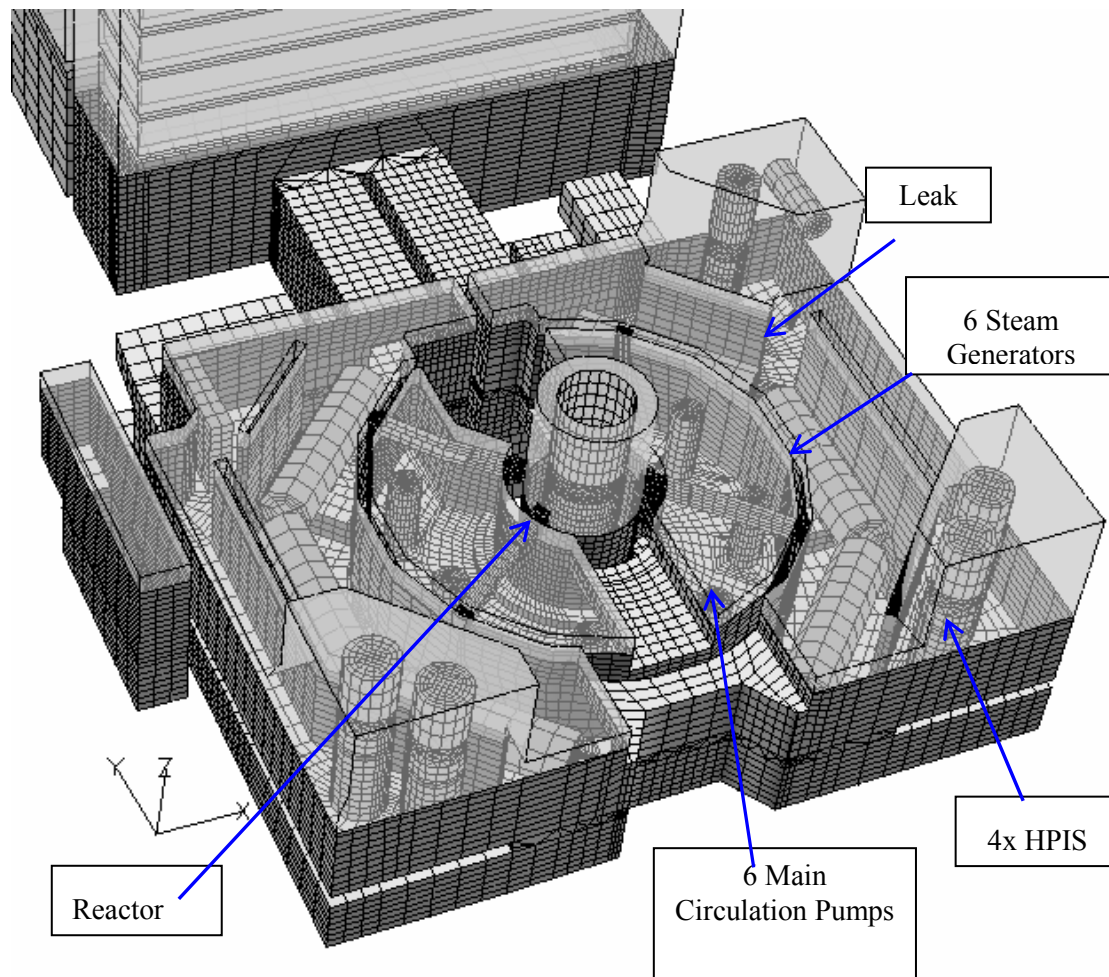


**Figure 11.25 View of main components and the surface mesh of the modeled containment**

The non-dimensional wall distance (see Section 6.2.3) was detected to stay well within an upper boundary of about 300.

All main components were built from hexahedral cells. Cylindrical bodies were handled by an internal "H-type" grid to avoid strongly distorted cells. In order to restrict the propagation of internal mesh structures too far from the location where they are needed, layers of tetrahedral cells were introduced. One example of this method can be seen in the upper end of the connecting channels before they merge into the tower of the bubble condenser.

The CFX grid for the simulation case including recombiners was modified from the grid in Figure 11.25 by splitting appropriate blocks down to the size of the recombiner boxes which is about 1.5 m by 1.4 m by 0.3 m (WxHxD).
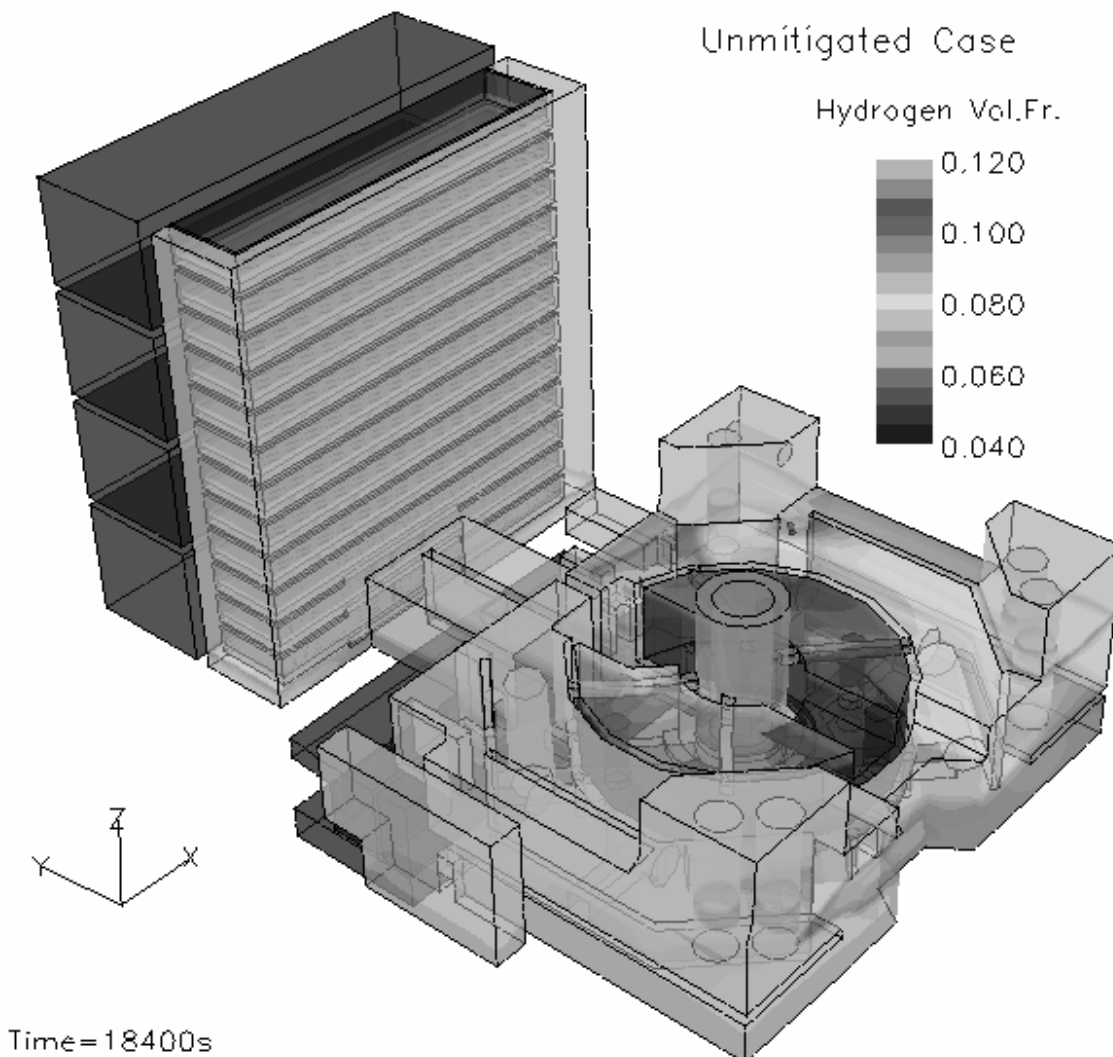


**Figure 11.26 Distribution of hydrogen in the containment in the unmitigated case**

Figure 11.26 and Figure 11.27 provide the hydrogen volume fraction in the containment for the unmitigated and mitigated cases . The time selected is after the first hydrogen release peak. In the unmitigated case there are many locations with hydrogen fractions higher than 12 %. However, high steam and low oxygen volume fractions in many locations at the same time (not shown) avoid ignitability even in this case. This illustrates the danger in looking only at hydrogen concentrations to reach a conclusion on combustion consequences. The integrated size of ignitable clouds (all cells with ignition limit fulfilled) in the containment is shown in Figure 11.28. This figure illustrates how drastically recombiners reduce the chance of ignition.

Figure 11.27 in comparison to Figure 11.26 proves the strong removal effect of catalytic recombiners in a more illustrative manner. The colored surface contours in Figure 11.27 show that there are no more locations exceeding 8 % of hydrogen. In combination with oxygen and steam molar fractions the history of burnable cloud sizes (Figure 11.28) can be deduced.
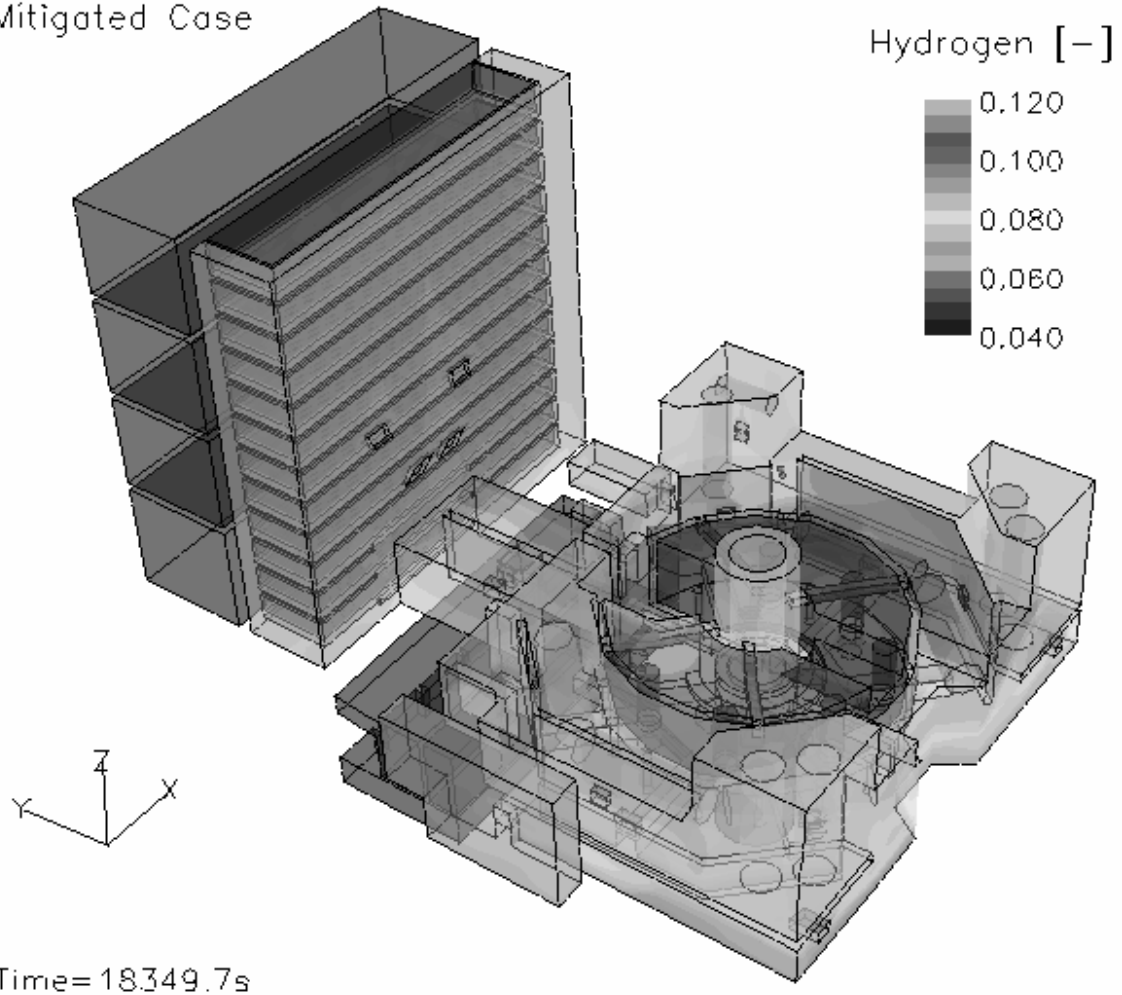


**Figure 11.27 Distribution of hydrogen in the containment with 20 recombiners installed**

## SG-Tube Rupture Accident in PAKS Containment

### - Size of Ignitable Cloud -
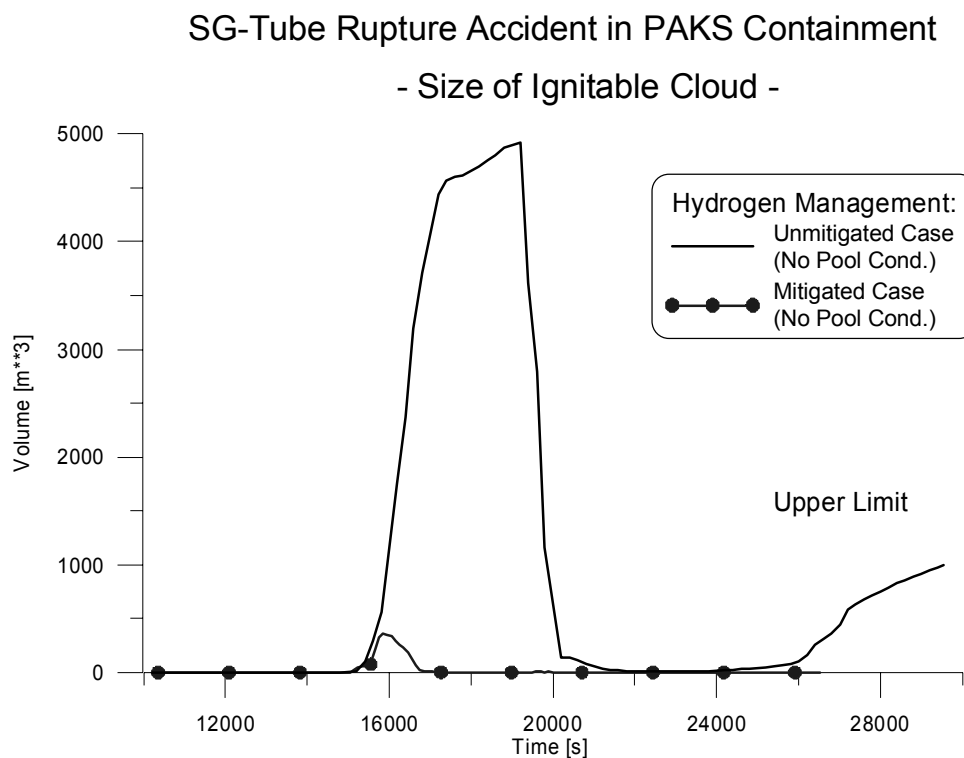
**Figure 11.28 Size of ignitable clouds for unmitigated and mitigated cases**

### *11.4.3    Conclusions*

Some results of the work carried out in the project "Hydrogen management for the VVER-440/213 containment" were presented to demonstrate the increasing capabilities of CFD in evaluating containment problems. The application of Best Practice Guidelines is currently restricted due to the prohibitive numerical effort to carry out mesh sensitivity studies and comprehensive investigations on different turbulence models. In the given context code benchmarks were defined to test the proper implementation of user models.

There is a continuous need to get more detailed information on hydrogen behaviour associated with severe accidents in order to design mitigation measures as reliably as possible. The work summarized gives new insights for this type of problems. There is also a generic significance of the simulations described because it is relatively easy to apply the same strategy to the containment of other and more recent reactor systems like EPR. It might even be easier to perform simulations as the complex bubble condenser system will not be available and containments consist of more open space.

# 12.    SUMMARY

As reflected in the content of this document, computer simulation is much more than generating input and observing results.  In an NRS project producing trusted results, these activities do not even occupy the majority of the staff time expended.  A project must begin with a clear written statement of the problem, including identification of the specific system and scenario to be analysed.  This statement is then reviewed by a panel of experts in a PIRT process, to identify parameters of interest and to rank physical phenomena (and by inference regions of the system) that most strongly influence these parameters.  This identification of important phenomena guides the analyst in selection of an appropriate CFD code and in selecting optional physical models within that code.  With knowledge of the system and significant physical phenomena, the panel is also responsible for identification of existing information that can be used to validate models over the range of conditions in the specified scenario.

The panel's identification of significant physical phenomena, and associated validation is also an initial guide for spatial (and if appropriate temporal) discretization. If a specific validation problem has already been performed with the selected code, it should be reviewed for appropriate nodalization. If new validation calculations are required, a verification process is necessary to estimate errors associated with discretization before any comparison with data.  This may result in an iterative adjustment of discretization until quantitative assurance is available that error associated with selection of the spatial mesh (and where appropriate time step) does not contaminate conclusions of the of the validation exercise.

If validation does not include simulations of the full system considered by the project, verification of the final discretization will also be needed before accepting results.  Frequently, available time and computer resources restrict the rigor in estimation of discretization error.  However, analysts must not use these restrictions as a excuse to abandon verification.  Useful information can be obtained from comparison with results from a mesh that is coarser than the one used for final results, and verification tests with subsections of the mesh can also be productive.

This document suffers from two major shortcomings.  The first is that we are producing a snapshot of guidelines at a relatively early phase in the use of CFD for nuclear reactor safety applications. In addition general claims of maturity for single phase CFD technology ignore the fact that most applications still must strike a balance between detail of modelling and reasonable execution time for the simulation.  As the natural growth continues in computer speed and memory, opinions on optimal discretization and model selection will shift.  As practical capabilities and associated experience expand, we expect extensions and revisions to all Best Practice Guidelines.  The second limitation is in the necessary decision to cover a wide range of CFD safety applications.  As more experience is gained through OECD sponsored benchmarks and other activities, we recommend that this document be used as a template for application specific best practice guidelines.  For example experience with ISP 47 could be used to generate detailed guidelines for modelling hydrogen mixing and combustion in a containment building.

Examples have been provided for two safety issues with a relatively long history of CFD analysis: boron dilution; and pressurized thermal shock.  In addition CFD analyses are described for the more recent issues of dry cask fuel storage, and hydrogen mixing in containment. None of these are intended as sample implementations of the guidelines provided in this document.  They do, however,

demonstrate important considerations in the area of model selection, and provide references to validation data for four specific problems in nuclear reactor safety.

The method of manufactured solutions is briefly outlined here because of its power for verification of a code's implementation of approximate solution methods to the underlying PDEs. It is a very simple process, although some of the algebra required for implementation can become complicated. You start with a partial differential equation or system of PDEs for which you want to verify the implementation of a discretized solution procedure. You choose a closed analytic form for the solution that you want for the final test problem. Next you substitute the analytic solution into the base PDEs to generate new or modified source terms in the equations. Finally, initial and boundary conditions for the test problem are obtained by evaluating the selected solution form at zero time and at whatever spatial locations constitute the boundary of the problem. For a given code primary consideration for use of MMS is the level of difficulty involved in specifying or adding source terms to all PDEs involved in the solution.

As an example, suppose that we wish to verify a finite difference solution method for a one-dimensional transient conduction problem represented by the equation:

$$\frac{\partial T}{\partial t} - \alpha \frac{\partial^2 T}{\partial x^2} = \frac{q}{\rho c_p} .$$

For this example a very simple functional form is chosen for the solution.

$$T(x,t) = 300 + (0.01 - x^2)t$$

Evaluating the differential operators gives:

$$\frac{\partial T}{\partial t} = 0.01 - x^2, \quad \frac{\partial^2 T}{\partial x^2} = -2t, \quad \frac{\partial T}{\partial t} - \alpha \frac{\partial^2 T}{\partial x^2} = 0.01 - x^2 + 2\alpha t$$

As a result the source term in the original model equation is specifically set as:

$$\frac{q}{\rho c_p} = 0.01 - x^2 + 2\alpha t$$

Looking at the original functional form, the initial conditions are T(x,0)=300, and boundary conditions for a 0.2 m thick metal slab would be T(-0.1,t)=300. and T(0.1,t)=300.

For most general purpose conduction solvers, the source term could be provided via tabulated input. However, complications can arise due to interpolation procedures applied to the input. For best results the source term should be installed as a function added to the program, or linked to the program via an interface provided to users by the code developers.

Verification testing of the code is very similar to a Richardson Extrapolation based mesh and time step sensitivity study. The error between the code and manufactured solution is followed for a sequence of mesh and a sequence of time step sizes. Any plot of error vs. mesh size (or time step) should trend clearly towards zero as the discretization approaches zero. In addition a fit of one of these curves to the equation

$$error = ah^p$$

provides a check of the order of accuracy quoted for the discrete approximation to the PDE.

For best results from a manufactured solution the following rules should be followed.

- The manufactured solution should be assembled using smooth analytic functions, i.e. trigonometric, exponential or polynomial functions. This ensures that the theoretical order of accuracy can be attained and also such functions are easy to differentiate.

- The solution should be general enough to exercise every term in the governing equation, including all dependent variables.

- The solution should have a sufficient number of non-trivial derivatives.

- The solution should not be a strongly varying function of space and time or have a singularity. This is accomplished by bounding a solution derivative by a relatively small constant.

- There is no requirement on physical realism or robustness. However, if the code contains assumptions, such as a positive solution or a positive equation term, make sure the manufactured solution satisfies those assumptions.

# REFERENCES

1. Menter, F., "CFD Best Practice Guidelines for CFD Code Validation for Reactor-Safety Applications," European Commission, 5th EURATOM Framework Programme, Report, EVOL-ECORA-D1, 2002.

2. Casey, M., and Wintergerste, T., (ed.), "Special Interest Group on 'Quality and Trust in Industrial CFD' Best Practice Guidelines, Version 1," ERCOFTAC Report, 2000

3. Casey, M., and Wintergerste, T., "The best practice guidelines for CFD - A European initiative on quality and trust," *American Society of Mechanical Engineers, Pressure Vessels and Piping Division (Publication) PVP*, v 448, n 1, p 1-10, 2002.

4. WS Atkins Consultants, "Best Practices Guidelines for Marine Applications of CFD," MARNET-CFD Report, 2002.

5. AIAA, "AIAA Guide for the Verification and Validation of Computational Fluid Dynamics Simulations," AIAA Report G-077-1988, 1998.

6. Roache, P.J., "Verification and Validation in Computational Science and Engineering," Hermosa Publishers, 1998.

7. Oberkampf, W. L. and Trucano, T. G., "Verification and Validation in Computational Fluid Dynamics, Progress in Aerospace Sciences, Vol. 38, pp. 209-272, 2002.

8. Oberkampf, W. L., Trucano, T. G., Hirsch, C., "Verification, Validation and Predictive Capability in Computational Engineering and Physics," Applied Mechanics Reviews, Vol. 57, pp. 345-384, 2004.

9. Mantlik F., Schmid J., Műhlbauer P., Pecha P., Zukov A. V., Usakov P. A., Sorokin A. P., Jurjev J. S., Bogoslovskaja G. P., Kolmakov A. P., Titov P. A., Tichomirov B. B.: Methods and computer codes for thermal-hydraulic analysis of fast reactor fuel assemblies. Zbraslav, Czech Republic. (In Russian), 1986.

10. Műhlbauer P., Schmid J., Kobeda Z.: Finite element analysis of turbulent flow in infinite rod bundles. Presented at the 4th Topical Meeting on Nuclear Reactor Thermalhydraulics NURETH-4, Karlsruhe, Germany, 1989.

11. Műhlbauer P., Mantlik F.: Computations of local developing temperature fields in fast reactor fuel subassemblies. Presented at the 6th Topical Meeting on Nuclear Reactor Thermalhydraulics NURETH-6, Grenoble, France, 1993.

12. Macek J., Műhlbauer P., Kral P.: Thermalhydraulic Analyses of NPPs with VVER-440/213 for the PTS Condition Evaluation. Presented at the 8th Topical Meeting on Nuclear Reactor Thermalhydraulics NURETH-8, Kyoto, Japan, 1997.

13. Gavrilas, M., Kiger, K., 'OECD/CSNI ISP Nr. 43: Rapid Boron-dilution Transient Tests for Code Verification', NEA/CSNI/R(2000)22, November 2000..

14. Műhlbauer P.: International Standard Problem ISP-43: Comparison of pre-test calculations with experimental results. Report ÚJV 11 464 T, Rez, December 2000.

15. Műhlbauer P.: Application of FLUENT 5 to the International Standard Problem ISP-43 "Rapid Boron-Dilution Transient Tests for Code Verification". 8th FLUENT User's Meeting, Prague, Czech Republic, October 10 2000.

16. Scheuerer M., Andreani M., Bestion D., Egorov Y., Heitsch M., Menter F., Műhlbauer P., Pigny S., Schwäger C., Willemsen S.: Condensed Final Summary Report. ECORA Deliverable D17, March 2005.

17. Vyskocil L.: CFD Simulation of Slug Mixing Tests of OKB Gidropress. 13th FLUENT User's Meeting, Mikulov, Czech Republic, June 8 - 10, 2005.

18. Rohde U., Höhne T., Kliem S., Scheuerer M., Hemström B., Toppila T., Dury T., Klepac J., Remis J., Műhlbauer P., Vyskocil L., Farkas I., Aszodi A., Boros I., Bezrukov Y., "The European project FLOMIX-R: Fluid mixing and flow distribution in the reactor circuit - Final summary report," Scientific-technical Report, Forschungszentrum Rossendorf; FZR-432 August 2005.

19. Smith B. et *al*, "Assessment of CFD Codes for Nuclear Reactor Safety Problem's", OECD Nuclear Energy Agency Report NEA/SEN/SIN/AMA(2005)3, January 2005.

20. Payen T., Chapuliot S., Gourdin C., Magnaud J.P. and Monavon A , "Hydro-thermal-mechanical Analysis of Thermal Fatigue in a Mixing Tee",

21.
    Third International Conference on Fatigue of Reactor Components, Seville, Spain, October 3-6, 2004

22. OECD/CSNI Report. 2003. First workshop on analytical activities related to the SETH-OECD project, Barcelona, 2003.

23. Bieder, U. et al, "Simulation of mixing effects in a VVER-1000 reactor"; Proceedings of The 11th International Topical Meeting on Nuclear Reactor Thermal-Hydraulics (NURETH-11), Avignon, October 2-6, 2005.

24. Tricot, N. and Menant, B., "Coupled ThermalHydraulic-Neutronic Calculation of Mixing Problem with the TRIO_U Code", CSNI Workshop on Advanced Thermal-Hydraulic and Neutronic Codes: Current and Future Applications, Barcelona, April 10-13, 2000

25. H. Mutelle and U. Bieder, "Study with the CFD Code TRIO_U of Natural Gas Convection for PWR Severe Accidents", NEA and IAEA workshop: Use of computational fluid dynamics (CFD) codes for safety analysis of reactor systems including containment , PISA (Italy), November 2002.

26. Bieder, U. et al, "Detailed thermalhydraulic analysis of induced break severe accidents using the massively parallel CFD code TRIO_U/PRICELES", SNA 2003 International conference on super computing in nuclear applications, 22-24 Sept. 2003

27. A. Beccantini et al., "H2 release and combustion in large-scale geometries: models and methods", .Proc. Supercomputing for Nuclear Applications, SNA 2003, Paris, France, 22-24 September 2003.

28. Beccantini, A. and Paillère, H., "Modeling of hydrogen detonation for application to reactor safety", Proc. ICONE-6, San Diego, USA, 1998

29. Cioni, O., et al "Thermalhydraulic 3D calculations on the core of High Temperature Gas Cooled Reactor", : HTR 2004, 22-24 septembre 2004, BEIJING, China

30. Coste, P., "Computational Simulation of Multi-D Liquid-Vapor Thermal Shock with Condensation", 5th ICMF Yokohama, Japan, May 30 – June 4, 2004.

31. Pigny, S., Coste, P., "Simulation and Modeling of Two-Phase Bubbly Flows", the 11th International Topical Meeting on Nuclear Thermalhydraulics (NURETH 11) Popes' Palace Conference Center, Avignon, France, October 2-6, 2005.

32. Pigny, S., Coste, P., "Rising and Boiling of a Drop of Volatile Liquid in a Heavier one: Application to the LMFBR Severe Accident", The 11th International Topical Meeting on Nuclear Thermalhydraulics (NURETH 11) Popes' Palace Conference Center, Avignon, France, October 2-6, 2005.

33. Aszodi, A.; Liewers, P.; Krepper, E.; Prasser, H.-M., 'Investigations of an externally heated storage vessel', Proceedings of 3rd Workshop 'Anlagen-, Arbeits- und Umweltsi-cherheit', Köthen, 1996.

34. Knebel, J.U. (FZK); R. Reinders (KWU); M. Scheuerer (GRS): ‚Anwendung von CFD-Codes in der Reaktortechnik', Jahrestagung Kerntechnik '98, Tagungsbericht, Bonn, Mai 1998

35. Cheng, X., 'Entwicklung experimentell gestützter analytischer Verfahren zur Auslegung der Containmentkühlung mit Luft durch Naturkonvektion', Scientific Report, FZKA-6056 Forschungszentrum Karlsruhe; IATF, 1998.

36. Heitsch, M., 'A Two-Dimensional Model of Internal Catalytic Recombiner Behavior', ICONE-6422, May 1998.

37. Scheuerer, M., Heitsch, M., Menter, F., Egorov, Y., Toth, I., Bestion, D., Pigny, S., Pail-lere, H., Martin, A., Boucker, M., et al., 'Evaluation of Computational Fluid Dynamic Methods for Reactor Safety Analysis (ECORA)', Nuclear Engineering and Design 235, 359-368, 2005.

38. Rohde, U.; S. Kliem, T. Höhne, R. Karlsson, B. Hemström, J. Lillington, T. Toppila, J. Elter, Y. Bezrukov: "Fluid mixing and flow distribution in the reactor circuit – measurement data base", Nucl. Engineering and Design Vol. 235 pp. 412-435, 2005.

39. Höhne, T.; S. Kliem, M. Scheuerer: "Experimental and numerical modelling of a buoyancy driven flow in a reactor pressure vessel", 11th Int. Topical Meeting on Nuclear Reactor Thermalhydraulics (NURETH-11), Avignon, France, paper 480, October 2-6, 2005.

40. Kliem, S.; U. Rohde, F.-P. Weiß: "Core response of a PWR to a slug of under-borated water" *Nuclear Engineering and Design, vol. 230, pp.121-132, May 2004.*

41. Höhne, T.; C. Vallee: "Experimental modelling and CFD simulation of air/water flow in a horizontal channel", 11th Int. Topical Meeting on Nuclear Reactor Thermalhydraulics (NURETH-11), Avignon, France, paper 479, October 2-6, 2005.

42. Krepper, E.; Grahn, A.; Alt, S.; Kästner, W.; Kratzsch, A.; Seeliger, A.: „Numerical investigations for insulation particle transport phenomena in water flow", 11th Int. Topical Meeting on Nuclear Reactor Thermalhydraulics (NURETH-11) , Avignon, France, paper 116, October 2-6, 2005.

43. Krepper, E.; Egorov, Y.: "CFD-modelling of subcooled boiling and application to simulate a hot channel of a fuel assembly", 13th Int. Conf. on Nuclear Engineering (ICONE-13), Chinese Nuclear Society, Peking, China, May 2005..

44. Shi, J.-M.; Frank, T.; Rohde, U.; Prasser, H.-M.: "Nx1 MUSIG model -- implementation and application to gas-liquid flows in a vertical pipe", 22nd CAD-FEM User Meeting 2004 and CFX & ICEM CFD Conference, Dresden, Germany, Nov. 10-12, 2004.

45. Prasser, H.-M.; Beyer, M.; Carl, H.; Gregor, S.; Lucas, D.; Pietruske, H.; Schütz, P.; Weiss, F.-P: "Evolution of the Structure of a Gas-Liquid Two-Phase Flow in a Large Vertical Pipe", 11th Int. Topical Meeting on Nuclear Reactor Thermalhydraulics (NURETH-11), Avignon, France, paper 399, October 2-6, 2005.

46. Frank, T.; Zwart, P.; Shi, J.-M.; Krepper, E.; Lucas, D.; Rohde, U.: Inhomogeneous "MUSIG model – a population balance approach for poly-dispersed bubbly flows", International Conference Nuclear Energy for New Europe 2005, Bled, Slovenia. 2005.

47. W. Ambrosini, N. Forgione, D. Mazzini, F. Oriolo, "Computational study on evaporative film cooling in a vertical channel", Heat Transfer Engineering, Volume 23 - Issue 5, pp. 25-35, 2002.

48. W. Ambrosini, N. Forgione, F. Oriolo, F. Varano, Condensation of an Air-Steam Mixture on a Flat Wall in a Vertical Square Channel, 21st UIT National Heat Transfer Conference 2003, Udine, pp. 197-202, June 23-25, 2003.

49. W. Ambrosini, N. Forgione, F. Oriolo, F. Varano, Steam Condensation in the Presence of Air: Prediction of Test Conditions by One-dimensional and CFD Codes , 22nd UIT National Heat Transfer Conference 2004, Genova, June 21-23, 2004, CD-ROM.

50. W. Ambrosini, N. Forgione, F. Oriolo, Experiments and CFD Analyses on Condensation Heat Transfer on a Flat Plate in a Square Cross Section Channel, Accepted at the 11th International Topical Meeting on Nuclear Reactor Thermal-Hydraulics (NURETH-11), Paper: 157, Popes' Palace Conference Center, Avignon, France, October 2-6, 2005.

51. N. Forgione, S. Paci, Computational Analysis of Vapour Condensation in Presence of Air in the TOSQAN Facility, Accepted at the 11th International Topical Meeting on Nuclear Reactor Thermal-Hydraulics (NURETH-11), Paper: 156, Popes' Palace Conference Center, Avignon, France, October 2-6, 2005.

52. W. Ambrosini, N. Forgione, J.C. Ferreri, M. Bucci "The effect of wall friction in single-phase natural circulation stability at the transition between laminar and turbulent flow", Annals of Nuclear Energy, Vol. 31, pp. 1833–1865 2004.

53. W. Ambrosini, J.C. Ferreri, N. Forgione, Finite-Volume analysis of natural convection in a 8:1 tall enclosure, First MIT Conference on Computational Fluid and Solid Mechanics, vol. 2, 1446, Cambridge, MA, June 12-15, 2001.

54. W. Ambrosini, J.C. Ferreri and N. Forgione "Sensitivity Analyses on Natural Circulation in a 8:1 Tall Enclosure using Finite-Volume Methods", International Journal of Heat and Technology, Vol. 21, No. 1, pp. 51-58, 2003.

55. B. Bordini, F. Fineschi, W. Ambrosini, A Computational Fluid Dynamic Code to Simulate Hydrogen Catalytic Recombiner, 21st UIT National Heat Transfer Conference 2003, Udine, pp. 495- 500, June 23-25, 2003.

56. Kamide, H., Hayashi, K., Isozaki, T., and Nishimura, M., "Investigation of Core Thermohydraulics in Fast Reactors- Interwrapper flow during natural circulation", Nuclear Technology vol.133 p.77-91, Jan.2001

57. Muramatu, et al., "Validation of Fast Reactor Thermomechanical and Thermohydraulic Codes", Final report of a co-ordinated research project 1996-1999, IAEA-TECDOC-1318, 2002

58. Takata, T. and Yamaguchi, A., "Numerical Approach to the Safety Evaluation of Sodium-Water Reaction", J. Nucl. Sci. Tech., Vol. 40, No. 10, pp.708-718, 2003

59. Morii, T. et al., " Improvement of hydraulic flow analysis code for APWR reactor internals," Presented at the Exploratory Meting of Experts on the Application of CFD to Nuclear Reactor Safety Problems, NEA/CSNI/R(2002)16, 2000.

60. Ishida, "Calculation of ISP-47 exercise with the DEFINE code", 2003.

61. Yagi, et al., "Two-phase flow analysis for secondary side in steam generator," ICONE10-22099, 2002.

62. Kwon, T.S.,  Song, C.-H., Baek, W.P., "A Three-Dimensional CFD Calculation for Boron Mixing Behaviors at the Core Inlet," NURETH-10, Seoul, 2003.10.

63. Kwon, T.S., Song, C-H, "Simulation of Delayed Borated Water during Steam Line Break," SNA-2003, Paris, 2003.

64. Kwon, T.S., Choi, C.-R., Song, C.-H, "Three-dimensional analysis of flow characteristics on the reactor vessel downcomer during the late reflood phase of a postulated LBLOCA," Nuclear Engineering & Design, Vol. 226, 2003.

65. Yoon, S. H., Kim, W. J., Suh, K. Y., Song, C.-H., "Characteristics of Steam Jet Impingement on Annulus," NUTHOS-6, Nara, 2004.10.

66. Jeong, J.H., Han, B.S., "A CFD Analysis of Flow Distribution in a PWR Reactor Vessel Based on CAD data," ICAPP'05, 2005.5.

67. Kim, K.-C., et al, , "An Unsteady Analysis on Thermal Stratification in the SCS Piping Branched off the RCS Piping," ASME PVP-2003, 2003.7.

68. Kang, H.S.,  Kim, Y. S., Chun, H. G., Yoon, Y. J., Song, C.-H., "CFD Analysis for the Thermal Mixing Phenomena in the Subcooled Water Tank," NTHAS-4,  Sapporo, 2004.11.

69. Lee, T.H. et. al.,"Local Flow Characteristics of Subcooled Boling Flow of Water in a Vertical Concentric Annulus", Int'l J. of Multiphase Flow, vol. 28, pp1351-1368.

70. Kim, J.T., Hong, S.W., Kim, S.B., Kim, H.D., "Hydrogen Mitigation Strategy of the APR1400 Nuclear Power Plant for a Hypothetical Station Blackout Accident," Nuclear Technology, vol.150, No.3, pp.263-282, 2005

71. Oh, M. T., Choi, J. H., Seo, J. T., "A Fuel Channel Integrity and Moderate Behavior during a LOCA in Pressurized Heavy Water Reactor," ICAPP'05, Seoul, May 17, 2005

72. Yoon, C., Rhee, B.W., and Min, B.-J., "Development and Validation of the 3-D CFD Model for CANDU-6 Moderator Temperature Predictions," Nuclear Technology, 148[3], 259 (2004).

73. Cho, H.K. et al., "Study on the Heat Transfer in the Water Pool Type Reactor Cavity Cooling System of the Very High Temperature Gas Cooled Reactor", ASME Fluid Eng'g Conf., Sanfrancisco, 2005, 7.

74. Lee, J.J., Kang, S.K., Yoon, S.J., Park, G.C. and Lee, W.J., "Assessment of Turbulence Models in CFD Cods and Its Application to Pebble Bed Reactor," HEFAT2005, 2005.9.

75. Yoon, H. Y., Joo, H.G., Hwang, Y.D., Kim, H.C., Zee, S. Q., "Development of a 3-D Performance Analysis Code for SMART Research Reactor," NTHAS-4, Sapporo, Japan, 2004.11.

76. Kim, J.-H., Kim, T.-W., Lee, S.-M., Park, G.-C., "Study on the Natural Circulation Characteristics of the Integral Type Reactor for Vertical and Inclined Conditions," Nuclear Engineering & Design, 207, pp.21-31, 2001.

77. Siccama, N.B., Houkema, M., and Komen, E.M.J., "CFD Analysis of Steam and Hydrogen Distribution in a Nuclear Power Plant", NEA and IAEA workshop on the Use of CFD Codes for Safety Analysis of Reactor System, including Containment, Pisa, Italy, 11-15 November 2002.

78. Willemsen, S.M. and Komen, E.M.J., "CFD Assessment of RANS CFD Modelling for Pressurised Thermal Shock Analysis", The 11th International Topical Meeting on Nuclear Thermal Hydraulics (NURETH 11) Popes' Palace Conference Center, Avignon, France, October 2-6, 2005.

79. Komen, E.M.J. and Roelofs, F. "Determination of Flow Stability and Flow Asymmetry and their Effect on the Heat Removal Capability of the ESS Target", The 11th International Topical Meeting on Nuclear Thermal Hydraulics (NURETH 11) Popes' Palace Conference Center, Avignon, France, October 2-6, 2005.

80. Roelofs, F. and Komen, E.M.J., "CFD Analyses of the Lead-Bismuth Flow Field in the Lower Plenum of the Myrrha Pool", The 11th International Topical Meeting on Nuclear Thermal Hydraulics (NURETH 11) Popes' Palace Conference Center, Avignon, France, October 2-6, 2005

81. Lycklama, J.A. and Hoehne, T., "CFD Modeling of the Mixing of Deborated with Borated Water in a Reactor Pressure Vessel", European Nuclear Congress 2005 (ENC2005), Versailles, France, December 11-14, 2005.

82. Roelofs, F. and Komen, E.M.J., "Heat Transfer to Supercritical Water in an SCWR Relevant Geometry", European Nuclear Congress 2005 (ENC2005), Versailles, France, December 11-14, 2005.

83. Tinoco, H. Personal communication. PIUS project within Asea-Atom (Only proprietary reports exist).

84. Hemström, B. and Tinoco, H. "Forsmark 1-2, Fukthalt i reaktorånga, numerisk simulering och beräkningar", Rapport UL-89:29, Vattenfall, Älvkarlebylaboratoriet, 1989.

85. Hemström, B. "Numerisk simulering av strömning i ånggeneratorer". Rapport VU-S 90:17, Vattenfall Utveckling AB, 1990.

86. Hemström, B., Lundström A. and Tinoco, H. "Mixing process in the downcomer of a BWR", Report VU-S 91:30, Vattenfall Utveckling AB, 1991.

87. Tinoco, H. and Alavyoon, F. "Numerisk förstudie av grundorsak till vibrationer i system 311/314", Rapport VU-S 93:B20, Vattenfall Utveckling AB, 1993.

88. Tinoco, H. and Hemström, B. "Dropperosion i titankondensorer – strömningstekniska studier", Rapport VU-S 93:B35, Vattenfall Utveckling AB, 1993.

89. Alavyoon, F. "Numerical investigations of rapid boron dilution transients for a 1/PWR mock up. – I. Grid convergence studies of the flow field." Report no. US 95:12, Vattenfall Utveckling AB, 1995.

90. Andreasson, P. and Hemström, B. "Simulation of rapid boron dilution transient (OECD/CSNI ISP NR 43). Report US 00:10, Vattenfall Utveckling AB, 2000.

91. Veber, P. and Andersson, L. "CFD calculation of flow and thermal mixing in a T-junction – time dependent calculation. Part 2 (BG-project)", Teknisk not 2004/21 Rev 0, Onsala Ingenjörsbyrå AB, 2004.

92. Müller, F. "Assessment of RELAP 5 against HDR-experiments", NOTHOS-6, Nara, Japan, Oct. 2004.

93. Veber, P. and Andersson, L. "On the validation and application of Fluid-Structure Interaction analysis of reactor vessel internals at loss of coolant accidents", Kärnteknik, Dec. 2004.

94. Anglart, H., Andersson, S. and Jadrny, R. "BWR steam line and turbine model with multiple piping capability", Nuclear Engineering and Design, vol. 137, pp.1-10, 1992.

95. Anglart, H. and Nylund, O. "CFD application to prediction of void distribution in two-phase bubbly flows in rod bundles", Nuclear Engineering and Design, vol. 163, pp.81-89, 1996.

96. Anglart, H., Nylund, O., Kurul, N. and Podowski, M.Z. "CFD prediction of flow and phase distribution in fuel assemblies with spacers", Nuclear Engineering and Design, vol. 177, pp. 215-228, 1997.

97. Anglart, H. "ABC-Advanced bundle code for thermal-hydraulics predictions in LWR fuel assemblies", Proc. Mathematics and Computation, Reactor Physics and Environmental Analysis in Nuclear Applications, vol. 1, pp.200-209, Madrid, Spain, Sept. 1999.

98. Windecker, G. and Anglart, H. "Phase distribution in a BWR fuel assembly and evaluation of a multidimensional multifield model", Nuclear Technology, vol. 134, pp. 49-61, 2001.

99. Anglart, H. and Podowski, M.Z. "Fluid mechanics of Taylor bubbles and slug flow in vertical channels", Nuclear Science and Engineering, vol. 140, pp. 165-171, 2002.

100. "OECD/SETH Large-scale investigation of gas mixing and stratification", 2nd Workshop on analytical activities, Analysis of PANDA experiments, Dec. 2004.

101. B. L. Smith, B. J. Broadhouse, A. Yerkess, "The Computer Code SEUBNUK/EURDYN (Release 1) Input and Output Specifications", EIR Report 591/AEEW-R 2070/EUR-10697 EN, May 1986.

102. N. E. Hoskin, M. J. Lancefield, "The COVA Programme for the Validation of Computer Codes for Fast Reactor Containment Studies", Nucl. Eng. Design, 46 17-46, 1978.

103. J. F. Jaeger, B. L. Smith, H. Palsson, "Modelling of an LMFBR Cover for Fluid-Structure Interaction Studies'', Trans. 8th Int. Conference on Structural Mechanics in Reactor Technology (SMiRT-8), Brussels, Belgium, Paper E7/7, 19-23 August 1985.

104. R. D. Lonsdale,"An Algorithm for Solving Thermal-Hydraulic Equations in Complex Geometry: The ASTEC Code", Int. Top. Mtg. on Advances in Reactor Physics, Math. and Computing, Paris, April 27-30 1987.

105. CFX-4.3, AEA Technology, Harwell, UK, 2000.

106. G. Yadigaroglu, J. Dreier, "Passive Advanced Light Water Reactor Designs and the ALPHA Program at the Paul Scherrer Institute, Kerntechnik, 63, 1-8.

107. S. V. Shepel, B. L. Smith, S. Paolucci, "Implementation of a Level Set Interface Tracking Method in the FIDAP and CFX-4 Codes", J. Fluids Eng., 127, 674-686, 2005.

108. M. Milelli, "A Numerical Analysis of Confined Turbulent Bubble Plumes", PhD Thesis No. 14799, Federal Technical University (ETH), Zurich, Switzerland, 2002.

109. B. L. Smith, S. V. Shepel, "CFD Analysis of a Possible Leakage of Coolant in the MEGAPIE Spallation Source Target", Proc. ASME Heat Transfer Conference HT2005, San Francisco, USA, Paper No. 726119, 17-22 Nov., 2005.

110. B. L. Smith, W. Leung, A. Zucchini, "Coupled Fluid/Structure Analyses of the MEGAPIE Spallation Source Target during Transients", Proc. 11th Int. Conf. on Nuclear Reactor Thermal-Hydraulics (NURETH-11), Paper 509, Avignon, France, Oct. 2-6, 2005.

111. T. V. Dury, "Simulation with CFX-4.3 of Steady-State Conditions in a 1/5th-Scale Model of a Typical 3-Loop PWR in the Context of Boron-Dilution Events", IAEA, OECD/NEA Technical Meeting on the Use of Computational Fluid Dynamics (CFD) Codes for Safety Analysis of Reactor Systems, Including Containment Pisa, Italy, CD-ROM, 11-14 November 2002,.

112. F. P. Weiss et al., "Fluid Mixing and Flow Distribution in the Reactor Circuit (FLOMIX-R)", FISA 2003 EU Research in Reactor Safety, 10-13 November 2003, Luxembourg, Luxembourg, 499-505, 2004.

113. Fischer, K., "International Standard Problem ISP-47 on Containment Thermal-Hydraulics, Step 2: ThAI. Volume 1: Specification Report," Becker Technologies GmbH, Eschborn, Report Nr. BF-R 70031-1, Revision 4, December 2004.

114. A. Dehbi, "Tracking of aerosol particles in large volumes with the help of CFD", 12th Int. Conf. on Nuclear Engineering (ICONE 12), 25-29 April 2004, Arlington, USA, CD-ROM, 2004.

115. Yagi, et al., "Two-phase flow analysis for secondary side in steam generator," Proceedings of ICONE10, Arlington Virginia, April 14-18, 2002.

116. Sha, W.T. , Domanus, H.M., Schmidt, R.C., Oras, J.J., Lin, E.I.H. , "COMMIX-1: A Three-Dimensional Transient Single-Phase Computer Program for Thermal-Hydraulic Analysis", NUREG/CR-0785, Argonne National Laboratory Report ANL-77-96, September, 1978.

117. Sha, W.T., Chao, B.T. and Soo, S.L., "Porous-Media Formulation for Multiphase Flow With Heat Transfer", Nuclear Engineering and Design, Vol. 82, pp 93-106, 1984.

118. Chao, D. Lumnsford, B. Chexal, B. and Layman, W., "Analysis of Mixing With Direct Safety Injection Into the Downcomer Region of a Westinghouse Two-Loop PWR", EPRI/NSAC-63, May 1984.

119. Sha, W.T., and Shah, V.L., "Natural Convection Phenomena in A Prototypic PWR During a Postulated Degraded Core Accident", EPRI TR-103574, January 1994.

120. Rivard, W.C, and Torrey, W.C., "K-FIX: A computer program for transient, two-dimensional, two-fluid flow", Los Alamos Scientific Laboratory report LA-NUREG-6623, April 1977.

121. Thurgood, M.J., Kelly, J.M., Basehore, K.L., and George, T.L., "COBRA-TF, A Three-Field Two-Fluid Model for Reactor Safety Analysis," 19th National Heat Transfer Conference, Orlando, Nov. 27-30, 1980.

122. George, T. L., Thurgood, M.J., Wiles, L.E., Wheeler, C.L., Merilo, M, "Containment Analysis with GOTHIC," 27th National Heat Transfer Conference, Minneapolis, Nov. 28-31, 1991.

123. J.K. Dienes, C.W. Hirt, W.C. Rivard, L.R. Stein, and M.D. Torrey ,"FLX: A shell code for coupled fluid-structure analysis of core barrel dynamics", Los Alamos Scientific Laboratory report LA-7927, NUREG/CR-0957, 1979

124. Rivard, W.C, and Torrey, W.C., "Application of the K-FIX code to fluid structure interaction phenomena in the HDR Geometry", Los Alamos Scientific Laboratory report LA-9138-MS, NUREG/CR-2477, 1981.

125. Chao, J., Lumnsford, D., Chexa, B., and Layman, W., "Analysis of Mixing With Direct Safety Injection Into the Downcomer Region of a Westinghouse Two-Loop PWR," EPRI Report, EPRI/NSAC-63, May 1984.

126. Sha, W.T., and Shah, V.L., "Natural Convection Phenomena in A Prototypic PWR During a Postulated Degraded Core Accident," EPRI Report, EPRI TR-103574, January 1994.

127. Boyd, C.F., Kiger, K., and Gavelli. F., "CFD Predictions and Experimental Data for Downcomer Mixing of an Infinite Slug in a Rapid Boron Dilution Transient," Proc. 8th International Conference on Nuclear Engineering (ICONE-8), ICONE-8224, Baltimore, USA, April 2-6, 2000.

128. Boyd, C.F., "Predictions of Spent Fuel Heatup After a Complete Loss of Spent Fuel Pool Coolant," U.S. Nuclear Regulatory Commission Report, NUREG-1726, June 2000.

129. Boyd, C.F., Helton, D.M., Hardesty, K., "CFD Analysis of Full-Scale Steam Generator Inlet Plenum Mixing During a PWR Severe Accident," U.S. Nuclear Regulatory Commission Report, NUREG-1788, May 2004.

130. Steger, J. L., Dougherty, F. C. and Benek, J. A., "A Chimera Grid Scheme," Advances in Grid Generation, K. N. Ghia and U. Ghia, eds., ASME FED-Vol. 5, June, 1983.

131. Boyack, B. et al., "Quantifying Reactor Safety Margins: Application of Code Scaling, Applicability, and Uncertainty Evaluation Methodology to a Large-Break, Loss-of-Coolant Accident," U.S. Nuclear Regulatory Commission Report, NUREG/CR-5249, December 1989.

132. Huhtanen, R. (Editor), "Hydrogen management for the VVER-440/213 containment," Phare project service contract No HU2002/000-632-04-01, Final Report, Dec. 2005.

133. Wilson, G.E. and Boyack, B.E., "The role of the PIRT process in experiments, code development and code applications associated with reactor safety analysis," Nuclear Engineering and Design, Vol. 186, pp. 23-37, 1998.

134. George, Th. L., *et al.*, GOTHIC containment analysis package - User Manual. Numerical Applications, Inc., NAI 8907-02 Rev. 7, prepared for EPRI (RP4444-1), 1997.

135. Heitsch, M., Schramm, B., Allelein, H-J., "Simulation of hydrogen mixing in the containment of the Paks NPP during a severe accident (Simulation der Wasserstoffverteilung im Sicherheitsbehälter des KKW Paks bei einem schweren Störfall)," Annual Meeting on Nuclear Technology 2006, Aachen, 2006

136. Smith, B.L., Milelli, M., Shepel, S., "Aspects of Nuclear Reactor Simulation Requiring the use of Advanced CFD Models", IAEA, OECD/NEA Technical Meeting on Use of Computational Fluid Dynamics (CFD) Codes for Safety Analysis of Reactor Systems, Including Containment, Pisa, Italy, 11-14 November 2002,

137. Gido, R.G., Koestel, A., "Containment Condensing Heat Transfer", 2nd International Topical Meeting on Nuclear Reactor Thermal-Hydraulics (NURETH-2), Santa Barbara, CA, USA, 11-14 January 1983.

138. Heitsch, M., Schramm, B., Allelein, H-J., Simulation of hydrogen mixing in the containment of the Paks NPP during a severe accident (Simulation der Wasserstoffverteilung im Sicherheitsbehälter des KKW Paks bei einem schweren Störfall), Annual Meeting on Nuclear Technology 2006, Aachen, 2006

139. Kastner, W. et. all, and "Calculation Code for Erosion Corrosion Induced Wall Thinning in Piping Systems", Nucl, Eng, and Design, Vol. 119, pp. 431-438, 1990.

140. "Benchmark Analysis of Rapid Boron Dilution Transient by the PLASHY Code", OECD/CSNI/ISP-43 Rapid Boron Transient Tests Code Verification NEA/CSNI/R (2000)22.

141. Appendix 4 of the final report on the Secondary Piping Rupture Accident at Mihama Power Station, Unit 3 of the Kansai Electric Power Co., Inc., (in Japanese). http://www.meti.go.jp/report/downloadfiles/g50330c02j.pdf, March 2005.

142. Chapuliot S., Gourdin C., Payen T., Magnaud J. P., Monavon A.: Hydro-thermal-mechanical analysis of thermal fatigue in a mixing tee. Nucl. Engng. Design, Vol. 235, pp. 575-596, 2005.

143. Kasahara N.: Thermomechanical and fracture mechanics analysis on a Tee junction of LMFBR secondary circuit due to thermal striping phenomena. In IAEA-TECDOC-1318, pp. 89-116, November 2002.

144. Validation of fast reactor thermomechanical and thermohydraulic codes. IAEA-TECDOC-1318, p. 13, November 2002.

145. Breitung, W., C. Chan, S. Dorofeev, A. Eder, B. Gelfand, M. Heitch, R. Klein, A. Malliakos, J. Shepherd, E. Studer, and P. Thibault "Flame Acceleration and Deflagration to Detonation Transition in Nuclear Safety", SOAR. NEA/CSNI/R(2000)7, August 2000

146. Magnussen, B. F., and Hjertager, B. H. "On Mathematical Modeling of Turbulent Combustion with Special Emphasis on Soot Formation and Combustion" Sixteenth Symp. (Int.) on Combustion, The Combustion In-stitute, p 719, 1976.

147. Said, R., and Borghi, R., "A simulation with a cellular automation for turbulent combustion modeling," 22nd Symposium (Int.) on Combus-tion, University of Washington - Seattle, USA, pp. 569-577, 1988.

148. Baraldi, D., Heitsch, M., Eyink, J., Movahed, M., Dorofeev, S., Kotchourko, A., Redlinger, R., Scholtyssek, W., Pailhories, P., Huld, T., Troyer, C., Alekseev, V., Efimenko, A., Kuznetsov, M., and Okun, M.V., "Application and Assessment of Hydrogen Combustion Models," The 10th Int. Topical Meeting on Nuclear Reactor Thermal Hy-draulics (NURETH-10), Seoul, Korea, 2003.

149. Baraldi, D,. Heitsch, M., Wilkening, H., " CFD Investigation of Hy-drogen Combustion in a Simplified EPR Containment with CFX and REACFLOW," The 11th Int. Topical Meeting on Nuclear Reactor Thermalhydraulics (NURETH-11), Paper 483, Avignon, France, 2005.

150. Heitsch, M., Fluid Dynamic Analysis of a Catalytic Recombiner to Remove Hydrogen, Nuclear Engineering and Design, 1-10, 201, 2000.

151. Brunone, B., Karney, B. W., Mecarelli, M., and Ferante, M., "Velocity Profiles and Unsteady Pipe Friction in Transient Flow," Water Resources Planning and Management, Vol 126, pp. 236-244, 2000.

152. Das, D. and Arakeri, J. H., "Transition of Unsteady Velocity Profiles with Reverse Flow," J. Fluid Mich., Vol. 374, pp. 251-283, 1998.

153. Ghidaoul, M. S., Zhao, M., McInnis, D. A., and Axworthy, D. H., "A Review of Water Hammer Theory and Practice," Applied Mechanics Reviews, Vol. 58, pp. 49-76, 2005.

154. Eckert, S., Gerbeth, G., "Local velocity measurements in lead-bismuth and sodium flows using the Ultrasound Doppler Velocimetry". NURETH-10, Seoul (Korea), Oct. 5-9, 2003.

155. Eckert, S., Cramer, A., Gerbeth, G., Velocity measurement techniques for liquid metal flows. "Magnetohydrodynamics: evolution of ideas and trends", S. Molokov, R. Moreau, H.K. Moffatt (Eds.), Springer/Kluwer, in press.

156. Carteciano, L. N., Grötzbach, G. "Validation of turbulence models in the computer code FLUTAN for a free hot sodium jet," Forschungszentrum Karlsruhe Scientific Report FZKA 6600, 2003.

157. Hanjalic, K., "One-point closure model for buoyancy-driven turbulent flows," Annual Review Fluid mechanics, Vol 34, pp. 321-347, 2002.

158. Kukita, Y. et al., "ROSA/AP600 testing: facility modifications and initial test results," J Nucl Sci Technol, V 33, pp 259-265, March 1996.

159. Barre, F., M. Parent, B. Brun, "Advanced numerical methods for thermalhydraulics," CSNI Specialist Meeting on Transient Two-Phase Flow, Aix-en-Provence, France, 1992.

160. Schnurr, N.M. et al., "TRAC-PF1/MOD2 Theory manual, Los Alamos National Laboratory," US Nuclear Regulatory Commission Report NUREG/CR-5673, 1992.

161. Bergeron, A., D. Caruge, P. Clément, "Assessment of the 3-D Thermal-Hydraulic Nuclear Core Computer Code FLICA-IV on Rod Bundle Experiments", in proceedings of NURETH-9; Volume 134, Number 1, pp. 71-83, April 2001.

162. Schultz, R. R., R. A. Riemke, C. B. Davis, G. Nurnberg, "Comparison: Relap5-3d© Systems Analysis Code & Fluent Cfd Code Momentum Equation Formulations," in 11th International Conference on Nuclear Engineering, Tokyo, Japan, ICONE11-36585, April 20-23, 2003.

163. Schultz R. R., W. L. Weaver, "Using The Relap5-3d Advanced Systems Analysis Code With Commercial And Advanced Cfd Software," 11th International Conference on Nuclear Engineering Tokyo, Japan, ICONE11-36545, April 20-23, 2003.

164. Schultz, R. R., W. L. Weaver, A. M. Ougouag, W. A. Wieselquist, "Validating & Verifying A New Thermal-Hydraulic Analysis Tool," Proceedings of ICONE10, 10th International Conference on Nuclear Engineering, Arlington, VA, ICONE10-22446, April 14-18, 2002.

165. Weaver, W. L., "A Mass and Energy Conserving, Form of Explicit Coupling, For Use With RELAP5-3D©," 2002 RELAP5 International Users Seminar, Park City, Utah, September 4-6, 2002

166. Gibeling, H. and J.H. Mahaffy, "Benchmarking Simulations with CFD to 1-D Coupling," Joint IAEA/NEA Technical Meeting on the use of Computational Fluid Dynamics (CFD) Codes for Safety Analysis of Reactor Systems, Pisa, Italy, November 11-13, 2002.

167. ERCOFTAC web site, http://ercoftac.mech.surrey.ac.uk/

168. Tzanos, C.T., "Performance of k-eps Turbulence Models in the Simulation of LWR Fuel Bundles fuel", ANS/ENS Annual Meeting, 2001.

169. Willemsen, S.M. and, Komen, E. M..J., "Assessment of RANS CFD Modelling for pressurized thermal shock analysis", Proceedings of the 11th International Topical Meeting on Nuclear Reactor Thermal-Hydraulics (NURETH-11), October 2-6, 2005.

170. "Benchmarking of CFD codes for Applications to Nuclear Reactor Safety"; CFD4NRS OECD/NEA International & International Atomic Energy Agency (IAEA) Workshop, 5-7 / 9 / 2006.

171. Ducros F., "Modélisation et simulation des écoulements turbulents", CLEFS CEA n°47

172. Baldwin, W.S. & Lomax H., "Thin-layer approximation and algebraic model for separated turbulent flows"; AIAA Paper 87-257, 1978.

173. Cebecci T., Smith, A.M.O., "Analysis of turbulent boundary layers", Series in Appl. Math. & Mech., Vol. XV, Academic Press, 1974.

174. Spalart, P. and Almaras, S.R., "A one-equation turbulence model for aerodynamic flows ", AIAA Paper 92-0439, 1992.

175. Smagorinsky, J., "General circulation experiments with the primitive equations", Month. Weath. Rev., Vol. 93, 99-165, 1963.

176. Menter, F.R., "Two-equation eddy-viscosity turbulence models for engineering applications", AIAA Journal, Vol. 32, pp.1598-1605, 1994.

177. Sagaut, P., "Introduction à la simulation des grandes échelles pour les écoulements incompressibles ", Springer, 1998.

178. Sagaut, P., "Large eddy simulation for incompressible flows", Springer-Verlag Eds., 2000.

179. Nicoud F, Ducros F, "Subgrid-scale stress modelling based on the square of the velocity gradient tensor ", Flow, Turbulence and Combustion, Vol. 62, p. 183-200, 1999.

180. Moin, P. Squires, K., Cabot, W. and Lee, S., "A dynamic subgrid scale modelling for compressible turbulence and scalar transport", Phys. of Fluids, 3, p. 2746-2757, 1991.

181. Stolz, S. Adams, N.A. and Kleiser, L., "The approximated deconvolution model for LES of compressible flows and its applications to shock-turbulent-boundary layer interaction", J. of Comput. Phys., 2001.

182. Bardina, J., Ferzigger, J.H., Reynolds W.C., "Improved subgrid-scale models for large eddy simulation", AIAA Paper 80-1357, 13th AIAA Fluid and Plasma Dynamics Conference, 1980.

183. Lartigue, G., "Simulation des grandes échelles et instabilités de combustion", PhD thesis of the National Polytechnique Institute of Toulouse, 2004.

184. Kaufmann A., "Vers la simulation des grandes echelles en formulation euler euler des écoulements réactifs diphasiques ", PhD thesis of the National Polytechnique Institute of Toulouse, 2004

185. Poinsot, T. & Veynante, D., "Theoretical and Numerical combustion ", R.T. Edwards, Inc Publishers, 2001

186. Lesieur , M., "Turbulence in Fluids ", Kluwer Academic Publishers, 1997.

187. Benarafa,, Y., "Application du couplage RANS-LES aux écoulements turbulents à haut nombre de Reynolds de l'industrie nucléaire"; PhD thesis, 2005.

188. " Turbulence modelling : Part 2, Limitations of the k-epsilon models" ; QNET-CFD, 2002

189. Höhne, T., and Bieder, U., "Modeling of A buancy-Driven Flow experiment at the rocom test facility using the CFD-codes CFX-5 and Trio_U", to appear in Nuclear Engineering and Design; 2006.

190. Bieder, U. Fauchet, G, Betin, S., Kolev, N. and Popov, D., "Simulation of mixing effect in a VVER-1000 reactor", to appear in Nuclear Eng. And Design

191. Rohde, U., 2005, "Final Summary Report", Flomix-R (FIKS-CT-2001-00197), 2001.

192. Schippers, M., 2005, "D10: Numerical Analysis of thermo-hydraulic tests", THERFAT R(13)/D10/2003.

193. Scheuerer, M., "Condensed Final Summary Report", EVOL-ECORA-D18, 2005.

194. Deadorff, J.W., "A numerical study of three dimensional turbulent channel flow at large Reynolds Numbers", Journal of Fluid Mech, 41, 453-465, 1970.

195. Nikitin, N.W., Nicoud, F., Wasistho B., Squires K.D., Spalart P.R., "An approach to wall modeling in large eddy simulations ", Physics of Fluids , 12, 1629-1632, 2000.

196. Spalart, P.R., Jou, W.H., Strelets, M. Allmaras, S.R., "Comments on the feasibility of LES for wings and on a hybrid RANS/LES approach", in Advances in DENS/LES, Z. Liu Ed., pp. 137-147, Greyden Press, 1997.

197. Fureby, C. and DeVore, C. R., "On MILES based on flux-limiting algorithms", F. F. Grinstein, International Journal for Numerical Methods in Fluids, Volume 47, Issue 10-11 , Pages 1043 – 1051, 2005.

198. Veber, P. & Andersson, L, "CFD calculation of flow and thermal mixing in a T-junction – time-dependent calculation part 2 (BG-project)," Teknisk not 2004/21, Rev 0, Onsala Ingenjörsbyrå, 2004.

199. Henriksson, M., Andersson, U. & Jungstedt, J., "Termisk blandning i T-stycke – Resultatrapportm," Report U02:134, Vattenfall Utveckling AB, 2002.

200. Menter F. R. and Egorov, Y., "Re-visiting the turbulent scale equation," Proc. IUTAM Symposium; One hundred years of boundary layer research, Göttingen, 2004.

201. Menter F. R. and Egorov, Y., "A Scale-Adaptive Simulation Model using Two-Equation Models", AIAA paper 2005-1095, Reno/NV, 2005.

202. Menter F.R. and Egorov, Y., "Turbulence Models based on the Length-Scale Equation", Fourth International Symposium on Turbulent Shear Flow Phenomena, Williamsburg, 2004 – Paper TSFP4-268, 2005.

203. Rotta, J. C., Turbulente Strömungen, Teubner Verlag, Stuttgart, 1972.

204. Menter F.R., "Two-equation eddy-viscosity turbulence models for engineering applications". AIAA-Journal, 32(8), pp. 269-289, 1994.

205. Weber C, Ducros F, Corjon A, "Assessment of implicit time integration for LES", AIAA Paper 99-3355, 2005.

206. Sergent, E., "Vers une méthodologie de couplage entre la simulation des grandes echelles et les modèles statistiques", PhD of Ecole Centrale de Lyon, 2002.

207. Schluter, J. U., Pitsch, H. and Moin, P., "Large Large Eddy Simulation Inow Conditions for Coupling with Reynolds-Averaged Flow Solvers ",AIAA Journal, 42(3):478-484, 2004.

208. Jarrin, N., Addad, Y., Laurence, D., "Synthetic turbulent inflow conditions based on a vortex method for large-eddy simulation", Sofiane Benhamadouche, Progress in Computational Fluid Dynamics, Vol. 6, No.1/2/3 pp. 50 – 57, 2006.

209. Udaykumar, H. S., Mittal, R., Shyy, W., "Computation of Solid-Liquid Phase Fronts in the Sharp Interface Limit on Fixed Grids," J. Comp. Phys., Vol.153, pp.535-574, 1999.

210. Hou, T. Y., Lowengrub, J. S., Shelley, M. J., "Boundary Integral Methods for Multicomponent Fluids and Multiphase Materials," J. Comp. Phys., Vol.169, pp.302-323, 2001.

211. Hirt, C.W., Amsden, A.A., and Cook, J.L., "An Arbitrary Lagrangian-Eulerian Computing Method for all Flow Speeds," J. Comp. Phys., 14, 227. 1974.

212. S. Koshizuka and Y. Oka, "Moving-Particle Semi-implicit Method for Fragmentation of Incompressible Fluid," Nucl. Sci. Eng. Vol. 123, pp. 421-434, 1996.

213. Osher, S., and Fedkiw, R. P., "Level Set Methods: an Overview and Some Recent Results," J. Comp. Phys., Vol.169, pp.463-502, 2001.

214. Sethian, J. A., "Evolution, Implementation, and Application of Level Set and Fast Marching Methods for Advancing Fronts," J. Comp. Phys., Vol.169, pp.503-555, 2001.

215. Jacqmin, D., "Calculation of Two-Phase Navier-Stokes Flows Using Phase-Field Modeling," J. Comp. Phys., Vol.155, pp.96-127, 1999.

216. Harlow, F.H. and Welch, J.E., "Numerical Calculation of Time-Dependent Viscous Incompressible Flow," Phys. Fluids 8, 2182 1965.

217. Hirt, C.W. and Nichols, B.D., "Volume of Fluid (VOF) Method for the Dynamics of Free Boundaries," J. Comp. Phys. 39, 201 1981.

218. Fluent Inc., Product Documentation, www.fluent.com, 2004.

219. Kunugi, T. MARS for Multiphase Calculation, Computational Fluid Dynamics Journal, Vol. 19, pp. 563-571, 2001.

220. T.Yabe and F.Xiao : Description of Complex and Sharp Interface during Shock Wave Interaction with Liquid Drop J.Phys. Soc. Japan Vol. 62, pp. 2537-2540, 1993.

221. FIDAP 8.60, Fluid Dynamics Analysis Package. Fluent Inc., 10 Cavendish Court, Lebanon, NH, 03766, USA , 2001.

222. CFX-4.3, AEA Technology, Harwell, Oxfordshire, OX11 0RA, UK, 2000.

223. Enright, D., Fedkiw, R., Ferziger, J., and Mitchell, I., A hybrid particle level set method for improved interface capturing. J. Comput. Phys., 183, 83 116, 2002.

224. Paterson, E. G., Poremba, J. E., Peltier, L. J., and Hambric, S. A. "A Physics Based Simulation Methodology for Predicting Hydrofoil Singing," Proceedings of the 25th Symposium on Naval Hydrodynamics, St. John's, Newfoundland and Labrador, CANADA, August 2004.

225. Hirt, C. W., "Heuristic stability theory for finite-difference, J. Comp. Phys., Vol 2. No. 2, pp. 339-355, 1967.

226. Vyskocil, L., "Numerical Diffusion in FLUENT 6," Proceedings of the 11th FLUENT User's Conference, pp. 117-127, 2005.

227. Levenspiel, )., "Chemical Reaction Engineering", 2nd Ed. New York, Wiley, 1972.

228. Macian, R. and Mahaffy, J.H., "Numerical Diffusion and the Tracking of Solute Fields in System Codes: Part I. One-Dimensional Flows," NED, Vol. 179, pp. 297- 319, 1998.

229. Richtmyer, R. D.,. Morton, K. W, *Difference methods for initial-value problems*, Wiley, New York, 1967.

230. Ferziger, J. H., Perić, M., *Computational Methods for Fluid Dynamics*, Springer Verlag, Berlin/Heidelberg, 1999.

231. Brackbill, J. U., Kothe, D. B., and Zemach, C., A continuum method for modeling surface tension. J. Comput. Phys., 100, pp, 335-354, 1992.

232. Roache, P. J., "Code Verification by the Method of Manufactured Solutions," Trans. ASME, J. Fluids Engineering, 124, pp. 4-10, 2002,

233. Richardson, L. F., "The Approximate Arithmetical Solution by Finite Differences Of Physical Problems Involving Differential Equations, with an Application to the Stresses in a Masonry Dam", Transactions of the Royal Society of London, Series A, Vol. 210, pp. 307-357, 1910.

234. Oberkampf, W. L. and Barone, M. F., "Measures of agreement between computation and experiment: Validation Metrics," J. Comp. Phys., Vol. 217, pp. 5-36, 2006.

235. "Guide to the Expression of Uncertainty in Measurement," ISO, 1995.

236. AIAA Standard, "Assessment of Wind Tunnel Data Uncertainty," *AIAA S-071-1995*.

237. ASME PTC 19.1-1998, "Test Uncertainty," 1998.

238. Coleman, H. G. and Steele, W. G., "Engineering Application of Experimental Uncertainty Analysis," *AIAA Journal*, Vol. 33, No. 10, pp. 1888 ~ 1896, 1995.

239. Coleman, H. G. and Steele, W. G. "Experimentation and Uncertainty Analysis for Engineers," John Wiley & Sons, 1989.

240. Brown, K. K., Coleman, H. W., Steele, W. G., and Taylor, R. P., "Evaluation of Correlated Bias Approximations in Experimental Uncertainty Analysis," *AIAA Journal*, Vol. 34, No. 5, pp. 1013 ~ 1018, 1996.

241. Steele, W. G., Maciejewski, P. K., James, C. A., Taylor, R. P., and Coleman, H. W., "Asymmetric Systematic Uncertainties in the Determination of Experimental Uncertainty," *AIAA Journal*, Vol. 34, No. 7, pp. 1458 ~ 1463, 1996.

242. Hemström, B., et al.: Validation of CFD codes based on mixing experiments (Final report on WP4). EU/FP5 FLOMIX-R report, FLOMIX-R-D11, Vattenfall Utveckling (Sweden), 2005.

243. Wilks, S. S., "Determination of sample sizes for setting tolerance limits," Ann. Math. Statist., Vol. 12, pp. 91-96. 1941.

244. Wilks, S.S., "Statistical prediction with special reference to the problem of tolerance limits," Ann. Math. Statist., Vol. 13, pp. 400-409, 1942.

245. Glaeser, H. G., "Large break LOCA uncertainty evaluation and comparison with conservative calculation." Proceedings of the International Meeting on Updates in Best Estimate Methods in Nuclear Installation Safety Analysis, BE-2004, pp. 118-123, 2004.

246. Attila Guba, A. Makai, and M., Pa´l, L. "Statistical aspects of best estimate method—I," Reliability Engineering and System Safety. Vol. 80, pp. 217-232, 2003.

247. Nutt, W. T. and Wallis, G. B., "Evaluation of nuclear safety from the outputs of computer codes in the presence of uncertainties," Reliability Engineering and System Safety. Vol. 83, pp. 57-77, 2004.

248. Orechwa, Y., "Comments on 'Evaluation of nuclear safety from the outputs of computer codes in the presence of uncertainties' by W.T. Nutt and G.B. Wallis," Reliability Engineering and System Safety. Vol. 87, pp. 133-135, 2005.

249. Wallis, G. B. and Nutt, W. T., "Reply to Comments on 'Evaluation of nuclear safety from the outputs of computer codes in the presence of uncertainties' by Y. Orechwa," Reliability Engineering and System Safety. Vol. 87, pp. 137-145, 2005.

250. Helton, J. C., and Oberkampf, W. L., "Alternate Representations of Epistemic Uncertainty," Reliability Engineering and System Safety, Vol. 85, pp. 1-10, 2004.

251. Helton, J. C., Johnson, J. D., Oberkampf, W. L., and Sallaberry, C. J. "Sensitivity analysis in conjunction with evidence theory representations of epistemic uncertainty," Reliability Engineering and System Safety, Vol. 91, pp. 1414-1434, 2006.

252. Oberkampf, W. L. and Helton. J. C., "Evidence Theory for Engineering Applications," Chapter 10 of the Engineering Design Reliability Handbook, Nikolaidis, E. et al Eds., CRC Press, 2005.

253. Trucano, T. G., Pilch M., and Oberkampf W. L., "General Concepts for Experimental Validation of ASCI Code Applications," SAND2002-0341, Sandia National Laboratories, March 2002.

254. Prasser, H.-M.; G. Grunwald, T. Höhne, S. Kliem, U. Rohde, F.-P. Weiss, "Coolant mixing in a Pressurized Water Reactor: Deboration Transients, Steam-Line Breaks, and Emergency Core Cooling Injection," Nuclear Technology 143 (1), p.37, 2003.

255. Rohde, U.; Kliem, S.; Höhne, T.; Karlsson, R.; Hemström, B.; Lillington, J.; Toppila, T.; Elter, J.; Bezrukov, Y., "Fluid mixing and flow distribution in the reactor circuit – Part 1: Measurement data base," Nuclear Engineering and Design 235, 421–443, 2005.

256. McKinnon M. A., Dodge, R. E., Schmitt, R. C., Eslinger, L. E. and Dineen, G.,. "Performance Testing and Analyses of the VSC-17 Ventilated Concrete Cask," TR-100305, Electric Power Research Institute, Palo Alto, California, 1992.

257. Spent Nuclear Fuel Effective Thermal Conductivity Report. Prepared by TRW Environmental Safety Systems, Inc., for US DOE, July 11, 1996.

258. McAdams W. H.. Heat Transmission. McGraw-Hill Book Company, Inc., New York, 1954.

259. Fluent User Guide Version 6., Fluent Inc, New Hampshire, 2004.

260. Téchy, Z., "Assessment of the Paks Nuclear Power Plant Safety for Large Radioactive Release. E1: Containment Event Trees and Severe Accident Analyses", VEIKI Report 20.22-017, October 2001.

261. Heitsch, M., Wilkening, H., Baraldi, D., "CFD Modelling of Gas-Transport and Mixing Phenomena in the Battelle Experimental Facility for Nuclear Safety Applications", 7th World Congress of Chemical Engineering, Glasgow, 2005.

262. Andreani, M., K. Haller, M. Heitsch, B. Hemström, I. Karppinen, J. Macek, J.Schmid, H. Paillere, I. Toth, "A Benchmark Exercise on the use of CFD Codes for Containment Issues using Best Practice Guidelines: a Computational Challenge", OECD NEA Workshop CFD4NRS, Garching, 2006.

263. Carcassi, M., M. Jordan, M. Heitsch, F. Martin Fuertes, R. Monti, T. Kanzleiter, "Improved Modelling of Turbulent Hydrogen Combustion and Catalytical Recombination for Hydrogen Mitigation (HYMI)", 4th Framework Programme of the EC, Final Summary Report, Pisa, 1999.

264. Heitsch, M. and Schramm, B.: "Simulation of the Unmitigated SG-Tube Rupture Accident at PAKS with CFX, Hydrogen Management for the VVER-440/213 Containment," HU2002/000-632-04-01, GRS Cologne, 2005.

265. Heitsch, M. and Schramm, B., "Simulation of the Mitigated SG-Tube Rupture Accident at PAKS with CFX, Hydrogen Management for the VVER-440/213 Containment," HU2002/000-632-04-01, GRS Cologne, 2005.

# GLOSSARY

AIAA    American Institute of Aeronautics and Astronautics

AP600   Advanced Pressurized water reactor, 600 Mw power (Westinghouse design

ASME   American Society of Mechanical Engineers

ATHLET    System TH code, used extensively in Germany

BPG    Best Practice Guidelines

CAD    Computer Aided Design

CATHARE  System TH code, used extensively in France

CFD    Computational Fluid Dynamics

CFL step    Courant-Friedrich-Levy number measures fraction of a cell crossed by flow in one time step

CHF    Critical Heat Flux

DDT    Deflagration to Detonation Transition

DES    Detached Eddy Simulation

DNS    Direct Numerical Simulation

DVI    Direct Vessel Injection

ECCS    Emergency Core Cooling System

ECORA    Evaluation of Computational Fluid Dynamic Methods for Reactor Safety Analysis

EPRI    Electric Power Research Institute

ERCOFTAC    European Research Community on Flow, Turbulence and Combustion

EVM    Eddy Viscocity Model

FAC    Flow accelerated corrosion

FBR    Fast Breeder Reactor

$Fr_{CL, HPI}$    "Superficial" Froude Number

GCR       Gas Cooled Reactor

HCDA    Hypothetical Core Disruptive Accident

HPI        High Pressure Injection

LBLOCA    Large Break Loss of Coolant Accident

LES        Large Eddy Simulation

LMFBR      Liquid Metal Fast Breeder Reactor

LPIS      Low Pressure Injection System

MILES       Monotonic Integrated for LES

NRS       Nuclear Reactor Safety

NPP       Nuclear Power Plant

PIRT      Phenomena Identification Ranking Table

PTS       Pressurized Thermal Shock

PWR      Pressurized Water Reactor

RANS     Reynolds-Averaged Navier-Stokes

RELAP5     U.S. DOE and NRC system TH code, used extensively in US and elsewhere

RNG      Renormalized Group Theory

RPV       Reactor Pressure Vessel

SG     Steam Generator

SMC      Second Moment Closure (class of turbulence model)

TH     Thermal-hydraulic

TRAC    Transient Reactor Analysis Code, old USNRC system TH code

TRACE      TRAC/RELAP Advanced Computational Engine, USNRC's current system TH code

V&V     Verification and Validation

**ANNEX I, CHECKLIST FOR A CALCULATION**

Initial Preparation

- Produce a clearly written problem description, specifying the system and scenario requiring analysis, and clearly listing study objectives (Section 3.2).

- Assemble a panel of experts and go through the PIRT process based upon the problem description (Section 3.2).

- Do special phenomena such as containment wall condensation require addition of models to a standard CFD code or use of a special purpose CFD package? (Section 3.3)

- With knowledge of the problem and physical processes select an appropriate CFD code and if necessary develop enhancements. (Section 4.3)

- Does the problem require full CFD or are classic thermalhydraulic (TH) codes adequate? .(Chapter 4)

- Is coupling required between a CFD and a TH code to supply boundary conditions to the CFD? (Section 4.4)

Geometry Generation

- Is the coordinate system correct?

- Are the units correct?

- Have any substantial modifications been made to the geometry?

- Is the geometry complete?

- Are there oversimplifications due to symmetry assumptions, etc.?

- Are inlet, outlet, symmetry and cyclic boundary condition regions located correctly?

Selection of Physical Models

- Develop a basic understanding of the prevalent physical phenomena and flow fields (part of the PIRT process)

- Select the appropriate level of turbulence representation (RANS, T-RANS, LES, hybrid approach, see Section 5.1.4)

- For RANS or T-RANS select an appropriate statistical model for turbulence (Section 5.1.4).

- Either resolve the wall boundary layer or choose a wall function model (Sections 5.1.4 and 6.2.3).

- Establish boundary conditions consistent with your choice of turbulence model. (Section 5.1.4)

Grid Generation (Section 6.2.3)

- Are the grid angles larger than 20° and less than 160°?

- Are the ratios of adjacent volumes less than 2?

- Are the aspect ratios below the values given in the solver manual (typically, 10 … 50)?

- Is the grid scalable?

- Are grid nodes concentrated in areas of foreseeable physical significance?

- Does the grid contain non-matching grid interfaces in critical regions?

- Is the grid compatible with the physical models (turbulence model, wall treatments, etc.)?

Numerical Methods

- Generally avoid use of first order upwind spatial discretization, and first order implicit time integration schemes.

- If first order methods are used, compare the numerical diffusion coefficient to an estimate of the turbulent diffusion coefficient at a number of locations in your mesh ( Section 0).

- When using LES, select a higher order central difference method, preferably 4th order.

Verification

- Check for round-off errors (Sections 8.2 & 8.3).

- Check for errors associated with selection of iteration convergence criteria (Sections 8.2 & 8.4).

- Check for errors associated with discretization of space and time (Sections 8.2, 8.5, & 8.6)

- Follow procedures to limit and locate user errors (Section 8.7) including:

  − selection of a high quality user interface to the CFD code; and

  − use of quality assurance practices.

Validation

- Follow a tiered approach comparing first to separate effects experiments (unit problems) and working up through complete system experiments (Section 9.1)

- Where possible use repeat experiments to help quantify experimental error

- Using guidance from the PIRT process, select target variables and metrics for agreement between calculation and experiment (Section 9.2).

- Characterize experimental uncertainty for all target variables, distinguishing between random and systematic (bias) contributions to the uncertainty (Section 9.3.1).

- If sufficient computer resources are available, perform uncertainty analysis on the simulation, to place bounds on results, and to cross-check the initial PIRT assumptions about relative importance of physical phenomena (Section 9.3.2).